BPS STATES IN STRING THEORY

BY EVGENY ANDRIYASH

A dissertation submitted to the
Graduate School—New Brunswick
Rutgers, The State University of New Jersey
in partial fulfillment of the requirements
for the degree of
Doctor of Philosophy
Graduate Program in Physics and Astronomy

Written under the direction of
Professor Gregory Moore
and approved by

_____

_____

_____

_____

_____

New Brunswick, New Jersey

October, 2010

ABSTRACT OF THE DISSERTATION

BPS states in string theory

by Evgeny Andriyash

Dissertation Director: Professor Gregory Moore

In this thesis we discuss a number of interesting and important properties of BPS states in string theory. We study wall-crossing behavior of BPS states at large volume limit and implications of it for the OSV conjecture. We find that the weak topological coupling OSV conjecture can be true at most in a special chamber of the Kähler cone.

We also clarify an interesting puzzle arising in the description of BPS states on the Higgs branch of supersymmetic quantum mechanics. Using methods of toric geometry we compute Hilbert spaces of BPS states on the compactified Higgs branch and arrive at completely consistent picture of spatial $Spin(3)$ structure of those spaces.

We introduce new kinds of walls, called Bound State Transformation(BST) walls, in the moduli space across which the nature of BPS bound states changes but the index remains continuous. These walls are necessary to explain the continuity of BPS index. BPS states can undergo recombination, conjugation or hybrids of the two when crossing a BST wall. Conjugation phenomenon happens near singularities in the moduli space and we relate massless spectra of BPS states at such singularities to monodromies around them. In cases when massless vector BPS particles are present we find new constraints on the spectrum and in particular predict the existence of magnetic monopoles becoming massless at such singularities.

We give a simple physical derivation of the Kontsevich-Soibelman wall-crossing formula. Considering galaxy-like configurations of BPS particles with a central supermassive black hole with a number of stellar BPS systems around it we derive a consistency requirement on the partition function of such BPS galaxies. This requirement turns out to be nothing but Kontsevich-Soibelman wall-crossing formula. Our approach gives a generalization of the formula for the

case when massless BPS particles are present.

Acknowledgements

I would like to thank my advisor, Greg Moore, for guiding me and helping me through my PhD years, for being supportive at all times, willing to invest his time in the discussions of physical problems with me, sharing his ideas and proposing interesting projects. It has been a pleasure to work with Greg and learn from him about the beautiful world of mathematical physics.

I am grateful to my collaborators Frederik Denef and Daniel Jafferis for a very fruitful work that resulted in very interesting ideas and taught me a lot about collaboration in general.

I would like to thank Emanuel Diaconescu for sharing his knowledge of algebraic geometry with me.

It is a pleasure to thank Diane Soyak, Ronald Ransome and Shirley Hinds for help with many organizational issues.

I wish to thank Dieter van den Bleeken, Jan Manschot, Wu-Yen Chuang, Alexey Litvinov, Gonzalo Torroba, Sam Klevtsov, Sergio Lukich, Jose Juknevich and Dmitrii Melnikov for many useful and productive conversations.

Evgeny Andriyash

Rutgers University

October 2010

Dedication

To my family.

Table of Contents

List of Figures

Chapter 1
Introduction

String theory is intrinsically connected with supersymmetry, which is the symmetry between bosonic and fermionic degrees of freedom. Low energy theories, describing the world around different vacua of string theory, are supersymmetric field theories, usually containing gauge fields and gravity. Since the discovery of supersymmetry in the early 70's it was known that supersymmetric field theories may contain short representations of supersymmetry, called BPS states. Those are states that are annihilated by half of the supersymmetry generators, thus giving a short representation. Since their discovery BPS states have played a prominent role in physics. They turned out to be responsible for a vast majority of phenomena in the low energy physics, including the low energy effective action of $N = 2$ supersymmetric field theories, found by Seiberg and Witten in the 90's [1].

BPS sates were also studied in supergravity theories and string theory. Due to the presence of supersymmetry certain properties of BPS states, such as the relation between mass and electromagnetic charge and their degeneracies, are protected in the sense that they do not change as the coupling constant of the theory is changed. This makes BPS states a natural playground for testing the large web of dualities between different string theories such that strong coupling regime of one can be described by weak coupling regime of the other. A famous example of BPS states usage is testing AdS/CFT duality, which in it's classic example is the duality between type II string theory on $AdS_5 \times S^5$ and $N = 4$ super Yang-Mills theory on R^4 [2].

In view of this last fact, it is clear that BPS states can have different incarnations. In the low energy limit of string theory, compactified on some internal 6D manifold, which is typically a supergravity theory in 4 dimensions with some additional particles and gauge fields, BPS states are represented as black hole solutions. This description of BPS states is good when the curvature of the resulting space-time is not too big which correspond to the so-called t'Hooft coupling being large. For small t'Hooft coupling, the more appropriate description is in terms of world-volume theory of D-branes, wrapping various cycles in the internal manifold. As BPS states are protected by supersymmetry, their degeneracy can be computed in the D-brane

picture, and then compared to the black hole entropy. Thus BPS states provide a framework to model microscopic structure of black holes, that account for the known entropy, which is known as Strominger-Vafa program of accounting for black hole entropy in terms of D-brane microstates [3].

Another more technical application of BPS states in string theory is the so-called Ooguri-Strominger-Vafa conjecture concerned with degeneracies of BPS states in type II string theory, compactified on a Calabi-Yau manifold [4]. It relates the partition function formed out of BPS black hole degeneracies with the so-called topological partition function. The latter partition function computes some part of the low energy effective action of string theory and the conjecture relates it to BPS states degeneracies directly. We will say more about this relation below.

In this thesis we study different properties and examples of BPS states in type II string theory. The Hilbert space of BPS states in this theory are graded by the values of their magnetic and electric charges $\Gamma = (p, q) \in \Lambda^{em}$. The main characteristic of interest to us will be the degeneracies, or more precisely indices of BPS states. The indices will be denoted $\Omega(p, q; t_\infty)$ and generically they are functions of the background moduli fields of type II string theory, denoted by t_∞. Although the introduced indices and degeneracies are different for finite charges Γ, in the limit of large charges the two become the same

$$\Omega(\Gamma; t_\infty) \sim e^{S(\Gamma)}, \tag{1.0.1}$$

where $S(\Gamma)$ is the corresponding entropy of the BPS state. Indices $\Omega(p, q; t_\infty)$ are integer-valued and piece-wise constant functions of the background moduli, i.e. they can change discontinuously across certain walls in the moduli space. The amount of jump is described by the famous Denef-Moore wall-crossing formula(WCF) [5], which we now explain. The index of the Hilbert space of BPS states with charge $\Gamma \in \Lambda^{em}$ at point t_∞, $\Omega(\Gamma; t_\infty)$, gets many different contributions from BPS states, represented by black holes, as well as from bound states of BPS objects, represented by multicentered black hole solution of the low energy supergravity theory. Suppose there are two charges $\Gamma_1, \Gamma_2 \in \Lambda^{em}$ such that BPS states with these charges can form a bound state of total charge $\Gamma = \Gamma_1 + \Gamma_2$ at point t_∞. The conditions for such bound state to exist was given in [6] and has the form

$$R = \frac{\langle \Gamma_1, \Gamma_2 \rangle}{2} \frac{|Z(\Gamma; t_\infty)|}{\mathrm{Im} Z(\Gamma_1; t_\infty) \overline{Z(\Gamma_2; t_\infty)}} > 0, \tag{1.0.2}$$

where $\langle \Gamma_1, \Gamma_2 \rangle$ is the intersection product of two charges in the symplectic lattice Λ^{em} and

$Z(\Gamma_{1,2};t_\infty)$ are the central charges of two BPS states, following from the supersymmetry algebra of the theory. Physically, R is the spatial distance between the two BPS states. The locus in the moduli space where the two central charges (anti-)align is called (Anti-)Marginal Stability ((A)MS) wall. If we cross the marginal stability wall from the negative side to the positive side across a generic point $t_{ms} \in MS(\Gamma_1,\Gamma_2)$ then the jump of index of BPS state with charge Γ is given by the primitive wall-crossing formula introduced in [5]

$$\Delta\Omega(\Gamma) = (-1)^{\langle\Gamma_1,\Gamma_2\rangle-1}|\langle\Gamma_1,\Gamma_2\rangle|\Omega(\Gamma_1;t_{ms})\Omega(\Gamma_2;t_{ms}). \tag{1.0.3}$$

The interpretation of this formula is simple: when t approaches $MS(\Gamma_1,\Gamma_2)$ the distance between the two BPS states goes to infinity, the state decays and the change in the index is roughly the product of indices of the two decay products times the Landau level degeneracy of one charge in the electromagnetic field of another. This WCF, as well the generalization thereof given by Kontsevich and Soibelman [7], will be the main focus of this thesis.

As we discuss in more details in chapter 2 the OSV conjecture relating BPS indices to the topological partition function does not specify the place in moduli space where the indices have to evaluated. In the large volume limit of compact manifold, given by $\mathrm{Im}\, t \to \infty$, the description of BPS states in terms of D-branes wrapping cycles of this manifold becomes accurate and much is known about the values of BPS indices. From the physics point of view the study was motivated by the Strominger-Vafa microstate counting program. From the mathematical perspective the hope is to identify BPS indices as something like "the Euler character of the moduli space of stable objects in the bounded derived category on X with stability condition t." As the BPS indices are well studied in this region, the large volume limit is natural place where we can test the OSV conjecture. In chapter 2 we study the indices of BPS states in the large volume limit with a focus on the possible jumps across MS walls going to infinity and implications of those jumps for the validity of the OSV conjecture. It was already noted in [8], that for $D4$ brane BPS states, realized as a bound state of two $D4$'s, the MS walls can go to infinity. We construct explicitly an example of such state. It is a bound state of a BPS black hole with $D4$ charge and another $D4$ charge, which itself is a bound state of $D6$ and $\bar{D}6$ BPS branes. We choose the total charge of BPS state such that it has also a realization as a single-centered black hole. When t_∞ crosses MS wall, 3-centered configuration disappears from the spectrum, and the index jumps. For a certain region of charges, namely when the $D4$ charge is very large, this jump can be exponentially larger than the single-centered contribution. As the original OSV conjecture was formulated precisely in this region, which corresponds to weak topological coupling region, we conclude that the conjecture cannot be true in this region. It

can be true at most in a certain chamber of the moduli space near the large volume point and we propose the candidate chamber.

As mentioned above BPS states in string theory usually allow two different descriptions in different regimes of the theory: supergravity description as single or multi-centered black hole configuration in the strong string coupling regime and D-brane world volume theory description in the weak string coupling regime. Sometimes the theory on the world volume of D-brane configuration is a conformal field theory(CFT) in which case one expects to find the complete duality between the two description and matching of the spectra on both sides. In such cases the geometry on the supergravity side contains as a part Anti de Sitter space and the observed duality is called AdS/CFT duality. A well-studied case of such duality is the single-centered black hole configuration, containing AdS_3 part, which is dual to some 2 dimensional CFT_2. The multicentered black holes can also be analyzed from AdS/CFT point of view. In [9], the authors considered certain limit of multicentered black hole configuration that lead upon lifting to 11-dimensional space geometries containing AdS_3 piece. This allowed [9] to identify the dual CFT_2 description. In particular, the entropy of such configurations is reproduced in the dual CFT_2 and is given by the entropy of the single centered configuration with the same total charge. Our 3-centered example, with entropy bigger than single-centered realization, could potentially lead to contradiction here, since it's contribution can not be seen in the dual CFT_2. We checked explicitly that our example does not survive the near-horizon limit of [9], actually corresponding to two infinitely separated AdS_3 geometries, and the contradiction is avoided. [9] also suggested a general criteria for multicentered BPS configuration to have a single AdS_3 geometry in the near-horizon limit. We give give a constructive argument in favor of this criteria.

Having discussed the two complementary descriptions of BPS states as applied to particular examples we move forward to some more general questions relating the two descriptions. On the supergravity side the moduli space of BPS objects, which are multicentered black hole solutions in this case, is described by the space of all possible positions of the black hole centers, subject to constraints following from equations of motion and supersymmetry. In the regime of weak string coupling constant the same objects are described by bound states of D-branes and excitations of those. It is very important to understand precisely how the matching of different BPS states in the two pictures occurs. An important step in this direction was made in [10]. It was shown there that in fact we should expect to have a smooth transition between the two regimes, in which all discrete characteristics, like the indices of BPS states, are preserved. Nevertheless there are still unanswered questions here. In the D-brane picture the bound states of BPS objects can be described using the powerful apparatus of algebraic geometry. For example [8]

studied stable holomorphic bundles on rigid surfaces and found the number of BPS states on two sides of a marginal stability wall. It turned out that enumeration of BPS states in algebraic geometry gives a very different answer for the number of BPS states than the answer that we expect from the supergravity description. More concretely supergravity picture tells us that BPS space is empty on one side of the wall and is populated on the other side. Algebraic-geometry picture gives non-empty spaces on both sides. This apparent contradiction is asking for a resolution.

In [10] the description of the abound state of BPS objects, that can be useful in both string and weak string coupling was given in terms of supersymmetric quantum mechanics(SSQM). The moduli space of this supersymmetric quantum mechanics has two branches: Coulomb branch which corresponds to the supergravity side and the Higgs branch which corresponds to the D-brane side of the full string theory description. [10] used this picture to show that in some cases the transition between the two descriptions is completely smooth. However, more generally Higgs branch is populated on both sides of marginal stability wall, while the Coulomb branch is populated only on the stable side, which leads to a similar contradiction as found for algebraic-geometry versus supergravity pictures. We will not try to resolve this problem in this thesis but instead concentrate on a related interesting paradox, arising in this setup. The Hilbert spaces of BPS states are representations of the Lorentz group, and in particular of the group of spatial rotations $Spin(3)$. As we move through the wall of marginal stability part of the Hilbert space decays. It turns out that in the Higgs branch description BPS states on both sides of MS wall as well as the decaying part of the Hilbert space form irreducible multiplets of $Spin(3)$ group. This leads to an apparent paradox since the sum of two irreducible representations cannot be an irreducible representation itself. We give a resolution of this paradox in chapter 3. The main idea is to consider the simplest compactification of the moduli space. We find a completely consistent picture for the BPS Hilbert spaces on both sides of the marginal stability wall. The simplest compactification that we consider also gives a hope to find the relation between algebro-geometric and SSQM pictures.

Despite the fact that there are two complementary descriptions of BPS states for the purposes of enumerating different contributions to their indices and computing the indices the supergravity picture of multicentered black hole is by far more powerful. In supergravity every multicentered black hole solution, representing BPS states, is given in terms of a map from our 3-dimensional space to the moduli space of the internal Calabi-Yau manifold. In the simplest case of a two centered solution there is a correspondence between this map and a certain graph in the moduli space, called Split Attractor Flow Tree in [11]. The image of space under the

map turns out to be a "thickening" of the attractor flow tree and the existence of the tree is equivalent to the existence of the full supergravity solution. This fact lead [11] to the

Split Attractor Flow Tree Conjecture: *Supergravity solution exists iff the corresponding Split Attractor Flow Tree exists. There is a one-to-one correspondence between components of the moduli space of supergravity solutions and Attractor Flow Trees.*

In practice it is very easy to formulate the existence conditions of attractor flow trees. It is a more computationally challenging problem to enumerate all possible attractor flow trees with given total charge Γ, existing at a given point t in the moduli space, although the algorithm is straightforward. We collect all the details on existence conditions of attractor flow trees in Appendix A. The conjecture gives a simple physical picture of the behavior of black hole "molecules" under the change of the background moduli. Suppose we move through the moduli space keeping track of a given attractor flow tree. As we cross the wall of marginal stability where this tree has it's first split the tree ceases to exist, decaying into the two constituents, represented by the two subtrees starting at this split. This gives a decomposition of BPS Hilbert space of the total charge into the Hilbert spaces of constituents. This process can be continued for the constituents also, moving along the edges of the tree away from the root. In all, the attractor flow tree gives a canonical way of (dis)assembling part of BPS Hilbert space, represented by this tree, into the Hilbert spaces of the constituents. This split attractor flow picture of BPS states, although originally coming from supergravity, is more general and applicable outside of the range of validity of supergravity.

The decay of BPS objects into constituents is subject to conservation of energy. For a decay $\Gamma \to \Gamma_1 + \Gamma_2$ that occurs at some point t_{ms} on the marginal stability wall $MS(\Gamma_1, \Gamma_2)$ this condition takes the form

$$|Z(\Gamma; t_{ms})| = |Z(\Gamma_1; t_{ms})| + |Z(\Gamma_2; t_{ms})|. \tag{1.0.4}$$

Together with an obvious relation, reflecting linearity of central charge with respect to the charge itself

$$Z(\Gamma; t_{ms}) = Z(\Gamma_1; t_{ms}) + Z(\Gamma_2; t_{ms}), \tag{1.0.5}$$

this mean that the state can only decay when the central charges align, i.e. only across MS wall. In fact the presence of a bound state $\Gamma_1 + \Gamma_2$ near anti-marginal stability wall $AMS(\Gamma_1, \Gamma_2)$ leads to a sharp contradiction with the conservation of energy, since approaching the AMS wall the radius of the bound state still has to go to infinity according to (1.0.2) and the energies

should add up. It is this contradiction, first pointed out in [12], that is the main motivating question for chapter 4. More precisely suppose that the bound state exists near the MS wall and there is a path in the moduli space connecting MS and AMS walls for this bound state such that the radius of it stays finite and positive along the whole path. This necessarily means that the bound state exists near AMS wall leading to a contradiction, unless something dramatic happened to it along the path.

We study the paradox in the most general set up using the split attractor flow picture in chapter 4. We find that there are several new phenomena and new kinds of walls that help to avoid the contradiction. We term these new walls collectively as Bound State Transformation(BST) walls since the nature of BPS states changes across these walls. These walls are different from marginal stability walls, thus BPS indices are expected to be constant across those walls. To avoid the contradiction the attractor tree must degenerate somehow and there are three basic ways how it can happen: the trunk of the tree can shrink to zero size, the internal edge can shrink to zero size or it can be the terminal edge of the tree. The first case is irrelevant since it would correspond to crossing (A)MS wall for the bound state $\Gamma_1 + \Gamma_2$ and we assumed that our path does not cross them.

When an internal edge shrinks to zero size, the bound state undergoes recombination phenomenon and we call the corresponding wall Recombination wall. Upon crossing this wall different components of multicentered state unbind from each other and become bound to other components. Although the content of the multicentered state does not change the bonds holding this molecular configuration together do change. The canonical recipe of (dis)assembling BPS Hilbert space also changes in accord with the change of attractor flow tree. A typical situation is when e.g. charge Γ_1 is realized as a bound state of two constituents with charges $\Gamma_3 + \Gamma_4$ and we denote this configuration as $((\Gamma_3, \Gamma_4), \Gamma_2)$. As we cross the recombination wall the internal edge of the attractor tree shrinks to zero size producing one 4-valent vertex, instead of two 3-valent ones, and on the other side we end up with two attractor flow trees of the form $((\Gamma_4, \Gamma_2), \Gamma_3)$ and $((\Gamma_2, \Gamma_3), \Gamma_2)$. BPS index should not change as we cross recombination wall and we prove that this is indeed the case.

When a terminal edge shrinks to zero size, the corresponding terminal charge must become massless and the conjugate particles will be created. Suppose that charge Γ_1 becomes massless along some locus in the moduli space. It is known [13] that massless particles in string theory are associated with singularities on the moduli space of Calabi-Yau manifold and the charges of BPS states undergo a typical monodromy of the form $\Gamma_2 \to \Gamma_2^M := \Gamma_2 + I\Gamma_1$ with $I = |\langle \Gamma_1, \Gamma_2 \rangle|$. As we cross the locus where Γ_1 constituent becomes massless a halo of I particles $-\Gamma_1$ is created

from vacuum around Γ_2 center. This halo is in fact a completely filled Fermi sea of fermionic particles Γ_1 and we call such process the Fermi flip. This process does not cost any energy since Γ_1 is massless and because of the monodromy the total charge of the final configuration $\Gamma_2 + I\Gamma_1 + (I-1)(-\Gamma_1)$ is equal to the initial total charge. The wall $AMS(\Gamma_1, \Gamma_2)$ now becomes marginal stability wall $MS(\Gamma_2^M, (I-1)(-\Gamma_1))$ and puzzle is resolved. Fermi flip effectively replaces Γ_1 particles by a certain number of conjugate particles $-\Gamma_1$ and we call the wall where this happens conjugation wall. It is easy to see that BPS index remains constant during this process.

Besides solving the puzzle the requirement that BPS indices are continuous when going from $MS(\Gamma_1, \Gamma_2)$ to $AMS(\Gamma_1, \Gamma_2)$ leads to non-trivial constraints on the spectrum of massless BPS states at the singularity. We find that when there is only one charge becoming massless at the singularity (Γ_1 and/or possibly some rational multiples of it) then BPS indices of such charges determine the monodromy of the local system of charges around the singularity.

The above resolution assumed that massless particles Γ_1 a fermionic. If it happens that massless vector particles are present at the singularity the only way BPS index can stay continuous is the presence in the spectrum of massless particles mutually non-local w.r.t. massless vectors. We predict that the spectrum will necessarily contain massless magnetic monopoles that will form bound states with Γ_1 and Γ_2. The structure of bound states with total charge Γ will become much more complicated compared to purely fermionic case. Particles Γ_1 and Γ_1^D(monopole charge) will form clusters orbiting around central Γ_2. Moving from $MS(\Gamma_1, \Gamma_2)$ to $AMS(\Gamma_1, \Gamma_2)$ we encounter a countable set of BST walls across which some hybrid of both conjugation and recombination porceses will take place and in the end BPS index will stay continuous. We illustrate our conclusions on a number of examples from the literature.

Halo picture of BPS states used in analyzing BPS indices near singularities can be fruitfully applied near a regular point in the moduli space. In chapter 5 we give a very simple physical derivation of the famous Kontsevich-Soibelman wall-crossing formula(KSWCF) [7] based on the halo picture. KSWCF is a generalization of the primitive(and semiprimitive) WCF (1.0.3) of [5] which relates BPS indices of charges of the form $m\Gamma_1 + n\Gamma_2$ on two sides of the marginal stability wall $MS(\Gamma_1, \Gamma_2)$. To formulate the KSWCF we introduce a complex symplectic torus $\tilde{T}_t$, associated to the local system of charges at point t in the moduli space, with coordinate functions X_γ, $\gamma \in \Lambda^{em}$ satisfying

$$X_\gamma X_{\gamma'} = X_{\gamma+\gamma'}. \tag{1.0.6}$$

There is a group of symplectomorphisms acting on this torus of the form

$$U_\gamma^t : X_{\gamma'} \to (1 - \sigma(\gamma) X_\gamma)^{\langle \gamma', \gamma \rangle \Omega(\gamma; t)} X_{\gamma'}, \tag{1.0.7}$$

where $\Omega(\gamma; t)$ is BPS index of charge γ and $\sigma(\gamma)$ is the "quadratic refinement" of the quadratic form $(-1)^{\langle \gamma', \gamma \rangle}$ obeying

$$\sigma(\gamma')\sigma(\gamma) = (-1)^{\langle \gamma', \gamma \rangle} \sigma(\gamma' + \gamma). \tag{1.0.8}$$

Consider a point $t_{ms} \in MS(\Gamma_1, \Gamma_2)$ and in a small neighborhood of this point choose t_+ in the stable side and t_- in the unstable side infinitesimally close to t_{ms}. At each of $t_\pm$ central charges of Γ_1 and Γ_2 do not align as they do at t_{ms}. Because of this there will be some natural ordering of charges of the form $m\Gamma_1 + n\Gamma_2$ according to the phases of their central charges $\alpha_{t_\pm}^{m,n}$ at $t_\pm$. The KSWCF is a relation

$$\prod_{\alpha_{t_+}^{m,n} \nearrow} U_{m\Gamma_1 + n\Gamma_2}^{t_+} = \prod_{\alpha_{t_-}^{m,n} \nearrow} U_{m\Gamma_1 + n\Gamma_2}^{t_-}. \tag{1.0.9}$$

This formula relates the indices $\Omega(m\Gamma_1 + n\Gamma_2; t_\pm)$ to each other and is the most general WCF for BPS indices in $N = 2$ supersymmetric field/string theories. In practice one expands both sides of (1.0.9) in powers of $X_{\Gamma_{1,2}}$ and equates the coefficients in front of different powers on both sides. In this way KSWCF reproduces the primitive and semi-primitive WCFs of [5] and provides a generalization thereof.

The first physical derivation of it in $N = 2$ field theory, based on a thorough analysis of hyper-Kähler metric on the moduli space, was given in [14]. In chapter 5 we give a different derivation of the formula valid in any $N = 2$ supergravity theory, based on the halo picture of BPS states and semiprimitive WCF. Our derivation is very similar in spirit to the derivation of (motivic) WCF in $N = 2$ field theories given in [15]. Inspired by the results from chapter 4 we also give a slight generalization of KSWCF for the cases when singularities are present. In that case the formula becomes a constraint on the massless spectrum of BPS states at the singularity and a relation of this spectrum to the monodromies of the local system of charges.

Chapter 2
Ample D4-D2-D0 decay

In this chapter we study the wall-crossing behavior of the index of BPS states for D4-D2-D0 brane systems on a Calabi-Yau 3-fold at large radius. We find that not only is the "BPS index at large radius" is chamber-dependent, but that the changes in the index can be large in the sense that they dominate single-centered black hole entropy. We discuss implications for the weak coupling OSV conjecture. We also analyze the near horizon limit of multicentered solutions, introduced in [9], for these particular configurations and comment on a general criterion, conjectured in [9], which identifies those multicentered solutions whose near horizon limit corresponds to a geometry with a single asymptotic $AdS_3 \times S^2$ boundary. This chapter is based on [16].

2.1 Review of OSV conjecture

In this section we fill in the details about OSV conjecture mentioned in the Introduction. We start with giving a more precise definition of the BPS index. Let's denote the Hilbert space of BPS states with charge $\Gamma = (p, q) = (p^0, P, Q, q_0)$ by $\mathcal{H}(\Gamma; t_\infty)$. Index of BPS states with this total charge is defined to be the second helicity supertrace

$$\Omega(\Gamma; t_\infty) = -2\mathrm{Tr}_{\mathcal{H}(\Gamma;t_\infty)} J_3^2 (-1)^{2J_3}. \tag{2.1.1}$$

Here J_3 is the third component of spatial angular momentum. Factoring out center-of-mass degrees of freedom, giving a half-hypermultiplet, we can rewrite the index as

$$\Omega(\Gamma; t_\infty) = \mathrm{Tr}_{\mathcal{H}'(\Gamma;t_\infty)} (-1)^{2J_3'}, \tag{2.1.2}$$

where J_3' is the reduced angular momentum. Using these indices it is natural to define a partition function, usually referred to as black hole partition function as

$$Z_{BH}(p, \phi; t_\infty) = \sum_q \Omega(p, q; t_\infty) e^{2\pi\phi^\Lambda} q_\Lambda. \tag{2.1.3}$$

This partition function has a meaning of a mixed ensemble of BPS states with fixed magnetic charges and chemical potential for the electric charges. In principle such partition function should arise naturally from string theory path integral. In practice it can be defined in the large charge limit using Wald's formula for the entropies of black holes, related to the indices via (1.0.1). In cases when black hole configuration admit a dual CFT description, as in the famous MSW theory [17], one can give a definition of black hole partition function valid for all charges, using CFT partition function

$$\mathcal{Z}_{CFT}(\tau = C_0 + i\frac{\beta}{g_{\rm IIA}}, C) = \mathrm{Tr}(-1)^{2J_3'} e^{-\beta H - 2\pi i q_0 C_0 - 2\pi i Q\cdot(C+\frac{P}{2})}. \tag{2.1.4}$$

In practice the dual CFT is obtained from the D-brane configuration, corresponding to black holes of given magnetic charge, and path integral over D-brane world-volume theory reduces to the CFT partition function. Parameters of the world-volume theory such as Ramond-Ramond potentials C_0, C_Λ and the radius of AdS_2 throat[1] are related to the usual modular parameter of CFT as in (2.1.4). Using this partition function the one in (2.1.3) can be defined as

$$\mathcal{Z}_{\rm BH}(p, \phi^0, \phi^\Lambda) = \mathcal{Z}_{\rm CFT}(\beta = 0, C_0 = i\phi^0, C = i\Phi - \frac{P}{2}). \tag{2.1.5}$$

Now we want to define another interesting object that exists on the Calabi-Yau manifolds used in string compactification models: topological partition function. Topological string theory on a Calabi-Yau manifold X is a twisted $(2,2)$ CFT with target space X (see [18] for a review). One defines vacuum amplitudes for embedding genus h string worldsheet into X

$$F_h(t) = \int_{\mathcal{M}_h} \langle \prod_{k=1}^{3h-3} (G_-, \mu_k)\ (G_\pm, \bar{\mu}_k)\rangle, \tag{2.1.6}$$

where $G_\pm$ are worldsheet supersymmetry generators, μ_k are Beltrami differentials and t are Kähler moduli of X. Topological partition function is formed using these amplitudes

$$F_{\rm top}(g_{top}, t) = \sum_{h=0}^{\infty} g_{top}^{2h-2} F_h(t). \tag{2.1.7}$$

This partition function is known to compute F-terms in the low energy effective action and thus is related to black hole entropies computed using Wald's formula. [4] made this precise and conjectured that there is a relation

[1] In IIA string theory black hole geometries for black holes with vanishing D6 charge contain an $AdS_2 \times S^2$ piece.

$$\mathcal{Z}_{\rm BH}(p,\phi^0,\phi^\Lambda;t_\infty)=|\mathcal{Z}_{\rm top}(g_{top},t)|^2,\ \text{where}$$
$$g_{top}=\frac{-4i\pi}{p^0+i\frac{\phi^0}{\pi}}\quad t^a=\frac{P^a+i\frac{\phi^a}{\pi}}{p^0+i\frac{\phi^0}{\pi}}. \tag{2.1.8}$$

This relation was derived for large charges, when BPS indices are saturated by black hole entropy as in (1.0.1), and in the weak topological coupling g_{top} limit. A major problem with this formula as originally formulated, is the dependence of black hole partition function on the background moduli t_∞ and independence from it of the topological partition function. A constructive proof of this relation was given in [5] where it was found that t_∞ has to be taken to infinity in the Kähler cone of Calabi-Yau X, i.e. BPS indices entering black hole partition function have to be evaluated around the large volume point of the Calabi-Yau.

2.2 Some general remarks on BPS indices at large radius

In this section we focus on the type IIA string theory compactified on a Calabi-Yau manifold X and study the indices of BPS states in the large volume limit. To define it we choose some vector $B+iJ$ in the complexified Kähler cone and consider the limit

$$\lim_{\Lambda\to\infty}\Omega(\Gamma;\Lambda(B+iJ)) \tag{2.2.9}$$

Charge Γ here is an element of symplectic lattice with components $\Gamma=(p^0,P,Q,q_0)$. We expect - on physical grounds - that this limit exists: In the large radius limit the physics is described by some D-brane gauge theory, and there should be a well-defined and finite-dimensional space of BPS states $\mathcal{H}(\Gamma;t)$. Somewhat surprisingly, it was pointed out in [8] that the limit (2.2.9) depends on the direction $B+iJ$ chosen in the Kähler cone, even for the D4-D2-D0 system studied in [17], and hence the "large-radius limit" of the index of BPS states is not well-defined without specifying more data. This fact has recently played an important role in [9]. Our point in this chapter is that in fact the dependence of the index on the direction $B+iJ$ can be large and this has significant implications, as explained in more detail below. In [5] it was pointed out that for D6-D4-D2-D0 systems there is nontrivial wall-crossing at infinite radius. In [8, 9] it was shown that even for the D4-D2-D0 system with ample $D4$ charge P, there are walls of marginal stability going to infinity. (Such examples are only possible when the dimension of the Kähler cone is greater than one [5].) One should therefore ask how large the discontinuities in Ω can be across walls at infinity. We show that they can be large in the following sense: If we consider charges Γ which support regular attractor points (hence the single-centered attractor

solutions of [19, 20]) then it is not consistent with wall-crossing to assume that the contribution of such states dominate the large radius limit of the index $\Omega(\Gamma)$. We show this by exhibiting an explicit example in Section 2.4.

Our example consists of a charge which supports a regular attractor point (hence a single-centered black hole), but which also supports a 3-centered solution. The three-centered solution decays across a wall in the Kähler cone which extends to arbitrarily large radius. The contribution of the single centered solution of charge Γ is predicted from supergravity to be

$$\log|\Omega| \sim S_{BH}(\Gamma) := 2\pi\sqrt{-\frac{\hat{q}_0}{6}P^3} \tag{2.2.10}$$

In our example Γ will support a boundstate of charge $\Gamma_1 + \Gamma_2$ where $\Omega(\Gamma_1)$ has bounded entropy and Γ_2 itself supports a regular attractor point, but $S_{BH}(\Gamma_2) > S_{BH}(\Gamma)$. Thus the discontinuities in the index are competitive with the single-centered entropy.

This effect of entropy dominance of multi centered configurations over single-centered ones is reminiscent of the "entropy enigma" configurations of [5, 21]. In that case, if we first take large J_∞ then under charge rescaling $\Gamma \to \Lambda\Gamma$ single centered entropy scales as $S_{BH} \sim \Lambda^2$ while the two-centered solutions contribute to entropy as $S_{2c} \sim \Lambda^3$. On the other hand, if one holds the moduli at infinity, J_∞, fixed and scales Γ, then the configuration will eventually become unstable and leave the spectrum. Here we again first take large J_∞ and find that under rescaling D4 charge $P \to \Lambda P$ (holding the remaining components of Γ fixed) the single centered entropy scales as $S_{BH} \sim c_{BH}\Lambda^{3/2}$ while the three-centered entropy scales as $S_{3c} \sim c_{3c}\Lambda^{3/2}$, with $c_{3c} > c_{BH}$. Thus here the entropy dominance of multicentered configuration over the singlecentered arises from the prefactor and not from the scaling exponent. In contrast to the entropy enigma configuration, if we fix moduli at infinity J_∞ and then scale P, the configuration does not leave the spectrum, as shown at the end of section 3 below.

Like the "entropy enigma" configurations, the boundstates considered here threaten to invalidate the weak-coupling version of the OSV conjecture [4] (or its refined version [5]). However, as discussed at length in [5], (see especially section 7.4.2), since Ω is an index there are potential cancellations between these configurations leading to the desired scaling $\log\Omega \sim \Lambda^2$ for uniformly scaled charges. Our main point here is that *even if we assume* that there are such miraculous cancellations the index will nevertheless have large discontinuities across the MS walls, even at large radius, and hence the weak coupling OSV conjecture is at best valid in special chambers of the Kähler cone. It is notable that the phenomenon we discuss cannot happen when the Kähler cone is one-dimensional. Moreover, our example only exists in the regime of weak topological string coupling, where $|\hat{q}_0|$ is not much larger than P^3. This regime

is already known to be problematical for the OSV conjecture [5].

Of course, given a charge $\Gamma = P + Q + q_0 dV$, with P in the Kähler cone, there is a natural direction singled out, namely the P direction. It is therefore natural to suppose that the refined OSV formula of [5] should apply to

$$\lim_{\Lambda\to\infty} \Omega(\Gamma; \Lambda z P) \tag{2.2.11}$$

where $z = x + iy$ is a complex number, and indeed, several of the arguments in [5] assumed (for simplicity) that J and P are proportional.

A second, related, implication of our example concerns the modularity of generating functions for BPS indices. In [5] a microscopic formulation of the "large radius" BPS indices was investigated by characterizing the BPS states as coherent sheaves supported on cycles in the linear system $|P|$. Put differently, a D4 brane wraps a cycle $\Sigma \in |P|$. There is a prescribed flux $F \in H^2(\Sigma; \mathbb{Z})$ and the system is bound to N anti-D0 branes. If we set $d(F, N) = (-1)^{\dim \mathcal{M}} \chi(\mathcal{M})$ where $\mathcal{M}$ is the moduli space of supersymmetric configurations of this type then, it was claimed, the large radius BPS indices are finite sums of the $d(F, N)$. On the other hand, duality symmetries of string theory imply that a certain generating function of the indices $d(F, N)$, denoted Z_{D4D2D0}, exhibits good modular behavior. It follows from the chamber dependence of the large radius limit of Ω that there must be chamber dependence of the $d(F, N)$. The chamber dependence of $d(F, N)$ raises the question of compatibility with the modularity of the partition function Z_{D4D2D0}. This partition function is also closely related to the $(0, 4)$ elliptic genus of the MSW string [22, 23], and hence similar remarks might apply to that elliptic genus. The statement of modularity of these partition functions follows from very basic duality symmetries in string theory and conformal field theory which, one might guess, should be valid in every chamber of the Kähler cone. One might therefore expect that the *change* in the partition function must also be modular. It might be easier to verify this than it is to verify the modularity of the full partition function. One might approach this using the results of [24]: One must compute the change of the polar polynomial across a chamber and show that the associated cusp form vanishes. This appears to be a challenging computation, but one well worth doing if possible.

2.3 Walls at large radius

In this section we analyze and enumerate marginal stability walls that exist around the large radius point. Let us consider a D4-D2-D0 charge $\Gamma = P + Q + q_0 dV$ splitting into a pair of

charges $\Gamma = \Gamma_1 + \Gamma_2$ with

$$\Gamma_i = r_i + P_i + Q_i + q_{0,i} dV \tag{2.3.12}$$

Then $r_1 = -r_2 = r$ and $I_{12} = \langle \Gamma_1, \Gamma_2 \rangle = P_1 \cdot Q_2 - P_2 \cdot Q_1 - r q_0$. The Denef stability condition [11] is governed by the sign of I_{12} times the sign of

$$\mathcal{Z}_{12} := \mathrm{Im} Z_{1,hol} Z^*_{2,hol}. \tag{2.3.13}$$

We are interested in the existence of walls at infinity. Let us consider walls which asymptotically contain lines in the Kähler moduli space. Thus, we set $t \to \Lambda t$ and take $\Lambda \to \infty$. If the leading term in $\mathcal{Z}_{12}$ at large Λ can change sign as the "direction" t is changed, then there will be asymptotic walls at infinity.

If r is nonzero then any wall that persists at infinity is necessarily an anti-MS wall, where the phases of $Z(\Gamma_1; t)$ and $Z(\Gamma_2; t)$ *anti*-align. There is no wall-crossing associated with such walls and thus we set $r = 0$.

When $r = 0$ (2.3.13) simplifies to

$$\begin{aligned} \mathcal{Z}_{12} = & \frac{1}{4} \mathrm{Im} P_1 \cdot t^2 P_2 \cdot \bar{t}^2 \\ & - \frac{1}{2} \mathrm{Im} \left(P_1 \cdot t^2 Q_2 \cdot \bar{t} + P_2 \cdot \bar{t}^2 Q_1 \cdot t \right) \\ & + \mathrm{Im} \left(Q_1 \cdot t Q_2 \cdot \bar{t} + \frac{1}{2} q_{0,1} P_2 \cdot \bar{t}^2 + \frac{1}{2} q_{0,2} P_1 \cdot t^2 \right) \\ & - \mathrm{Im} \left(q_{0,1} Q_2 \cdot \bar{t} + q_{0,2} Q_1 \cdot t \right) \end{aligned} \tag{2.3.14}$$

For the generic direction t the leading behavior for $\Lambda \to \infty$ will be governed by the sign of

$$\mathrm{Im} P_1 \cdot t^2 P_2 \cdot \bar{t}^2 = (P_1 \cdot B \cdot J) P_2 \cdot B^2 - (P_2 \cdot B \cdot J) P_1 \cdot B^2 - (P_2 \cdot J^2 P_1 \cdot B \cdot J - P_1 \cdot J^2 P_2 \cdot B \cdot J) \tag{2.3.15}$$

This vanishes in the one-modulus case, but is generically nonzero in the higher dimensional cases. Moreover, it is odd in B. Therefore, just by changing the sign of B we change from a region of Denef stability to instability, and hence there are definitely walls at infinity.

As an example we analyze (2.3.15) for two particular examples of Calabi-Yau manifolds with a 2-parameter moduli space. The first case is the elliptic fibration $\pi : X \to P^2$. A basis of divisors is $D_1 = \alpha_f, D_2 = h$ with intersection products given by $\alpha_f^3 = 9$, $\alpha_f^2 h = 3$, $\alpha_f h^2 = 1$ and $h^3 = 0$. The second example is a blow-up of a hypersurface in $\mathbb{P}^{(1,1,2,2,2)}[8]$ [25]. A basis of divisors is H and L with intersection products given by $H^3 = 8$, $H^2 L = 4$, $H L^2 = 0$, $L^3 = 0$. It turns out that in the elliptic fibration case (2.3.15) takes the form (here, superscripts denote components w.r.t. the basis D_1, D_2 above):

$$16((B^1)^2 + (J^1)^2)(P_1^2 P_2^1 - P_1^1 P_2^2)(B^2 J^1 - B^1 J^2) \tag{2.3.16}$$

and thus vanishes whenever P_1 becomes parallel to P_2 or B becomes parallel to J. Assuming P_1 not parallel to P_2 there is exactly one wall, going to infinity with $B \propto J$. In the case of $\mathbb{P}^{(1,1,2,2,2)}[8]$ (2.3.15) looks like:

$$(3B_1B_2 + B_2^2 + 3J_1J_2 + J_2^2)(P_1^{(2)}P_2^{(1)} - P_1^{(1)}P_2^{(2)})(B_2J_1 - B_1J_2) \tag{2.3.17}$$

Here in addition to $B \propto J$ wall there is another wall for $3B_1B_2 + B_2^2 + 3J_1J_2 + J_2^2 = 0$, provided that $9B_1^2 - 12J_1J_2 - 4J_2^2 > 0$. It is easy to see that on the $B \propto J$ wall the phases of the central charges align and hence, this is an MS and not an anti-MS wall. For simplicity we will choose $B = 0$ in which case the stability condition at large Λ is governed by the sign of

$$(P_2 \cdot J^2 Q_1 \cdot J - P_1 \cdot J^2 Q_2 \cdot J) \tag{2.3.18}$$

Again, in the one-modulus case this expression has a definite sign in accord with the analysis in [5], however, in the higher dimensional case it is perfectly possible for this quantity to change sign as J changes direction in the Kähler cone.

2.4 An example

We now give an explicit example of a split of a D4D2D0 charge, which supports a single centered black hole, but which admits marginal stability walls at infinity describing a splitting into a pair of D4D2D0 systems in which the change in index $\Delta\Omega$ is larger than the single-centered entropy.

In order to have a single-centered solution we must assume P is in the Kähler cone and the discriminant is positive. Therefore,

$$\hat{q}_0 < 0 \qquad \hat{q}_0 := q_0 - \frac{1}{2}Q^2|_P \tag{2.4.19}$$

where we recall that $Q^2|_P := (D_{ABC}P^C)^{-1}Q_AQ_B$.

In some chambers this charge can also support a multicentered solution where the first split in the attractor flow tree is given by

$$\begin{aligned} \Gamma &\to \Gamma_1 + \Gamma_2 \\ \Gamma_1 &= P_1 + \frac{\chi(P_1)}{24}dV \\ \Gamma_2 &= P_2 + Q + q_{0,2}dV \end{aligned} \tag{2.4.20}$$

Here, Γ_1 is a pure D4-brane and Γ_2 is a $D4$-brane charge supporting a single-centered black hole: We will consider only charge configurations so that $\hat{q}_{0,2} < 0$, and hence Γ_2 has a regular attractor point.

Using the summary of split attractor flows in the appendix A, we see that a necessary condition for the existence of the split realization is that the flow crosses $MS(\Gamma_1, \Gamma_2)$ at a positive value of the flow parameter s. Using notations from Appendix A the flow parameter is given by:

$$s^{12}_{ms} = 2\frac{-(Q\cdot J - P\cdot B\cdot J)\,(\frac{1}{2}P_1\cdot(J^2-B^2)+\frac{\chi(P_1)}{24}) - (\frac{1}{2}P\cdot(J^2-B^2)+Q\cdot B - q_0)\,P_1\cdot B\cdot J}{\sqrt{\frac{4}{3}J^3}|\frac{1}{2}P\cdot(J^2-B^2)+Q\cdot B - q_0 + iQ\cdot J - iP\cdot B\cdot J|\;P_1\cdot Q}|_\infty \tag{2.4.21}$$

Here $|_\infty$ means that complexified Kähler moduli $t = B+iJ$ are evaluated at spatial infinity. The vanishing locus of s_{ms} is the wall of marginal stability. This is a rather complicated expression, but it simplifies if the starting point is chosen to have zero B-field. In that case the parameter along the flow s^{12}_{ms}, for which the wall is crossed is

$$s^{12}_{ms} = 2\frac{-Q\cdot J\,(\frac{1}{2}P_1\cdot J^2+\frac{\chi(P_1)}{24})}{\sqrt{\frac{4}{3}J^3}|\frac{1}{2}P\cdot J^2 - iQ\cdot J - q_0|\;P_1\cdot Q}|_\infty \tag{2.4.22}$$

which further simplifies in the large J limit to

$$s^{12}_{ms} = -2\frac{Q\cdot J\;P_1\cdot J^2}{\sqrt{\frac{4}{3}J^3}P\cdot J^2\;P_1\cdot Q}|_\infty \tag{2.4.23}$$

The condition $s^{12}_{ms} > 0$ (which is equivalent to the Denef stability condition) imposes a restriction on Q, because we must have $(QJ_\infty)(P_1Q) < 0$ while both P_1 and J_∞ are in Kähler cone. There are plenty of charges that satisfy this condition and we'll give a numerical example below.

We are not quite done constructing the split attractor flow tree because Γ_1 is a polar charge, and must itself be realized as a multicentered solution. As discussed in appendix A, for an attractor tree to exist all its edges must exist and moreover all its terminal charges must support BPS states. The charge Γ_2 supports a regular black hole. Meanwhile, Γ_1 is realized as a flow, splitting into $D6$ and $\overline{D6}$ as in [5]:

$$\begin{aligned}\Gamma_1 &\to \Gamma_3 + \Gamma_4\\ \Gamma_3 &= e^{P_1/2}\\ \Gamma_4 &= -e^{-P_1/2}\end{aligned} \tag{2.4.24}$$

So for the whole tree to exist we need

- $s^{12}_{ms} > 0$ for the split $\Gamma \to \Gamma_1 + \Gamma_2$ to exist
- $s^{34}_{ms} > 0$ for the split $\Gamma_1 \to \Gamma_3 + \Gamma_4$ to exist
- $s^{34}_0 > s^{34}_{ms}$ where s^{34}_0 is the value when the flow reaches zero of the charge $Z(\Gamma_1)$

These conditions are sufficient because the charges Γ_3 and Γ_4 exist everywhere in moduli space and Γ and Γ_2 support black holes. It is also easy to see that both walls are MS and not anti-MS walls. It turns out that above conditions are always satisfied if

- J_∞ is on stable side of the wall, corresponding to $s^{12}_{ms} > 0$
- $P_1 \ll J_\infty$ component-wise in a basis of Kähler cone

To see this we estimate s^{34}_{ms} and s^{34}_0 in the large J_∞ limit. Recall from appendix A that

$$s^{34}_{ms} = \frac{\langle \Gamma_3, \Delta H\rangle - \langle \Gamma_3, \Gamma\rangle s^{12}_{ms}}{\langle \Gamma_3, \Gamma_4\rangle}. \tag{2.4.25}$$

Now plugging the expression for ΔH from (1.0.6) we can estimate $\langle \Gamma_3, \Delta H\rangle \sim \frac{J^3_\infty}{3\sqrt{4/3 J^3_\infty}}$. Using $\langle \Gamma_3, \Gamma_4\rangle = -\frac{P_1^3}{6}$ and the fact that $s^{12}_{ms} \sim O(\frac{1}{J^{1/2}})$ is small we get

$$s^{34}_{ms} \sim \frac{2J^3_\infty}{\sqrt{4/3 J^3_\infty} P_1^3}. \tag{2.4.26}$$

To find s^{34}_0 we equate the central charge to zero $Z(\Gamma_1; t) = 0$ to get the vanishing locus:

$$-\frac{\chi(P_1)}{24} - \frac{1}{2} P_1 \cdot B^2 + \frac{1}{2} P_1 \cdot J^2 = 0, \qquad P_1 \cdot B \cdot J = 0. \tag{2.4.27}$$

Moduli along the flow of charge Γ_1 are determined again by (1.0.6) with $\Gamma(s) = s\Gamma_1 + s^{12}_{ms}\Gamma - \Delta H$. Recalling that $s^{12}_{ms} \sim O(\frac{1}{J^{1/2}})$ this can be written as

$$\Gamma(s) = \left(O(\frac{1}{J^{5/2}_\infty}), sP_1 + O(\frac{1}{J^{1/2}_\infty}), O(\frac{1}{J^{1/2}_\infty}), s\frac{\chi(P_1)}{24} - \frac{J^3_\infty}{2\sqrt{\frac{4}{3} J^3_\infty}} \right). \tag{2.4.28}$$

Plugging this $\Gamma(s)$ into (1.0.6) and taking into account that $s_0^{34} \sim O(J^{3/2})$, as we will see below, we find that

$$J(s_0^{34})^a \sim P_1^a \sqrt{\frac{-6}{P_1^3}\left(\frac{\chi(P_1)}{24} - \frac{J_\infty^3}{2s_0^{34}\sqrt{\frac{4}{3}J_\infty^3)}}\right)}, \tag{2.4.29}$$

and $B^a(s_0^{34})$ is small. Now we can solve (2.4.27) for s_0^{34} to find:

$$s_0^{34} \sim \frac{6J_\infty^3}{\sqrt{4/3J_\infty^3}(P_1)^3}. \tag{2.4.30}$$

Thus we see from (2.4.26) and (2.4.30) that the existence conditions are indeed satisfied: $s_0^{34} > s_{ms}^{34}$.

We conclude with a numerical example, checking explicitly that such split solutions exist. We consider again the elliptic fibration example and $\mathbb{P}^{(1,1,2,2,2)}[8]$ of [25]. The initial charge is of the form $\Gamma = P + Q + q_0 dV$, where $P = (50, 50)$, $Q = (-1, 3)$, $q_0 = -10$. The starting point of the flow is $J_\infty = (500, 100)$, which indeed lies on stable side of MS wall in (2.4.22). The pure $D4$ has charge $P_1 = (1, 2)$. All the existence conditions are found to be satisfied for both Calabi-Yau manifolds. As we'll discuss in the next section, the entropy of this three-centered configuration is expected to be larger than the one from the single-centered realization of the same total charge. The numerical examples confirm this claim in both cases.

Now we will justify the remark made in the Section 2.2 about the existence of the 3-centered configuration for $P \to \infty$. We take $B_\infty = 0$ and evaluate (2.4.21). Evaluating (2.4.22) in the limit $P \to \infty$ and with fixed J_∞ produces an expression almost identical to (2.4.23). In particular, it remains positive, but does go to zero. The second split $\Gamma_1 \to \Gamma_3 + \Gamma_4$ will therefore happen very close to starting point in moduli space and hence $J_\infty \gg P_1$ will guarantee that the second split exists. This proves that our example exists in the $P \to \infty$ limit if it existed in $J_\infty \to \infty$ limit.

2.5 Comparison of the entropies

Now let us compare the discontinuity $\Delta\Omega$ of the BPS index with the contribution of the single-centered (black hole) solutions to the "large radius" index $\Omega(\Gamma; J_\infty)$. We first *assume* that the dominant contribution to the large radius entropy is that of the single-centered solutions, if they exist. We will then show that this assumption is inconsistent with the wall-crossing phenomena. The black hole contribution to Ω can be approximated using the equation from the attractor mechanism

$$\Omega_{BH}(\Gamma) := \exp S_{BH}(\Gamma) = \exp\left[2\pi\sqrt{-\hat{q}_0 P^3/6}\right]. \tag{2.5.31}$$

The discontinuity of the index across the wall $\Gamma \to \Gamma_1 + \Gamma_2$ is given by

$$\Delta_{12}\Omega(\Gamma; t_{ms}) = (-1)^{\langle\Gamma_1,\Gamma_2\rangle-1}|\langle\Gamma_1,\Gamma_2\rangle|\,\Omega(\Gamma_1; t^{12}_{ms})\,\Omega(\Gamma_2; t^{12}_{ms}). \tag{2.5.32}$$

Here the indices of Γ_1 and Γ_2 are evaluated on the MS wall. As we have said, the state with charge Γ_1 is realized as a split attractor flow splitting into pure $D6$ and $\overline{D6}$ with fluxes. The index of Γ_1 is polynomial in charges and is given by $\Omega(\Gamma_1) = (-1)^{I(P_1)-1} I(P_1)$ where $I(P) := \frac{P^3}{6} + \frac{c_2(X)\cdot P}{12}$. Again using our assumption we would estimate that the index of Γ_2 can again be approximated by the black hole contribution:

$$\Omega(\Gamma_2, J_\infty) \sim \Omega_{BH}(\Gamma_2) = \exp\left[2\pi\sqrt{-\hat{q}_{0,2}P_2^3/6}\right] \tag{2.5.33}$$

since Γ_2 supports a single-centered black hole.

We now consider a limit of large charges. We hold P_1 fixed and take $P \to \infty$ along some direction in the Kähler cone. Then from Eqs.(2.5.31), (2.5.33) the indices of Γ and Γ_2 will be exponentially large for large P while $\Omega(\Gamma_1)$ is a known, bounded function of P_1. This means that to compare the contributions (2.5.31) and (2.5.32) we need to compare the exponents:

$$-\hat{q}_0 P^3 \quad \text{vs} \quad -\hat{q}_{0,2}P_2^3. \tag{2.5.34}$$

In this limit we can write

$$P_2^3 = P^3 - 3P^2\cdot P_1 + ... = P^3\left(1 - \frac{3P^2\cdot P_1}{P^3} + \mathcal{O}(1/|P|^2)\right). \tag{2.5.35}$$

Moreover, since q_0 is conserved at the vertex

$$\hat{q}_{0,2} = \hat{q}_0 + \frac{1}{2}Q^2|_P - \frac{\chi(P_1)}{24} - \frac{1}{2}Q^2|_{P_2}. \tag{2.5.36}$$

In taking our charge limit we can make $q_{0,2}$ sufficiently negative that $\hat{q}_{0,2}$ and $\hat{q}_0$ are both negative. Now we can write

$$-\hat{q}_{0,2}P_2^3 = -\hat{q}_0 P^3\left(1 - \frac{\chi(P_1)}{24\hat{q}_0} - \frac{1}{2\hat{q}_0}(Q^2|_{P_2} - Q^2|_P) - \frac{3P^2\cdot P_1}{P^3} + \mathcal{O}(1/|P|^2)\right). \tag{2.5.37}$$

Since $\hat{q}_0$ is negative we see from (2.5.37) that the contribution of the $\Gamma \to \Gamma_1+\Gamma_2 \to (\Gamma_3+\Gamma_4)+\Gamma_2$ split attractor flow will be greater in the $P \to \infty$ limit provided that

$$\frac{\chi(P_1)}{24|\hat{q}_0|} + \frac{1}{2|\hat{q}_0|}(Q^2|_{P_2} - Q^2|_P) - \frac{3P^2\cdot P_1}{P^3} > 0. \tag{2.5.38}$$

The first term of (2.5.38) is always positive, while the second term can have both signs. The third term is always negative. However, for parametrically large P and fixed Q the second and third terms are suppressed, so the expression is positive. Thus we find that in the limit described above, the split flow configuration has *greater* entropy than the black hole contribution:

$$\Omega_{BH}(\Gamma) \ll \Delta_{12}\Omega(\Gamma; t_{ms}). \tag{2.5.39}$$

So not only does the value of the index Ω depend on the direction in which J is taken to infinity, but this dependence can be very strong, and even dominate single-centered black hole entropy.

One might worry that there are other split flow realizations of the charge Γ, with the same wall of marginal stability as the one we are studying, which produce a cancellation in $\Delta\Omega$. For example, the charge Γ_2 might well support multi-centered solutions. However, by our hypothesis, the single-centered entropy dominates the multi-centered ones, so such a cancellation cannot occur. Then (2.5.39) leads to a contradiction and hence we conclude that it cannot be that single-centered entropy dominates the entropy at infinity in all chambers.

Remarks

1. In the context of topological string theory the topological string coupling is $g_{top} \sim \sqrt{-\hat{q}_0/P^3}$ [4]. The effect we are discussing does not appear in the strong coupling regime, in harmony with the arguments in [5]. However, it does appear in the problematic weak coupling regime.

2. Interestingly, this phenomenon will not occur with splits into two single-centered attractors. If $q_{0,i} < 0$ for both $i = 1, 2$ and P_1, P_2 are in the Kähler cone then (taking $Q_i = 0$ for simplicity) one can show that

$$S_{BH}(\Gamma) > S_{BH}(\Gamma_1) + S_{BH}(\Gamma_2) \tag{2.5.40}$$

   as expected. We do not know of a proof of the analogous statement for $Q_i \neq 0$.

3. In principle the example we have given can be extended by replacing Γ_1 by an arbitrary extreme polar state in the sense of [5]. Following [5], the charges $\Gamma_1 \to \Gamma_3 + \Gamma_4$ can be parametrized as

$$\Gamma_3 = re^{S_1}(1-\beta_1+n_1 w)$$
$$\Gamma_4 = -re^{S_2}(1-\beta_2+n_2 w)$$
$$\Gamma_1 = r\left(0, \hat{P}, \frac{\hat{P}S}{2}+\Delta\beta, \frac{\hat{P}^3}{24}+\frac{\hat{P}S^2}{8}-\frac{\hat{P}\beta}{2}+\frac{S\Delta\beta}{2}-\Delta n w\right) \qquad (2.5.41)$$

where $\hat{P} = S_1 - S_2$, $S = S_1 + S_2$, $\beta = \beta_1 + \beta_2$, $\Delta\beta = \beta_2 - \beta_1$, $\Delta n = n_2 - n_1$. For sufficiently small β_i and n_i and $S_1 \equiv P_1/2$, $S_2 \equiv -P_1/2$, the charge Γ_1 is very close to a pure $D4$-brane and all existence conditions are still satisfied. The 3-centered entropy dominance also continues to hold.

2.6 M-theory lift and its near-horizon limit

In this section we check what happens to our boundstate configurations in the near horizon scaling limit recently introduced in [9]. This is important since our observations regarding the entropy have the potential to lead to a troublesome contradiction with the AdS/CFT conjecture. If our configurations corresponded to states in the Cardy region of the holographic dual to an asymptotically $AdS_3 \times S^2$ geometry then there would be such a contradiction. Fortunately, our example turns out to be quite similar to that discussed in [9]: The first split $D4 \to D4 + D4$ corresponds to two infinitely separated $(AdS_3 \times S^2)$-like geometries, so there is no contradiction. These curious limiting geometries, and especially their holographic dual interpretation, deserve to be understood much better. Indeed, the existence of these $D4 \to D4 + D4$ decays suggests that in general one *cannot* identify the partition function Z_{D4D2D0} of [5] with the M5 elliptic genus of [22, 23]! They might nevertheless agree in certain chambers of the Kähler cone (e.g. at the "AdS point" described in [9]). Clearly, this issue deserves to be understood better.

The solution to the attractor equations in the effective 4d $\mathcal{N} = 2$ SUGRA for a general multicentered configuration can be written (in the regime of large Kähler classes) in terms of harmonic functions ([9], eq. (2.8)):

$$\begin{aligned} ds_{4d}^2 &= -\frac{1}{\Sigma}(dx_0 + \sqrt{G_4}\,\omega)^2 + \Sigma\,(d\vec{x})^2\,, \\ \mathcal{A}^0 &= \frac{\partial \log\Sigma}{\partial H_0}\left(\frac{dx_0}{\sqrt{G_4}} + \omega\right) + \omega_0\,, \\ \mathcal{A}^A &= \frac{\partial \log\Sigma}{\partial H_A}\left(\frac{dx_0}{\sqrt{G_4}} + \omega\right) + \mathcal{A}_d^A\,, \\ t^A &= \frac{H^A}{H^0} + \frac{y^A}{Q^{\frac{3}{2}}}\left(i\Sigma - \frac{L}{H^0}\right), \end{aligned} \qquad (2.6.42)$$

where

$$\begin{aligned}
\star\, d\omega &= \frac{1}{\sqrt{G_4}}\langle dH, H\rangle\,, \quad d\omega_0 = \frac{1}{\sqrt{G_4}}\star dH^0 \\
d\mathcal{A}^A_d &= \frac{1}{\sqrt{G_4}}\star dH^A\,, \quad \Sigma = \sqrt{\frac{Q^3 - L^2}{(H^0)^2}} \\
L &= H_0(H^0)^2 + \frac{1}{3}D_{ABC}H^AH^BH^C - H^AH_AH^0\,, \\
Q^3 &= (\frac{1}{3}D_{ABC}y^Ay^By^C)^2\,, \quad D_{ABC}y^Ay^B = -2H_CH^0 + D_{ABC}H^AH^B \\
H &\equiv (H^0, H^A, H_A, H_0) := \sum_a \frac{\Gamma_a\sqrt{G_4}}{|\vec{x} - \vec{x}_a|} - 2\mathrm{Im}\ (e^{-i\alpha}\Omega)|_{\vec{x}=\infty}\,,
\end{aligned} \tag{2.6.43}$$

$A = 1, \ldots, h^{1,1}(X)$ are components relative to a basis D_A for $H^2(X, \mathbb{Z})$, $\star$ is the Hodge star with respect to the Euclidean metric $d\vec{x}^2$ on $\mathbb{R}^3$, and we choose a solution y^A of the quadratic equations such that y^AD_A is in the Kähler cone. The Calabi-Yau volume in string units is given by

$$\tilde{V}_{IIA} = \frac{D_{ABC}}{6}J^AJ^BJ^C = \frac{1}{2}\frac{\Sigma^3}{Q^3} \tag{2.6.44}$$

and G_4 is the 4-dimensional Plank constant, determined in terms of the string length l_s and string coupling g_s by

$$G_4 = \frac{l_s^2g_s^2}{32\pi^2\tilde{V}_{IIA,\infty}}. \tag{2.6.45}$$

The above equations assume $H^0(\vec{x})$ is nonzero, but they have a smooth limit as $H^0 \to 0$. (See [26] eq. (9.21) for the relevant expansions.)

This solution of 4d supergravity can be lifted to 5d supergravity. To do this we use the standard relation between M-theory and IIA geometries

$$\begin{aligned}
ds^2_{5d} &= \frac{R^2}{4}e^{\frac{4}{3}\phi}\left(d\psi + \mathcal{A}^0\right)^2 + e^{-\frac{2}{3}\phi}\,ds^2_{4d}\,, \\
Y^A &= \tilde{V}_{IIA}^{-1/3}\,J^A\,, \quad A^A_{5d} = \mathcal{A}^A + B^A\left(d\psi + \mathcal{A}^0\right)\,.
\end{aligned} \tag{2.6.46}$$

Here R is the M-theory circle radius, $\psi \sim \psi + 4\pi$, Y^A are 5d SUGRA moduli, and $\phi(\vec{x})$ is the 10d dilaton field, normalized as $\phi(\infty) = 0$. Note that the Calabi-Yau volume in 11d Planck units is

$$\tilde{V}_M = e^{-2\phi}\frac{\tilde{V}_{IIA}}{g_s^2}. \tag{2.6.47}$$

The near horizon limit of the M-theory solution, introduced in [9], may be described as follows. Beginning with a solution (2.6.42) we introduce a family of BPS solutions of the 4d supergravity equations, parametrized by $\lambda \in [1, \infty)$. The expressions that get modified under

this deformation are given by

$$\begin{aligned} ds^2_{4d\,,\lambda} &= -\frac{1}{\Sigma^\lambda}(dx_0+\lambda^{-3/2}\sqrt{G_4}\,\omega^\lambda)^2+\lambda^{-6}\Sigma^\lambda\,(d\vec{x})^2\,, \\ \mathcal{A}^0_\lambda &= \frac{\partial\log\Sigma^\lambda}{\partial H^\lambda_0}\left(\lambda^{3/2}\frac{dx_0}{\sqrt{G_4}}+\omega^\lambda\right)+\omega^\lambda_0\,, \\ \star d\omega^\lambda &= \frac{\lambda^{-3/2}}{\sqrt{G_4}}\langle dH^\lambda, H^\lambda\rangle\,, \quad d\omega^\lambda_0=\frac{\lambda^{-3/2}}{\sqrt{G_4}}\star dH^0_\lambda \\ H^\lambda &:= \lambda^{3/2}\sum_a\frac{\Gamma_a\sqrt{G_4}}{|\vec{x}-\vec{x}^\lambda_a|}-2\mathrm{Im}(e^{-i\alpha}\Omega)|_{B_\infty+i\lambda J_\infty} \end{aligned} \tag{2.6.48}$$

Here, $\Omega=-\frac{1}{\sqrt{4/3J^3}}e^{B+iJ}$ and for brevity we omit the corresponding formulae for $\mathcal{A}^A_\lambda$ and $\mathcal{A}^A_{d\,,\lambda}$. The vectors $\vec{x}^\lambda_a$ used to define H^λ can be taken to be any solution of the integrability constraints

$$\sum_{b\neq a}\frac{\langle\Gamma_a,\Gamma_b\rangle}{x^\lambda_{ab}}=-\lambda^{-3}\sqrt{\frac{3}{G_4J^3_\infty}}\mathrm{Im}\,\left(e^{-i\alpha_{\infty,\lambda}}\int\Gamma_b e^{-(B_\infty+i\lambda J_\infty)}\right)\qquad\forall b. \tag{2.6.49}$$

where $x^\lambda_{ab}:=|\vec{x}^\lambda_a-\vec{x}^\lambda_b|$ and $e^{i\alpha_{\infty,\lambda}}$ is the phase of the total central charge at $B_\infty+i\lambda J_\infty$. We choose $\vec{x}^\lambda_a$ to coincide with our original solution at $\lambda=1$, and let them depend continuously on λ. Clearly there is some degree of arbitrariness at this stage. [2]

The above family of solutions can be obtained from original ones by scaling (2.6.43)

$$\begin{aligned} &\vec{x}\to\lambda^{-3}\vec{x} \\ &l_s\to\lambda^{-3/2}l_s \\ &g_s^2\to\lambda^3 g_s^2 \\ &G_4\to\lambda^{-3}G_4 \\ &J_\infty\to\lambda J_\infty \\ &B_\infty\to B_\infty \end{aligned} \tag{2.6.50}$$

but we prefer to keep $\vec{x}, l_s, G_4$ fixed and change the solution according to (2.6.48). The constant G_4, and the coordinate system, in these equations is λ-independent.

Now consider the corresponding λ-deformed 5d geometries. Since the moduli $t^A(\vec{x};\lambda)$ determined by (2.6.42) scale as λ^0 for $\lambda\to\infty$ (at least when $H^0(\vec{x})\neq 0$) it is clear that if the $\vec{x}^\lambda_a$ have a well-defined limit then there are well-defined limiting moduli $\tau^A(\vec{x}):=\lim_{\lambda\to\infty}t^A(\vec{x};\lambda)$. One must be careful because the limits $\vec{x}\to\infty$ and $\lambda\to\infty$ do not commute. Indeed $t^A(\vec{x};\lambda)\to B^A_\infty+i\lambda J^A_\infty$ as $\vec{x}\to\infty$ for any fixed λ while $\tau^A(\vec{x})$ has asymptotics for large $x=|\vec{x}|$:

$$\tau^A=D^{AB}Q_B+\mathcal{O}(1/x)+i\sqrt{\frac{3|x|}{P^3}}(J^3_\infty/3)^{1/4}P^A\,(1+\mathcal{O}(1/x)) \tag{2.6.51}$$

[2] In principle some components of the moduli space of solutions to (2.6.49) might be obstructed by the positivity of the discriminant.

This implies that the 5d SUGRA moduli $Y^A(\vec{x})$ have well-behaved large $\vec{x}$ asymptotics

$$Y^A(\vec{x}) = \frac{P^A}{(P^3/6)^{1/3}} + \mathcal{O}(1/|\vec{x}|). \tag{2.6.52}$$

Moreover, since the 10d dilaton scales according to (2.6.47) as $e^{2\phi^\lambda} = \frac{\tilde{V}_{IJA}^\lambda}{\lambda^3 g_s^2 \tilde{V}_M}$ ($\tilde{V}_M$ is λ independent), $e^{2\phi^\lambda(\vec{x})}$ for fixed $\vec{x}$ scales as λ^{-3}. Note, however, that in the other order of limits $\phi^\lambda(\infty) = 0$. The corresponding 5d metric for the deformed solution $\lambda^2 ds^2_{5d,\,\lambda}$ has a well-defined limit. Reference [9] shows that this limiting solution defines a geometry which is asymptotically $AdS_3 \times S^2$, where there is a nontrivial connection on the (trivial) S^2 bundle over the asymptotic AdS_3 region.

The upshot is that *if* we can choose the centers $\vec{x}_a^\lambda$, constrained by (2.6.49), so that the $\vec{x}_a^\lambda$ have a well-defined finite limit as $\lambda \to \infty$ then, by AdS/CFT, the BPS states corresponding to the multicentered solution at $\lambda = 1$ should correspond to BPS states in the MSW conformal field theory. However, it can happen that as $\lambda \to \infty$ the distances between the centers $\vec{x}_a^\lambda$ cannot remain bounded. In this case the behavior of the limiting geometry is more complicated, and might involve, for example, "several $AdS_3 \times S^2$ geometries at infinite separation." In particular, note that if the total $D6$ charge vanishes then $\alpha_{\infty,\lambda} \to 0$ and hence those integrability equations (2.6.49) with $\Gamma_b^0 = 0$ have a zero on the RHS. This might force some centers to move to infinity.

In view of the above results we next turn to our 3-centered configuration and examine the integrability conditions [11] on the positions of the three centers. For the set of charges described in section 3 we have two independent equations:

$$\begin{aligned} -\frac{\langle \Gamma_2, \Gamma_3 \rangle}{x_{23}^\lambda} + \frac{\langle \Gamma_3, \Gamma_4 \rangle}{x_{34}^\lambda} &= \theta_3^\lambda \\ -\frac{\langle \Gamma_2, \Gamma_4 \rangle}{x_{24}^\lambda} - \frac{\langle \Gamma_3, \Gamma_4 \rangle}{x_{34}^\lambda} &= \theta_4^\lambda \end{aligned} \tag{2.6.53}$$

where θ_b^λ denote (minus) the right-hand-sides of (2.6.49). The intersections of charges take the form:

$$\begin{aligned} \langle \Gamma_3, \Gamma_4 \rangle &= -\frac{P_1^3}{6} := c \\ \langle \Gamma_2, \Gamma_3 \rangle &= \left(\frac{P \cdot P_1^2}{8} - \frac{P_1^3}{8} + q_{0,2} \right) - \frac{Q \cdot P_1}{2} := a - b \\ \langle \Gamma_2, \Gamma_4 \rangle &= -\left(\frac{P \cdot P_1^2}{8} - \frac{P_1^3}{8} + q_{0,2} \right) - \frac{Q \cdot P_1}{2} := -a - b \end{aligned} \tag{2.6.54}$$

Using the charges of section 2.4 and the limit $P \to \infty$ holding P_1 fixed, we have $a \gg b, c$ and $c < 0$. As for the sign of b we first choose $b > 0$ and explain the case $b < 0$ later. Equations

(2.6.53) determine x_{23}^λ and x_{24}^λ in terms of x_{34}^λ. As discussed above, there is still freedom in choosing the dependence of x_{34}^λ on λ. One way to fix this freedom is to choose x_{34}^λ independent of λ. The relations between x_{ab}^λ, following from (2.6.53) are subject to the triangle inequalities. The moduli space of solutions will generically consist of several intervals on the x_{34}^λ line. The relation between these intervals and topologies of attractor flow trees is the essence of the Split Attractor Flow Conjecture (SAFC) [11], which we recall in Appendix A for convenience.

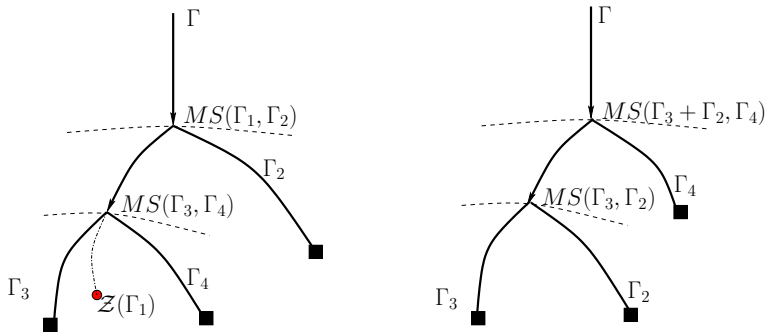

Figure 2.1: The two contributing topologies of attractor trees.

In the present case the two possible attractor flow tree topologies are shown in Figure 2.1. To identify the region corresponding to the left tree, we tune the moduli at infinity to be close to the $MS(\Gamma_2, \Gamma_1)$ wall. This means choosing $\theta_2^\lambda = -(\theta_3^\lambda + \theta_4^\lambda)$ close to zero. We can then write the triangle inequalities as follows:

$$\begin{aligned} \frac{a-b}{c-\theta_3^\lambda x_{34}} + \frac{a+b}{c+\theta_4^\lambda x_{34}} &\geq 1 \\ \frac{a-b}{c-\theta_3^\lambda x_{34}} + 1 &\geq \frac{a+b}{c+\theta_4^\lambda x_{34}} \\ 1 + \frac{a+b}{c+\theta_4^\lambda x_{34}} &\geq \frac{a-b}{c-\theta_3^\lambda x_{34}} \end{aligned} \tag{2.6.55}$$

Close to the MS wall $\theta_2^\lambda = 0$, we can write $\theta_3^\lambda = -\theta_4^\lambda - \theta_2^\lambda$, solve inequalities (2.6.55) and expand the solution to first order in θ_2^λ. Using in addition the relations between the magnitudes of a, b, c, we get the following solutions to (2.6.55):

$$\begin{aligned} &-\frac{c}{\theta_4^\lambda} + \frac{c}{2(\theta_4^\lambda)^2}\theta_2^\lambda \leq x_{34} \leq \frac{2a}{\theta_4^\lambda} - \frac{c}{\theta_4^\lambda} - \frac{a}{(\theta_4^\lambda)^2}\theta_2^\lambda \\ &x_{34} \leq \frac{-2b-c}{\theta_4^\lambda} - \frac{a(2b+c)}{2b(\theta_4^\lambda)^2}\theta_2^\lambda \quad \text{or} \quad -\frac{c}{\theta_4^\lambda} + \frac{ac}{2b(\theta_4^\lambda)^2}\theta_2^\lambda \leq x_{34} \\ &x_{34} \leq -\frac{c}{\theta_4^\lambda} + \frac{ac}{2b(\theta_4^\lambda)^2}\theta_2^\lambda \quad \text{or} \quad \frac{2b-c}{\theta_4^\lambda} + \frac{a(2b-c)}{2b(\theta_4^\lambda)^2}\theta_2^\lambda \leq x_{34} \end{aligned} \tag{2.6.56}$$

It is easy to see from these inequalities that for $\theta_2^\lambda < 0$ the solution consists of a point and an interval:

$$x_{34} \in \{-\frac{c}{\theta_4^\lambda} + \frac{ac}{2b(\theta_4^\lambda)^2}\theta_2^\lambda\} \bigcup \{\frac{2b-c}{\theta_4^\lambda} + \frac{a(2b-c)}{2b(\theta_4^\lambda)^2}\theta_2^\lambda,\ \frac{2a}{\theta_4^\lambda} - \frac{a}{(\theta_4^\lambda)^2}\theta_2^\lambda\}. \tag{2.6.57}$$

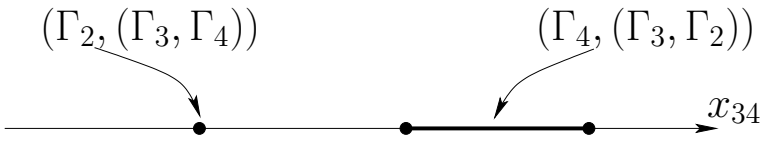

Figure 2.2: The two intervals, corresponding to topologies of Figure 2.1.

On the other hand for $\theta_2^\lambda > 0$ the point disappears, and the solution is just an interval. Thus, under the SAFC correspondence, the attractor tree topology of our main example is identified with the component of the moduli of solutions to (2.6.53), given by the point on the x_{34}^λ line. In the above we have chosen a definite sign of b, but it is easy to check that choosing $b < 0$ would lead to the existence of a point for $\theta_2^\lambda > 0$, and absence of it for $\theta_2^\lambda < 0$. This can also be seen from the stability condition for the $D4 \to D4D4$ split, $-\frac{\theta_2}{\langle\Gamma_1,\Gamma_2\rangle} > 0$, taking into account $\langle\Gamma_1,\Gamma_2\rangle = 2b$.

Having identified the intervals with the corresponding topologies we can investigate what happens to each interval as we change λ from 1 to ∞. From the functional form of θ_a^λ it is easy to see that $\theta_2^\lambda = \mathcal{O}(\lambda^{-2})$ and $\theta_4^\lambda = O(1)$ as $\lambda \to \infty$. Thus in the near horizon limit the point on the $|\vec{x}_{34}^\lambda|$ line corresponding to the topology of interest goes to $|\vec{x}_{34}^\lambda| = -\frac{c}{\theta_4^\infty}$. This means that $\vec{x}_{23}^\lambda, \vec{x}_{24}^\lambda \to \infty$ as $\lambda \to \infty$ and we get an infinite separation between charges Γ_2 and $\Gamma_3 + \Gamma_4$.

The conclusion is that our 3-centered configuration *does not* correspond to a single smooth geometry with $AdS_3 \times S^2$ asymptotics in the near horizon limit of [9].

2.7 Some general remarks on holographic duals of $D4D4$ boundstates.

As a byproduct of our investigation of the previous section we would like to make some more general remarks concerning the relation between the split attractor flows and the existence of a near horizon geometry with a single $AdS_3 \times S^2$ boundary. In [9] it is stated that configurations with the first split of the type $D4 \to D4 + D4$ do not correspond to geometries with a single $AdS_3 \times S^2$ boundary. In this section we will refine this statement. We begin with the integrability conditions:

$$\sum_{b \neq a} \frac{\langle\Gamma_a,\Gamma_b\rangle}{x_{ab}} = \theta_a \qquad \theta_a := 2\mathrm{Im}(e^{-i\alpha} Z(\Gamma_a))_\infty, \tag{2.7.58}$$

where the sum runs over all centers of multicentered solution, and denote by $M(\theta)$ the moduli space of solutions in $\vec{x}_a$ to (2.7.58). The decomposition of the charges in the first split defines a disjoint decomposition of the charges into two sets $A \amalg B$. Then, summing (2.7.58) over all charges in one cluster we get:

$$\sum_{a\in A, b\in B} \frac{\langle \Gamma_a, \Gamma_b\rangle}{x_{ab}} = \theta_A := 2\mathrm{Im}(e^{-i\alpha} Z(\Gamma_A))_\infty. \tag{2.7.59}$$

Conjecture 1: *The component of $M(\theta)$ that corresponds to a topology with the first split $D4 \to D4 + D4$ according to $A \amalg B$ under the SAFC, has the property: if $\sum_{a\in A} \theta_a \to 0$, then $x_{ab} \to \infty$ for $\forall a \in A\,, b \in B$.*

We do not know the proof of this statement but our previous 3-centered example can serve as an illustration of it. A suggestive argument here is the following: Tune the moduli at infinity t_∞ close to the MS wall of the first split. Then, according to the SAFC, for the $D4 \to D4D4$ component of moduli space the $D4$ clusters will become separated, and denoting the maximum size of these clusters by d, we can write (2.7.59) as

$$\frac{\langle \Gamma_A, \Gamma_B\rangle}{r_{AB}} \left(1 + O(\frac{d}{r_{AB}})\right) = \theta_A. \tag{2.7.60}$$

If one could argue, that as $\theta_A \to 0$ the sizes of clusters will remain much smaller than the separation between them $d \ll r_{AB}$, then we necessarily have $r_{AB} \to \infty$ and Conjecture 1 follows. Unfortunately, in general the sizes of clusters can grow as we change θ_a's, so this argument does not always apply and one needs a more detailed knowledge of the moduli space of solutions to (2.7.58).

A related issue that we wish to address is a conjecture of [9], relating multicentered solutions with single $AdS_3 \times S^2$ near horizon geometry and attractor flow trees at the "AdS point." The "AdS point" is given by

$$t_{AdS} = D^{AB} Q_B + i\infty P^A \tag{2.7.61}$$

This is a point on the boundary of moduli space given by $\lim_{u\to\infty} D^{AB}Q_B + iuP^A$ and we are considering limits of attractor flows with $D^{AB}Q_B + iuP^A$ as an initial point. Note that it is naturally selected by the near horizon limit (2.6.51). [9] noticed that the component of moduli space with first split $D4 \to D4 + D4$ does not correspond to a single $AdS_3 \times S^2$, and this component also does not exist at the AdS point, which lead them to

Conjecture 2: *There is a one to one correspondence between (i) components of the moduli space of lifted multicentered solutions with a single $AdS_3 \times S^2$ asymptotic geometry and (ii) attractor flow trees starting at the AdS point.*

We now give an argument in favor of this conjecture. As discussed in Appendix A, the attractor tree is specified by the H-functions:

$$H(s^{(a)}) = \Gamma^{(a)} s^{(a)} - \Delta H^{(a)}, \tag{2.7.62}$$

where $s^{(a)}$ is the parameter along the flow on the a-th edge. The rescaling in (2.6.48) leading to the near horizon limit of [9] results in changing the H-functions to

$$H(s^{(a)}) \to H^{\lambda}(s^{(a)}) = \lambda^{3/2}\Gamma^{(a)} s^{(a)} - \Delta H^{(a)}_{\lambda}. \tag{2.7.63}$$

According to (1.0.3), $\Delta H^{(a)}_{\lambda}$ depend linearly on and are completely determined in terms of ΔH_{λ}, and $\Delta H_{\lambda} = 2\mathrm{Im}(e^{-i\alpha}\Omega)_{t^{\lambda}_{\infty}}$, where $t^{\lambda}_{\infty} := B_{\infty} + i\lambda J_{\infty}$. As the solution for the moduli (2.6.42) are homogeneous of degree zero in H, we can replace these H^{λ}-functions with:

$$\begin{aligned} &H^{\lambda}(s^{(a)}) \to \tilde{H}^{\lambda}(s^{(a)}) = \Gamma^{(a)} s^{(a)} - \Delta\tilde{H}^{\lambda}_{(a)}, \\ &\Delta\tilde{H}^{\lambda} = \lambda^{-3/2} 2Im(e^{-i\alpha}\Omega)|_{t^{\lambda}_{\infty}}. \end{aligned} \tag{2.7.64}$$

We will refer to the split flow defined by (2.7.64) as a λ-deformed flow. Note that for λ-deformed flows the values of MS wall crossings parameters $s^{(a)\,\lambda}_{ms}$ in (1.0.4) will depend on λ. Our argument will be based on two assumptions:

Assumption 1: *There is a λ-deformed version of the SAFC, i.e. the components of the moduli space of λ-deformed solutions (2.6.48) are in one to one correspondence with λ-deformed attractor flow trees.*

Assumption 2: *The λ-deformed solution "survives" the near horizon limit, i.e. it corresponds to an asymptotically $AdS_3 \times S^2$ geometry, iff the corresponding λ-deformed attractor flow tree has all its flow parameters $s^{(a)\,\lambda}_{ms}$ nonzero (and positive) in the limit $\lambda \to \infty$. The attractor flow tree exists at the AdS point iff all it's flow parameters $s^{(a)}_{ms}$ stay nonzero (and positive) as it's starting point approaches AdS point.*

The second assumption is of course closely related to Conjecture 1 above, because for the first split $D4 \to D4 + D4$ we have $s_{ms} = \frac{\sum_{a\in A}\theta_a}{\langle\Gamma_A\Gamma_B\rangle}$. Given the above assumptions we want to prove that there is a one to one correspondence between λ-deformed attractor flow trees, that "survive" the near horizon limit in the sense of Assumption 2, and regular (not λ-deformed) attractor flow trees, that start at the AdS point.

First, we note that the first split of a λ-deformed flow that "survives" the limit must be $D4 \to D6 + \overline{D6}$. To see this we use (1.0.6), to estimate the λ dependence of $\Delta\tilde{H}^{\lambda}$:

$$\Delta\tilde{H}^{\lambda} = (\Delta\tilde{H}^{0}, \Delta\tilde{H}^{A}, \Delta\tilde{H}_{A}, \Delta\tilde{H}_{0}) \sim (\lambda^{-4}, \lambda^{-2}, \lambda^{-2}, \lambda^{0}). \tag{2.7.65}$$

From this we find that for $D4 \to D6 + \overline{D6}$ the flow parameter of the first split is $s^{\lambda}_{ms} \sim \lambda^{0}$, while for $D4 \to D4 + D4$ it is $s^{\lambda}_{ms} \sim \lambda^{-2}$. This means that only $D4 \to D6 + \overline{D6}$ is a valid split in the limit $\lambda \to \infty$.

For the chosen attractor trees we next look at the first edge of the flow tree in the moduli space. Using formula (1.0.6) from Appendix A, the complexified Kähler moduli are:

$$\begin{aligned} B^{A}_{\lambda}(s) &= D^{AB}\left(sP^{C} - \Delta\tilde{H}^{C}_{\lambda}\right)(sQ_{B} - \Delta\tilde{H}^{\lambda}_{B}) \\ J^{A}_{\lambda}(s) &= (sP^{A} - \Delta\tilde{H}^{A}_{\lambda})\sqrt{-6(sq_{0} - \Delta\tilde{H}^{\lambda}_{0} - 1/2Q^{2}(s))/(sP - \Delta\tilde{H}^{0}_{\lambda})^{3}} \end{aligned} \tag{2.7.66}$$

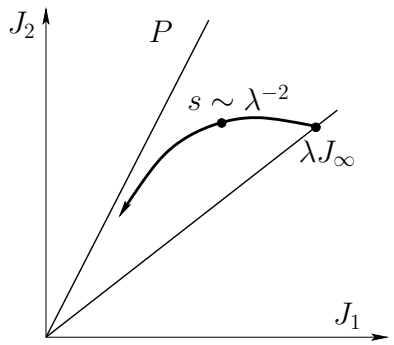

Figure 2.3: Behavior of the flow for the first edge of the tree.

Figure 2.3 shows that the flow starts at t^{λ}_{∞}, but for the flow parameter $s \sim \frac{1}{\lambda^2}$ the first term in $(sP^{A} - \Delta\tilde{H}^{A}_{\lambda})$ becomes comparable with second term and then starts to dominate, so that the flow will go along the P direction. The transition from J_∞ asymptotics to P asymptotics occurs around $s \sim \frac{1}{\lambda^2}$. Also note that the first split $D6\bar{D}6$ occurs long after this region at $s^{\lambda}_{ms} \sim \lambda^{0}$.

Now choose a value $\tilde{s}^{\lambda}$ of the flow parameter that goes to zero more slowly than $\frac{1}{\lambda^2}$, e.g. $\tilde{s}^{\lambda} \sim \frac{1}{\lambda^{2-\epsilon}}$, with small $\epsilon > 0$. From (2.7.66), it follows that $J^{A}(\tilde{s}^{\lambda})$ will approach the P direction as $\lambda \to \infty$, and grow as $\lambda^{1-\epsilon/2}$, i.e.

$$t^{A}(\tilde{s}^{\lambda}) \sim D^{AB}(P)Q_{B}(1 + O(\lambda^{-\epsilon})) + i\lambda^{1-\epsilon/2}P^{A}\, const\,(1 + O(\frac{1}{\lambda})). \tag{2.7.67}$$

We can think of the part of the attractor flow tree that starts at $J^{A}(\tilde{s}^{\lambda})$ as a tree on its own. It is again constructed in terms of H-functions, but now the $\Delta\tilde{H}^{\lambda}$ function will look like:

$$\Delta\tilde{H}^{\lambda} = \lambda^{-3/2} 2Im(e^{-i\alpha}\Omega)|_{t(\tilde{s}^{\lambda})}. \tag{2.7.68}$$

The only difference of this $\Delta\tilde{H}^\lambda$ with the ΔH of the λ-undeformed flow with starting point given by (2.7.67), is the overall factor $\lambda^{-3/2}$. Denoting the flow parameters for all edges of the tree collectively by s, we can introduce new parameters $s' = \lambda^{3/2}s$, in terms of which the H-functions will look like the ones for the λ-undeformed flow with starting point given by (2.7.67). It follows from Appendix A that the existence conditions, written in terms of parameters s', are the same as those written in terms of s, and furthermore the non-zero $s^{(a)\,\lambda}_{ms}$ will correspond to non-zero $s'^{(a)\,\lambda}_{ms}$ since $s'^{(a)\,\lambda}_{ms} = \lambda^{3/2}s^{(a)\,\lambda}_{ms}$. By virtue of Assumption 2, the λ-deformed flow tree that "survives" the near horizon limit has all its flow parameters $s^{(a)\,\lambda}_{ms}$ non-zero, and the corresponding λ-undeformed flow tree with starting point (2.7.67) exists at the AdS point.

In order to prove Conjecture 2 in the other direction consider a family of attractor flow trees whose initial point approaches the AdS point. Note that only the trees with the first split $D4 \to D6\overline{D6}$ exist in this limit, as shown in [9], eq.(3.64). Without loss of generality, for sufficiently large λ we can choose the initial points to be given by the right-hand side of (2.7.67) for some t_∞. Now, due to Assumption 2, the existence of the attractor flow tree at the AdS point means that in the limit $\lambda \to \infty$ all the flow parameters of these trees, $s'^{(a)\,\lambda}_{ms}$, stay non-zero. The dependence on λ in $s'^{(a)\,\lambda}_{ms}$ originates from the dependence in the starting point (2.7.67). We can use the discussion above to argue that there exists a corresponding λ-deformed flow tree, starting at t_∞ and passing through the point (2.7.67) at some parameter $\tilde{s}^\lambda$. For this λ-deformed flow tree to "survive" the limit $\lambda \to \infty$ we must have all $s^{(a)\,\infty}_{ms}$ non-zero and positive, due to Assumption 2. As the relation between the flow parameters for the two trees is $s^{(a)\,\lambda}_{ms} = \lambda^{-3/2}s'^{(a)\,\lambda}_{ms}$, some of the $s^{(a)\,\lambda}_{ms}$ of the λ-deformed flow might go to zero in the limit $\lambda \to \infty$, leading to trouble. We will now argue that in fact this cannot happen. To this end, first introduce a notation, analogous to the one in (2.7.58):

$$\theta(\Gamma) := 2\mathrm{Im}(e^{-i\alpha}Z(\Gamma))_\infty \tag{2.7.69}$$

According to (1.0.4), for each edge a the flow parameter $s^{(a)}_{ms}$ is given by a linear combination, with rational coefficients, of $\theta(\Gamma_i)$, where i runs over all the intermediate charges occurring in the path from the root of the tree to the edge a. For the λ-deformed flow these $\theta(\Gamma_i)$ have a definite scaling under λ-scaling. For instance, since the first split is always $\Gamma(D4) \to \Gamma_1 + \Gamma_2$ where Γ_1 and Γ_2 have nonzero (and opposite) $D6$ charge, we have $\theta(\Gamma_1) = -\theta(\Gamma_2) \sim \lambda^0$ and $\theta(\Gamma_1)$ will enter the expressions for all $s'^{(a)\lambda}_{ms}$. Other $\theta(\Gamma_i)$ will in general have $\mathcal{O}(\lambda^0)$ scaling (i.e. those with nonzero $D6$ charge) but, examining examples, we find that the coefficient of the λ^0 term will be some complicated nonlinear expression in terms of the intersection products of the charges, which does not vanish in these examples and hence we expect does not vanish

generically. For example for figure 2.7, $s^{(4)}_{ms}$ for the edge with Γ_4, it is a combination of the form:

$$s^{(4)}_{ms} = \frac{\theta_5 - \frac{\langle\Gamma_5,\Gamma_2\rangle}{\langle\Gamma_3,\Gamma_4\rangle}\theta_3 + \frac{\langle\Gamma_3,\Gamma\rangle\langle\Gamma_5,\Gamma_2\rangle}{\langle\Gamma_1,\Gamma_2\rangle\langle\Gamma_3,\Gamma_4\rangle}\theta_1 - \frac{\langle\Gamma_5,\Gamma\rangle}{\langle\Gamma_1,\Gamma_2\rangle}\theta_1}{\langle\Gamma_5,\Gamma_6\rangle}. \tag{2.7.70}$$

Here $\theta_5 \sim \lambda^{-2}$, $\theta_1 \sim \lambda^0$, $\theta_3 \sim \lambda^0$. If we assume that all $D6$ branes have $D6$ charges ± 1, then in the limit $\lambda \to \infty$ $\theta_1 = -\theta_3$, the leading coefficient of $s^{(4)}_{ms}$ is proportional to

$$-\langle\Gamma_3,\Gamma_6\rangle\langle\Gamma_5,\Gamma_1\rangle + \langle\Gamma_1,\Gamma_5\rangle\langle\Gamma_5,\Gamma_6\rangle + \langle\Gamma_1,\Gamma_6\rangle\langle\Gamma_5,\Gamma_6\rangle + \langle\Gamma_1,\Gamma_6\rangle\langle\Gamma_5,\Gamma_3\rangle, \tag{2.7.71}$$

which has no reason to vanish. In this way we can argue that all $s'^{(a)\,\lambda}_{ms}$ will have an order $\sim \lambda^0$ contribution whose coefficient will not scale to zero as $\lambda \to \infty$, at least not in general.

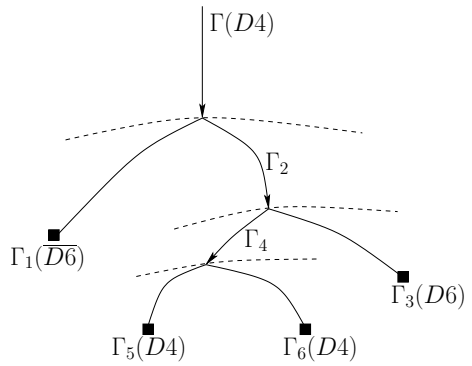

Figure 2.4: An example of attractor flow tree.

To summarize, we have shown that there is a one to one correspondence between λ-deformed attractor flow trees that "survive" the near horizon limit, and regular attractor flow trees, starting at AdS point. If one grants Assumptions 1 and 2 this would actually prove Conjecture 2, and hence the conjecture of [9].

Chapter 3

Spin paradox

In this chapter we will discuss an interesting question arising in the study of the moduli space of BPS objects in string theory. As discussed in the introduction in the supergravity approximation to string theory there is a wide class of BPS solutions, introduced in ([27], [11],[28]) represented by multicentered black hole solutions. The moduli space of such objects is described by the space of all possible positions of the black hole centers, subject to constraints following from equations of motion and supersymmetry. On the other hand the same BPS objects can be studied in the regime of weak string coupling constant when the lightest states are described by bound states of D-branes and excitations of those (for a good review see [29]). Of course, according to the common lore supersymmetry ensures that certain properties like degeneracies and mass/central charge relations are preserved when the coupling constant is changed, so the two pictures should give the same answer. One of the major applications of this statement is the so-called Strominger-Vafa program of accounting for black hole entropy in terms of D-brane microstates (see [3],[20], [17]). In view of this it is very important to understand precisely how the matching of different BPS states in the two pictures occurs. An important step in this direction was made in [10]. It was shown there that in fact we should expect to have a smooth transition between the two regimes, in which all discrete characteristics, like the number of BPS states, are preserved. Nevertheless there are still unanswered questions here. In the D-brane picture the bound states of BPS objects can be described using the powerful apparatus of algebraic geometry. For example [8] studied stable holomorphic bundles on rigid surfaces and found the number of BPS states on two sides of a marginal stability wall, across which BPS space undergoes a jump [5]. It turned out that enumeration of BPS states in algebraic geometry gives a very different answer for the number of BPS states than the answer that we expect from the supergravity description. More concretely supergravity picture tells us that BPS space is empty on one side of the wall and is populated on the other side. Algebraic-geometry picture gives non-empty spaces on both sides. This apparent contradiction is asking for a resolution.

In [10] the description of the abound state of BPS objects, that can be useful in both string and weak string coupling was given in terms of supersymmetric quantum mechanics(SSQM).

We review this description briefly in Section 3.1. The moduli space of this supersymmetric quantum mechanics has two branches: Coulomb branch which corresponds to the supergravity side and the Higgs branch which corresponds to the D-brane side of the full string theory description. Generically Higgs branch is populated on both sides of marginal stability wall, while the Coulomb branch is populated only on the stable side [10]. Apart from the mismatch between the number of BPS states on the two branches there is another interesting paradox that will be the focus of this chapter. As discussed at length in the Introduction the Hilbert spaces of BPS states are functions of the background moduli and can jump as the background moduli cross marginal stability walls. Part of the Hilbert space decays as the corresponding states "move off to infinity" in the moduli space. A paradox arises when we recall that BPS states are representations of $Spin(3)$ group of spatial rotations. On the Higgs branch, as we show in Section 3.1, Hilbert spaces on both sides of the marginal stability wall are irreducible multiplets of $Spin(3)$, as well as the decaying part of the Hilbert space. This leads to an apparent paradox since the sum of two irreducible representations cannot be an irreducible representation itself. We give a resolution of this paradox in Section 3.2, which also sheds some light on the relation between algebro-geometric and SSQM pictures.

3.1 Quantum quivers and spin paradox.

In this section we review the SSQM description of bound states of BPS objects, given in [10]. Suppose we have two D-branes, wrapping two rigid S^3 cycles of CY manifold, and placed at $\vec{x}_1$ and $\vec{x}_2$ in $\mathbb{R}^3$ space. In the weak string coupling regime the lightest modes are described by the world sheet gauge theory of these two D4 branes, which is $U(1)\times U(1)$ theory in this case. There will be additional light modes coming from bi-fundamental fields, living on the intersections of the two D-branes. In all the low energy theory will be the SSQM theory, obtained from this gauge theory by dimensional reduction with the Lagrangian:

$$
\begin{aligned}
L = \frac{\mu}{2}(\dot{\vec{x}}^2 + D^2 + 2i\bar{\lambda}\dot{\lambda}) - \theta D + |\partial_\tau \phi_+|^2 + |\partial_\tau \phi_-|^2 - (\vec{x}^2 + D)|\phi_+|^2 - (\vec{x}^2 - D)|\phi_-|^2 + \\
+ i\bar{\psi}_+\partial_\tau\psi_+ - \bar{\psi}_+\vec{x}\cdot\vec{\sigma}\psi_+ - i\sqrt{2}\left(\bar{\phi}_+\psi_+\cdot\lambda_+ + \phi_+\bar{\lambda}_+\cdot\bar{\psi}_+\right) + |F_+|^2 + \\
+ i\bar{\psi}_-\partial_\tau\psi_- + \vec{x}\cdot\vec{\sigma}\psi_- + i\sqrt{2}\left(\bar{\phi}_-\psi_-\cdot\lambda_- + \phi_-\bar{\lambda}_-\cdot\bar{\psi}_-\right) + |F_-|^2. \qquad (3.1.1)
\end{aligned}
$$

Here, $\vec{x}$ is the relative position of the D-branes, $(\vec{x}, \lambda, D)$ comes from the vector multiplet of $N = 1$ SYM in 4 dimensions, $(\phi_\pm, \psi_\pm, F_\pm)$ are hypermultiplets coming from the string modes, living on the intersections of two D-branes. We have $k_\pm$ fields $\phi_\pm$ so that $\phi_\pm \in \mathbb{C}^{k_\pm}$. Denoting

by $\alpha_{1,2}$ the phases of central charges of the two branes near the marginal stability wall we have the relations

$$\theta = \mu(\alpha_2 - \alpha_1), \quad \mu \sim \frac{1}{g_s}. \tag{3.1.2}$$

Eliminating the auxiliary fields the Lagrangian becomes:

$$\begin{aligned} L = {} & \frac{\mu}{2}(\dot{\vec{x}}^2 + 2i\bar{\lambda}\dot{\lambda}) + |\partial_\tau \phi_+|^2 + |\partial_\tau \phi_-|^2 - \vec{x}^2(|\phi_+|^2 + |\phi_-|^2) - \frac{(\theta + |\phi_+|^2 - |\phi_-|^2)^2}{2\mu} + \\ & + i\bar{\psi}_+ \partial_\tau \psi_+ + \bar{\psi}_+ \vec{x} \cdot \vec{\sigma} \psi_+ - \bar{\psi}_- i\sqrt{2}\left(\bar{\phi}_+ \psi_+ \cdot \lambda_+ + \phi_+ \bar{\lambda}_+ \cdot \bar{\psi}_+\right) + \\ & + i\bar{\psi}_- \partial_\tau \psi_- - \vec{x} \cdot \vec{\sigma} \psi_- + i\sqrt{2}\left(\bar{\phi}_- \psi_- \cdot \lambda_- + \phi_- \bar{\lambda}_- \cdot \bar{\psi}_-\right). \end{aligned} \tag{3.1.3}$$

Depending on the value of the string coupling constant that enters μ the space of vacua of this Lagrangian changes. First, following [10], we consider the regime

$$\sqrt{\Delta\alpha} \ll \frac{\Delta k}{2\mu\Delta\alpha} \ll 1. \tag{3.1.4}$$

In this regime we can integrate out the chiral fields, which induces the following potential for the positions field $\vec{x}$:

$$V_C = \frac{\theta^2}{2\mu} + k_+\sqrt{\vec{x}^2 + \frac{\theta}{\mu}} + k_-\sqrt{\vec{x}^2 - \frac{\theta}{\mu}} - (k_+ + k_-)|\vec{x}| + \frac{1}{2\mu}\left(\frac{k_+}{2\sqrt{\vec{x}^2 + \frac{\theta}{\mu}}} - \frac{k_-}{2\sqrt{\vec{x}^2 - \frac{\theta}{\mu}}}\right)^2 + O(\frac{1}{\mu^2}) \tag{3.1.5}$$

Assuming that $|\vec{x}|^2 \gg |\Delta\alpha|$ we further get

$$V_C = \frac{\theta^2}{2\mu}\left(\theta + \frac{(k_+ - k_-)}{2|\vec{x}|}\right) + O(\frac{1}{\mu^2}). \tag{3.1.6}$$

Minimizing this potential gives the relative positions of D-branes in the supersymmetric bound state (essentially the Coulomb branch of the SSQM) coinciding with the supergravity result:

$$R = -\frac{k_+ - k_-}{2\theta} = \frac{k_- - k_+}{2\mu(\alpha_2 - \alpha_1)}. \tag{3.1.7}$$

Now we can justify the conditions (3.1.4): we required $\sqrt{\Delta\alpha} \ll R$ in order to have large and positive mass squared for $\phi_\pm$ fields and the requirement $R \ll 1$ justifies the usage of SSQM. Positivity of the above radius is equivalent to Denef's stability conditions [11], which looks like

$$\frac{k_- - k_+}{2\theta} > 0. \tag{3.1.8}$$

Let's assume that $k_- - k_+ > 0$ and the stable side is $\theta > 0$. As we cross the marginal stability wall θ goes through zero and becomes negative, the radius of the bound state goes to infinity

and the bound state decays. [10] showed that on the stable side the Hilbert space of BPS states forms and irreducible representation of spatial $Spin(3)$ of spin $\frac{k_- - k_+ - 1}{2}$. On the unstable side the Hilbert space is empty.

Now let's turn to the Higgs branch description of the theory. In the regime of parameters[1]

$$\mu |\Delta\alpha|^{3/2} \gg 1, \tag{3.1.9}$$

we can integrate out $\vec{x}$ modes in the Lagrangian (3.1.3). $\phi_\pm$ fields will have a potential

$$V_H = \frac{(\theta + |\phi_+|^2 - |\phi_-|^2)^2}{2\mu}, \tag{3.1.10}$$

and the space of minima of this potential modulo gauge invariance, acting on $\phi_\pm$, constitute the Higgs branch of the theory. This theory is known as $N = 4$ supersymmetric non-linear sigma model and the Hilbert space of BPS states in this model is given by the Dolbeault cohomology of the classical moduli space. The moduli space in our example is

$$\mathcal{M} = \{(\phi_\pm) : \ -|\phi_+|^2 + |\phi_-|^2 = \theta, \quad (\phi_\pm \sim e^{\pm i\alpha}\phi_\pm)\}. \tag{3.1.11}$$

It is very convenient to use quiver notation to denote such moduli spaces. The moduli space is given by the moduli space of a two node quiver, given on Figure 3.1.

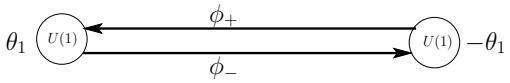

Figure 3.1: Quiver for the moduli space $\mathcal{M}$.

The nodes represent gauge groups here, the arrows represent the bi-fundamental fields $\phi_\pm$ and $\pm\theta_1$ are the so-called D-term parameters that enter the D-term equations as in (3.1.11). Now let's find the Hilbert spaces of BPS states on both sides of the marginal stability wall. The stable side is given by $\theta_1 > 0$ and the quiver moduli space is a fibration V_+^0:

$$\begin{array}{c} O(-1)^{\oplus k_+} \\ \downarrow \\ \mathbb{P}^{k_- - 1} \end{array} \tag{3.1.12}$$

As mentioned above BPS states are represented by the elements of Dolbeault cohomology of this space. As the space is non-compact we have to specify what cohomology we are talking

[1]Notice that this regime is complimentary to (3.1.4).

about. In fact we have to restrict ourselves to just cohomology of the base of the fibration because as the fibers are non-compact we restrict to states having zero momentum in the fiber direction. This gives the Hilbert space of BPS states

$$\mathcal{H}_{\theta_1>0} = J_{\frac{k_- -1}{2}}, \quad \dim\mathcal{H}_{\theta_1>0} = k_-. \tag{3.1.13}$$

Here $J_{\frac{k_- -1}{2}}$ is spin $\frac{k_- -1}{2}$ representation of $Spin(3)$ and we are focusing only on the $Spin(3)$ structure of the Hilbert space. We can repeat the above calculation for the unstable side $\theta_1 < 0$ to get the moduli space V_-^0

$$\begin{array}{c} O(-1)^{\oplus k_-} \\ \downarrow \\ \mathbb{P}^{k_+-1} \end{array} \tag{3.1.14}$$

together with the Hilbert space

$$\mathcal{H}_{\theta_1<0} = J_{\frac{k_+ -1}{2}}, \quad \dim\mathcal{H}_{\theta_1>0} = k_+. \tag{3.1.15}$$

First thing to note here is that the space is not empty, unlike in the supergravity (Coulomb branch) description. We will not try to resolve this discrepancy between Coulomb and Higgs branches here but just mention an argument from [30]: although the potential on the Coulomb branch (3.1.5) on the unstable side does not have a minimum, it decreases to a non-zero value for $\vec{x}^2 = \frac{\theta_1}{\mu}$ where the Coulomb branch approximation breaks down. This might be an indication that the minimum is actually on the Higgs branch and the BPS space is non-empty.

Setting aside this problem we concentrate on the $Spin(3)$ structure of Hilbert spaces on the Higgs branch. We know that $\mathcal{H}_{\theta_1>0} = J_{\frac{k_- -1}{2}}$ and $\mathcal{H}_{\theta_1<0} = J_{\frac{k_+ -1}{2}}$ and also from the Coulomb branch description we know [10] that the part of Hilbert space that decays across the marginal stability wall is $\Delta\mathcal{H} = J_{\frac{k_- -k_+ -1}{2}}$. Obviously there is a paradox here since we cannot have $\mathcal{H}_{\theta_1>0} = \mathcal{H}_{\theta_1<0} \oplus \Delta\mathcal{H}$ due to the difference in $Spin(3)$ representations. We will call this spin paradox in what follows.

3.2 Spin paradox: resolution

In this section we describe the resolution of the spin paradox. As noted above the moduli space on the Higgs branch in (3.1.11) is non-compact, which makes non-obvious what cohomology of this space corresponds to BPS states in the quantum theory. Further more, as discussed in

[30], in the algebro-geometric picture one has a certain compactification of the moduli space on both sides of the marginal stability wall. So the simplest resolution is to compactify the moduli space (3.1.11) by adding an additional node to the quiver Figure 3.1.[2] In Figure 3.2 we show the proposed quiver describing the compactified Higgs branch. The moduli space of this quiver

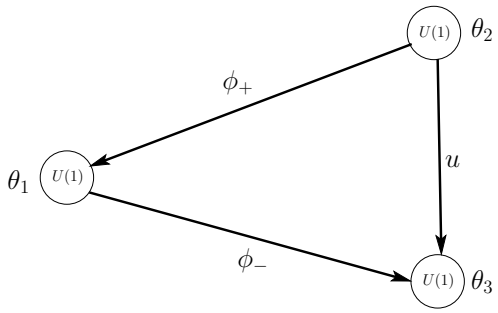

Figure 3.2: Quiver for compactified moduli space.

is given by 3 moment map (D-term) equations

$$\begin{aligned} |\phi_+|^2 + |u|^2 &= \theta_2 \\ -|\phi_-|^2 - |u|^2 &= \theta_3 \\ |\phi_-|^2 - |\phi_+|^2 &= \theta_1, \end{aligned} \tag{3.2.16}$$

and gauge invariance $(\phi_+, u, \phi_-) \to (e^{i\alpha^a Q_a^+}\phi_+, e^{i\alpha^a Q_a^u}u, e^{i\alpha^a Q_a^-}\phi_-)$ with $a = 1..3$ and

$$\begin{aligned} Q_1 &= (-1_+, 0, , 1_-) \\ Q_2 &= (-1_+, 1, , 0_-) \\ Q_3 &= (0_+, -1, , -1_-). \end{aligned} \tag{3.2.17}$$

We want to find cohomology of this variety for both stable $\theta_1 > 0$ and unstable $\theta_1 < 0$ sides and compare the results with non-compact case as well as with the Coulomb branch results. In order to do this we will use methods of toric geometry as this is a toric variety given in the form of symplectic reduction.[3] For another application of toric geometry and introductory remarks on it see Appendix G. To keep formulas simple we will do the calculation in all details for a particular simple but non-trivial case $k_+ = 1, k_- = 2$ and after that generalize it to arbitrary values of $k_\pm$.

[2]This suggestion is due to Frederik Denef.

[3]For a good review of applications of toric geometry in physics see for example [31].

3.2.1 $k_+ = 1, k_- = 2$

Toric variety, defined by (3.2.16), (3.2.17) depends on the values of parameters θ_i. As $\theta_3 = -\theta_1 - \theta_2$ we can parametrize the space of resulting varieties by $(\theta_1, \theta_2) \in \mathbb{R}^2$. Not every value (θ_1, θ_2) corresponds to a non-empty toric variety, but rather the set of such values forms a fan inside $\mathbb{R}^2$, called secondary fan. Different cones of this fan correspond to topologically distinct toric varieties, connected to each other by a series of flop transitions. Our main interest is to study the transition between varieties V_+ in the region $\theta_1 > 0$ and V_- in the region $\theta_1 < 0$.

To describe toric varieties explicitly we will use the holomorphic quotient construction, reviewed in appendix G. As discussed there, all information is encoded in the fan of the variety which can be constructed from (3.2.16), (3.2.17) data as follows. First we find linear subspace of $\mathbb{R}^{k_+ + k_- + 1} \equiv \mathbb{R}^4$ orthogonal to the charges (3.2.17):

$$\sum_I Q_a^I n_i^I = 0, \tag{3.2.18}$$

where I runs over $(+, u, -)$ indices. Solving this equation we get

$$\begin{pmatrix} n_1 \\ n_2 \end{pmatrix} = \begin{pmatrix} 1 & -1 & 1 & 0 \\ 0 & 0 & 1 & -1 \end{pmatrix}. \tag{3.2.19}$$

The columns of this matrix are points in some lattice $\mathbb{N}$ and generate 1-dimensional cones of the toric fan, given on Figure 3.3. Each edge of the fan corresponds to one of the coordinates (ϕ_+, u, ϕ_-). Each coordinate corresponds to a divisor of toric variety given by putting the coordinate to zero. We denote the corresponding divisors by (ξ_+, ξ_u, ξ_-). In the holomorphic quotient construction, toric variety is given by

$$V = (C^4 - Z) \bmod G, \tag{3.2.20}$$

where $(\phi_+, u, \phi_-) \in C^4$, group G is given in (3.2.17) and the excluded locus Z is encoded in the fan. Each 1-dimensional cone corresponds to one of the coordinates (ϕ_+, u, ϕ_-) and for each set of 1-dimensional cones that do not form a cone of our fan but such that any subset does, the zero locus of corresponding coordinates is included in Z. For the fan on Figure 3.3 we find

$$Z = \{\phi_+ = u = 0\} \cup \{\phi_-^1 = \phi_-^2 = 0\}. \tag{3.2.21}$$

There is a region in the (θ_1, θ_2) plane where (3.2.16) leads to precisely such excluded locus, namely $\theta_1 \geq 0, \theta_2 \geq 0$. In this indirect way we have found the Kähler cone of this toric variety.

We depict it in Figure 3.4 along with the Kähler cone for the $\theta_1 < 0$ variety that we derive later.

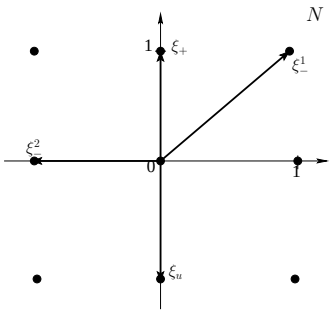

Figure 3.3: Fan of toric variety V_+.

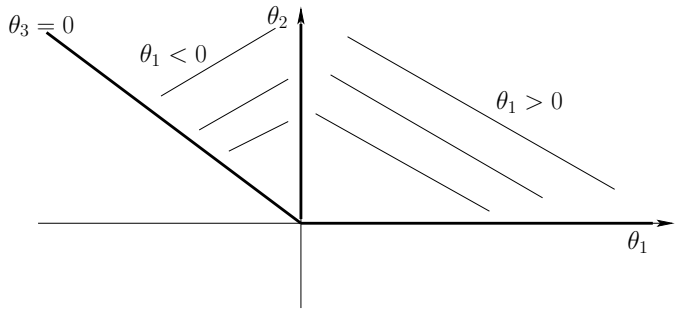

Figure 3.4: Kähler cones for $\theta_1 > 0$ and $\theta_1 < 0$ varieties.

V_+ is known as Hirzebruch surface F_1 and topologically this is a $\mathbb{P}^2$ with blown-up point in it. In Figure 3.3 we depict the four divisors $\xi_+, \xi_u, \xi_-^{1,2} \in \mathrm{H}^2(F_1)$, associated to each 1-dimensional cone in the fan. Since the Kähler cone is given by $\theta_1 > 0, \theta_2 > 0$, we can introduce the basis elements $\eta_{1,2} \in \mathrm{H}^2(F_1)$ and write the Kähler form of F_1 as

$$w = \theta_1 \eta_1 + \theta_2 \eta_2. \tag{3.2.22}$$

Other divisors can be expanded in this basis using charges Q_1 and Q_2 in (3.2.17) as

$$\begin{aligned} \xi_+ &= -\eta_1 + \eta_2 \\ \xi_u &= \eta_2 \\ \xi_-^i &= \eta_1. \end{aligned} \tag{3.2.23}$$

The last thing we need is the ring structure of $\mathrm{H}^*(F_1)$, which is determined by the fan as follows: for each component of the excluded locus we equate to zero intersection of the corresponding divisors. This produces

$$\xi_+\xi_u = 0 \quad \xi_-^1\xi_-^2 = 0, \tag{3.2.24}$$

which translates into the following conditions on the $\mathrm{H}^2(F_1)$ generators η_1, η_2:

$$\eta_1^2 = 0 \quad \eta_2^2 = \eta_1\eta_2. \tag{3.2.25}$$

To find the normalization of the intersection ring we choose any cone of maximal dimension in the fan of F_1 and require the intersection of corresponding divisor to be equal to 1:[4]

$$\xi_+\xi_-^1 = \xi_+\xi_-^2 = \xi_u\xi_-^1 = \xi_u\xi_-^2 = 1, \tag{3.2.26}$$

which leads to

$$\eta_2^2 = \eta_1\eta_2 = 1. \tag{3.2.27}$$

Finally we can write the decomposition of $\mathrm{H}^*(F_1)$ into $Spin(3)$ multiplets as

$$\begin{aligned} &\text{triplet}: \ 1, \ w, \ w^2, \\ &\text{singlet}: w^{(1)} = \theta_3\eta_1 + \theta_2\eta_2, \end{aligned} \tag{3.2.28}$$

There is a standard action of $Spin(3)$ group on the cohomology of toric (or more generally Kähler) varieties, called Lefschetz representation and generated by

$$\begin{aligned} S^+ &= -w_{m\bar{n}} dz^m \wedge d\bar{z}^{\bar{n}} \\ S^- &= w^{m\bar{n}} \frac{\partial}{\partial dz^n} \wedge \frac{\partial}{\partial d\bar{z}^{\bar{n}}} \\ S^3 &= \frac{1}{2}\left(d\bar{z}^{\bar{m}} \frac{\partial}{\partial d\bar{z}^{\bar{m}}} + dz^m \frac{\partial}{\partial dz^m} \right) - \frac{\dim_{\mathbb{C}}}{2}. \end{aligned} \tag{3.2.29}$$

Although it is a known fact that supersymmetric ground state of $N = 4$ SSQM are in one-to-one correspondence with Dolbeault cohomology of the moduli space ([32], [33]), the relation between spatial $Spin(3)$ ground and Lefschetz $SU(2)$ action is not obvious. We will demonstrate it in details in Appendix B.

The space $\mathrm{H}^2(F_1)$ is two dimensional with generators $\eta_{1,2}$ and is decomposed into two classes: w - Kähler form and w_1, determined by the condition $w_1 w = 0$. In the next Section we will

[4]This is always true for smooth varieties. In general intersection of n divisors of n-dimensional toric variety is equal to $\frac{1}{\mathrm{index}(v_1,\ldots v_n)}$, where v_i are generators of 1-dimensional cones in the n-dimensional cone and $\mathrm{index}(v_1,\ldots v_n)$ is the index of lattice generated by $(v_1,\ldots v_n)$ in $\mathbb{N}$. For varieties with quotient singularities this index can be greater than 1.

show how such decomposition works for arbitrary $k_\pm$. Having found the spin content of BPS states in $\theta_1 > 0$ region we would like to repeat the analysis for $\theta_1 < 0$ region. When $\theta_1 < 0$ the excluded set Z will contain $\{\phi_+ = 0\} \in Z$. This means that we have to remove the generator ξ_+ from the fan (3.3). After that the condition $\theta_2 > 0$ does not make sense since it leads to excluded locus $\phi_+ = u = 0$ which will remove the ξ_u cone from the fan in Figure 3.3 and give non-compact variety. On the other hand requiring $\theta_3 > 0$ corresponds to excluding the locus $\phi_u = \phi_-^{1,2} = 0$ and produces a fan 3.5. This is a fan of $\mathbb{P}^2$. The Kähler cone is 1-dimensional

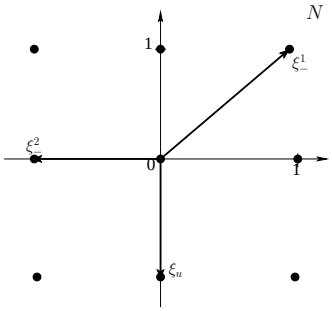

Figure 3.5: Fan of toric variety V_-.

and we can immediately write the spin structure of $\mathrm{H}^*(V_-)$:

$$\begin{aligned} &\mathrm{H}^*(V_-) : \{1,\, w,\, w^2\} \,-\, \text{triplet} \\ &w = -\theta_3 \eta. \end{aligned} \tag{3.2.30}$$

The spectra (3.2.28), (3.2.30) lead to a completely consistent picture: as we cross the wall the singlet state disappears as $\mathbb{P}^1$ inside F_1 is blown down and on the other side we have only triplet. The singlet is exactly the spin $\frac{k_- - k_+ - 1}{2}$ multiplet that we expect from supergravity picture.

Before generalizing the discussion to arbitrary $k_\pm$ it is interesting to see what happens to $V_\pm$ varieties as we decompactify them and go from quiver on Figure 3.2 to the one on Figure 3.1.

For $\theta_1 > 0$, quiver Figure 3.1 gives a toric variety (3.1.12) with a fan in Figure 3.6. We see that to decompactify all we need to do is to remove the edge ξ_u from the fan. In a way the fan on Figure 3.3 is really *the simplest possible* compactification of the fan on Figure 3.6. This becomes even more evident for the $\theta_1 < 0$ case, where the decompactification leads to variety (3.1.14) with a fan on Figure 3.7. In this case (3.1.14) is just $\mathbb{C}^2$ and compactifying it by adding an edge to the fan gives $\mathbb{P}^2$ which is the simplest compactification.

Decompactifying V_+ effectively removes η_2 from the cohomology ring and leaves

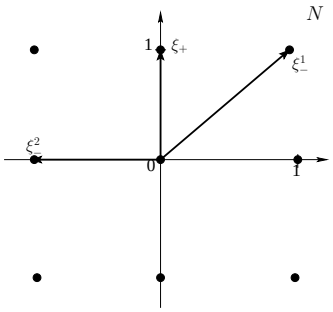

Figure 3.6: Fan of toric variety V_+^0.

$$\mathrm{H}^*(V_+^0):\ 1,\ w=\theta_1\eta_1, \tag{3.2.31}$$

that is with the cohomology of just the base $\mathbb{P}^1$ of the fibration (3.1.12). We observe a dramatic change of $Spin(3)$ structure, starting with singlet+triplet and ending up with a doublet. It is this dramatic change that leads to the spin paradox for the non-compact quiver (3.1). Decompactifying $V_- = \mathbb{P}^2$ also removes η from the cohomology and leaves a 0-form only, which is a change of $Spin(3)$ structure of BPS space form a triplet to a singlet. In summary, when we decompactify the two varieties $V_\pm$ there is a dramatic change of $Spin(3)$ structure of BPS space on both sides of the marginal stability wall which eventually leads to the spin paradox. As we mentioned above, in algebraic geometry the moduli space is also given some natural compactification. It would be very interesting to understand if the two compactifications coincide.

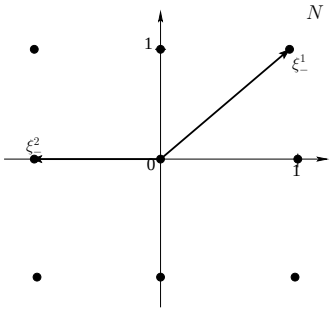

Figure 3.7: Fan of toric variety V_-^0.

3.2.2 Arbitrary $k_\pm$

First, it is straightforward to carry the above analysis of toric varieties from $k_- = 2, k_+ = 1$ to $k_- > 2, k_+ = 1$. In this case V_- will be just $\mathbb{P}^{k_-}$ and V_+ will be $\mathbb{P}^{k_-}$ with a blown up point, which is blown up to a $\mathbb{P}^{k_- -1}$. As before, V_+ will have one additional divisor ξ_+ in comparison to V_-, which is Poincar dual to the blow up cycle $\mathbb{P}^{k_- -1}$. The $Spin(3)$ structures

of cohomologies of $V_\pm$ will also work in a similar way. For V_+ we will have:

$$\begin{aligned}
&\mathrm{H}^*(V_+):\ J_{\frac{k_-}{2}} \oplus J_{\frac{k_- -1}{2}},\\
&J_{\frac{k_-}{2}} = \{1, w, ..., w^{k_-}\},\\
&J_{\frac{k_- -2}{2}} = \{w_1, w_1 w, ..., w_1 w^{k_- -2}\}
\end{aligned} \tag{3.2.32}$$

where

$$w = \theta_1\eta_1 + \theta_2\eta_2 \tag{3.2.33}$$

The 2-form w_1 is determined by the condition $w_1 w^{k_- -1} = 0$. The ring structure is similar to (3.2.25) and can be easily read off the fan:

$$\eta_1^{k_-} = 0 \quad \eta_2^{k_- -1}(\eta_2 - \eta_1) = 0. \tag{3.2.34}$$

Using these relations we can find the form w_1 to be

$$w_1 = (\theta_1 + \theta_2)^{k_- -1}\eta_1 + \left(-(\theta_1 + \theta_2)^{k_- -1} + \theta_1^{k_- -1}\right)\eta_2. \tag{3.2.35}$$

Going to the other side of marginal stability wall we have

$$\begin{aligned}
&\mathrm{H}^*(V_-):\ J_{\frac{k_-}{2}},\\
&J_{\frac{k_-}{2}} = \{1, w, ..., w^{k_-}\},
\end{aligned} \tag{3.2.36}$$

and the multiplet that left the spectrum is again the one expected from supergravity picture $J_{\frac{k_- - k_+ -1}{2}}$. As in the previous Section we can decompactify both $V_\pm$ by removing ξ_u edge from the fan and get back to the spin paradox.

Allowing for arbitrary values of k_+ makes the toric description of $V_\pm$ more complicated. In each particular case we can obtain the fan and the Kähler cone numerically. On the other hand, we do not really need this to resolve our spin paradox: all we need is the structure of $\mathrm{H}^*(V_\pm)$ as a $Spin(3)$ module.

For arbitrary $k_\pm$ the cohomology rings of $V_\pm$ are generated by $\eta_{1,2}$, subject to the relations

$$V_+ : \ \eta_1^{k_-} = 0, \quad (\eta_2 - \eta_1)^{k_+}\eta_2 = 0$$
$$V_- : \ (\eta_2 - \eta_1)^{k_+} = 0, \quad \eta_1^{k_-}\eta_2 = 0. \tag{3.2.37}$$

These relations follow directly form the excluded loci Z for both varieties, that can be read off the quiver (3.2.16). Let's demonstrate how the cohomology ring can be decomposed into irreducible representations of Lefschetz $Spin(3)$. Starting with V_+ we first identify the longest multiplet

$$J_{\frac{k_-+k_+-1}{2}} = \{1, w, ..., w^{k_-+k_+-1}\}. \tag{3.2.38}$$

As $\dim \mathrm{H}^2(V_+) = 2$ we can choose the form $w_1 \in \mathrm{H}^2(V_+)$ subject to the constraint $w_1 w^{k_-+k_+-2} = 0$, which will furnish another multiplet:

$$J_{\frac{k_-+k_+-3}{2}} = \{w_1, w_1 w, ..., w_1 w^{k_-+k_+-3}\}. \tag{3.2.39}$$

It is obvious that this form is linearly independent from w, as well as that each form $w_1 w^n$ is independent form w^{n+1}. Now $\dim \mathrm{H}^4(V_+) = 3$ with a basis $\eta_1^2, \eta_1\eta_2, \eta_2^2$ and we can always choose the form $w_2 \in \mathrm{H}^4(V_+)$, subject to the constraint $w_2 w^{k_-+k_+-4} = 0$, which will give another multiplet

$$J_{\frac{k_-+k_+-5}{2}} = \{w_2, w_2 w, ..., w_2 w^{k_-+k_+-5}\}. \tag{3.2.40}$$

Again, in every space $\mathrm{H}^{2n}(V_+)$, $n = 2..k_- + k_+ - 3$ we have 3 independent elements w^n, $w_1 w^{n-1}$ and $w_2 w^{n-2}$. We can continue this process: as each subsequent space $\mathrm{H}^{2n}(V_+)$ has dimension 1 higher than the previous one, there will be a new multiplet $J_{\frac{k_--k_+-2n-1}{2}}$, starting with w_{n-1}, subject to $w_n w^{k_-+k_+-2n} = 0$. However when we reach $n = k_+ + 1$ the relation $(\eta_2 - \eta_1)^{k_+}\eta_2 = 0$ kicks in and for $n = k_+ + 1...k_- - 1$ the dimensions of $\mathrm{H}^{2n}(V_+)$ will be constant and equal to $k_+ + 1$. For $n \geq k_-$ the second relation $\eta_1^{k_-} = 0$ will come into play and the dimensions will decrease. In all we get the usual structure of a tensor product of $Spin(3)$ representations, that is decomposed into the sum of irreducible multiplets:

$$\mathrm{H}^*(V_+) : \ J_{\frac{k_-+k_+-1}{2}} \oplus J_{\frac{k_-+k_+-3}{2}} \oplus ... \oplus J_{\frac{k_--k_+-1}{2}}. \tag{3.2.41}$$

Repeating this calculation for V_- we find

$$\mathrm{H}^*(V_-):\ J_{\frac{k_-+k_+-1}{2}} \oplus J_{\frac{k_-+k_+-3}{2}} \oplus ... \oplus J_{\frac{k_--k_++1}{2}}. \tag{3.2.42}$$

The difference between the two spaces is the $J_{\frac{k_--k_+-1}{2}}$ multiplet that leaves the spectrum as we cross the wall. Recall that for the simplest case $k_- = 2, k_+ = 1$ there was a simple interpretation of the transition $V_+ \to V_-$ as blowing down an exceptional divisor of V_+, which naturally lead to the disappearance of a part of the cohomology. Here we do not have such clear interpretation. As for the decompactification of $V_\pm$ that brings them to (3.1.12), (3.1.14) the interpretation is exactly the same: as we decompactify, $\xi_u \in \mathrm{H}^2(V_\pm)$ leaves cohomology as it's support spreads out, this effectively puts $\eta_2 = 0$ and changes the spin structure form (3.2.41), (3.2.42) to (3.1.13), (3.1.15).

3.3 Summary

In this chapter we briefly discussed the correspondence between the Hilbert spaces of BPS states in the two complementary regimes: on the Higgs and Coulomb branches. We posed an apparent paradox in the Higgs branch description in the $Spin(3)$ structure of BPS spaces on the two sides of some marginal stability wall. Compactifying the moduli space we showed that the paradox is completely resolved. This resolution also gave us a tentative picture of the Higgs branch of supersymmetric quantum mechanics which is fully consistent with algebro-geometric picture. It still remains to make an explicit check if the structure of the Higgs branch, i.e. the spectrum of BPS states and their degeneracy, that we propose is related to the one in algebro-geometric picture.

Chapter 4
Bound state transformation walls

In this chapter we address an interesting problem arising in the study of BPS states in four dimensional N=2 supergravity theories. BPS bound states near marginal stability are described by configurations of widely separated constituents with nearly parallel central charges. When the vacuum moduli can be dialed adiabatically until the central charges become *anti*-parallel, a paradox arises. We show that this paradox is always resolved by the existence of Bound State Transformation(BST) walls across which the nature of the bound state changes, although the index does not jump. We find that there are two distinct phenomena that can take place on these walls, which we call recombination and conjugation. The latter is associated to the presence of singularities at finite distance in moduli space. Consistency of conjugation and wall-crossing rules near these singularities leads to new constraints on the BPS spectrum. Singular loci supporting massless vector bosons are particularly subtle in this respect. We argue that the spectrum at such loci necessarily contains massless magnetic monopoles, and that bound states around them transform by intricate hybrids of conjugation and recombination. This chapter is based on [34].

4.1 Qualitative discussion of basic ideas

The spectrum of BPS states in four dimensional $\mathcal{N} = 2$ supersymmetric theories shows interesting behavior when the vacuum moduli are varied. Well known are jumps at walls of marginal stability, where BPS bound states can decay into, or be assembled from, mutually supersymmetric constituents. In supergravity these bound states are described by multicentered black hole or particle configurations [11, 35], providing an intuitive "molecular" picture of such bound states and their wall crossing behavior [5] (for recent reviews, see [36, 37]). However as pointed out e.g. in [12], this picture leads to an apparent paradox, reviewed below.

4.1.1 Puzzle

The simplest example of a BPS bound state in supergravity is a 2-centered bound state of charges Γ_1 and Γ_2. The equilibrium distance between the two centers is given by [11]

$$R = \frac{\langle \Gamma_1, \Gamma_2 \rangle}{2} \frac{|Z_1 + Z_2|}{\mathrm{Im}(Z_1 \overline{Z}_2)} \tag{4.1.1}$$

where the central charges Z_i of Γ_i are evaluated at spatial infinity. Existence of the bound state requires $R > 0$. When one dials the moduli at infinity through a marginal stability wall, the equilibrium distance R diverges and the BPS state decays. The same is true when the two centers themselves are replaced by clusters of black holes or particles, or by a multi-particle 'halo' [10]. This simple physical picture has led to a number of notable successes, including the derivation of universal wall crossing formulae [5, 38].

These successes notwithstanding, it does not take much effort to arrive at the following disturbing observation. It is often possible [11, 6, 12] to dial the moduli *while keeping R positive and finite*, from a marginal to an *anti*-marginal stability wall, as illustrated in fig. 4.1. At an anti-marginal stability wall, the phases of Z_1 and Z_2 anti-align. It would appear from (4.1.1) that this simply leads to $R \to \infty$ again and a decay $\Gamma \to \Gamma_1 + \Gamma_2$. However, this obviously violates conservation of energy: the energy of the BPS bound state at the anti-marginal stability wall is $|Z| = ||Z_1| - |Z_2||$, while the total energy of the decay products equals $|Z_1| + |Z_2|$! Either we have created a perpetuum mobile, or something dramatic must have happened to the bound state along the way.

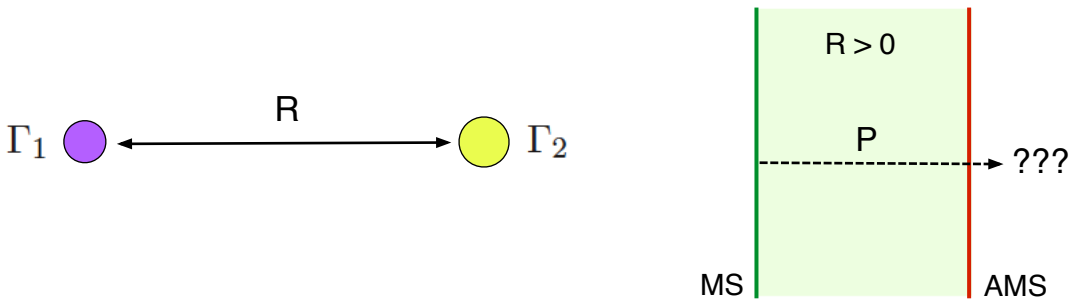

Figure 4.1: BPS bound states appear to be adiabatically transportable from marginal stability to anti-marginal stability keeping $R > 0$, violating conservation of energy.

The puzzle is not tied to the supergravity approximation; it similarly arises, perhaps even more sharply, when thinking of BPS bound states as characterized by attractor flow trees [11, 27, 6, 5]. The branches of such trees are attractor flows, splitting on walls of marginal stability, terminating on the attractor points of the constituents, and rooted at the vacuum

value of the moduli. A flow tree can be thought of as the "skeleton" of a supergravity solution,[1] but can be given a meaning independent of supergravity [39, 5], as a canonical recipe to assemble or disassemble a BPS state. What makes an attractor flow special compared to other paths in moduli space is that for any pair of constituent charges it either crosses a marginal stability wall once, or an anti-marginal stability wall once, or it crosses neither. In particular it is not possible to cross both a marginal and an anti-marginal stability wall. Our puzzle is then how to reconcile this with the fact that the root point of the tree can be moved along the path $\mathcal{P}$ shown in fig. 4.1, seemingly forcing the trunk to cross both the AMS and the MS wall. A related puzzle has been discussed in [40].

4.1.2 Resolution

The most straightforward resolution of the puzzle would appear to be that somewhere along the path, the BPS state simply gets lifted. Indeed for classical solutions this "elevation" phenomenon was noticed some time ago already [6] (fig. 18); see also fig. 4.4 below. However, this is only possible at the quantum level if the BPS index was zero to begin with. If the index is nonzero, as in the situation raised in [12], something more dramatic needs to happen to prevent the paradox.

In the flow tree picture something dramatic can only happen when the flow tree degenerates, i.e. when an edge shrinks to zero size. This edge can be the trunk, an internal edge or a terminal edge. The first case corresponds to crossing a marginal stability wall, which we have excluded from the start. The second case is associated to constituents rearranging themselves, and the third case to constituents becoming massless and charge conjugate particles being created. They will be referred to as recombination resp. conjugation walls.

1. **Recombination wall** (fig. 4.2): If the charges Γ_1 and Γ_2 themselves are composite bound states, it is possible that along the way the different constituents recombine into new clusters. This invalidates the hidden assumption in the formulation of the puzzle that the BPS state can at all times be viewed as a bound state with well separated clusters of charge Γ_1 and Γ_2. What happens instead is that before the troubling AMS wall is reached, the constituents rearrange themselves to make the AMS wall irrelevant. A sketch of possible

[1] The Split Attractor Flow Conjecture, mentioned in the Introduction and reviewed in Appendix A was originally formulated in [5]. In the course of this work we noticed this is not quite correct: the loci in moduli space where solution spaces split and join do not exactly coincide with loci in moduli space where flow trees split and join; see section 4.5.3 for details. None of the results on indices and wall crossing in the literature are affected by this, as those required only the interpretation of flow trees as canonical procedures to assemble or disassemble BPS states. For this reason we are careful to phrase definitions of bound state transformation walls in terms of trees, not solutions.

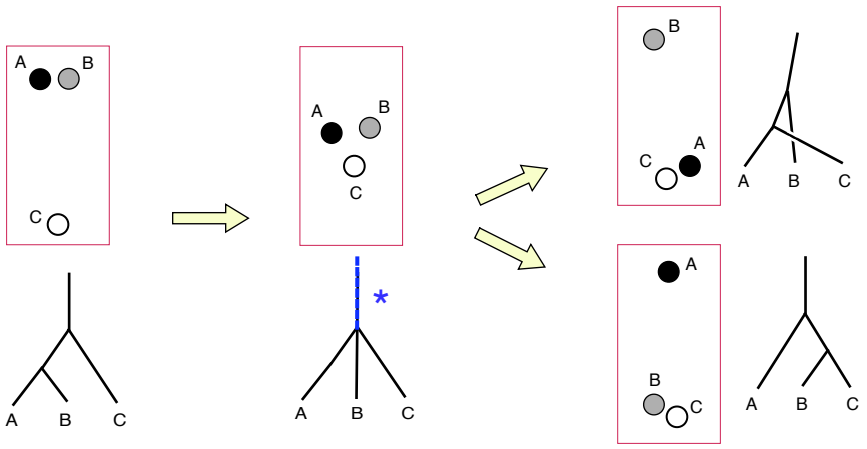

Figure 4.2: **Recombination:** Constituents rearrange themselves into different clusters. The example represents a family of configurations with A tightly bound to B evolving into a family with A tightly bound to C, and a family with C tightly bound to B. The corresponding attractor flow tree evolves from an $((A,B),C)$ tree to a $((C,A),B)$ tree plus a $((B,C),A)$ tree. At the transition point, the flow tree has two 3-valent vertices coalescing into a 4-valent vertex. The recombination wall is the blue line with the asterisk next to it.

recombination processes is shown in fig. 4.2. In the corresponding flow trees we see two 3-valent vertices coalesce into a 4-valent vertex, which then again separates into 3-valent vertices, but with a different tree structure. The degenerate 4-valent vertex lies at the intersection of the marginal stability walls for the different partitions of the constituents. The union of critical ingoing flows, i.e. the set of all moduli values flowing into the degenerate vertex, forms a codimension 1 wall in moduli space, the recombination wall. We will check that both index and spin character remain constant across a recombination wall, provided we sum over all trees of the given charge. An example of such a recombination process appeared in fig. 14 of [5]. More recently it was also discussed in [41].

2. **Conjugation wall**: The second possibility is more subtle, and is the one that solves the particular instance of the puzzle raised in [12]. It is associated to a vanishing terminal edge of the flow tree. This is only possible if the end point of this edge is a singularity, since regular attractor points can never lie on marginal stability walls. Thus, for example, it occurs when one of the constituents, say Γ_1, is a particle in a hypermultiplet which becomes massless at a singular locus, where the MS and AMS walls meet. In such cases there is a log-monodromy around the massless locus: $\Gamma_2 \to \Gamma_2 + I\Gamma_1$, where $I = |\langle\Gamma_1,\Gamma_2\rangle|$. As was pointed out in [11], trying to pull a single Γ_2 attractor flow through such a massless locus going from MS(Γ_1,Γ_2) to AMS(Γ_1,Γ_2) will cause the creation of a new tree branch, corresponding to charge $-I\Gamma_1$, terminating on the massless locus, as shown in fig. 4.3 on the left. This is required by charge conservation. The spacetime picture of this is that

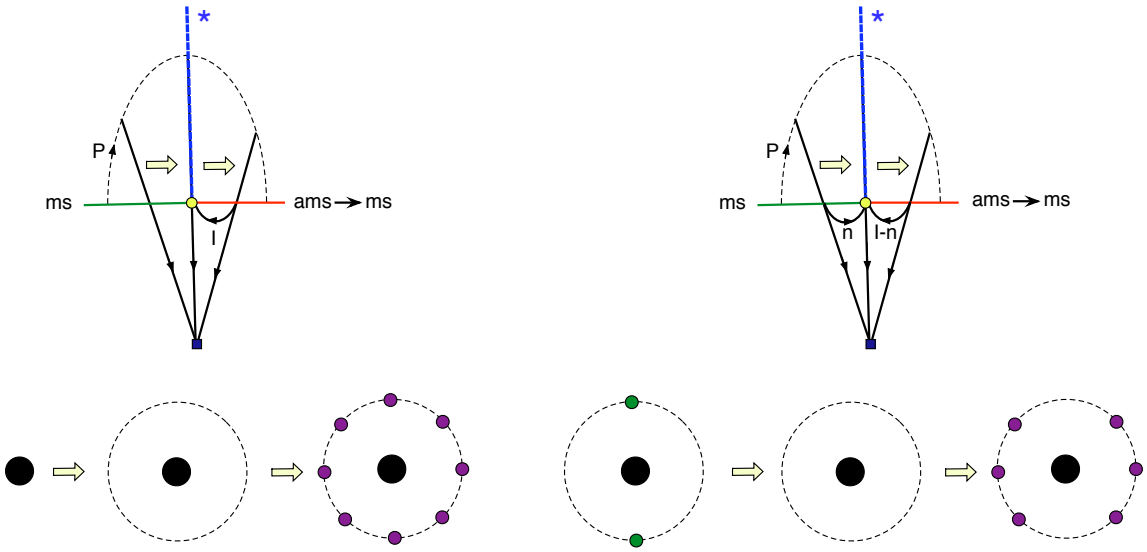

Figure 4.3: **Conjugation:** Left: a single centered Γ_2 flow turns into a $(\Gamma_2, -I\Gamma_1)$ split flow when pulled through the locus where the hyper Γ_1 becomes massless and around which we have a monodromy $\Gamma_2 \to \Gamma_2 + I\Gamma_1$. The corresponding spacetime picture is the creation of a fully filled fermi shell of I particles of charge $-\Gamma_1$. Right: a $(\Gamma_2, n\Gamma_1)$ split flow turns similarly into a $(\Gamma_2, (I-n)(-\Gamma_1))$ split flow.

a shell of I particles of charge $-\Gamma_1$ gets created as a halo around a core of charge Γ_2 at the radius where the moduli pass through the massless locus. It was shown in [10] that these newly created particles form a completely filled fermi shell of spin 1/2 fermions. If we start off with a bound state of Γ_1 and Γ_2, the fermi shell of I particles of charge $-\Gamma_1$ will again be generated, but now one $-\Gamma_1$-particle will annihilate with the Γ_1 particle already present, leaving behind a hole in the fermi shell, i.e. $I-1$ particles of charge $-\Gamma_1$. The troublesome AMS wall for Γ_1 and Γ_2 is now reinterpreted as a trouble-free MS wall for Γ_2 and the remaining particles of charge $-\Gamma_1$. In particular the state remains BPS: we go from a flow tree (Γ_2, Γ_1) to a flow tree $(\Gamma_2, (I-1)(-\Gamma_1))$. Similarly, if $n \leq I$ Γ_1 particles were present, we end up with n holes or $I-n$ particles of charge $-\Gamma_1$. In flow tree language we go from a (Γ_2, Γ_1) tree to a $(\Gamma_2, (I-n)(-\Gamma_1))$ tree. This is shown in fig. 4.3 on the right. We call this process the fermi flip.

When $n > I$ this does not work: we end up with particles of charge Γ_1 rather than $-\Gamma_1$, the flow tree ceases to exist since splits on AMS walls are not allowed, and the bound state goes from being classically BPS to being classically non-BPS (the minimum of the interaction potential is no longer at the BPS bound). At the classical level, this is a realization of the elevation phenomenon mentioned earlier as the most straightforward resolution of the puzzle. At the quantum level, what happened here wasn't quite elevation, because there

were initially no quantum BPS states at all. This is because more fermions were present (n) than the number of available 1-particle states (I). In some cases[2] elevation processes may occur also at the quantum level. An example is a bound state of some magnetically charged particle and an electrically charged $\mathcal{N} = 4$ vector multiplet, illustrated in fig. 4.4.

The above list is exhaustive, since the only possible degenerations of flow trees are collapses of edges. In general we can also get recombination-conjugation hybrids, at singularities where mutually nonlocal BPS states become massless. But the basic building blocks are given by the above classification.

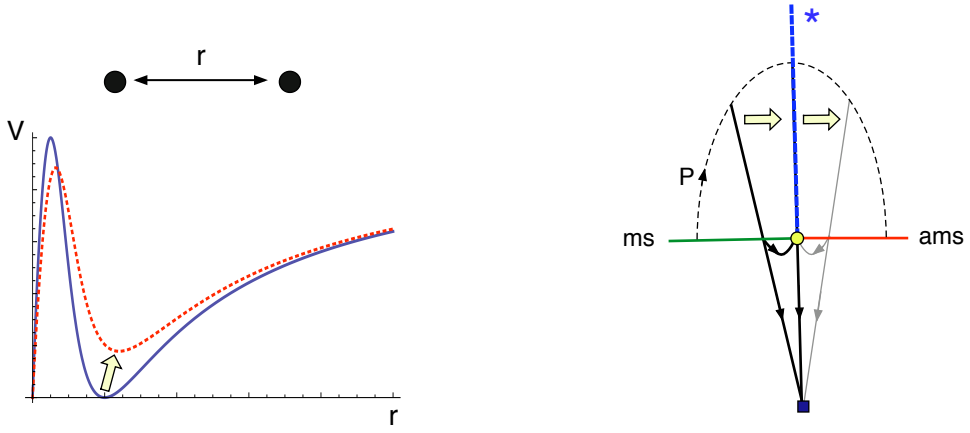

Figure 4.4: **Elevation:** The initially BPS-saturated minimum of the interaction potential $V(r)$ gets lifted, and the bound state becomes classically non-BPS. The corresponding flow trees are shown on the right. The blue line with the asterisk is the elevation wall. It corresponds to a critical attractor flow hitting a locus in (a suitable finite cover of) moduli space where the mass of one of the constituent particles vanishes but there is no charge monodromy around it, as is the case for example if an $\mathcal{N} = 4$ vector multiplet becomes massless. The tree on the right is shown in grey because it does not represent an actual BPS flow tree, since the split occurs on an anti-marginal stability wall.

The definitions we have given here will be made more precise in the following sections, and we will study more systematically under what conditions these phenomena occur. Besides solving the puzzle raised in [12], these considerations will also lead to interesting constraints on the BPS spectrum. More precisely these follow from continuity of BPS indices across bound state transformation walls. For example, if only particles of charge proportional to γ become massless at a certain locus at finite distance in moduli space, we find that the monodromy around this locus must be given by

$$\Gamma \to \Gamma + I\,\gamma\,, \qquad I = \langle \gamma, \Gamma \rangle \sum_{k=1}^{\infty} k^2 \Omega(k\gamma)\,. \tag{4.1.2}$$

[2]This may require fine tuning of hypermultiplet moduli, and requires the absence of quantum tunneling phenomena pairing up and lifting unprotected BPS states.

Furthermore, if some $\Gamma_1 = k\gamma$ supports massless BPS vector particles with $\Omega(k\gamma) \neq 0$, we clearly run into trouble, since we could start with a BPS configuration $(\Gamma_2, n\Gamma_1)$ with $n > I$ vector-particles (as this is no longer forbidden by the exclusion principle), and after crossing the bound state transformation wall end up with $n - I > 0$ particles of charge Γ_1, leading to a classically non-BPS configuration. By continuity of the index, this implies $\Omega(\Gamma_2 + n\Gamma_1) = 0$ on either side of the BST wall. The only way this is possible is if by some bizarre conspiracy the sum of all (nonzero) indices of individual configurations with total charge $\Gamma_2 + n\Gamma_1$ equals zero, for *any* choice of Γ_2 and n. More plausibly, this situation simply cannot occur. A more precise version of this argument is given in Sections 4.3.4 and 4.3.9 below. Indeed the following independent argument corroborates this. We only expect massless vectors at the quantum level when the low energy gauge theory is IR free or conformal. For IR free gauge theories we can trust the smooth classical BPS monopole solutions that such theories have on their Coulomb branch. These monopoles have mass proportional to the W-boson mass, and so we will always get BPS states with mutually nonlocal charges becoming massless at the same locus as the vector, contradicting the assumption that only charges proportional to γ become massless. See Section 4.6.3 for further discussion.

Of course the BPS spectrum near singularities, including constraints from monodromy and stability, is a well-studied subject, going back to the original works [42, 43, 1]. Scattered examples of supergravity bound state transformation phenomena have appeared before in the literature [11, 6, 5, 41]. Related phenomena have been exhibited in other pictures of BPS bound states; for example the conjugation phenomenon which we describe is related to quiver mutations or Seiberg dualities in cases where the quiver description of BPS bound states holds [44, 45], and to the string - string junction transition in the D-string description of BPS states in brane engineered field theories [46, 47, 48]. The goal of [34], on which the present chapter is based, was to study bound state transformations in full generality in the supergravity attractor flow tree picture of BPS states, and to determine how they constrain the BPS spectrum. We believe our constraints on the spectrum of massless states discussed in Sections 4.3.4 and 4.6.3 are new.

The organization of this chapter is the following: in section 4.2 we give a general and precise description of BST walls. In section 4.3 we review multicentered halo solutions of supergravity. We investigate the conjugation wall and the way BPS Hilbert spaces change across it, detailing the physical conjugation process and its relation to monodromy around the singularity. Finally we discuss constraints on the spectrum of BPS states following from the continuity of BPS index. In section 4.4 we give the simplest example of a conjugation wall, associated to a single

massless hypermultiplet, as in the example from [12]. In Section 4.5 the recombination walls are presented and we show how index and spin character are preserved. In addition we revisit the split attractor flow conjecture of [11] and add some important amendments to it. In Section 4.6 we describe the situation with a massless vector multiplet appearing at the singularity, and in section 4.7 we give a representative set of examples. One important conclusion we draw from the example of Section 4.7.3 is that the spectrum of low energy particles in some models with extremal transitions has not been fully understood in the past. We found this because published spectra disagreed with the general conclusions we had reached in Section 4.3. We have concluded that the published spectra were incomplete, and do not constitute counterexamples to the prediction of Section 4.3.4.

4.2 Walls from attractor flow trees

One way to describe BPS boundstates in supergravity is via attractor flow trees [11, 27, 6, 5].[3] Such trees describing a boundstate of two subcomponents of charge (Γ_1, Γ_2) (necessarily in a stable region) begin with single-centered attractor flow for the total charge $\Gamma := \Gamma_1 + \Gamma_2$. When describing boundstates of two constituents Γ_1, Γ_2 the tree then splits on a marginal stability wall $MS(\Gamma_1, \Gamma_2)$:

$$MS(\Gamma_1, \Gamma_2) := \{t \in \widetilde{\mathcal{M}} \mid 0 < Z(\Gamma_1; t)/Z(\Gamma_2; t) < +\infty\} \tag{4.2.3}$$

where $\widetilde{\mathcal{M}}$ denotes the universal cover of vectormultiplet moduli space. (In general our notation follows [5].)

Let us now suppose we are in the situation of our puzzle. The region of stability is defined by

$$\langle \Gamma_1, \Gamma_2 \rangle \mathrm{Im} Z(\Gamma_1; t) \overline{Z(\Gamma_2; t)} > 0. \tag{4.2.4}$$

Suppose that the path $\mathcal{P}$ is contained in the region of stability, connecting a point t_{ms} on $MS(\Gamma_1, \Gamma_2)$ to a point t_{ams} on $AMS(\Gamma_1, \Gamma_2)$

$$AMS(\Gamma_1, \Gamma_2) := \{t \in \widetilde{\mathcal{M}} \mid -\infty < Z(\Gamma_1; t)/Z(\Gamma_2; t) < 0\}. \tag{4.2.5}$$

The boundary of a region of stability is the set:

$$W(\Gamma_1, \Gamma_2) = \{t \in \widetilde{\mathcal{M}} \mid \mathrm{Im}\left[Z(\Gamma_1; t)\bar{Z}(\Gamma_2; t)\right] = 0\}, \tag{4.2.6}$$

[3] In fact, the description of BPS boundstates via attractor flow trees is applicable in a far more general context than just the supergravity approximation.

which can be decomposed as:

$$W(\Gamma_1,\Gamma_2) = MS(\Gamma_1,\Gamma_2) \amalg AMS(\Gamma_1,\Gamma_2) \amalg (\mathcal{Z}(\Gamma_1) \cup \mathcal{Z}(\Gamma_2)), \tag{4.2.7}$$

where

$$\mathcal{Z}(\Gamma) := \{t \in \widetilde{\mathcal{M}} | Z(\Gamma;t) = 0\}. \tag{4.2.8}$$

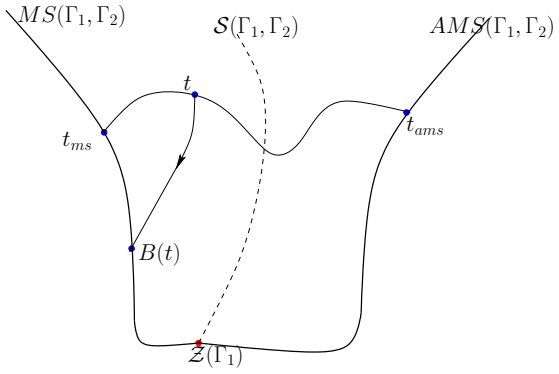

Figure 4.5: Location of the $\mathcal{S}(\Gamma_1,\Gamma_2)$ wall.

In figure 4.5 we depict a caricature of the location of different components of $W(\Gamma_1,\Gamma_2)$ in a real dimension 2 surface in the moduli space. Denote by t a point on $\mathcal{P}$ and consider the behavior of the attractor flow tree as t moves along $\mathcal{P}$ from t_{ms} towards t_{ams}. We want to prove the following

Statement: *There exists a point $t \in \mathcal{P}$, such that the attractor flow for $\Gamma_1+\Gamma_2$, starting at t, ends on either $\mathcal{Z}(\Gamma_1)$ or $\mathcal{Z}(\Gamma_2)$.*

One can use the following simple argument. Notice that when t is close to t_{ms}, the attractor flow for $\Gamma_1+\Gamma_2$ will almost immediately hit $MS(\Gamma_1,\Gamma_2)$. On the other hand, when t is close to t_{ams}, the flow will hit $AMS(\Gamma_1,\Gamma_2)$. Indeed, according to Property 3 from Appendix C, the attractor flow always has the direction from stable to unstable side in the vicinity of an (anti)marginal stability locus. As one can continuously get from $MS(\Gamma_1,\Gamma_2)$ to $AMS(\Gamma_1,\Gamma_2)$ only through the loci $\mathcal{Z}(\Gamma_1)$ or $\mathcal{Z}(\Gamma_2)$, it is almost obvious that for some $t \in \mathcal{P}$ the attractor flow will crash on those zeros. The only thing to check is that the attractor flow for $\Gamma_1+\Gamma_2$ does not run to a boundary of the moduli space at infinite distance when we move t from t_{ms} to t_{ams}. Let $B(t)$ denote the point where the flow hits $W(\Gamma_1,\Gamma_2)$. Property 2 from Appendix C says that $B(t)$ exists for all t on path $\mathcal{P}$ and Property 1 ensures that it is unique. Now define a real-valued function

$$\lambda(t) := \frac{Z(\Gamma_1;B(t))}{Z(\Gamma_2;B(t))} \in \mathbb{R} \cup \{\pm\infty\}. \tag{4.2.9}$$

We showed that it can be defined for every t. Given that $\lambda(t) > 0$ for t near t_{ms} and $\lambda(t) < 0$ for t near t_{ams}, there must be some point where $\lambda(t)$ changes sign, going either to zero or infinity. $\lambda(t)$ having zero corresponds to crossing a wall $\mathcal{S}(\Gamma_1, \Gamma_2)$ and $\lambda(t)$ having infinity corresponds to crossing a wall $\mathcal{S}(\Gamma_2, \Gamma_1)$ wall, where

$$\mathcal{S}(\Gamma_1, \Gamma_2) := \{t \mid (\Gamma_1 + \Gamma_2) \text{ flow from } t \text{ crashes on } \mathcal{Z}(\Gamma_1)\}. \tag{4.2.10}$$

In principle, $\lambda(t)$ could have changed its sign more than once along the path $\mathcal{P}$, crossing one or both of $\mathcal{S}(\Gamma_1, \Gamma_2)$, $\mathcal{S}(\Gamma_2, \Gamma_1)$ walls possibly several times. For resolving our puzzle it will suffice to understand what happens when we cross just one wall.

Coming back to the fate of the BPS bound state $(\Gamma_1 + \Gamma_2)$, we suppose for definiteness that $\lambda(t)$ has a zero, the path $\mathcal{P}$ crosses $\mathcal{S}(\Gamma_1, \Gamma_2)$ and $Z(\Gamma_1)$ has a zero. The physical discussion of BPS states depends on the following dichotomy:

1. Near the locus $\mathcal{Z}(\Gamma_1)$, BPS states with charge γ_1 parallel to Γ_1 exist. That is, there is a positive rational number and a charge $\gamma_1 = r\Gamma_1$ so that

$$\mathcal{H}(\gamma_1, t)|_{t \in \mathcal{Z}(\Gamma_1)} \neq \emptyset, \tag{4.2.11}$$

2. No such states exist in the neighborhood of $\mathcal{Z}(\Gamma_1)$.

There are known examples of both possibilities. The first possibility gives rise the conjugation phenomenon across $\mathcal{S}(\Gamma_1, \Gamma_2)$. We will define the wall $\mathcal{S}(\Gamma_1, \Gamma_2)$, subject to the constraint (4.2.11), to be the conjugation wall.

In the second case the charge Γ_1 is not populated around $\mathcal{Z}(\Gamma_1)$, but by assumption, it is populated in the neighborhood of t_{ms} and thus should be realized as a multicentered solution [11]. An example of this situation, when Γ_1 is a bound state of $\Gamma_3 + \Gamma_4$, is given in figure 4.6 [4]. The bound state of $\Gamma_3 + \Gamma_4$ has to decay as one approaches $\mathcal{Z}(\Gamma_1)$, so that $MS(\Gamma_3, \Gamma_4)$ has to separate some region around $\mathcal{Z}(\Gamma_1)$ from the path $\mathcal{P}$, as in figure 4.6. Introducing the notation of nested lists to denote different attractor tree topologies the bound state just described is denoted as $(\Gamma_2, (\Gamma_3, \Gamma_4))$. Let's also denote

$$\begin{aligned} &\Gamma_{ij} := \langle \Gamma_i, \Gamma_j \rangle, \\ &\Gamma_{ij,k} := \Gamma_{ik} + \Gamma_{jk}, \quad \Gamma_{k,ij} := -\Gamma_{ij,k} \end{aligned} \tag{4.2.12}$$

[4] We depict charges Γ_2, Γ_3 and Γ_4 as single-centered attractor flows, but the discussion is applicable to the most general case with all charges being some multicentered configurations. The notation $t_*(\Gamma)$ in the figure is used for the regular attractor point of charge Γ.

for $i, j, k \in (2, 3, 4)$ and all different. The set of points in moduli space, such that attractor flow for charge $\Gamma_{total} = \Gamma_2 + \Gamma_3 + \Gamma_4$ with at least one $\Gamma_{ij,k}$ non-zero, starting at those points, passes through the locus where all three central charges are aligned defines a *recombination wall* (RW) [5], which we will denote by

$$RW(\Gamma_2, \Gamma_3, \Gamma_4) = \{t | (\Gamma_2 + \Gamma_3 + \Gamma_4)\text{-flow from t crashes on } MS(\Gamma_3 + \Gamma_4, \Gamma_2) \cap MS(\Gamma_3, \Gamma_4)\}. \tag{4.2.13}$$

The definition is in fact symmetric as will be explained in Section 4.5. It is clear from the

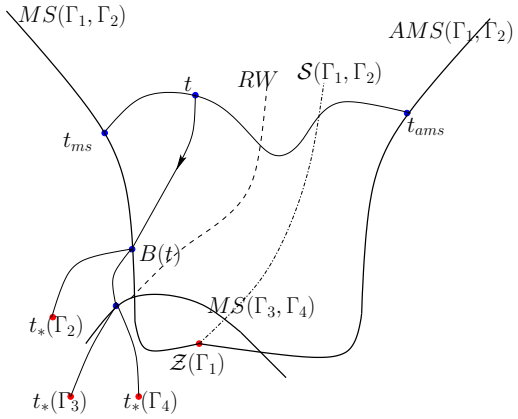

Figure 4.6: Charge Γ_1 is realized as a bound state of $\Gamma_3 + \Gamma_4$. The dashed line is the recombination wall RW between $(\Gamma_2, (\Gamma_3, \Gamma_4))$ and $(\Gamma_4, (\Gamma_2, \Gamma_3))$+$(\Gamma_3, (\Gamma_2, \Gamma_4))$.

picture that as we move t along $\mathcal{P}$ from t_{ms} and before crossing the $\mathcal{S}(\Gamma_1, \Gamma_2)$ wall, we will hit $RW(\Gamma_2, \Gamma_3, \Gamma_4)$. Section 4.5 gives a detailed account of how the bound states transform across $RW(\Gamma_2, \Gamma_3, \Gamma_4)$ wall and once again the puzzle from SEction 4.1.1 gets resolved.

4.3 Conjugation Walls and Fermi Flips

In this section we describe what happens to the bound state when the background moduli cross a conjugation wall. Changing slightly the notation from the previous section, we will be interested in bound states of a single particle of charge Γ with one or more particles with charges proportional to a primitive charge γ where $\langle \Gamma, \gamma \rangle \neq 0$. Our considerations will force us to consider, more generally, a particle of charge $\Gamma + m\gamma$ bound to one or more particles whose charges are proportional to γ.

4.3.1 Rules of the game

We assume that $\mathcal{Z}(\gamma)$ is located on the boundary of the moduli space at a finite distance. This locus is complex codimension one in moduli space $\mathcal{M}$ and can be thought of as lying on a real codimension one boundary of the covering space $\widetilde{\mathcal{M}}$. We will reduce arguments to one-complex-dimensional slices so one should keep in mind the analogy of $\widetilde{\mathcal{M}}$ as the upper half-plane with coordinate τ and $\mathcal{M}$ as the unit disk with parameter $q = e^{2\pi i \tau}$. Then $\widetilde{\mathcal{Z}}(\gamma)$ is $\mathbb{Q} \cup \{i\infty\}$ and $\mathcal{Z}(\gamma)$ is $q = 0$. All our arguments should be understood as pertaining to some sufficiently small and generic neighborhood $\mathcal{U}$ of $\mathcal{Z}(\gamma)$ in $\mathcal{M}$.

The lattice Λ of electromagnetic charges forms a local system over $\mathcal{M}$. That is, there is a flat connection on Λ. Moreover, the Hilbert space $\mathcal{H}^{\rm one-particle}$ of *all* one-particle states has a flat connection on $\mathcal{M}$, and furthermore $\mathcal{H}^{\rm one-particle}$ has a compatible grading by Λ. Typically, the local system Λ will have nontrivial monodromy around $\mathcal{Z}(\gamma)$. We will assume that γ is monodromy invariant. [5]

We will make some assumptions about the nature of certain BPS spaces in $\mathcal{U}$. First, we assume that $\mathcal{H}(\ell_i\gamma;t)|_{t\in\mathcal{Z}(\gamma)} \neq \emptyset$ for some collection of integers ℓ_i.[6] Second, we assume that these spaces are "constant" or t-independent in $\mathcal{U}$. By "constant" we mean there is a flat connection on the vector bundle of BPS states of charge $\ell\gamma$ whose fiber at t is $\mathcal{H}(\ell\gamma;t)$. Using the flat connection we trivialize the bundle and just speak of $\mathcal{H}(\ell\gamma)$. Third, it can very well happen that there is a linearly independent charge γ' with the same vanishing locus $\mathcal{Z}(\gamma) = \mathcal{Z}(\gamma')$. However, we assume that if such charges arise they are not populated, that is, $\mathcal{H}(n\gamma + m\gamma';t) = 0$ in $\mathcal{U}$ whenever $m \neq 0$. As we will see in Section 4.6, this is a crucial assumption; one which is not always satisfied in physically interesting situations.

Finally, returning to our charge Γ such that $\langle\Gamma,\gamma\rangle \neq 0$ we make some assumptions about $\mathcal{H}(\Gamma;t)$. Again, by taking $\mathcal{U}$ sufficiently small we know that the only relevant walls of (anti)marginal stability are in $W(\gamma,\Gamma)$. As we have explained, the locus $\mathcal{Z}(\gamma)$ divides $W(\gamma,\Gamma)$ into two connected components, $\mathcal{U}\cap MS(\gamma,\Gamma)$ and $\mathcal{U}\cap AMS(\gamma,\Gamma)$. We assume that our neighborhood of $\mathcal{U}$ is sufficiently small that, for all $n\in\mathbb{Z}$, $\mathcal{H}(\Gamma+n\gamma;t)$ is "constant" on these two components in the sense explained above. Therefore we can speak of well-defined spaces $\mathcal{H}^{ms}(\Gamma+n\gamma)$ and $\mathcal{H}^{ams}(\Gamma+n\gamma)$. We assume that $\mathcal{H}^{ms}(\Gamma)$ is nonzero, but we do *not* assume that $\mathcal{H}^{ms}(\Gamma+n\gamma) \cong \mathcal{H}^{ams}(\Gamma+n\gamma)$. Indeed, such a statement is meaningless if Γ is not

[5] We might need to pass to a finite cover of $\mathcal{U}$ if $Z(\gamma;t)$ has a multiple zero on $\mathcal{Z}(\gamma)$.

[6] Here we deviate slightly from the notation of [5] by using $\mathcal{H}$ for the reduced statespace of single-particle BPS states where the half-hypermultiplet degrees of freedom from the center of mass have been factored out. Thus $\mathcal{H}$ was denoted by $\mathcal{H}'$ in [5] and hence the BPS index – the second helicity supertrace – is given by $\Omega(\Gamma;t) = \mathrm{Tr}_{\mathcal{H}(\Gamma;t)}(-1)^{2J_3}$ throughout the thesis.

invariant under the monodromy action around $\mathcal{Z}(\gamma)$.

4.3.2 Review of halo states

Multicentered Halo Solutions

Four dimensional N=2 supergravity has stationary multicentered BPS black hole solutions [49, 11, 35], which are typically true bound states with constrained center positions whenever the centers have mutually nonlocal charges [11, 35]. It was shown in [10] that there is a distinguished class of multicentered solutions of supergravity known as *halo solutions*. In these solutions there is one center, known as the *core* with a charge Γ while all the other centers carry charges proportional to a primitive charge γ. The name derives from the fact that when the solution exists all the halo centers must lie on a sphere of fixed radius. For total charge of the form $\Gamma + n\gamma$ the halo radius is

$$R_n(t) = \frac{1}{2}\langle\Gamma,\gamma\rangle \frac{|Z(\Gamma+n\gamma;t)|}{\mathrm{Im}Z(\Gamma;t)\overline{Z(\gamma;t)}} \tag{4.3.14}$$

The total halo charge $n\gamma$ might be divided up between different halo centers in different ways corresponding to several centers of charges $\ell_i\gamma$, with $\sum \ell_i = n$.

Multi-centered halo configurations might or might not constitute acceptable solutions to supergravity. The existence criterion for acceptable multi-centered solutions of supergravity are rather complex and difficult to check in general. However, for halo solutions there are two simple necessary and sufficient criteria for existence:

1. The halo centers all must have parallel charges. That is the charges must be of the form $\ell_i\gamma$ where the integers ℓ_i all have the same sign.

2. The single-centered attractor flow from t with total charge $\Gamma + n\gamma$ must split on a wall of *marginal stability* $MS(\gamma,\Gamma)$ if $n > 0$ and it must split on a wall of *anti-marginal stability* if $n < 0$.

The first criterion is easy to understand. As we cross a wall of marginal stability the halo radius $R_n(t)$ goes to infinity. If some particles had ℓ_i of opposite sign then energy could not be conserved. Alternatively, if there were particles of opposite sign we could bring them together adiabatically and annihilate them. Thus, the original configuration could not have been BPS.

The shell approximation

The multi-centered halo solutions are rather intricate, and lead to rather complicated variations of moduli $t(\vec{x})$ in space. Some useful intuition can be gleaned by examining a much simplified

"shell approximation" to the multicentered solutions. This shell approximation is closely related to the split attractor flow description.

In the "shell approximation" we replace the multicentered supergravity solution by a spherically symmetric shell solution [11] (see figure 4.7). The supergravity field configuration is radially symmetric. For $r > R$ it is given by the attractor flow for $\Gamma + n\gamma$. Following the lead of split attractor flow, we choose the radius R to be $R = R_n(t)$. Thus, the local vectormultiplet moduli at $r = R$ are given by the point in $\mathcal{M}$ where the attractor flow of charge $\Gamma + n\gamma$ hits $W(\Gamma, \gamma)$, denoted in what follows by $B_n(t)$. We next insert a shell of uniform charge with total charge $n\gamma$ at the radius $r = R$. Then, we continue the solution to $r < R$ using single centered attractor flow for Γ. Let us compute the energy of such a field configuration. The energy is a sum of three terms $E_> + E_R + E_<$, the energy of the fields for $r > R$, $r = R$ and $r < R$, respectively. These are given by

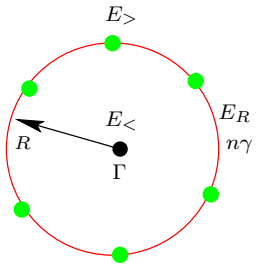

Figure 4.7: Shell configuration.

$$
\begin{aligned}
E_> &= |Z(\Gamma + n\gamma; t)| - |e^U Z(\Gamma + n\gamma; B_n(t)| \\
E_R &= |e^U Z(n\gamma; B_n(t))| \\
E_< &= |e^U Z(\Gamma; B_n(t))|,
\end{aligned}
\tag{4.3.15}
$$

with the total energy given by the sum

$$
E = |Z(\Gamma + n\gamma; t)| + 2\theta |e^U Z(n\gamma; B_n(t))|, \tag{4.3.16}
$$

where $\theta = 0$ if $B_n(t)$ lies on $MS(\gamma, \Gamma)$ and $\theta = 1$ if $B_n(t)$ lies on $AMS(\gamma, \Gamma)$. When $\theta = 1$ the field configuration is certainly not BPS and might not even be a solution of the equations of motion. Thus, we have recovered the second existence criterion for halo boundstates mentioned above: $B_n(t)$ must lie on $MS(\gamma, \Gamma)$.

Halo Fock Spaces

Upon quantization multi-centered solutions of supergravity correspond to states in the Hilbert space of BPS states. These states are to be thought of as boundstates of BPS particles. For the halo solutions we have a *core particle* of charge Γ and *halo particles* whose charges are proportional to γ. The corresponding quantum states are known as *halo states*.

Thus far we have been referring to a single core particle. In general the core charge Γ in a multi-centered solution might correspond to several particles and might not even have a single-centered realization. Nevertheless, if the boundstate radius $R_n(t)$ is large compared to any dimensions of the multi-centered solution of charge Γ then we can still meaningfully distinguish between the core and the halo and we can speak meaningfully of the "halo contribution to the BPS space $\mathcal{H}(\Gamma + n\gamma; t)$." We will restrict attention to such regions and think of the BPS space as a direct sum

$$\mathcal{H}(\Gamma + n\gamma; t) = \mathcal{H}^{halo}(\Gamma + n\gamma; t) \oplus \mathcal{H}'(\Gamma + n\gamma; t), \tag{4.3.17}$$

where $\mathcal{H}^{halo}(\Gamma + n\gamma; t)$ is the halo contribution and $\mathcal{H}'(\Gamma + n\gamma; t)$ is the core contribution. By taking a sufficiently small neighborhood $\mathcal{U}$ of a generic point on $\mathcal{Z}(\gamma)$ any possible mixing between $\mathcal{H}^{halo}(\Gamma; t)$ and $\mathcal{H}'(\Gamma; t)$ can be made small. By the correspondence principle we expect that we can focus on $\mathcal{H}^{halo}(\Gamma; t)$.

Let us now recall the description of the halo states given in [5]. It is useful to consider a "generating Hilbert space"

$$\oplus_{n\geq 0}\, \mathcal{H}^{halo}(\Gamma + n\gamma; t). \tag{4.3.18}$$

Since the halo particles are mutually BPS and noninteracting, the Hilbert space of all halo-type boundstates with a core particle of charge Γ form a $\mathbb{Z}_2$-graded Fock space:

$$\mathcal{H}^{halo}_{\Gamma} := \mathcal{H}^{ms}(\Gamma) \otimes_{\ell\geq 1} \mathcal{F}\left[(J_{\Gamma,\ell\gamma}) \otimes \mathcal{H}(\ell\gamma)\right] \tag{4.3.19}$$

Here $J_{\Gamma,\ell\gamma} = \frac{1}{2}(|\langle \Gamma, \ell\gamma\rangle| - 1)$ is an $SU(2)$ spin and $(J_{\Gamma,\ell\gamma})$ is the corresponding representation space of $SU(2)$ with generators $J_i^{(1)}$ while $\mathcal{H}(\ell\gamma)$ is also an $SU(2)$ representation space with generators $J_i^{(2)}$. The finite-dimensional vector space $(J_{\Gamma,\ell\gamma}) \otimes \mathcal{H}(\ell\gamma)$ is $\mathbb{Z}_2$-graded by $-(-1)^{2J_3^{(2)}}$ and the Fock space construction is applied in the $\mathbb{Z}_2$-graded sense. The physical reason for this seemingly strange choice of $\mathbb{Z}_2$-grading is explained in detail in [10]. In particular, halo particles which are *hypermultiplets* behave like free fermions and halo particles which are *vectormultiplets* behave like free bosons. Note that because of our assumptions, the space (4.3.19) does not depend on t.

There are three important subtleties one must be mindful of when using (4.3.19).

1. First, at a given value of t it is not true that all of the Hilbert space (4.3.19) contributes to (4.3.18). Only those states contribute for which the corresponding halo solutions exist. In particular, for contributions to $\mathcal{H}^{halo}(\Gamma + n\gamma; t)$ with $n > 0$ the point $B_n(t)$ must lie on $MS(\gamma, \Gamma)$ and hence t must lie on the appropriate side of the conjugation wall $\mathcal{S}(n\gamma, \Gamma)$. In Appendix D we discuss the arrangement of the walls $\mathcal{S}(n\gamma, \Gamma)$ as a function of n (see Figure D.1) and the consequences for (4.3.18).

2. The second subtlety is that the halo Fock space (4.3.19) singles out a special "core charge" Γ. When speaking of the "halo contribution to the space $\mathcal{H}(\Gamma + n\gamma; t)$" we should bear in mind that there can also be core charges of the form $\Gamma + m\gamma$ surrounded by halos of particles of total charge $(n - m)\gamma$, where m can be any integer, and thus when working out the contributions to (4.3.18) we should really sum over such core charges:

$$\oplus_{m\in\mathbb{Z}}\, \mathcal{H}^{halo}_{\Gamma+m\gamma}. \tag{4.3.20}$$

   Once again, only values of m such that the corresponding supergravity solutions exist will contribute to (4.3.18). Note that the BST walls $\mathcal{S}((n - m)\gamma, \Gamma + m\gamma)$ are the same for all $m \in \mathbb{Z}$.

3. Third, it is possible that there is nontrivial "mixing" between different halo states. This would result from tunneling amplitudes between halo particles and core states. It is clearly exponentially suppressed for large halo radius, but might in principle be nonvanishing. Such mixing would alter our description of the Hilbert space of BPS states. This would have an important impact on our description of the spin characters, but it would not impact our description of the BPS indices.

In (4.3.18) we have considered halo states with halo particles whose charge is parallel to γ. There is an analogous story for halo states with halo particles whose charge is anti-parallel to γ. For these we should sum over negative values of n in the analog of (4.3.18), the analogous Fock space (4.3.19) involves particles drawn from $\mathcal{H}(-\ell\gamma)$ with $\ell \geq 1$, etc.

4.3.3 The puzzle

Let us now return to the situation described in the previous sections. We have a path $\mathcal{P}$ joining t_{ms} to t_{ams} as in figure 4.5. Now imagine moving t along the path $\mathcal{P}$ and consider boundstates of total charge $\Gamma + n\gamma$ with $n > 0$. For t near t_{ms} we know there are halo boundstates with halo particles of charge parallel to γ. For t near t_{ams} such boundstates cannot exist. Indeed,

when t crosses the wall $\mathcal{S}(n\gamma, \Gamma)$ the halo bound states will cease to exist. Again we ask: *what happened to these BPS states*?

The simplest thing that can happen is that BPS states smoothly pair up and become non-BPS states as t crosses $\mathcal{S}(n\gamma, \Gamma)$. We called this the elevation phenomenon. An example of this will be given in Section 4.7.2, where $\mathcal{N} = 2$ vector- and hypermultiplets will pair up to form massive vectormultiplets. This mechanism is indeed suggested by the shell model. The field configuration we have written is clearly a solution of the equations of motion for $t \in \mathcal{P}_{ms}$, since it satisfies the BPS bound. On the other hand, it ceases to be a BPS configuration for $t \in \mathcal{P}_{ams}$. Nevertheless, the energy as a function of t continuously increases from the BPS bound. (Of course, this is not a proof that the states smoothly evolve into non-BPS states since the field configuration for $t \in \mathcal{P}_{ams}$ might no longer solve the equations of motion, but we consider it suggestive.)

Nevertheless, it is clear that this standard mechanism cannot be the whole story. The reason is that one can easily compute the contribution of the halo states to the BPS index $\Omega(\Gamma + n\gamma; t)$ from (4.3.19), and this contribution is typically nonzero. Indeed, this is what happens in the example of [12]. The lifting mechanism can only apply to states whose total contribution to the index vanishes. When the index does not vanish, the wall being crossed is the conjugation wall and there must be at least some other kind of phenomenon to account for what happened to the BPS states. In sections 4.3.5 and 4.3.6 we describe two new phenomenon - the *Fermi flip* and the *fadeout* – which can account for the disappearance of BPS states which contribute to an index. In sections 4.4 and 4.7.2 we show how these mechanisms nicely accounts for the fate of BPS boundstates in the neighborhood of common types of discriminant loci of Calabi-Yau manifolds. In order to motivate the Fermi flip it is useful to try to write out quantitatively the condition that all the indices $\Omega(\Gamma + n\gamma; t)$, $n \in \mathbb{Z}$ are continuous functions along the path $\mathcal{P}$. We turn to this in the next subsection.

4.3.4 BPS Indices

BPS indices can only change across walls of marginal stability. Let us see what this implies for our setup with a path $\mathcal{P}$ connecting t_{ms} to t_{ams}. We will define the "partition function":

$$F(\Gamma; t) := \sum_{n=-\infty}^{\infty} q^n \Omega(\Gamma + n\gamma; t). \tag{4.3.21}$$

This is a formal series in q, q^{-1} and we will demand its continuity along the path $\mathcal{P}$. As we have explained, we may focus on the contributions of the halo states with core charges of the form $\Gamma + m\gamma$, $m \in \mathbb{Z}$.

When t is infinitesimally close to t_{ms} all halo states with halo particles of charge parallel to γ will contribute to the partition function. No halo states with halo particles with charges anti-parallel γ will contribute. Therefore, the limiting value as t approaches the marginal stability line factorizes:

$$F(\Gamma; t_{ms}^{+}) = F_{\text{core}}^{\text{ms}} \cdot F_{\text{halo}}^{\text{ms}} \tag{4.3.22}$$

$$F_{\text{core}}^{\text{ms}} := \sum_{n=-\infty}^{\infty} q^n \Omega^{ms}(\Gamma + n\gamma) \tag{4.3.23}$$

$$F_{\text{halo}}^{\text{ms}} := \prod_{k>0} (1 - (-1)^{k|\langle \Gamma, \gamma \rangle|} q^k)^{k|\langle \Gamma, \gamma \rangle| \Omega(k\gamma)}. \tag{4.3.24}$$

Here t_{ms}^{+} means a point infinitesimally displaced from $MS(\gamma, \Gamma)$ into the stable region. By the same token, near the point t_{ams} all halo states with halo particles of charge parallel to $-\gamma$ will contribute, while no such states with halo particles of charge parallel to γ will contribute. Therefore we have the factorization:

$$F(\Gamma; t_{ams}^{+}) = F_{\text{core}}^{\text{ams}} \cdot F_{\text{halo}}^{\text{ams}} \tag{4.3.25}$$

$$F_{\text{core}}^{\text{ams}} := \sum_{n=-\infty}^{\infty} q^n \Omega^{ams}(\Gamma + n\gamma) \tag{4.3.26}$$

$$F_{\text{halo}}^{\text{ams}} := \prod_{k>0} (1 - (-1)^{k|\langle \Gamma, \gamma \rangle|} q^{-k})^{k|\langle \Gamma, \gamma \rangle| \Omega(k\gamma)}. \tag{4.3.27}$$

Since (for sufficiently small $\mathcal{U}$) our path does not cross any walls of marginal stability the two partition functions above must be equal:

$$F(\Gamma; t_{ms}^{+}) = F(\Gamma; t_{ams}^{+}). \tag{4.3.28}$$

Combining this continuity requirement with the above factorization statements leads to some interesting constraints on BPS indices.

Note first that since there are no walls of marginal stability in the unstable region $F(\Gamma; t)$ cannot jump in this region. This suggests that $F_{\text{core}}^{\text{ms}}$ and $F_{\text{core}}^{\text{ams}}$ must be identical, but that is not quite the case because the charges live in a local system. In stating (4.3.28) we have implicitly assumed that the local system has been trivialized throughout the closure of the stable region in $\mathcal{U}$. Therefore, we must choose a "cut" in the unstable region. (See Figure 4.8 and Section 4.3.8 below.) Taking into account the monodromy of the local system we see that instead

$$F_{\text{core}}^{\text{ms}} = q^{-I} F_{\text{core}}^{\text{ams}} \tag{4.3.29}$$

for some integer I. Equating the coefficient of q^n on both sides gives:

$$\Omega^{ms}(\Gamma + n\gamma) = \Omega^{ams}(\Gamma + (n + I)\gamma). \tag{4.3.30}$$

Now, equations (4.3.28) and (4.3.29) together would seem to imply

$$F^{\rm ams}_{\rm halo} = q^{-I} F^{\rm ms}_{\rm halo} \tag{4.3.31}$$

and indeed formal manipulation of the product formulae above lead to such an identity with

$$I := |\langle \Gamma, \gamma \rangle| \sum_{k=1}^{\infty} k^2 \Omega(k\gamma). \tag{4.3.32}$$

However, we must stress that (4.3.31) is only a formal identity! The left-hand side is a series in negative powers of q. On the other hand, the right-hand side is a series in positive powers of q times q^{-I}, and thus the power series is bounded below. This necessarily implies that the power series is bounded both above and below and moreover that $F^{\rm ms}_{\rm halo}$, and $F^{\rm ams}_{\rm halo}$ must be *polynomials* and finally that $I \geq 0$ with $I = 0$ only when $F^{\rm ms}_{\rm halo} = F^{\rm ams}_{\rm halo}$ is a constant in q. Thus, if we are in a situation where (4.3.31) holds then we can conclude:

1. At a generic point of a discriminant locus, if $\Omega(k\gamma) \neq 0$ for some k then the quantity I defined in (4.3.32) must be *positive*. In particular, it is impossible to have $\Omega(k\gamma) \leq 0$ for all $k \in \mathbb{Z}$.

2. The spectrum must be such that the product

$$P(q) := \prod_{k>0} (1 - q^k)^{k\Omega(k\gamma)} \tag{4.3.33}$$

   is a *polynomial* in q.

The quantity $\sum_{k>0} k^2 \Omega(k\gamma)$ has a nice physical interpretation, associated with the key insights of [1] and [13]. It is the coefficient of the β-function for the $U(1)$ coupling defined by the direction γ in the charge lattice, that is

$$4\pi i \mu \frac{\partial}{\partial \mu} \tau = I \tag{4.3.34}$$

where μ is the low energy scale at which the coupling is measured. Thus, our conclusion would seem to be that, given the hypotheses of Section 4.3.1 the low energy field theory should be IR free.

Before stating this conclusion we must hasten to add that there is a logical gap in the above derivation. The difficulty is that one must be careful because manipulation with formal power series in q, q^{-1} can be tricky. As a simple example note that

$$(\sum_{n \in \mathbb{Z}} q^n)(1 - q) = 0,$$

so formal power series can have zero-divisors. From the mathematical standpoint we must consider three cases: In the first case, $F^{\rm ms}_{\rm halo}$ is a polynomial in q and the above reasoning holds. In the second case $F^{\rm ms}_{\rm halo}$ is a rational function. In the third case $F^{\rm ms}_{\rm halo}$ is an infinite product.

We will have nothing to say about the third case, other than to note that it can happen. (For example the $D0$ halo factor around a $D6$ brane is a copy of the McMahon function [5].) The second case, where $F^{\rm ms}_{\rm halo}$ is a rational function would seem to be very physical since while (half)hypermultiplets have $\Omega = +1$, vectormultiplets have $\Omega = -2$, which can lead to nontrivial denominators in the product formula for $F^{\rm ms}_{\rm halo}$. Somewhat surprisingly, as we discuss in Section 4.6 below, in all examples we have analyzed, points in moduli space leading to massless vectormultiplets violate the hypotheses stated in Section 4.3.1. Indeed, we show in Section 4.3.9 below that the second case leads to some rather peculiar physical predictions, and we suspect there are no examples.

Thus we conclude that *if we assume: 1.) the hypotheses of Section 4.3.1 2.) the low energy effective field theory is a conventional field theory, and 3.) the halo factor is not an infinite product, then $I > 0$ and (4.3.33) is a polynomial in q.*

Remark: The formula (4.3.32) for I can also be derived from the Kontsevich-Soibelman wall-crossing formula using the relation between that formula and monodromy pointed out in [50] and elaborated in [38]. In particular, the requirement that the product of KS transformations denoted $U_{k\gamma}$ in [38] in fact has a well-defined action on $F(\Gamma; t)$ leads to an alternative argument in favor of (4.3.33). A version of this argument is given in Section 4.7.1 below.

4.3.5 The Fermi Flip

In this section we describe one way in which the Hilbert spaces of halo states can change upon crossing conjugation walls.

Restricting attention to the halo subsector of Hilbert space the discussion of subsection 4.3.2 shows that for $t = t^+_{ms}$ the Hilbert space of halo states of total charge $\Gamma + n\gamma$ is

$$\mathcal{H}(\Gamma + n\gamma; t)|_{t\in\mathcal{P}_{ms}} \simeq \oplus_{m\geq 0}\Big(\mathcal{H}^{ms}(\Gamma + (n-m)\gamma) \otimes \Big\{\otimes_{\ell\geq 1}\mathcal{F}[(J_{\Gamma,\ell\gamma}) \otimes \mathcal{H}(\ell\gamma)]\Big\}_m\Big). \quad (4.3.35)$$

The Fermi Fock spaces are graded by a $U(1)$ charge corresponding to γ and the subscript m means the subspace of the Fermi Fock space of total $U(1)$ charge $m\gamma$. For $t \in \mathcal{P}_{ms}$ only halo particles with charges parallel to γ can contribute, and in particular the only nonzero contributions come from $m \geq 0$. The sum on m comes about because it is possible to have different core charges.

After crossing the wall $\mathcal{S}(n\gamma,\Gamma)$ the Hilbert space becomes:

$$\mathcal{H}(\Gamma+n\gamma;t)|_{t\in\mathcal{P}_{ams}} \simeq \oplus_{m\geq 0}\Big(\mathcal{H}^{ams}(\Gamma+(n+m)\gamma)\otimes\Big\{\otimes_{\ell\geq 1}\mathcal{F}[(J_{\Gamma,\ell\gamma})\otimes\mathcal{H}(-\ell\gamma)]\Big\}_{-m}\Big). \quad (4.3.36)$$

Now, it is possible for (4.3.35) and (4.3.36) to be isomorphic through the following mechanism. For simplicity of exposition suppose that $\mathcal{H}^{ms}(\Gamma)\neq\emptyset$ but $\mathcal{H}^{ms}(\Gamma+n\gamma)=\emptyset$ for $n\neq 0$. It follows from (4.3.30) that $\Omega^{ams}(\Gamma+m\gamma)$ can only be nonzero for $m=I$, and this suggests that $\mathcal{H}^{ams}(\Gamma+m\gamma)=0$ unless $m=I$. We will make that assumption. Then (4.3.35) and (4.3.36) simplify to

$$\mathcal{H}(\Gamma+n\gamma;t)|_{t\in\mathcal{P}_{ms}} \cong \mathcal{H}^{ms}(\Gamma)\otimes[\otimes_{\ell\geq 1}\mathcal{F}[(J_{\Gamma,\ell\gamma})\otimes\mathcal{H}(\ell\gamma)]]_n \quad (4.3.37)$$

$$\mathcal{H}(\Gamma+n\gamma;t)|_{t\in\mathcal{P}_{ams}} \cong \mathcal{H}^{ams}(\Gamma+I\gamma)\otimes[\otimes_{\ell\geq 1}\mathcal{F}[(J_{\Gamma,\ell\gamma})\otimes\mathcal{H}(-\ell\gamma)]]_{n-I} \quad (4.3.38)$$

In (4.3.37) we must have $n\geq 0$ while in (4.3.38) we must have $n-I\leq 0$. Thus, there can only be non-empty spaces for $0\leq n\leq I$. This means that the Fock space (4.3.19) must be finite dimensional, i.e. the halo particles of charge proportional to γ must be fermionic.

If we put $n=I$ and equate (4.3.37) with (4.3.38) then we find that

$$\mathcal{H}^{ams}(\Gamma+I\gamma)\cong\mathcal{H}^{ms}(\Gamma)\otimes\mathcal{L} \quad (4.3.39)$$

where $\mathcal{L}$ is the complex line:

$$\mathcal{L}=\Lambda^{max}\Big(\oplus_{\ell\geq 1}(J_{\Gamma,\ell\gamma})\otimes\mathcal{H}(\ell\gamma)\Big). \quad (4.3.40)$$

One can view (4.3.40) as the entirely filled Fermi Fock space, which of course furnishes a "flipped Fermi sea." More generally, equating the Hilbert spaces at $t=t_{bst}$ we find

$$\mathcal{L}\otimes\Big\{\otimes_{\ell\geq 1}\mathcal{F}[(J_{\Gamma,\ell\gamma})\otimes\mathcal{H}(-\ell\gamma)]\Big\}_{n-I}\cong\Big\{\otimes_{\ell\geq 1}\mathcal{F}[(J_{\Gamma,\ell\gamma})\otimes\mathcal{H}(\ell\gamma)]\Big\}_n \quad (4.3.41)$$

The equation (4.3.41) suggests the following interpretation. We should associate to the halo particles a Clifford algebra.[7] On the LHS of (4.3.41) we have a subspace of a Fock space with creation operators associated to particles of charge $-\ell\gamma$, $\ell>0$. On the RHS we have a subspace of a Fock space with creation operators associated to particles of charge $\ell\gamma$, $\ell>0$. The isomorphism corresponds to a Bogolyubov transformation that exchanges creation and annihilation operators. The transformation of Fock vacua may be referred to as "flipping the Fermi sea." An example of this situation is the conifold point, which we consider in greater detail in Section 4.4. In that case the only available halo particles have charge $\pm\gamma$ and form a hypermultiplet, so all the assumptions are met.

[7] Presumably this is simply the algebra of BPS states [51, 52, 53].

The Fermi flip nicely accounts for how the BPS spaces change across conjugation walls when the halo particles are all fermionic. In cases when $\mathcal{H}(\ell\gamma)$ contains bosonic degrees of freedom for some ℓ, we do not expect an isomorphism between $\mathcal{H}(\Gamma + n\gamma; t)|_{t\in\mathcal{P}_{ms}}$ and $\mathcal{H}(\Gamma + n\gamma; t)|_{t\in\mathcal{P}_{ams}}$ and in fact in section 4.3.7 we will see that in general it cannot be the case. (Nevertheless, the index is continuous.)

4.3.6 The Fadeout

The Fermi flip described in section 4.3.5 implies that as t crosses the conjugation wall $\mathcal{S}(n\gamma, \Gamma)$ the supergravity description of the boundstate changes in an interesting way. Consider first the case $n = I$. For $t \in \mathcal{P}_{ms}$ there is a core charge at a single point in $\mathbb{R}^3$ and it is surrounded by a halo of particles with charges parallel to γ of total charge I. After crossing the BST wall we have a single core charge of total charge $\Gamma + I\gamma$ and *no* halo particles! More generally, for $0 \leq n \leq I$, a state with core charge Γ and halo particles with charge parallel to γ of total halo charge $n\gamma$ evolves into a state with core charge $\Gamma + I\gamma$ and halo particles with charge anti-parallel to γ with total halo charge $-(I-n)\gamma$. This sounds like a very discontinuous process, but, remarkably, the process is in fact physically smooth. Nothing violent happens to our boundstates. In particular we stress that the boundstate radius $R_n(t)$ is finite and smooth in the neighborhood of t_{bst}.

First, let us address how a state with halo particles of charge parallel to γ can smoothly evolve into a state with halo particles of charge anti-parallel to γ. Recall that as t crosses the conjugation wall the central charge $Z(\gamma; t(\vec{x}))$ vanishes at the halo radius (in the shell approximation). Now, let us consider a probe BPS halo particle of charge γ in an attractor background of charge $\Gamma + n\gamma$. It has Lagrangian [10]

$$L = -2e^U |Z(\gamma; t(\vec{x}))|(1 - \cos(\alpha_\gamma - \alpha)) \tag{4.3.42}$$

where α_γ is the phase of $Z(\gamma; t(\vec{x}))$ and α is the phase of $Z(\Gamma + n\gamma; t(\vec{x}))$. The term proportional to the cosine comes from the interaction with the electromagnetic field, and the other term comes from the rest mass of the BPS particle. Since $Z(\gamma; t(\vec{x})) \to 0$ on the halo radius $R_n(t)$ as t crosses $\mathcal{S}(n\gamma, \Gamma)$ we see that the halo particles have both a mass and coupling to the background gauge fields which approaches zero. Thus, as t crosses the BST wall $\mathcal{S}(n\gamma, \Gamma)$ the halo particles decouple from any possible *local* physical measurement! We call this process the *fadeout*.

The fadeout takes care of the halo particles, but the reader might still be disturbed because our description of the core charge has changed discontinuously as t crosses the BST wall, namely a core of charge Γ appears to have jumped suddenly to a core of charge $\Gamma + I\gamma$. The process is

in fact physically smooth, but this aspect is best explained after we have discussed monodromy in Section 4.3.8

4.3.7 Spin character

Hilbert spaces of BPS states are representations of the spatial rotation group $SU(2)$. As such they are completely classified by their character. In this section write out what the description of halo states of section 4.3.2 above implies for the spin character.

To begin, let us define the spin character of halo particles to be:

$$\mathrm{Tr}_{\mathcal{H}(\ell\gamma;t)}(-z)^{2J_3} := \Omega(\ell\gamma;-z;t) = \sum_{-M_\ell}^{M_\ell} a_{m,\ell} z^m \tag{4.3.43}$$

By assumption the integers $a_{m,\ell}$ are independent of $t \in \mathcal{U}$. Because of our $\mathbb{Z}_2$ grading the particles contributing to m even (for which $a_{m,\ell} > 0$) correspond to *fermionic* particles in the Fock space while those contributing to m odd (for which $a_{m,\ell} < 0$) correspond to *bosonic* particles in the Fock space. In particular, if $M_\ell \leq 1$ then a_0 counts *hypermultiplets* in four dimensions and $a_{\pm 1}$ counts *vectormultiplets* in four dimensions. By rotational invariance $a_{m,\ell} = a_{-m,\ell}$. By CPT invariance $a_{m,\ell} = a_{m,-\ell}$. In particular, $\Omega(\ell\gamma;y;t) = \Omega(-\ell\gamma;y;t) = \Omega(\ell\gamma;y^{-1};t)$.

Now we introduce a generating function for the spin characters of the positive halo Fock spaces:

$$F(q,y;t) := \sum_{n\in\mathbb{Z}} q^n \mathrm{Tr}_{\mathcal{H}^{halo}(\Gamma+n\gamma;t)} y^{2J_3} \tag{4.3.44}$$

This is a formal power series in q whose coefficients are finite Laurent polynomials in y. The contribution to this generating function from boundstate halo particles of charge $\pm\ell\gamma$ is

$$F^{(\pm\ell)}(q,y) = \prod_{m=-M_\ell}^{M_\ell} \prod_{j=-J_{\Gamma,\ell\gamma}}^{J_{\Gamma,\ell\gamma}} (1+(-1)^m y^{2j+m} q^{\pm\ell})^{a_{m,\ell}} \tag{4.3.45}$$

and in the spirit of our discussion around (4.3.22)-(4.3.25), we can write down the full generating function at points t^+_{ms} and t^+_{ams}:

$$F(q,y;t^+_{ms}) = \Omega^{ms}(\Gamma;y) \prod_{\ell=1}^{\infty} F^{(\ell)}(q,y) \tag{4.3.46}$$

$$F(q,y;t^+_{ams}) = \Omega^{ams}(\Gamma;y) \prod_{\ell=1}^{\infty} F^{(-\ell)}(q,y) \tag{4.3.47}$$

where $\Omega^{ms}(\gamma;y)$ is the spin character of $\mathcal{H}^{ms}(\Gamma)$, etc.

It is easy to see that when γ has bosonic internal degrees of freedom, $F(q,y;t^+_{ms})$ is an infinite series in positive powers of q. The cancellation mechanism mentioned below (4.3.33)

is no longer operative. Similarly, in this case $F(q,y;t^+_{ams})$ will be an infinite series in negative powers of q. Thus, (4.3.46) and (4.3.47) can never be equal. We conclude that when halo particles include bosonic degrees of freedom the spin character must change across conjugation walls.

On the other hand when the only BPS particles with charge parallel to γ are fermionic, we can apply the analog of (4.3.31), which states that:

$$\prod_{\ell=1}^{\infty} F^{(\ell)}(q,y) = q^I \prod_{\ell=1}^{\infty} F^{(-\ell)}(q,y), \tag{4.3.48}$$

In this case, the spin character will be smooth across conjugation walls provided the analog of (4.3.29), is satisfied:

$$\sum_m \Omega^{ms}(\Gamma + m\gamma; y) q^m = \sum_m \Omega^{ams}(\Gamma + m\gamma; y) q^{m-I}. \tag{4.3.49}$$

which would follow, for example, if $\mathcal{H}^{ms}(\Gamma + n\gamma) \cong \mathcal{H}^{ams}(\Gamma + (n+I)\gamma)$ upon parallel transport with the flat connection. When all halo particles are fermionic this is quite a reasonable condition, as we explain in section 4.3.8.

4.3.8 Monodromy

It is now time to understand the meaning of the identity (4.3.30). First let us note that the choice of Γ is rather general. After all, there will be many charges Γ which are not local with γ and furthermore support regular attractor points and hence support single-centered black hole solutions in the supergravity approximation. Indeed in the local system of charges Λ (trivialized on $\widetilde{\mathcal{M}}$), there should be an open set of such charges in $\Lambda \otimes \mathbb{R}$. Since the charges are sections

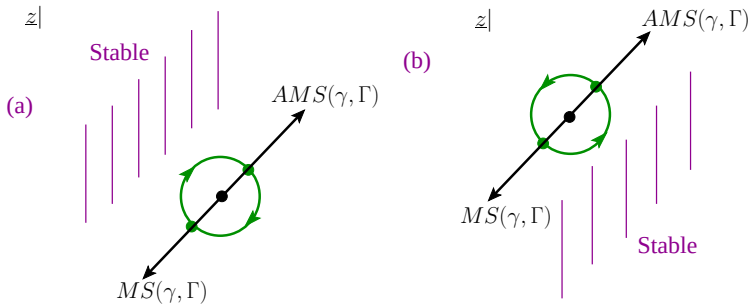

Figure 4.8: A figure of the z-plane where $Z(\gamma;t) = z$. When $\langle\Gamma,\gamma\rangle < 0$ the stable region is the shaded region in (a), and when $\langle\Gamma,\gamma\rangle > 0$ it is the shaded region in (b). The transformation of charge $\Gamma \to \Gamma + I\gamma$ corresponds to a monodromy transformation around the closed paths indicated in green.

of a local system Λ when comparing indices in an equation such as (4.3.30) we must specify a path along which charges have been parallel transported. We have implicitly assumed that the

charges are related by parallel transport through the stable region. On the other hand, the BPS Hilbert space should remain "constant" in the unstable region, and hence equation (4.3.30) is naturally explained if Λ undergoes a monodromy transformation

$$\Gamma \to M \cdot \Gamma = \Gamma + I\gamma. \tag{4.3.50}$$

along a closed path winding once around $\mathcal{Z}(\gamma)$. The direction of the path is determined by noting that in the argument used in section 4.3.4 we parallel transport the charge Γ from $MS(\gamma, \Gamma)$ to $AMS(\gamma, \Gamma)$ through the stable region. Since the spaces are "constant" in the unstable region a path beginning on $AMS(\gamma, \Gamma)$ and passing through the unstable region does not change Γ, and hence we should consider a closed path that begins on $AMS(\gamma, \Gamma)$, first passes through the unstable region to $MS(\gamma, \Gamma)$ and then returns through the stable region back to $AMS(\gamma, \gamma)$, as shown in figure 4.8. Thus, the sign of the winding is correlated with the sign of $\langle \Gamma, \gamma \rangle$ and hence we can say that the monodromy transformation for a *clockwise* oriented curve of winding number one is

$$\Gamma \to M \cdot \Gamma = \Gamma + \bar{I}\gamma. \tag{4.3.51}$$

where

$$\bar{I} = \langle \Gamma, \gamma \rangle \sum_{k=1}^{\infty} k^2 \Omega(k\gamma) \tag{4.3.52}$$

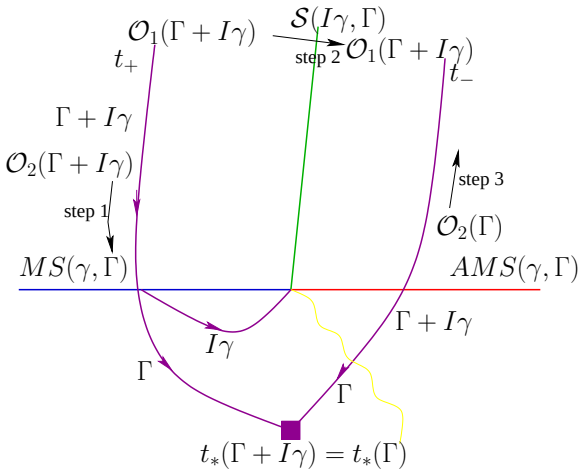

Figure 4.9: The steps in the Gedankenexperiment shown in terms of paths on moduli space. The conjugation wall is shown in green. There is a cut for the local system Λ shown in yellow, and the attractor flows are illustrated in purple. The entire experiment involves parallel transport of the charge lattice once around the locus $\mathcal{Z}(\gamma)$ in $\mathcal{M}$.

Monodromy and the Fermi Flip: A Gedankenexperiment

A monodromy transformation of the form (4.3.51) around $\mathcal{Z}(\gamma)$ also nicely explains how the Fermi flip transformation of Section 4.3.5 above is in fact a continuous physical process. Again, let us work locally on moduli space in the neighborhood $\mathcal{U}$ of $\mathcal{Z}(\gamma)$. Let us imagine there are two observers $\mathcal{O}_1$ and $\mathcal{O}_2$ in a laboratory located very far from the halo core, effectively at infinite radius. The vectormultiplet moduli at this radius are denoted t. Let us suppose the background modulus t is initially at t^+_{bst}, on the $\mathcal{P}_{ms}$ side of $\mathcal{S}(I\gamma,\Gamma)$. Both $\mathcal{O}_1$ and $\mathcal{O}_2$ can measure the total charge within a fixed radius r. (For example, they can measure fluxes with local test particles and integrate the flux.) They both measure the charge of the boundstate to be $\Gamma + I\gamma$. We now consider a four step experiment. In step one, one observer, say $\mathcal{O}_2$, travels radially inward toward the core (potentially observing attractor flow of the vectormultiplet moduli along the way). As $\mathcal{O}_2$ passes through the radius $R_n(t^+_{bst})$ there will be some mild disturbance, but, because of the fadeout phenomenon, this disturbance will be arbitrarily mild. For $r < R_n(t^+_{bst})$, as r decreases to the horizon at $r = 0$ $\mathcal{O}_2$ measures total charge Γ, and concludes that the core has charge Γ. In step two, observer $\mathcal{O}_1$ changes the vectormultiplet moduli t, crossing the conjugation wall from t^+_{bst} to t^-_{bst} proceeding from $\mathcal{P}_{ms}$ to $\mathcal{P}_{ams}$. Nothing discontinuous has happened either to $\mathcal{O}_1$ or to $\mathcal{O}_2$. In particular $\mathcal{O}_1$ continues to measure charge $\Gamma + I\gamma$ of the boundstate. At the same time, $\mathcal{O}_2$ also sees nothing discontinuous happening and continues to measure the charge Γ. In step three the observer $\mathcal{O}_2$ travels radially outward from $r = 0$ back to the laboratory of $\mathcal{O}_1$. In this third step $\mathcal{O}_2$ notes that no halo is encountered. Now, for the final step four of our experiment $\mathcal{O}_1$ and $\mathcal{O}_2$ compare their results for the electromagnetic charge of the core. $\mathcal{O}_2$ agrees that there is a single-centered boundstate, and declares its charge to be Γ, while $\mathcal{O}_1$ insists that the charge is $\Gamma + I\gamma$. They are both right, because the Gedankenexperiment we have just described involves a closed loop in moduli space around $\mathcal{Z}(\gamma)$ as shown in figure 4.9. In our description of the Fermi flip in section 4.3.5 we used the viewpoint of $\mathcal{O}_1$. However, in order to investigate if something discontinuous has happened to the core while crossing $\mathcal{S}(I\gamma,\Gamma)$ we must send out the observer $\mathcal{O}_2$ to report core activity from the scene of the crime. As we have explained, $\mathcal{O}_2$ saw nothing dramatic happening.

Area code walls and basins of attraction

There is an interesting interpretation of conjugation walls in terms of walls between basins of attraction for attractor flow, *i.e.* "area code walls" [54]. This relation will be used in the covering space description of our Gedankenexperiment in Section 4.3.8 below.

Let us assume that $\Gamma + I\gamma$ has at least one regular attractor point. Consider the attractor flows for $\Gamma + I\gamma$ on the covering space $\widetilde{\mathcal{M}}$. The wall $\widetilde{\mathcal{S}}(I\gamma, \Gamma)$ is a set of attractor flows. If this wall separates $\widetilde{\mathcal{M}}$ into more than one component then, since attractor flows cannot intersect except at a regular attractor point or a singular point the attractor flows cannot cross the wall $\widetilde{\mathcal{S}}(I\gamma, \Gamma)$.

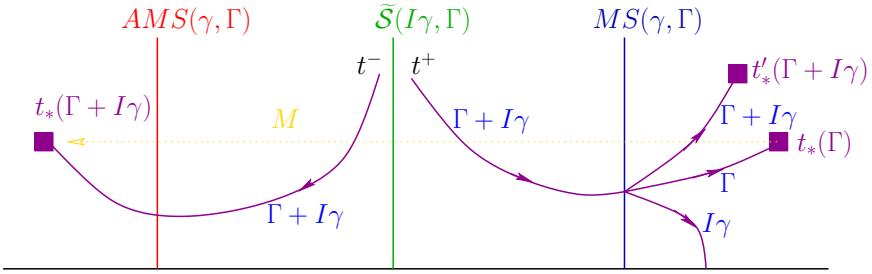

Figure 4.10: Illustrating why the conjugation wall $\widetilde{\mathcal{S}}(I\gamma, \Gamma)$ is an area code wall. The attractor flow for $\Gamma + I\gamma$ (shown in purple) from t^+ has a split attractor flow, splitting into flows for Γ and $I\gamma$. We assume the attractor flow for Γ has a regular attractor point at $t_*(\Gamma)$. In the Fermi flip scenario the action of the monodromy group M (shown in gold) on $t_*(\Gamma)$ produces the regular attractor point $t_*(\Gamma + I\gamma)$ for flows which begin from t^-. Note that t^- is on the other side of the conjugation wall $\widetilde{\mathcal{S}}(I\gamma, \Gamma)$. On the other hand, the $\Gamma + I\gamma$ flow from t^+ can be continued from its intersection with $MS(\gamma, \Gamma)$ and, unless $t_*(\Gamma)$ is a regular attractor point of rank two, the flow will continue and end on a point other than $t_*(\Gamma)$. We have denoted this distinct point by $t'_*(\Gamma + I\gamma)$. We claim that $t'_*(\Gamma + I\gamma)$ is also distinct from $t_*(\Gamma + I\gamma)$, and therefore $\widetilde{\mathcal{S}}(I\gamma, \Gamma)$ separates basins of attraction for $\Gamma + I\gamma$ flow. In our local model, where the inverse attractor flow on $\widetilde{\mathcal{S}}(I\gamma, \Gamma)$ extends infinitely far upwards, the flow cannot cross back to the point $t_*(\Gamma + I\gamma)$ on the left because in order to do so it would have to cross $\widetilde{\mathcal{S}}(I\gamma, \Gamma)$, which is impossible. (In addition it would also have to cross two walls $MS(\gamma, \Gamma)$ and $AMS(\gamma, \Gamma)$, which is also impossible by Property 1 of Appendix A.) Thus - in our local model - if the attractor flow for $\Gamma + I\gamma$ from t^+ terminates on a regular attractor point it must be a distinct point from $t_*(\Gamma + I\gamma)$.

It is difficult to give a completely general argument that $\widetilde{\mathcal{S}}(I\gamma, \Gamma)$ is an area code wall because one must take into account global properties of covering space. However, a very natural scenario is illustrated and explained in figure 4.10. In this case, $\widetilde{\mathcal{S}}(I\gamma, \Gamma)$ is a wall between basins of attraction for the flow $\Gamma + I\gamma$.

Gedanken Again

Since discussions of this nature are apt to cause confusion it is worthwhile to describe the same experiment using the language of the covering space $\widetilde{\mathcal{U}}$ of $\mathcal{U}$. Now we must take into account the action of a gauge transformation by a generator M of the covering (i.e. modular) group. Under this transformation all physical quantities are invariant, so for example

$$Z(M \cdot \Gamma; M \cdot t) = Z(\Gamma; t) \tag{4.3.53}$$

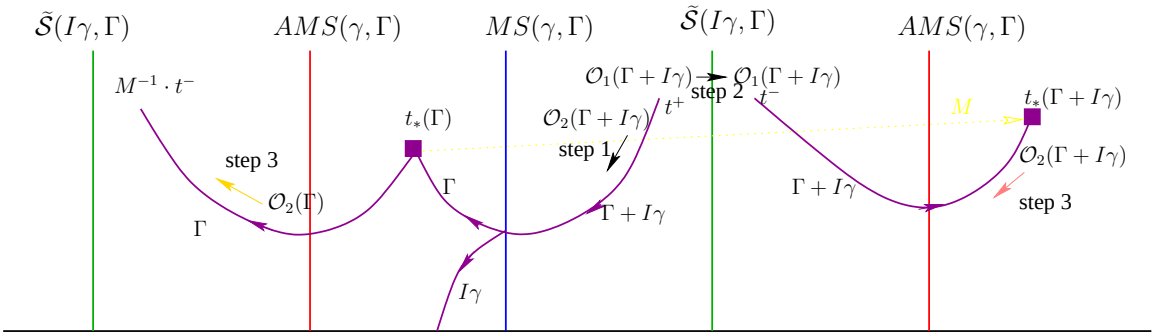

Figure 4.11: Steps in the Gedankenexperiment as described in the covering space. The blue vertical lines are the marginal stability walls, the red vertical lines are the anti-marginal stability walls and the green vertical lines are the conjugation walls. Attractor flows are shown in purple. The group of Deck transformations is generated by M and corresponds to a shift by $+1$. In step 3 $\mathcal{O}_2$ can choose to reverse the attractor flow from $t_*(\Gamma)$ as indicated in gold. Alternatively, $\mathcal{O}_2$ can make a gauge transformation while at $r=0$ and reverse the attractor flow from $t_*(\Gamma+I\gamma)$ as indicated in pink. Note the discontinuous nature of the attractor flow as t crosses the conjugation wall.

and,

$$\mathcal{H}(M\cdot\Gamma;M\cdot t)\cong\mathcal{H}(\Gamma;t). \tag{4.3.54}$$

We illustrate the Gedankenexperiment expressed in the language of the covering space in figure 4.11. A crucial new point comes at step 3 where $\mathcal{O}_2$ makes the return trip in $\mathbb{R}^3$ radially back outward to infinity. Now, if $\mathcal{O}_2$ traverses the inverse attractor flow for charge $\Gamma+I\gamma$ from $t_*(\Gamma)$, as shown in step 3 of figure 4.11 she measures the charge Γ of the core, but ends up expressing her measurements in terms of the point in $M^{-1}\cdot t^-_{bst}\in\widetilde{\mathcal{U}}$ which differs from the point t^-_{bst} used by $\mathcal{O}_1$. In order to compare results with $\mathcal{O}_1$ the experimenters must be on the same page - which in our case literally corresponds to being on the same sheet of the covering space. One of the two experimenters must transform the data by the action of $M^{\pm1}$. Once this is done they will *agree* on the total charge of the single-centered state, as they must, since the local system Λ has been trivialized on $\widetilde{\mathcal{U}}$. Alternatively, as indicated by the pink arrow in step three of figure 4.11 $\mathcal{O}_2$ might make a gauge transform while at $r=0$ in order for the return trip to $r=\infty$ to take her data to t^-_{bst}. Thus she starts not from $t_*(\Gamma)$ but rather from its modular image

$$t_*(\Gamma+I\gamma)=t_*(M\cdot\Gamma)=M\cdot t_*(\Gamma) \tag{4.3.55}$$

It is at this point that $\mathcal{O}_2$ decides the core has charge $\Gamma+I\gamma$. She does not think this is a discontinuous change from step 2, because she has merely applied a gauge transformation. In step 4, $\mathcal{O}_1$ and $\mathcal{O}_2$ are now on the same page and once again, they agree on the value of the core charge.

Remark: Relation to the monodromy of the derived category

A formula for the autoequivalences in the derived category induced by monodromy around loci where branes become massless was conjectured in [55]. (See Conjecture 1 on page 6.) If an object $\mathbf{A}$ in the derived category becomes massless on a component of the discriminant locus $\mathcal{Z}$ (and we assume $\mathbf{A}$ corresponds to a single D-brane which is stable in some sufficiently small neighborhood $\mathcal{U}$ of $\mathcal{Z}$) then when one considers a loop in $\mathcal{U}$ around $\mathcal{Z}$ which winds once around $\mathcal{Z}$ the monodromy action on the objects in the derived category is claimed to be:

$$\mathbf{B} \to \mathrm{Cone}\left(\mathrm{Hom}(\mathbf{A},\mathbf{B})\otimes\mathbf{A}\to\mathbf{B}\right). \tag{4.3.56}$$

If one takes the Chern character of this equation, setting $\mathrm{ch}(\mathbf{A}) = k\gamma$ and $\mathrm{ch}(\mathbf{B}) = \Gamma$, then (4.3.56) becomes the standard Lefshetz formula

$$\Gamma \to \Gamma + \langle\Gamma, k\gamma\rangle k\gamma. \tag{4.3.57}$$

There is therefore some tension between (4.3.56) and our formula (4.3.50), (4.3.52). The latter involves a *sum* over all charges parallel to γ and is moreover weighted by the BPS index $\Omega(k\gamma)$. Since the group of autoequivalences of the derived category does not depend on a stability condition our expression involving I might seem somewhat strange. However, since we have explicitly assumed that the $\Omega(\gamma;t)$ are constant in the neighborhood of $\mathcal{Z}(\gamma)$ there is not a strict contradiction here. Clearly this point needs to be understood better.[8]

4.3.9 The case when $F_{\rm halo}$ is a rational function

Let us now return to the logical possibility, mentioned in Section 4.3.4, that $F^{\rm ms}_{\rm halo}(q)$ is a rational function of q. We will show that this leads to some physical predictions which are so peculiar that we suspect that there are no examples.

To begin we prove a small Lemma from High School Mathematics:

Lemma: Let $R(q)$ be a rational function of q with a convergent power series around $q=0$, $R(q) = 1+\mathcal{O}(q)$. Suppose R has poles, and all the poles lie on the unit circle. Then there exists a positive integer L such that $R(q)$ has a power series expansion of the form

$$R(q) = \sum_{r=0}^{L-1}\sum_{n\geq 0} a_{r,n} q^{r+nL} \tag{4.3.58}$$

where, for some r, n_0 we have $a_{r,n}\neq 0$ for all $n\geq n_0$.

[8] We thank Emanuel Diaconescu for useful discussions about this point.

Proof: First note that $R(q)$ has a continued fraction expansion of the form:

$$R(q) = r(q) + \sum_{\rho,s} \frac{a_{\rho,s}}{(1-\rho q)^s} \tag{4.3.59}$$

where $r(q)$ is a polynomial and the sum over ρ runs over a finite set of roots of unity and s runs over a finite set of positive integers. The coefficients $a_{\rho,s}$ are complex numbers.

Note that if ρ is an L^{th} root of unity then

$$\frac{1}{(1-\rho q)^s} = \sum_{r=0}^{L-1} \sum_{n\geq 0} p_r(n) q^{r+nL} \tag{4.3.60}$$

where, for each r, $p_r(n)$ is a polynomial in n. ($p_r(n)$ might depend on r and is of order $(s-1)$). Now let L be any integer such that all ρ which occur in (4.3.59) are L^{th} roots of unity and observe that a non vanishing polynomial can have at most a finite number of roots ■

Now we claim that if $F^{\rm ms}_{\rm halo}$ is a rational function of q with poles on the complex q-plane, (as can happen if there are bosons in the halo) then $F(\Gamma;t)$ is a finite Laurent polynomial in q. In particular, $F^{\rm ms}_{\rm core}(q)$ is a finite Laurent polynomial in q whose set of zeroes includes the set of poles of $F^{\rm ms}_{\rm halo}(q)$ and $F^{\rm ms}_{\rm halo}(q^{-1})$, counted with multiplicity.

To prove this we need need three ingredients: First, as we have seen, it follows from the monodromy that we have (4.3.29), an identity of formal series in q, q^{-1}. Second, continuity of the index away from walls of marginal stability implies (4.3.28). Third, finiteness of the number of attractor flow trees implies that if we write $F^{\rm ms}_{\rm core}(q) = \sum b_m q^m$ and $F^{\rm ms}_{\rm halo}(q) = \sum c_n q^n$, then, for all N,

$$d_N = \sum_{n+m=N} b_m c_n \tag{4.3.61}$$

is a *finite* sum.

Now if $F^{\rm ms}_{\rm halo}(q)$ has a pole then by the Lemma above we know that for some L, r, n_0 we have $a_{r,n} \neq 0$ for all $n \geq n_0$ in the expansion:

$$F^{\rm ms}_{\rm halo}(q) = \sum_{r=0}^{L-1} \sum_{n\geq 0} a_{r,n} q^{r+nL} \tag{4.3.62}$$

Next, suppose the exponents of q in the expansion of $F^{\rm ms}_{\rm core}(q)$ is unbounded below. That is, $\{m | b_m \neq 0\}$ is unbounded below. Then choosing L as above, it must be that for some residue r' and some n_0' we have $b_{-r-nL} \neq 0$ for $n > n_0'$. Then the coefficient of $q^{r-r'}$ contains the infinitely many terms

$$\sum_{n > \max[n_0, n_0']} b_{-r'-nL} a_{r,n} \tag{4.3.63}$$

But this violates the ingredient 3 above, based on the finiteness of the number of attractor flow trees, and hence we conclude that $F^{\rm ms}_{\rm core}(q)$ has coefficients bounded blow.

On the other hand, $F^{\rm ams}_{\rm halo}(q) = F^{\rm ms}_{\rm halo}(q^{-1})$ so exactly the same reasoning implies that $F^{\rm ams}_{\rm core}(q)$ has coefficients bounded above. It now follows from equation (4.3.29) that $F^{\rm ms}_{\rm core}(q)$ is a finite Laurent polynomial. Applying the same reasoning and now using the equality of indexes, (4.3.28) shows that $F^{\rm ms}_{\rm core}(q)F^{\rm ms}_{\rm halo}(q)$ must also be a finite Laurent polynomial. Therefore, the poles of $F^{\rm ms}_{\rm halo}(q)$ must also be zeroes of $F^{\rm ms}_{\rm core}(q)$, including multiplicity. But the same reasoning applied to $q^I F^{\rm ms}_{\rm core}(q)F^{\rm ams}_{\rm halo}(q)$ shows that the poles of $F^{\rm ams}_{\rm halo}(q)$ must also be zeroes of $F^{\rm ms}_{\rm core}(q)$. This concludes the proof ■

Now, the above structure of $F_{\rm halo}$ and $F_{\rm core}$ is rather odd. The poles of $F_{\rm halo}$ only depend on γ. On the other hand, there is a wide choice of Γ's for which the rules of the game in Section 4.3.1 apply. Indeed, we expect that there is an open set of such elements in the space of charges. For all these charges $F_{\rm core}$ must be a Laurent polynomial with zeroes at the poles of $F_{\rm halo}$. This means that for some collection of roots of unity ρ (depending only on γ) we must have

$$\sum_{n\in\mathbb{Z}} \Omega^{ms}(\Gamma + n\gamma)\rho^n = 0 \tag{4.3.64}$$

for all charges Γ mutually nonlocal with respect to γ and supporting, say, single-centered attractor flows. Such constraints seem to us physically unreasonable. We certainly know of no examples, and we find the above a compelling argument that $F^{\rm ms}_{\rm halo}$ is either a finite Laurent expansion or an infinite product.

4.4 An Example: Conifold-Like Singularities

In this Section we discuss in detail a simple example of the setup of Section 4.3, in which the spectrum of massless states of charge γ consists of a single hypermultiplet. Such massless BPS states are present when a Calabi-Yau manifold develops a conifold singularity. In the IIA picture, the halos are made of light D2/D0 branes wrapping a rational curve, bound to a heavy core D6 brane filling the entire Calabi-Yau manifold. The local geometry of the Calabi-Yau near the rational curve is $\mathcal{O}(-1)\oplus\mathcal{O}(-1)\to\mathbb{P}^1$, and a hypermultiplet becomes massless at the singular point in the Kähler moduli space where the class of the rational curve vanishes. The massless state is a pure fermion with $\Omega(\gamma) = 1$ and from the discussion in Section 4.3.5 we know the structure of the halo bound states of core D6 with D2/D0 particles near the singularity, their BPS indices and Hilbert spaces. In particular, the Hilbert spaces of halo states transform smoothly across the conjugation walls through the Fermi flip of Section 4.3.5. The generating function of the index of such BPS states as a function of the Kähler moduli was first computed in [56, 57] from the quiver category point of view, generalizing the results in special chambers found in [58] and [59].

4.4.1 The resolved conifold

Since the puzzle of Section 4.1.1 was origianlly raised in [12], we now briefly review the setting of that puzzle and describe it's resolution. We will describe how the local geometry of the covering space near the conifold point fits together with the patch of the moduli space in which the volume of the entire Calabi-Yau is taken very large. (This was used in [12] to derive the partition function of D6/D2/D0 bound states using the semi-primitive wall crossing formula.) Consider the local limit of a Calabi Yau 3-fold X, with only one homology class, a rigid rational curve, dual to $\beta \in H^4(X,\mathbb{Z})$, remaining small. The Kähler parameter is $t = z\mathcal{P} + Le^{i\phi}\mathcal{P}'$, where $L \to \infty$ in the local limit, $\mathcal{P}\beta = 1$, for a positive integral class $\mathcal{P}$, and $\mathcal{P}'\beta = 0$ for a semi-positive class $\mathcal{P}'$. This parameterization is only valid for $\phi \in (0,\pi)$ and $Im(z) > 0$, which corresponds to a patch in the full covering space. In this patch the large volume expression for the periods can be used, and for instance (here Z_h is the holomorphic central charge):

$$Z_h(1) = \frac{1}{3}L^3 e^{3i\phi} \quad , \quad Z_h(\beta) = z \quad \text{and} \quad Z_h(dV) = -1. \tag{4.4.65}$$

BPS states with charges of the form $\Gamma_{m,n} = 1 - m\beta + ndV$, where dV is a generator of $H^6(X;\mathbb{Z})$, are realized as multicentered solutions in supergravity description. As argued in [12], in the neighborhood of the wall $\phi = \frac{1}{3}\arg z + \frac{\pi}{3}$ only the pure D6 brane with charge $\Gamma_0 = 1$ exists as a single centered object (out of the set of objects with charges of the form $\Gamma_{m,n}$). We are interested in configurations that consist of this core $D6$ charge surrounded by halos of $D2$-$D0$ particles $\gamma_{m,n} = -m\beta + ndV$. [12] computed the D6/D2/D0 partition function defined by

$$F(u,v;t_\infty) := \sum_{N\in\mathbb{Z},\beta\in H^4(X,\mathbb{Z})} u^N v^\beta \Omega(1-\beta+NdV;t_\infty), \tag{4.4.66}$$

in all chambers of the Kähler cone, parametrized in the local limit $L \to \infty$ by (z,ϕ). Fixing some value of z the ϕ interval can be divided into chambers, bounded by (anti)marginal stability walls $\mathcal{W}_n^m$ of D6 with $\gamma_{m,n}$ as in figure 4.12, found to be

$$\begin{aligned}
\mathcal{W}_n^m &= \{(z,\phi) : \phi = \frac{1}{3}arg(z+n/m) + \frac{\pi}{3}\} \\
\mathcal{W}_n^{-m} &= \{(z,\phi) : \phi = \frac{1}{3}arg(z-n/m)\} \\
\mathcal{W}_{-n}^{-m} &= \{(z,\phi) : \phi = \frac{1}{3}arg(z+n/m)\},
\end{aligned} \tag{4.4.67}$$

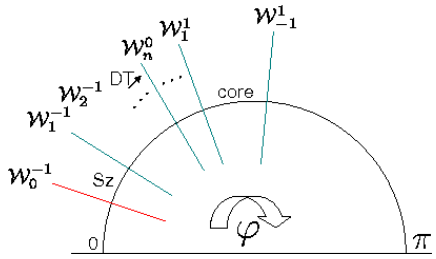

Figure 4.12: Arrangement of $\mathcal{W}_n^m$ walls along the ϕ line.

with both $n \geq 0$, $m \geq 0$. One can see that there is a path from $\mathcal{W}_n^m$ to $\mathcal{W}_{-n}^{-m}$ along the ϕ direction and we can form "positive" ("negative") halos around the D6 with particles $\gamma_{m,n}$ ($-\gamma_{m,n}$) near $\mathcal{W}_n^m$ ($\mathcal{W}_{-n}^{-m}$), but these halos cannot exist near $\mathcal{W}_{-n}^{-m}$ ($\mathcal{W}_n^m$). As all particles $\gamma_{m,n}$ are mutually local, we can focus on one of them to see the resolution. Also the index of particles with $|m| > 1$ is zero, so we can take some charge $\gamma_{1,n}$ as an example. The moduli space has conifold singularities at the loci $z = n$, where $\gamma_{\pm 1,\mp n}$ becomes massless. Locally around each point $z = n$ the moduli space will look like an infinite sheeted cover of the z-plane, described by a coordinate $u_n = \log(z - n)$, and the charge lattice will have the monodromy $\Gamma \mapsto \Gamma - \langle \Gamma,\ \gamma_{1,n} \rangle \gamma_{1,n}$. However, it is clear that in the large L limit for fixed u_n, ϕ, and to leading order in $1/L$, the periods will be given exactly as above. Therefore walls of marginal stability will approach being periodic in the u_n-plane for large L. We now describe the conjugation behavior in a single patch $Im(z) > 0,\ \phi \in (0, \pi)$, which will be repeated periodically in the u_n-plane.

The location of the conjugation walls for Γ with each of the $\gamma_{1,n}$ can be determined precisely in the limit of large L. In terms of the period vector $\Omega(t)$ the attractor flow of the total charge is determined by

$$2e^{-U}\mathrm{Im}(e^{-i\alpha}\Omega(t)) = -\tau\Gamma + H_\infty(t_\infty), \tag{4.4.68}$$

where τ is the parameter along the flow and $\Gamma = \Gamma_0 + \gamma_{1,n}$. We are interested in finding the locus t_∞, such that $t(\tau)$ will intersect the discriminant locus of vanishing $Z(\gamma_{1,n})$. Note that such a $t(\tau)$ necessarily satisfies

$$\mathrm{Im}\ \left[\bar{Z}(\gamma_{1,n}; t) Z(\Gamma_0; t)\right] = 0, \tag{4.4.69}$$

which immediately determines the value of τ at the intersection, due to the linearity of the attractor equation for the periods. Now we impose that this t is on the discriminant locus. Of course, to solve (4.4.69) and find the location of the conjugation wall we need to know the periods of D6 and D2/D0 close to the singularity, where they do get corrections from the D2/D0

becoming massless. It turns out that in the limit of large L the point $t(\tau)$ will also have an order L component in the direction of $\mathcal{P}'$. Thus in the neighborhood of the conjugation wall the corrections to the periods at $t(\tau)$ will still be of order $1/L$, which allows us to solve (4.4.69) in this limit (see Appendix E). The conjugation walls $\mathcal{S}(\gamma_{m,n}, \Gamma_0)$ turn out to be located at

$$\phi = \frac{1}{2} \arg\left(-\frac{m}{n} z - 1\right) + \frac{\pi}{2}, \tag{4.4.70}$$

in the patch of the Teichmüller space that we are discussing. Comparing (4.4.67) and (4.4.70) we see that the conjugation wall is indeed located in the region of bound state stability between the corresponding marginal and anti-marginal stability walls. Notice that the conjugation walls for all charges $k\gamma_{m,n}$ coincide, unlike the picture in z-plane near the singularity that we had before in Figure D.1. This is of course an artifact of using the large volume expression for the periods, or in other words as $L \to \infty$ all the conjugation walls for $k\gamma_{m,n}$ asymptote to (4.4.70) .

The particles $\gamma_{m,n}$ that inhabit the halos in this example have indices given by

$$\begin{aligned} &\Omega(\pm\beta + ndV) = 1, \text{for all } n, \\ &\Omega(ndV) = -2, \text{for } n \neq 0, \end{aligned} \tag{4.4.71}$$

where the D2/D0 states with charges $\pm\beta + ndV$ are the free hypermultiplet at the conifold point and its images under the large gauge transformations $B \mapsto B - n\mathcal{P}$. The attractor flows of objects with only D0 charge flow to large volume, where n D0 branes can form precisely one bound state, giving a massless vector multiplet. The expression (4.4.70) shows that there are no conjugation walls for the D6 brane with the D0 particles, confirming the general argument that $\Omega(\gamma)$ must be positive. This can also be seen directly: the attractor flow of the D6 with D0's can never reach the large volume point since then the period of the D6 brane would be increasingly well approximated by the large volume form, which grows without bound at large volume, contradicting the gradient flow.

On the other hand, $\gamma_{1,n}$ particles will have conjugation walls with the D6. Upon crossing those, a filled Fermi sea of n $\gamma_{1,n}$ particles appears at the halo radius. From Section 4.3.4 we know that the partition function for each individual halo particle $\gamma_{1,n}$ stays constant across the conjugation walls, so we can write the partition function for halos of all $\gamma_{1,n}$'s in all chambers of (4.4.67) as[9]

[9]The first two lines were already presented in [12], but the third line is a new result.

$$
\begin{aligned}
F(u,v;[\mathcal{W}_n^1\mathcal{W}_{n+1}^1]) &= \prod_{j=1}^{n}\left(1-(-u)^j v\right)^j \\
F(u,v;[\mathcal{W}_{n+1}^{-1}\mathcal{W}_n^{-1}]) &= \prod_{j>0}\left(1-(-u)^j\right)^{-2j}\left(1-(-u)^j v\right)^j \prod_{k>n}\left(1-(-u)^k v^{-1}\right)^k \\
F(u,v;[\mathcal{W}_{-n-1}^{-1}\mathcal{W}_{-n}^{-1}]) &= \left(\prod_{\ell=1}^{n}(u^\ell v)^\ell\right)\prod_{j>0}\left(1-(-u)^j\right)^{-2j}\prod_{j>0}\left(1-(-u)^j v^{-1}\right)^j \prod_{k>n}\left(1-(-u)^k v\right)^k ,
\end{aligned}
\tag{4.4.72}
$$

with $n \geq 0$. The last expression is evaluated in the chamber $[\mathcal{W}_{-n-1}^{-1}\mathcal{W}_{-n}^{-1}]$, where all halos of particles $-\gamma_{1,k}$, $k = 1..n$ have decayed after crossing $MS(\Gamma, -\gamma_{1,k})$ from stable to unstable side, and the factor $\prod_{\ell=1}^{n}(u^\ell v)^\ell$ accounts for the change of the core charge Γ_0 due to monodromy. It comes about through the identity

$$
(1-(-u)^\ell v)^\ell = (u^\ell v)^\ell\,(1-(-u)^{-\ell}v^{-1})^\ell, \tag{4.4.73}
$$

where the second factor is the contribution of all halos of $-\gamma_{1,n}$ particles. After crossing the conjugation walls $\mathcal{S}(\gamma_{1,\ell}, \Gamma_0)$, $\ell = 1..n$ the core charge changes according to the monodromy

$$
\Gamma_0 \to \Gamma_0 - \sum_{\ell=1}^{n}\langle\Gamma,\ \gamma_{1,\ell}\rangle\gamma_{1,\ell} = \Gamma_0 + \sum_{\ell=1}^{n}\ell\gamma_{1,\ell}. \tag{4.4.74}
$$

In particular, the "pure D6" brane with core charge Γ_0 *does not exist* after crossing the first conjugation wall. It gets replaced according to (4.4.74). Also note that to be more precise one might want to rewrite (4.4.72) using the left-hand side of (4.4.73) before crossing the wall $\mathcal{S}(\gamma_{1,\ell}, \Gamma_0)$, and right-hand side after crossing it. This is straightforward using (4.4.70) and (4.4.67), but the result would look rather messy which is why we don't do it here.

Note that for fixed z, taking ϕ to zero involves crossing infinitely many conjugation walls and marginal stability walls. In fact, the limits $\phi \to 0$ and $L \to \infty$ do not commute, since when ϕ is too close to 0, the imaginary part of the Kähler form becomes small, and the large volume approximation to the periods breaks down. Moreover,

$$
\lim_{\phi\to 0}\left(\lim_{L\to\infty} Z(u,v;t_\infty = z\mathcal{P} + Le^{i\phi}\mathcal{P}')\right)
$$

does not exist. To proceed further would require specifying a particular compact Calabi-Yau with a conifold degeneration.

4.5 Recombinaton walls

4.5.1 BPS index

In this Section we describe what happens to the BPS state when it crosses the recombination wall. Going back to Figure 4.6, let us first describe the $RW(\Gamma_2, \Gamma_3, \Gamma_4)$ in more detail. As mentioned above (4.2.13) at least one of $\Gamma_{ij,k}$ is nonzero. Using an identity $\Gamma_{ij,k}+\Gamma_{jk,i}+\Gamma_{ki,j} = 0$ we see that two of them have to be non-zero. Without loss of generality we have $\Gamma_{34,2} \neq 0$, $\Gamma_{24,3} \neq 0$. In what follows we also take $\Gamma_{23,4} \neq 0$ and comment on the case $\Gamma_{23,4} = 0$ in the end of this section. Although the definition appears to depend on the entire attractor flow, the position of this wall can be expressed entirely in terms of the periods evaluated at t_∞. By definition, the recombination wall consists of points $\{t|\tau_{ms}(\Gamma_{total}, \Gamma_2; t) = \tau_{ms}(\Gamma_{total}, \Gamma_3; t)\}$, as the central charge of Γ_4 will then also be aligned at the point $t(\tau_{ms})$. Thus by equation (3.0.4), it is given by

$$\mathrm{Im}\left[\frac{Z(\Gamma_3+\Gamma_4;t)Z(\bar{\Gamma_2};t)}{\langle\Gamma_3+\Gamma_4,\Gamma_2\rangle}\right] = \mathrm{Im}\left[\frac{Z(\Gamma_2+\Gamma_4;t)Z(\bar{\Gamma_3};t)}{\langle\Gamma_2+\Gamma_4,\Gamma_3\rangle}\right]. \tag{4.5.75}$$

This equation can be expressed in the form

$$\begin{aligned} &\mathrm{Im}\, Z(\Gamma_a;t)\bar{Z}(\Gamma_b;t) = 0, \text{ where} \\ &\Gamma_a = \Gamma_2\langle\Gamma_{total},\Gamma_3\rangle - \Gamma_3\langle\Gamma_{total},\Gamma_2\rangle \\ &\Gamma_b = \Gamma_{total}. \end{aligned} \tag{4.5.76}$$

(4.5.76) can be interpreted as the MS wall for charges Γ_a and Γ_b, satisfying $\langle\Gamma_a, \Gamma_b\rangle = 0$.

Returning to Figure 4.6, we see that the path $\mathcal{P}$ necessarily crosses the recombination wall, and we claim that the bound state $\Gamma_2 + (\Gamma_3 + \Gamma_4)$ on the left is transformed into two bound states $\Gamma_3 + (\Gamma_2 + \Gamma_4)$ and $\Gamma_4 + (\Gamma_3 + \Gamma_2)$ on the right. Figure 4.13 shows one of the two bound states on the right of the recombination wall. In [5, 9] this situation was illustrated in particular examples, and it was found that on the level of the index the transition is smooth, so that the two bound states on the right have exactly the same index as the one on the left. Note that our puzzle from the Introduction gets resolved since the bound state of $\Gamma_1 = \Gamma_3 + \Gamma_4$ and Γ_2 does not exist when t reaches t_{ams} and the total charge $\Gamma_2 + \Gamma_3 + \Gamma_4$ has a different realization.

Now we will explain in complete generality why the above claim is true: that is, why there are precisely two attractor trees on one side of the wall and one tree on the other side, and why

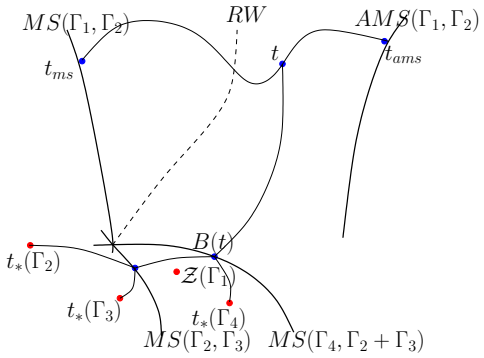

Figure 4.13: Bound state of charges $\Gamma_4 + (\Gamma_3 + \Gamma_2)$ on the right of the recombination wall.

the net BPS index is the same and also why the spin character does not change.[10] The locus where all three central charges align is complex codimension 1 in the moduli space, and we can parametrize the transverse plane with complex coordinate z, $z = 0$ being the alignment point. To understand the phenomenon it is enough to work in a small neighborhood of $z = 0$. There will be six walls of marginal stability for pairs of charges $(\Gamma_2, \Gamma_3+\Gamma_4)$, $(\Gamma_3, \Gamma_4+\Gamma_2)$, $(\Gamma_4, \Gamma_2+\Gamma_3)$, (Γ_2, Γ_3), (Γ_3, Γ_4), (Γ_4, Γ_2), all intersecting at $z = 0$. To understand which attractor trees exist on each side of the recombination wall, we will find the intersection points of the attractor flow with $(\Gamma_2, \Gamma_3 + \Gamma_4)$, $(\Gamma_3, \Gamma_4 + \Gamma_2)$, $(\Gamma_4, \Gamma_2 + \Gamma_3)$, and then see whether these points lie on the stable side of $MS(\Gamma_3, \Gamma_4)$, $MS(\Gamma_4, \Gamma_2)$ and $MS(\Gamma_2, \Gamma_3)$ respectively.

In a small neighborhood of $z = 0$ we can expand all central charges in powers of z to first order

$$Z(\Gamma_i; z) \approx Z(\Gamma_i; 0) + \partial_z Z(\Gamma_i; z)|_{z=0}\, z, \tag{4.5.77}$$

for $i = 2, 3, 4$. We will assume that the two terms in this expansion are nonzero. In this approximation the marginal stability walls can be written as

$$\begin{aligned} &MS(\Gamma_i, \Gamma_j) = \{z : \mathrm{Im}\, \rho_{ij}\, \bar{z} = 0\}, \\ &MS(\Gamma_i + \Gamma_j, \Gamma_k) = \{z : \mathrm{Im}\, (\rho_{ik} + \rho_{jk})\, \bar{z} = 0\}, \\ &\rho_{ij} := Z(\Gamma_i; 0)\, \partial_{\bar{z}} \bar{Z}(\Gamma_j; \bar{z})|_{\bar{z}=0} - Z(\Gamma_j; 0)\, \partial_{\bar{z}} \bar{Z}(\Gamma_i; \bar{z})|_{\bar{z}=0}. \end{aligned} \tag{4.5.78}$$

The recombination wall of the total charge $\Gamma_2 + \Gamma_3 + \Gamma_4$ is determined from (4.5.75) and can be written in parametric form as

$$z(s) = s \frac{(\rho_{23}\Gamma_{23,4} + \rho_{24}\Gamma_{3,42} + \rho_{43}\Gamma_{2,34})}{|\rho_{23}\Gamma_{23,4} + \rho_{24}\Gamma_{3,42} + \rho_{43}\Gamma_{2,43}|}, \tag{4.5.79}$$

[10] In some independent work Jan Manschot found another version of this proof [41].

where $s \in \mathbb{R}$ is a parameter. The attractor flows on the two sides of the recombination wall can be analogously written as

$$z_{\pm}(s) = (\pm i\varepsilon + s)\frac{(\rho_{23}\Gamma_{23,4} + \rho_{24}\Gamma_{3,42} + \rho_{43}\Gamma_{2,34})}{|\rho_{23}\Gamma_{23,4} + \rho_{24}\Gamma_{3,42} + \rho_{43}\Gamma_{2,43}|}, \tag{4.5.80}$$

where $\varepsilon > 0$ is a very small shift off the recombination wall. Let us choose for definiteness the plus sign in (4.5.80), find the value of s where the flow intersects the wall $MS(\Gamma_2, \Gamma_3 + \Gamma_4)$, and check if this point is on the stable side of the wall $MS(\Gamma_3, \Gamma_4)$. Some simple algebra yields the condition:

$$-\frac{\Gamma_{34}}{\Gamma_{34,2}}\frac{\mathrm{Im}\rho_{23}\bar{\rho}_{34} + \mathrm{Im}\rho_{34}\bar{\rho}_{42}}{\mathrm{Im}\rho_{42}\bar{\rho}_{23} + \mathrm{Im}\rho_{23}\bar{\rho}_{34} + \mathrm{Im}\rho_{34}\bar{\rho}_{42}} > 0 \tag{4.5.81}$$

If this condition is true, then the attractor flow $z_+(s)$ will cross $MS(\Gamma_2, \Gamma_3 + \Gamma_4)$ on the stable side of $MS(\Gamma_3, \Gamma_4)$ and the attractor tree $(\Gamma_2, (\Gamma_3, \Gamma_4))$ will exist. Using the definition of ρ_{ij} from (4.5.78) together with the fact that all the $Z(\Gamma_i, 0)$ have the same phase, we can, after a bit more algebra, rewrite (4.5.81) as

$$-\frac{\Gamma_{34}}{\Gamma_{34,2}}\frac{|Z(\Gamma_3;0)| + |Z(\Gamma_4;0)|}{|Z(\Gamma_2;0)| + |Z(\Gamma_3;0)| + |Z(\Gamma_4;0)|} > 0. \tag{4.5.82}$$

Repeating the calculation for the two remaining trees $(\Gamma_3, (\Gamma_4, \Gamma_2))$ and $(\Gamma_4, (\Gamma_2, \Gamma_3))$ and getting rid of positive factors we get

$$\begin{aligned}
(\Gamma_2, (\Gamma_3, \Gamma_4)): &\quad -\Gamma_{34}\,\Gamma_{34,2} > 0 \\
(\Gamma_3, (\Gamma_4, \Gamma_2)): &\quad -\Gamma_{42}\,\Gamma_{42,3} > 0 \\
(\Gamma_4, (\Gamma_2, \Gamma_3)): &\quad -\Gamma_{23}\,\Gamma_{23,4} > 0.
\end{aligned} \tag{4.5.83}$$

This is the main result of the above calculation. Taking into account that

$$\Gamma_{34}\,\Gamma_{34,2} + \Gamma_{42}\,\Gamma_{42,3} + \Gamma_{23}\,\Gamma_{23,4} = 0, \tag{4.5.84}$$

we see that it is impossible to have all three trees to be present on one side of the recombination wall. Furthermore, since choosing the attractor flow on the other side of the recombination wall $z_-(s)$ will give the same existence conditions with $>$ exchanged with $<$, precisely the trees that exist on one side of the recombination wall will cease to exist on the other and vise versa. It is

also clear now how the index gets preserved across the recombination wall: the index of each tree $(\Gamma_i,(\Gamma_j,\Gamma_k))$ is given by[11]

$$\Omega_{(\Gamma_i,(\Gamma_j,\Gamma_k))}=(-1)^{\Gamma_{ij}+\Gamma_{jk}+\Gamma_{ki}}\,|(\Gamma_{ij}-\Gamma_{ki})\Gamma_{jk}|\,\Omega(\Gamma_i)\Omega(\Gamma_j)\Omega(\Gamma_k),$$

and if the trees $(\Gamma_i,(\Gamma_j,\Gamma_k))$ and $(\Gamma_j,(\Gamma_k,\Gamma_i))$ exist on the " + " side of the recombination wall and $(\Gamma_k,(\Gamma_i,\Gamma_j))$ exists on the " − " side, then from (4.5.83) we have

$$\begin{aligned}\Gamma_{jk}(\Gamma_{ij}-\Gamma_{ki})>0\\ \Gamma_{ki}(\Gamma_{jk}-\Gamma_{ij})>0\\ \Gamma_{ij}(\Gamma_{ki}-\Gamma_{jk})<0,\end{aligned}\tag{4.5.85}$$

which leads to

$$\Omega_{(\Gamma_i,(\Gamma_j,\Gamma_k))}+\Omega_{(\Gamma_j,(\Gamma_k,\Gamma_i))}=\Omega_{(\Gamma_k,(\Gamma_i,\Gamma_j))}.$$

One thing to mention here is the fact that by looking at the marginal stability walls and recombination wall on the z-plane for given charges Γ_1, Γ_2, Γ_3 it is not possible to determine on which side of the recombination wall two trees exist and on which side only one tree exists. Resolving this ambiguity requires the knowledge of the actual periods.

Now let's comment on the case when not all $\Gamma_{ij,k}\neq 0$, but rather $\Gamma_{34,2}\neq 0$, $\Gamma_{24,3}\neq 0$ and $\Gamma_{23,4}=0$. According to (4.5.76), the recombination wall coincides with $MS(\Gamma_4,\Gamma_2+\Gamma_3)$. It is clear that there will be a single configuration on each side of $RW(\Gamma_2,\Gamma_3,\Gamma_4)$, $(\Gamma_2,(\Gamma_3,\Gamma_4))$ on one side and $(\Gamma_3,(\Gamma_4,\Gamma_2))$ on the other side. BPS index will again be preserved through (4.5.84). The recombination wall in this particular case is called the Threshold Stability(TS) wall, introduced first in [9]. Physically, in $(\Gamma_2,(\Gamma_3,\Gamma_4))$ configuration charge Γ_4 is bound to Γ_3, and after crossing the recombination wall it leaves Γ_3 and binds to Γ_2. Exactly on the recombination wall we have a bound state $\Gamma_2+\Gamma_3+\Gamma_4$ at threshold, as described in [9].

4.5.2 Spin character

Finally let us show that the spin character is invariant across the recombination wall. The spin character of the bound state of two charges Γ_j and Γ_k can be written as

$$\Omega_{(\Gamma_j,\Gamma_k)}(y)=\sum_{m=-\frac{|\Gamma_{jk}|-1}{2}}^{\frac{|\Gamma_{jk}|-1}{2}}y^{2m}\,\Omega(\Gamma_j,y)\Omega(\Gamma_k,y)=\frac{y^{|\Gamma_{jk}|}-y^{-|\Gamma_{jk}|}}{y-y^{-1}}\,\Omega(\Gamma_j,y)\Omega(\Gamma_k,y).\tag{4.5.86}$$

[11] We do not write explicitly the dependence of the BPS index on the moduli, meaning that all indices are evaluated at $z=0$.

Generalizing this to a three-centered configuration $(\Gamma_i,(\Gamma_j,\Gamma_k))$ one gets

$$\Omega_{(\Gamma_i,(\Gamma_j,\Gamma_k))}(y)=\frac{1}{(y-y^{-1})^2}(y^{|\Gamma_{jk}|}-y^{-|\Gamma_{jk}|})(y^{|\Gamma_{ij}-\Gamma_{ki}|}-y^{-|\Gamma_{ij}-\Gamma_{ki}|})\,\Omega(\Gamma_i,y)\Omega(\Gamma_j,y)\Omega(\Gamma_k,y). \tag{4.5.87}$$

The conservation of the spin character across the recombination wall is the consequence of a simple identity:

$$(y^a-y^{-a})(y^{c-b}-y^{-c+b})+(y^b-y^{-b})(y^{a-c}-y^{-a+c})+(y^c-y^{-c})(y^{b-a}-y^{-b+a})\equiv 0, \tag{4.5.88}$$

true for any a,b,c and y. Consider, for example, the case (4.5.85) again. In this case Γ_{jk} and $\Gamma_{ij}-\Gamma_{ki}$ have the same sign and thus their absolute values in (4.5.87) can be replaced simultaneously by their actual values. The same is true for Γ_{ki} and $\Gamma_{jk}-\Gamma_{ij}$ entering the expression for $\Omega_{(\Gamma_j,(\Gamma_k,\Gamma_i))}(y)$, but Γ_{ij} and $\Gamma_{ki}-\Gamma_{jk}$ have different signs and so dropping the absolute value signs gives additional minus sign in the expression for $\Omega_{(\Gamma_k,(\Gamma_i,\Gamma_j))}(y)$, leading to the desired result:

$$\Omega_{(\Gamma_i,(\Gamma_j,\Gamma_k))}(y)+\Omega_{(\Gamma_j,(\Gamma_k,\Gamma_i))}(y)=\Omega_{(\Gamma_j,(\Gamma_k,\Gamma_i))}(y). \tag{4.5.89}$$

4.5.3 Attractor Flow Conjecture revisited

It is interesting to see what happens to the moduli space of the supergravity solutions as one crosses the recombination wall. Recall that the Split Attractor Flow Conjecture (SACF) [11] states that the components of the moduli spaces of the multicentered BPS solutions with constituent charges Γ_i and background t_∞ , are in 1-1 correspondence with the attractor flow trees beginning at t_∞ and terminating on attractor points for Γ_i. Thus we expect to observe that the number of components of the supergravity solution changes discontinuously as we cross the recombination wall.

Let us write explicitly the stability conditions for the supergravity solution with three charges Γ_2, Γ_3, Γ_4:

$$\begin{aligned}
&-1+\frac{-\Gamma_{42}}{-\Gamma_{23}+\theta_2 x_{23}}+\frac{\Gamma_{34}}{\Gamma_{23}+\theta_3 x_{23}}\geq 0\\
&1-\frac{-\Gamma_{42}}{-\Gamma_{23}+\theta_2 x_{23}}+\frac{\Gamma_{34}}{\Gamma_{23}+\theta_3 x_{23}}\geq 0\\
&1+\frac{-\Gamma_{42}}{-\Gamma_{23}+\theta_2 x_{23}}-\frac{\Gamma_{34}}{\Gamma_{23}+\theta_3 x_{23}}\geq 0.
\end{aligned} \tag{4.5.90}$$

Here the moduli space is 1-dimensional and we chose to parametrize it with x_{23} - the distance between charges Γ_2 and Γ_3. The $\theta' s$ are defined as follows:

$$\theta_i=2\mathrm{Im}\left[Z(\Gamma_i,t_\infty)\bar{Z}(\Gamma_{tot},t_\infty)\right]. \tag{4.5.91}$$

In this case the moduli space will be represented by one or two intervals in x_{23}. Let us suppose that the configuration $(\Gamma_2, (\Gamma_3, \Gamma_4))$ exists on the left of the recombination wall, at some point t_L, and $(\Gamma_3, (\Gamma_4, \Gamma_2))$, $(\Gamma_4, (\Gamma_2, \Gamma_3))$ on the right at a point t_R. It is easy to see that for t_R and t_L sufficiently close to the recombination wall there will be only one component of the moduli space in some open region, containing these two points.[12] This means that the SAFC as it was originally formulated *does not hold*!

Nevertheless it is clear that there is a relation between attractor trees and the components of the moduli space. To understand this relation let us first look at the moduli space parametrized by the absolute value squared of the angular momentum of the configuration. As discussed in [60] each component of the moduli space will be an interval of the form $[J_d, J_u]$ with $J_{d,u}$ determined by the intersection numbers of the charges. For the example at hand there will an interval for each topology of the attractor tree:

$$\begin{aligned}
&(\Gamma_2, (\Gamma_3, \Gamma_4)) : \; I_{2,34} = [\Gamma_{42} - \Gamma_{23} - \Gamma_{34}, \Gamma_{42} - \Gamma_{23} + \Gamma_{34}] \\
&(\Gamma_3, (\Gamma_4, \Gamma_2)) : \; I_{3,42} = [\Gamma_{42} - \Gamma_{23} + \Gamma_{34}, \Gamma_{42} + \Gamma_{23} - \Gamma_{34}] \\
&(\Gamma_4, (\Gamma_2, \Gamma_3)) : \; I_{4,23} = [\Gamma_{42} + \Gamma_{23} - \Gamma_{34}, \Gamma_{42} - \Gamma_{23} - \Gamma_{34}].
\end{aligned} \tag{4.5.92}$$

We see that $I_{2,34} = I_{3,42} \amalg I_{4,23}$ and the moduli space always consist of only one interval $I_{2,34}$, which becomes partitioned into two on the right of the recombination wall. This leads us to a modified version of the SACF as follows: *The classical BPS configuration space and the quantum BPS Hilbert space are partitioned by attractor flow trees.* The partitioning in the classical case is defined as follows: start with some value of the background moduli, then adiabatically deform it by dialing the moduli at infinity along the attractor flow for the total charge. If there are several configurations of attractor flow trees then upon crossing MS walls they will decay and the corresponding components of the moduli space will disappear. As we saw above different components do not have to be disjoint, but the point is that the change of the moduli space will be discontinuous which allows to identify the part of the moduli space with the attractor flow tree. The quantum case is analogous, although we now have to allow for evolution into linear superpositions of different decay outcomes if there are multiple trees. The Hilbert space of BPS states will be partitioned in states which have only nonzero amplitudes to decay adiabatically into the constituents of each corresponding attractor tree.

[12] Finding the roots of numerators and denominators of the rational functions entering (4.5.90) one can check than none of them become equal on the recombination wall, which means that the number of components cannot change as one crosses this wall.

4.6 Massless Vectormultiplets

In this section we discuss a class of examples where the spectrum at the singularity contains massless vector multiplets. The BPS index of a vectormultiplet has $\Omega = -2$ and therefore (4.3.33) might very well be an infinite series and not a finite polynomial. In various important developments in string theory, such as geometrical engineering of gauge theories and heterotic/type II duality, these kinds of singularities played a key role. Some of the models with massless vectormultiplets which have appeared in this literature appear to conform to our basic assumptions in Section 4.3.1 and thus threaten to pose counterexamples to our prediction (4.3.33). In this Section and the next we examine these examples and demonstrate that in fact there are no counterexamples to our prediction.

We divide the zoo of examples into three groups:

- singularities with the spectrum of an asymptotically free gauge theory,
- conformal fixed points of gauge theories with vanishing β-function,
- theories with electric spectrum (with respect to some duality frame) being that of IR free gauge theory.

4.6.1 Asymptotically free gauge theories

Consider the simplest example of $SU(2)$ $N_f = 0$. This can emerge at a singularity in type II string compactification, and a simple example was discussed in [61]. The CY in this case is a K3 fibration over $\mathbb{P}^1$, which develops an A_1 singularity. Classically at the singularity there is a massless vector multiplet with index $\Omega(\gamma) = -2$ and this clearly contradicts our conclusions from Section 4.3.4. In particular, the quantity I which was associated with the beta-function there is negative and the product $P(q)$ of equation (4.3.33) is

$$P(q) = \frac{1}{(1-q)^2} \tag{4.6.93}$$

and is certainly not a polynomial!

However the full quantum moduli space does not have a singularity with massless vector multiplets at finite distance in the moduli space ([62], [63], [64]). Indeed one recovers the full moduli space of the $SU(2)$ gauge theory, including the strong coupling region, in a certain double scaling limit on IIA side. Part of the IIA string moduli space can be parameterized by the Kähler moduli t_b and t_f of the base of K3 fibration and it's fiber respectively. There will be two discriminant loci, corresponding to the monopole and the dyon. These intersect on the

boundary of the moduli space $t_b = 0$. It is on this codimension 2 intersection where one expects to have massless vector multiplets. This boundary is a nongeneric point on the discriminant locus and so this example does not meet the requirements of Section 4.3.1. In fact if we try to consider bound states of some massive black hole Γ with the W-boson γ near the codimension 2 locus where the W-boson is massless, we find that the attractor flow of $\Gamma + \gamma$ will never pass through this locus, because the attractor flow will always have the direction away from the boundary divisor $t_b = 0$. Thus for any t_∞ the flow of $\Gamma + \gamma$ will intersect $MS(\Gamma, \gamma)$ at some point with $t_b \neq 0$ and the W-boson will be realized as a bound state of well-separated monopole and dyon. As we move t_∞ in the t_f plane around the origin our paradox is resolved through the recombination process of the 3-centered bound state $\Gamma + (\gamma_{monopole} + \gamma_{dyon})$.

It is natural to assume that this conclusion extends to all cases where one engineers an asymptotically free gauge theory: there will be no places in the moduli space at finite distance where on a codimension 1 locus a vector multiplet becomes massless. The singularity will always "split" and there will be a number of conifold-like singularities, around each of which the picture is as described in Section 4.3.4.

4.6.2 Conformal fixed points

These theories are conformal fixed points of gauge theories with vanishing beta-function $I = 0$. It is known that in such theories the spectrum necessarily contains mutually non-local populated charges that becomes massless at the conformal point. This violates our assumptions that there is only one charge γ (and possibly some other parallel charges), that is massless and populated at the singularity. Although there is no notion of particles in such theories, away from the superconformal point the theory does contain particles. One can form halo bound states of these light particles with some massive black hole near the superconformal point and talk about wall-crossing phenomenon. We examine an example of this situation in Section 4.7.1.

4.6.3 Electrically IR-free gauge theories

This class of theories at first sight seems to conform to our assumptions from Section 4.3.1. The light spectrum near the singularity is that of an IR free gauge theory. Examples include the model [65] and the model based on a chain of heterotic/IIA duals first discussed in [66] and further analyzed in [67]. In Section 4.7.3 we consider an example where the electrically charged spectrum gives a non-polynomial expression for (4.3.33).

We will now argue that although the spectrum near the singularity is that of an IR free

gauge theory, at the singularity itself there is a violation of the central assumption of 4.3.1 that the only massless BPS particles have charge parallel to γ. If we parametrize the plane transverse to the singularity by the expectation value of the adjoint scalar v from the light vector multiplet then the W-boson will have mass $\sim |v|$. On the other hand, the theory will also have BPS monopoles that can be reliably constructed as large, smooth, classical solutions to the YM field equations. The mass of the monopole is, as usual, proportional to the vacuum expectation value of scalars from the vector multiplet $\frac{|v|}{g^2(v)}$, where $g(v)$ is the coupling at the scale v. At energies smaller than the monopole mass the dependence of the running coupling on the scale v is given by $\frac{1}{g(v)^2} = \beta \log(\mu/v)$. As the energy scale set by v goes to zero the relation between the mass of the monopole and W-boson does not get spoiled by the quantum corrections, and in the IR limit these masses are still proportional. Taking $v \to 0$ and keeping μ to be some fixed string scale, both masses of W-boson and monopole go to zero. Thus we have mutually non-local massless states at $v = 0$, violating a key assumption of 4.3.1.

We should remark that some care is required when interpreting the above massless monopole. The ratio of monopole mass to W-boson mass goes to to infinity as $v \to 0$ so with an appropriate cutoff the IR free theory is indeed a free theory. On the other hand, one generally expects when one approaches a locus with mutually nonlocal massless particles the theory should become a nontrivially interacting conformal field theory. We believe that there are some important order of limits questions here. In particular, the monopole also becomes larger and more diffuse, since its typical length scale is set by v^{-1}. For purposes of BPS statecounting and the computation of Ω one should include this particle. For purposes of the computation of loop diagrams one should exclude it.

We will examine two examples of this type. In Section 4.7.2 we consider a model whose electric spectrum is that of an IR free gauge theory which has massless vectors provided the hypermultiplet moduli are tuned appropriately. In this case, there are cancelations between vectors and adjoint hypers so that (4.3.33) is still polynomial. Moreover, the massless monopoles have vanishing index, and thus do not affect the partition function of the index of BPS states. In Section 4.7.3 we consider another famous example of this kind. As a check of our conclusion about the spectrum we show that there are two dual CY periods, vanishing at the singularity. The above reasoning implies they are both populated. Note that our picture of the massless spectrum at the singularity is very different from the one advocated in [67].

4.7 Examples with massless vectors

4.7.1 The FHSV Model

In this section we describe a particular example of a model where one has massless vector multiplets at certain places on the moduli space and the theory at the singularity is superconformal. The model is referred to as the FHSV model [68]. Due to the high amount of symmetry the moduli space of this theory is known exactly. From the S-duality symmetry we also can make a good guess about the massless spectrum at the singularity. This spectrum contains both electrically and magnetically charged states. The purpose of this subsection is to illustrate the very nontrivial wall-crossing phenomenon around such a singularity.

Basic Setup for the model

We recall that the FHSV model is an example of a type II compactification with a heterotic dual which is in fact simply an asymmetric orbifold of the heterotic string on T^6. Both the vectormultiplet and hypermultiplet moduli spaces are known exactly. The vectormutiplet moduli space has universal cover

$$\widetilde{\mathcal{M}_V} = \frac{SU(1,1)}{U(1)} \times \frac{SO(10,2)}{SO(10)\times SO(2)}. \tag{4.7.94}$$

It is convenient to choose coordinates on 4.7.94 (we follow conventions of [69]). Let $\mathbb{C}^{1,r}$ denote the $r+1$ dimensional complex vector space equipped with a Lorentzian bilinear form of signature $(+,-^r)$. Let $\mathcal{H}^{1,r}$ be the subspace of with positive definite imaginary part. Then our coordinates are $(\tau,\vec{y})$, where $\tau \in \mathcal{H}^{1,1}$ and $\vec{y}$ is a "tube domain" coordinate of $\mathcal{H}^{1,9}$. We also introduce $u := (\vec{y}, 1, -\frac{\vec{y}^2}{2}) \in \mathbb{C}^{2,10}$. The lattice of electric charges is $II^{2,10} = II^{1,9} \oplus II^{1,1}$ with a quadratic form:

$$(v,v) = \vec{v}^2 + 2v_+v_- \quad \text{where } v := (\vec{v}, v_+, v_-) \in II^{2,10}. \tag{4.7.95}$$

Elements of the full electromagnetic lattice $\Lambda = II^{2,10} \oplus II^{2,10}$ will have the form (q,p), with $q,p \in II^{2,10}$. Using the quadratic form on $II^{2,10}$ we construct the symplectic form on Λ

$$\langle \Gamma, \Gamma' \rangle = (q,p') - (p,q') \tag{4.7.96}$$

where $\Gamma = (q,p)$ and $\Gamma' = (q',p')$ The holomorphic central charge can be written as:

$$Z_h(\Gamma) = (\vec{q}\cdot\vec{y}) - q_+\frac{\vec{y}^2}{2} + q_- + \tau\left((\vec{p}\cdot\vec{y}) - p_+\frac{\vec{y}^2}{2} + p_-\right). \tag{4.7.97}$$

The model has two kinds of singularities on the moduli space with enhanced gauge symmetry. The first kind is given by

$$\vec{\alpha}\cdot\vec{y}=0,\quad \text{with } \vec{\alpha}^2=-2, \tag{4.7.98}$$

and corresponds to $\mathcal{N}=4$ $SU(2)$ SYM gauge theory in the infrared. The second kind is the locus

$$\left((\vec{0},-1,1),(\vec{y},1,-\frac{\vec{y}^2}{2})\right)=1+\frac{\vec{y}^2}{2}=0, \tag{4.7.99}$$

and corresponds to $\mathcal{N}=2$ $N_f=4$ $SU(2)$ gauge theory. We will describe them on the same footing as loci where

$$(\alpha,u)=0,\quad \text{where } (\alpha,\alpha)=-2 \tag{4.7.100}$$

for $\alpha\in II^{2,10}$.

The superconformal theory at the two singularities has S-duality symmetry but the spectrum of massless states at the singularity and the structure of halo states will be different in the two cases. In both cases there will be two BPS states with mutually non-local charges $\gamma=(\alpha,0)$ and $\gamma_D=(0,\alpha)$, $\langle\gamma,\gamma_D\rangle=-2$, that become massless. The spectrum in the case of the $SU(2)$, $\mathcal{N}=4$ singularity is given by

$$\begin{aligned}\mathcal{H}(m\gamma+n\gamma_D)\neq\emptyset,\ \Omega(m\gamma+n\gamma_D)=0 \qquad &\text{if} \quad gcd(m,n)=1,\\ \mathcal{H}(m\gamma+n\gamma_D)=\emptyset, \qquad &\text{otherwise.}\end{aligned} \tag{4.7.101}$$

In case of the $SU(2)$, $N_f=4$ singularity the spectrum is

$$\begin{aligned}&\mathcal{H}(m\gamma+n\gamma_D)\neq\emptyset, \quad \Omega(m\gamma+n\gamma_D)=8, && gcd(m,n)=1,\\ &\mathcal{H}(m\gamma+n\gamma_D)\neq\emptyset, \quad \Omega(m\gamma+n\gamma_D)=-2, && gcd(m,n)=2,\\ &\mathcal{H}(m\gamma+n\gamma_D)=\emptyset, && \text{otherwise.}\end{aligned} \tag{4.7.102}$$

We are interested in the behavior of BPS indices and the structure of Hilbert spaces of charges

$$\Gamma_{m,n}:=\Gamma+m\gamma+n\gamma_D \tag{4.7.103}$$

around the superconformal point. Here $\Gamma=(q,p)$ is some charge, mutually non-local to γ and γ_D, such that $\Omega(\Gamma)\neq 0$ and constant in the neighborhood of $\mathcal{Z}(\gamma)$. (Let us say it supports a heavy single-centered black hole with a regular attractor point near $\mathcal{Z}(\gamma)$.) It is convenient to choose basis so that $\langle\Gamma,\gamma\rangle=0$ and $a:=\frac{1}{2}\langle\Gamma,\gamma_D\rangle<0$. In particular we are taking:

$$(p,\alpha)=0 \qquad (q,\alpha)=2a<0. \tag{4.7.104}$$

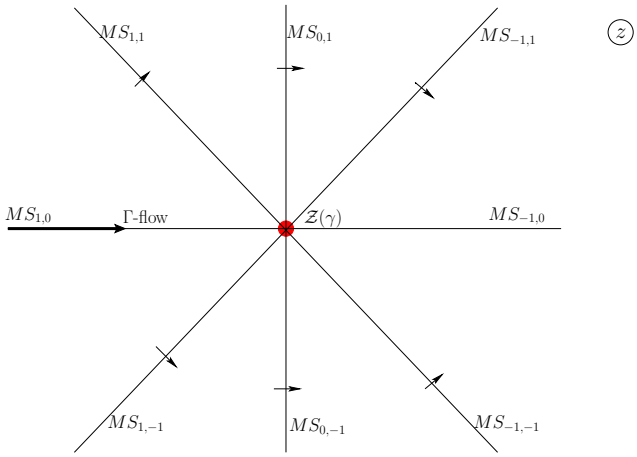

Figure 4.14: Marginal stability walls $MS_{m,n}$ for charge Γ with charges $\gamma_{m,n} = m\gamma + n\gamma_D$. The walls form a dense set, labeled by the rational numbers in lowest terms. The arrows point in the direction of stable to unstable region appropriate to that wall of marginal stability.

Attractor flows and walls of marginal stability

As another preliminary we describe relevant walls of marginal stability and the attractor flows. It is convenient to parameterize the plane transverse to $\mathcal{Z}(\gamma)$ by $z := (\alpha, u)$, the period of γ, and to project the walls of marginal stability and the attractor flows into this plane.

First, let us plot the walls of marginal stability. Let $\gamma_{m,n} := m\gamma + n\gamma_D$. There will be a dense set of walls of marginal stability $MS_{m,n} := MS(\Gamma, \gamma_{m,n})$ for all $(m,n) \in \mathbb{Z}^2$, $gcd(m,n) = 1$. For the $N_f = 4$ case there will also be such walls for $gcd(m,n) = 2$. As usual these walls will sit in the locus:

$$\text{Im } Z(\Gamma; \tau, y)(m\bar{z} + n\bar{\tau}\bar{z}) = 0. \tag{4.7.105}$$

The marginal stability walls will end at $z = 0$. We work in an arbitrarily small neighborhood of $z = 0$ and hence can treat $Z(\Gamma; t)$ as a constant. We will normalize $Z(\Gamma, t)$ to be $Z(\Gamma, t) = -1$ at $z = 0$ and moreover we will take $\tau = i$ for simplicity. In the linear approximation the walls $MS_{m,n}$ will be

$$MS_{m,n} = \{\rho(-m + in) : \rho > 0\}. \tag{4.7.106}$$

The marginal stability walls are in the upper half-plane for $n > 0$ and for $m \to +\infty$ they asymptote to the negative x axis, while for $m \to -\infty$ they asymptote to the positive x axis. Some of the walls are illustrated in Figure 4.14. Again, because we are working at small z we can in fact identify

$$MS(\Gamma_{m,n}, \gamma_{m',n'}) \cong MS(\Gamma, \gamma_{m',n'}), \tag{4.7.107}$$

an approximation which will be used throughout.

The stable side of the walls is readily computed from

$$\langle \Gamma, \gamma_{m,n} \rangle \mathrm{Im}\, Z_\Gamma \bar{Z}_{\gamma_{m,n}} = 2na(nx + my) \tag{4.7.108}$$

where $z = x + iy$. Note that for $x \to +\infty$ the dominant term in the expression, $2an^2x$, is always negative, hence the unstable side is always on the right in Figure 4.14, as indicated by the arrows.

Next, let us turn to the attractor flows. In the small z approximation the attractor flows for $\Gamma_{m,n}$ can be written for both cases in a uniform way:

$$\dot{z} \sim -(\alpha, q) + 2m + \bar{\tau}\left(-(\alpha, p) + 2n\right), \tag{4.7.109}$$

which, for our choice of parameters $\tau = i$ and (4.7.104) is simply

$$\Gamma_{m,n} - \text{flow}: \qquad \dot{z} = (m - a) - in, \tag{4.7.110}$$

and similarly we have

$$\gamma_{m,n} - \text{flow}: \qquad \dot{z} = m - in. \tag{4.7.111}$$

Here we have neglected the variation in τ, again using the small z approximation. (We also rescaled time by a factor of 2.)

In order to prove (4.7.110) and (4.7.111) let us start with the $\mathcal{N} = 4$ singularity with $z = \vec{\alpha} \cdot \vec{y}$. Writing the attractor equation as in (4.0.1), we get

$$\dot{z} = \alpha_a \dot{y}^a \sim -\alpha_a g^{a\bar{b}} \partial_{\bar{y}^{\bar{b}}} \left(|Z_h(\Gamma_{m,n}; \tau, y)| e^{K/2} \right) |_{z=0}. \tag{4.7.112}$$

Taking into account that the Kähler potential is given by $K = -\log\left(4(\mathrm{Im}\vec{y})^2\right) - \log\left(\mathrm{Im}\tau\right)$ gives

$$\dot{z} \sim -\vec{\alpha} \cdot \vec{q} + 2m + \bar{\tau}\left(-\vec{\alpha} \cdot \vec{p} + 2n\right). \tag{4.7.113}$$

Repeating the same calculation for the $\mathcal{N} = 2$ singularity we get:

$$\begin{aligned} \dot{z} &= \left(1 + \frac{\vec{y}^2}{2}\right)^{\cdot} = y_a \dot{y}^a \sim -y_a g^{a\bar{b}} \partial_{\bar{y}^{\bar{b}}} \left(|Z_h(\Gamma_{n,m}; \tau, y)| e^{K/2} \right) |_{z=0}, \\ \dot{z} &\sim -(q_+ - q_-) + 2m + \bar{\tau}\left(-(p_+ - p_-) + 2n\right). \end{aligned} \tag{4.7.114}$$

thus establishing (4.7.110), from which one can also deduce (4.7.111).

We remark that

1. The attractor flows for $\Gamma_{m,n}$ are parallel to the marginal stability walls $MS_{(m-a),n}$. In particular, the flows for Γ itself are parallel to the x-axis in the direction of increasing x.

2. In particular, the bound state transformation wall $\mathcal{S}(\gamma_{m,n}, \Gamma)$ is precisely the marginal stability wall $MS_{m-a,n}$. We will see that it is really a hybrid of conjugation and recombination walls in this example.

3. The attractor flow for $\gamma_{m,n}$ is parallel to the walls of marginal stability $MS_{m,n}$

4. Attractor flows always proceed from stable to unstable regions, in accord with Property 3 of Appendix C.

Monodromy

It will be important in our story below to take into account the $\mathbb{Z}_2$-monodromy of the local system of charges around $z = 0$. The z-plane is simply a double-cover of the moduli space under $z \to -z$. The action on a general charge $\lambda \in \Lambda = II^{2,10} \oplus II^{2,10}$ is

$$M \cdot \lambda = \lambda - \langle \lambda, \gamma \rangle \gamma_D + \langle \lambda, \gamma_D \rangle \gamma. \tag{4.7.115}$$

This takes $\gamma \to -\gamma$, $\gamma_D \to -\gamma_D$, and is the identity on charges orthogonal to both γ, γ_D. Thus, if we write $\Gamma = \Gamma_0 - a\gamma$ where Γ_0 is orthogonal to γ and γ_D then the monodromy image is $\Gamma_M := M \cdot \Gamma = \Gamma + 2a\gamma = \Gamma_0 + a\gamma$.

Since there are no basins of attraction in the FHSV model, both charges Γ and Γ_M will be populated charges in the neighborhood of the singularity and will have isomorphic Hilbert spaces.

Attractor flow trees

Now let us turn our attention to the attractor flow trees for $\Gamma_{m,n}$.

We are interested in attractor flow trees relevant to considering Γ as a core charge, that is, trees of the form:

$$\Gamma_{m,n} \to (\gamma_{m_1,n_1} + (\gamma_{m_2,n_2} + ...(\gamma_{m_{L-1},n_{L-1}} + (\Gamma + \gamma_{m_L,n_L}))...)). \tag{4.7.116}$$

Of course, charge conservation requires

$$\sum_i m_i = m \qquad\qquad \sum_i n_i = n. \tag{4.7.117}$$

The attractor flow trees are systematically constructed from two principles: First, the flow must split from the stable to the unstable side on the wall of marginal stability and second, the charges must be conserved at each vertex of the tree.

In Appendix F we give an algorithm for enumerating the trees and show, in particular, that the number of such trees is finite. If $n > 0$ then the initial point of the tree can only be in the upper half plane. Moreover, the initial point must be to the right of the BST wall $\mathcal{S}(\gamma_{m,n}, \Gamma)$, otherwise there are no acceptable trees. The reason for this is that simple geometry forces the trees that begin on the left of the BST wall $\mathcal{S}(\gamma_{m,n}, \Gamma)$ to intersect marginal stability walls $MS_{m',n'}$ in a direction from unstable to stable side. But this is a forbidden vertex. This would appear to pose a serious problem for continuity of the index. We discuss that point in the next subsection.

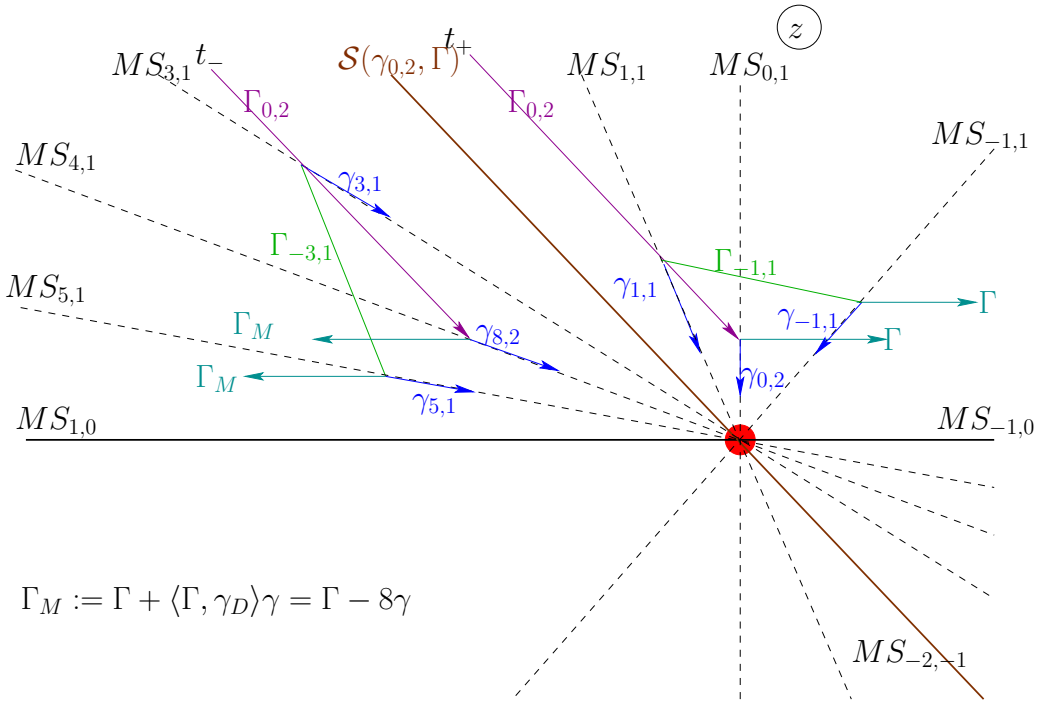

Figure 4.15: Attractor trees, contributing to the realization of charge $\Gamma_{0,2}$ on two sides of $\mathcal{S}(\gamma_{0,2}, \Gamma)$. We have chosen a=-4. Attractor flows of core with halos are purple, green and cyan colored line, attractor flows of halo particles are blue lines.

As an example, consider the attractor trees contributing to the realization of charge $\Gamma_{0,2}$. These are shown in Figure 4.15. Starting at t_+ there will be only two valid trees. One is a two centered solution $\Gamma + \gamma_{0,2}$ and the other is a 3-centered solution $(\Gamma + \gamma_{1,1}) + \gamma_{-1,1}$. If, on the other hand, we move the initial point t_∞ from t_+ to t_- across the BST wall then these two attractor flow trees cease to exist!

Continuity of the index

In the previous subsection we remarked that attractor flows of type (4.7.116) with final core charge Γ do not exist for initial point t_∞ to the left of the BST wall $\mathcal{S}(\gamma_{m,n}, \Gamma)$. As we noted, this

would appear to pose a serious problem for the index. The only way the index can be continuous across $\mathcal{S}(\gamma_{m,n},\Gamma)$ is if there exists another core charge that can form halos with $\gamma_{m',n'}$-particles of the same total charge $\Gamma_{m,n}$. Because of the $\mathbb{Z}_2$-monodromy there is indeed another natural core charge, namely $\Gamma_M = \Gamma + 2a\gamma = \Gamma_{2a,0}$. The attractor flows for Γ_M are parallel to the x-axis but the flow is to the left. Similarly, the stable and unstable sides of all the walls of marginal stability are flipped. (All this becomes more obvious if we write $\Gamma = \Gamma_0 - a\gamma$ and $\Gamma_M = \Gamma_0 + a\gamma$ as in Section 4.7.1.) One can write out conditions similar to those in Appendix F for enumerating the attractor flow trees corresponding to core charge Γ_M. Again there will be finitely many such trees. In particular, the initial point for a flow tree with terminating with core charge Γ_M must lie to the *left* of the BST wall

$$\mathcal{S}(\gamma_{m,n},\Gamma) = \mathcal{S}(\gamma_{m-2a,n},\Gamma_M) \tag{4.7.118}$$

Continuity of the index leads us to expect, and hence we conjecture, the following: *The sum of contributions to the index from flow trees terminating on core* Γ *with initial point* t_+ *infinitesimally to the right of* $\mathcal{S}(\gamma_{m,n},\Gamma)$ *is equal to the sum of contributions to the index from flow trees terminating on the core charge* Γ_M *with initial point* t_- *infinitesimally to the left of* $\mathcal{S}(\gamma_{m,n},\Gamma)$.

As a simple check on this idea consider charges of type $\Gamma_{m,1}$. These only support a single branch. At a point t_+ just to the right of the wall $\mathcal{S}(\gamma_{m,1},\Gamma)$ there is only a single tree $\Gamma_{m,1} \to \Gamma + \gamma_{m,1}$. This contributes to the index

$$\Delta\Omega(\Gamma_{m,1} \to \Gamma + \gamma_{m,1}) = (-1)^{\langle\Gamma,\gamma_{m,1}\rangle - 1}|\langle\Gamma,\gamma_{m,1}\rangle|\Omega(\gamma_{m,1})\Omega(\Gamma) = -16a\Omega(\Gamma). \tag{4.7.119}$$

At a point t_- just to the left of the wall this tree does not exist, but the tree $\Gamma_{m,1} \to \Gamma_M + \gamma_{m-2a,1}$ does exist. The latter contributes

$$\Delta\Omega(\Gamma_{m,1} \to \Gamma_M + \gamma_{m-2a,1}) = (-1)^{\langle\Gamma_M,\gamma_{m-2a,1}\rangle - 1}|\langle\Gamma_M,\gamma_{m-2a,1}\rangle|\Omega(\gamma_{m-2a,1})\Omega(\Gamma_M) = -16a\Omega(\Gamma_M). \tag{4.7.120}$$

Now, thanks to the $\mathbb{Z}_2$ monodromy $\Omega(\Gamma) = \Omega(\Gamma_M)$ and so indeed the contributions to the index are continuous.

As a second check we return to the example of the previous section. For t_+ on the right of $\mathcal{S}(\Gamma_{0,2})$ with $a = -4$ the tree with one branching contributes

$$\Delta\Omega = -16\Omega(\gamma_{0,2})\Omega(\Gamma) = 32\Omega(\Gamma) \tag{4.7.121}$$

and the second tree contributes

$$\Delta\Omega = 32\Omega(\gamma_{1,1})\Omega(\gamma_{-1,1})\Omega(\Gamma) = 2^{11}\Omega(\Gamma) \tag{4.7.122}$$

On the other hand, going back to Figure 4.15, starting from t_- there will be two solutions with the core charge Γ_M of the form $\Gamma_M + \gamma_{8,2}$ and $(\Gamma_M + \gamma_{5,1}) + \gamma_{3,2}$. The first tree contributes $32\Omega(\Gamma_M)$ and the second $2^{11}\Omega(\Gamma_M)$.

For charges of type $\Gamma_{m,2}$ we must take into account trees with one and two branches and the computation becomes more elaborate. We have performed this check and the index is continuous. The computation is very similar to that in given in the next subsection. In general, upon crossing the BST wall we have conjugation - since the core charge is replaced by a monodromy image - at the same time as recombination - so the walls in this example exhibit a hybrid of the conjugation and recombination mechanisms.

Wall-Crossing near a superconformal point

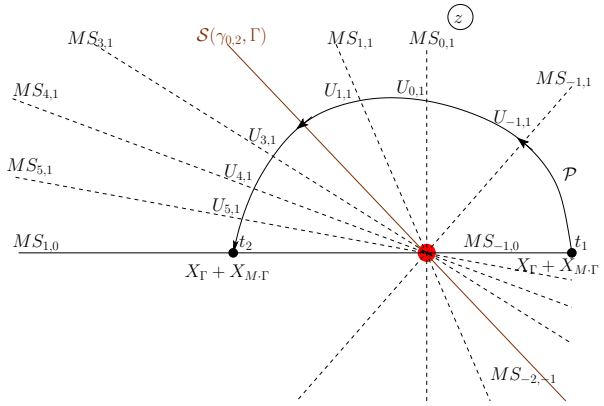

Figure 4.16: Transformation of the partition function through operators $U_{m,n}$ along a path $\mathcal{P}$ from t_1 to t_2.

In the next chapter, which is based on [38], we give a simple proof of the Kontsevich-Soibelman wall-crossing formula based on supergravity halos. Moreover, as explained in Section 4 of [38], the line of reasoning adopted there suggests a generalization of the KSWCF. The FHSV model provides a nice example in which to illustrate the ideas.

Following [38] we consider the partition function

$$F(q,p;t) = \sum_{m,n} q^{m-a} p^n \, \overline{\underline{\Omega}}_\Gamma(\gamma_{m,n};t), \tag{4.7.123}$$

where $\overline{\underline{\Omega}}_\Gamma(\gamma_{m,n};t)$ are the "framed" BPS indices described in [38]. The sum here runs over $n \geq 0$ and $m \in \mathbb{Z}$. For our purposes these framed BPS indices can be identified with the halo contributions to the total index $\Omega(\Gamma_{m,n};t)$ with $\Omega(\Gamma)$ factored out. (This is also what we were considering in Section 4.3.4.)

Let us consider the path $\mathcal{P}$ shown in Figure 4.16 going from t_1 to t_2. Using the reasoning of [38] we see that the partition function at a point $z = x + iy$ on $\mathcal{P}$ is given in terms of that at $z = t_1$ by

$$F(q,p;z) = \prod_{my+nx<0\,\&\,n>0} U_{m,n} F(q,p;t_1). \tag{4.7.124}$$

Here the operators $U_{m,n}$ are defined in terms of basic KS-transformations:

$$T_{m,n} := (1 - q^m p^n)^{D_{m,n}} \tag{4.7.125}$$

where $D_{m,n}$ is a differential operator defined by $D_{m,n} q^\alpha p^\beta := 2(n\alpha - m\beta) q^\alpha p^\beta$ and

$$U_{m,n} = T_{m,n}^8 T_{2m,2n}^{-2}. \tag{4.7.126}$$

The $U_{m,n}$ are only defined for $gcd(m,n) = 1$ and this restriction is understood on the product (4.7.124) and similar products below. The restriction $my + nx < 0$ on the terms in the product applies because only the walls $MS_{m,n}$ (defined by $my + nx = 0$) that have been crossed while moving along $\mathcal{P}$ should be included. Finally, the factors in the product are ordered so that terms with increasing argument $\arg(-m + in)$ are placed to the left.

If we identify the framed BPS index with the index of states which can be described as halo states around a core of charge Γ then at $z = t_1$ there are no halo states and hence the core simply contributes a factor of q^{-a}. We have already seen in the halo description that such states do not give a continuous index across the BST walls and we should expect trouble here too if we only include q^{-a} in $F(q,p;t_1)$. Indeed, the examples below will bear that out. Thus we should include the monodromy image Γ_M and its halo states. Again, at $z = t_1$ the only halos around Γ_M are the single core state itself. Recalling that $\Gamma_M = \Gamma + 2a\gamma$ we see that including these two cores gives

$$F(q,p;t_1) = q^a + q^{-a}. \tag{4.7.127}$$

Substituting this into (4.7.124) and expanding as a series in $p, q^{\pm 1}$ we observe that the number of terms in the expansion of the product contributing to a given monomial $q^{m-a}p^n$ is finite. Indeed, we can observe that we need to choose a partition of n to account for the power of p. The power of q is more complicated. The walls crossed in the first quadrant all have $m < 0$, but for $x < 0$ there will be a finite number of walls with $0 \le m < -nx/y$. Once these nonnegative values of m have been chosen, the remaining negative values of m constitute a partition, and therefore there are only finitely many choices. Thus the infinite product will be well-defined.

As an example of the issues involved let us examine the product

$$\prod_{my+nx<0\,\&\,n>0} U_{m,n}(q^a + q^{-a}) \tag{4.7.128}$$

and let us extract the coefficients of $q^{m-a}p$ and $q^{m-a}p^2$. We first consider the case of $q^{m-a}p$. There are only two terms which can contribute to $q^{m-a}p$. First, there is the term coming from the expansion of

$$(1-q^m p)^{8D_{m,1}}q^{-a} = (1-q^m p)^{-16a}q^{-a} \tag{4.7.129}$$

which enters the product when $my + x < 0$, i.e. when $m < -x/y$ and contributes $16a$ to the coefficient. The other term which can contribute comes from the expansion of

$$(1-q^{m-2a}p)^{8D_{m-2a,1}}q^{a} = (1-q^{m-2a}p)^{16a}q^{-a} \tag{4.7.130}$$

This contributes $-16a$ to the coefficient and enters the product when $m - 2a < -x/y$. Thus the coefficient of $q^{m-a}p$ (that is, the framed BPS degeneracy) is given by

$-\frac{x}{y} < m$	0
$m < -\frac{x}{y} < m-2a$	$16a$
$m-2a < -\frac{x}{y}$	0

Now, a short computation shows that the BST wall $\mathcal{S}(\gamma_{m,1}, \Gamma)$ is given by $-x/y = m - a$, and hence the index is continues across it.

A slightly more elaborate computation is required to compute the coefficient of $q^{m-a}p^2$. The power of p^2 can come from a single factor, or from two distinct factors. We have listed the cases in the table below together with the contribution of that factor and the range in which it applies: [13]

I	$(1-q^m p^2)^{-2D_{m,2}}q^{-a}$	$-8aq^{m-a}p^2$	$\frac{m}{2} < -\frac{x}{y}$
II	$(1-q^{m-2a}p^2)^{-2D_{m-2a,2}}q^{a}$	$8aq^{m-a}p^2$	$\frac{m}{2} - a < -\frac{x}{y}$
III	$(1-q^{\frac{m}{2}}p)^{8D_{\frac{m}{2},1}}q^{-a}$	$8a(16a+1)q^{m-a}p^2$	$\frac{m}{2} < -\frac{x}{y}$
IV	$(1-q^{\frac{m}{2}-a}p)^{8D_{\frac{m}{2}-a,1}}q^{a}$	$8a(16a-1)q^{m-a}p^2$	$\frac{m}{2} - a < -\frac{x}{y}$
V_μ	$(1-q^{\mu}p)^{8D_{\mu,1}}(1-q^{\mu_2}p)^{8D_{\mu_2,1}}q^{-a}$	$-2^8 a(m-a-2\mu)$	$\left(\substack{\frac{m}{2}<\mu<-\frac{x}{y} \\ \mu+\mu_2=m}\right)$
VI_μ	$(1-q^{\mu}p)^{8D_{\mu,1}}(1-q^{\mu_2}p)^{8D_{\mu_2,1}}q^{a}$	$2^8 a(m-a-2\mu)$	$\left(\substack{\frac{m}{2}-a<\mu<-\frac{x}{y} \\ \mu+\mu_2=m-2a}\right)$

The range of μ in the last two rows is derived as follows. The expression

$$(1-q^{\mu_1}p)^{8D_{\mu_1,1}}(1-q^{\mu_2}p)^{8D_{\mu_2,1}}q^{-a} \tag{4.7.131}$$

can contribute to $q^{m-a}p^2$ when $\mu_1 + \mu_2 = m$. The factors are properly ordered for

$$0 < \mathrm{Im}(-\mu_1 + i)\overline{(-\mu_2 + i)} = \mu_1 - \mu_2$$

[13] We have taken m to be even for simplicity. A slightly different computation applies when m is odd.

and hence $m/2 < \mu_1$. On the other hand, for the second factor to contribute we must have $\mu_1 y + x < 0$ and hence $\mu_1 < -x/y$. The range for VI_μ is derived similarly.

When $-x/y > m/2$ we can evaluate the contribution of V_μ using the identity

$$\sum_{\frac{m}{2}<\mu\leq N}(m-a-2\mu) = \left(\frac{a+1}{2}\right)^2 - \left(N - \frac{m-a}{2} + \frac{1}{2}\right)^2. \tag{4.7.132}$$

Now we can add up the contributions. For $-\frac{x}{y} < \frac{m}{2}$ there are no contributions, and the coefficient is 0. In the range $\frac{m}{2} < -\frac{x}{y} < \frac{m}{2} - a$ terms of types I, III and V_μ all contribute. The sum of the contributions of type I and III is 2^7a^2. Using (4.7.132) we can evaluate the contribution of terms of type V_μ and thus derive the index

$$2^7a^2 - 2^6a(a+1)^2 + 2^8a\left(N_{x,y} - \frac{m-a}{2} + \frac{1}{2}\right)^2 \tag{4.7.133}$$

where $N_{x,y} = \lfloor -x/y \rfloor$. This is to be evaluated for $-x/y$ nonintegral.

When $\frac{m}{2} - a < -\frac{x}{y}$ the index is zero. The way this comes about is interesting: The terms I and II cancel and III and IV add up to give 2^8a^2. Moreover V_μ and VI_μ together have canceling terms for $\frac{m}{2} - a < \mu$ and the sum of these two terms becomes the constant (as a function of x, y) given by

$$-2^8a \sum_{\frac{m}{2}<\mu\leq\frac{m}{2}-a}(m-a-2\mu). \tag{4.7.134}$$

The range of this sum can be written as $a \leq m - a - 2\mu < -a$ and hence (4.7.134) is trivially equal to -2^8a^2, thus leading to total index 0.

In particular for our example $\Gamma_{0,2}$ with $a = -4$ discussed in Figure 4.15 above we have

$-\frac{x}{y} < 0$	0
$0 < -\frac{x}{y} < 1$	2^{11}
$1 < -\frac{x}{y} < 3$	2^{12}
$3 < -\frac{x}{y} < 4$	2^{11}
$4 < -\frac{x}{y}$	0

A number of interesting lessons can be drawn from these examples:

1. The BST wall $\mathcal{S}(\gamma_{m,2}, \Gamma)$ is at $-\frac{x}{y} = \frac{m-a}{2}$. Note that at t_+ on the right of this wall $N_{x,y} = \frac{m-a}{2} - 1$ and at t_- on the left $N_{x,y} = \frac{m-a}{2}$. Thus, from equation (4.7.133) we see that the index is indeed constant across the BST wall.

2. Different terms from the product can be identified with different kinds of attractor trees. Terms of type I correspond to single-branched flows with core Γ while terms of type II correspond to single-branched flows with core Γ_M. Terms of type III and IV correspond to 2-particle haloes with core Γ and Γ_M, respectively. Some of the terms of type V_μ and VI_μ can be associated with two-branched trees with cores Γ and Γ_M, respectively.

3. If we considered only one core charge Γ, corresponding to $F(q,p,t_1) = q^{-a}$ then terms of type V_μ would not give a well-defined index as the point z on $\mathcal{P}$ approaches t_2 since $N_{x,y}$ goes to infinity and the sum of terms of type V_μ grows without bound. On the other hand, when we include the monodromy image q^a there is a term-by-term cancellation between V_μ and VI_μ so that the index is in fact well-defined.

We expect the features of the above example to hold for general coefficients of $q^{m-a}p^n$ with $n > 2$. In particular, following the path $\mathcal{P}$ all the way from t_1 to t_2 should yield an identity of the form

$$F(q,p;t_2) = \prod_{\frac{m}{n}\in(-\infty,\infty),\, n>0} U_{m,n}\, F(q,p;t_1). \tag{4.7.135}$$

Just like t_1, at t_2 all halo states are unstable and the partition functions have only two contributions from core charges Γ and Γ_M so:

$$F(q,p;t_2) = q^{-a} + q^a \tag{4.7.136}$$

and hence we arrive at the following (somewhat strange) identity for formal power series in q and p:

$$q^{-a} + q^a = \prod_{\frac{m}{n}\in(-\infty,\infty),\, n>0} U_{m,n}\left(q^{-a} + q^a\right). \tag{4.7.137}$$

It is worth stressing that the operator $\prod_{\frac{m}{n}\in(-\infty,\infty),\, n>0} U_{m,n}$ does not act well on general power series or even on general rational functions of q, p. As we have seen above, it does have a well-defined action on $q^a + q^{-a}$ (and hence on finite sums of such terms). Thus, requiring that such infinite products have well defined actions on partition functions puts a nontrivial constraint on the spectrum of BPS states. This is the sense in which the approach of [38] constitutes a generalization of the Kontsevich-Soibelman wall-crossing formula.

4.7.2 Massless vectors with adjoint hypermultiplets

In this section we consider an example with massless vector multiplets at the singularity, introduced by Katz, Morrison and Plesser (KMP) in [65]. The massless spectrum at the singularity is that of an $\mathcal{N} = 2$, $SU(2)$ gauge theory with some number of adjoint hypermultiplets. One

distinctive feature of this example is that there are massless vector bosons at the singularity in the Kähler moduli space only at some special value of hypermultiplet (complex structure) moduli. If one moves off this special value of hypermultiplet moduli, the $\mathcal{N}=2$ vector multiplet will become massive and the massless spectrum will consist of some number of hypermultiplets. At the special locus where there are massless vectormultiplets we can invoke the discussion of Section 4.6.3 above to conclude that the spectrum will also include massless monopoles/dyons. Note that when moving away from the special locus the monopoles will become confined due to the dual Meissner effect and will not be present in the massless spectrum either. This means that the monopoles must have zero BPS index.

As we discussed in more detail in Section 4.7.1 at the special locus the spectrum leads to a very complicated wall-crossing phenomena of halos states and there must be some hybrid BST walls, across which both conjugation and recombination take place. On the other hand the BPS index is preserved exactly as in the conifold like case, i.e. the index jumps across marginal stability walls of the core charge with hypermultiplet halo particles. The rest of the massless spectrum has index zero and thus across marginal stability walls with halo particles containing W-boson and monopole charges, as well as across BST walls for such halos, the index is trivially constant. Thus the index of halo states changes exactly the same way as for generic complex structure with a conifold-like singularity. In the latter case the conditions of Section 4.3.1 are met, and our main puzzle is resolved through the presence of the conjugation walls.

For completeness, in the remainder of this Section we recall a few details of the KMP model and justify the above statements a bit more. KMP considered the compactification of type II string theory on a Calabi-Yau which is a $K3$ fibration over a genus g curve $\mathcal{C}$. In particular, the fibration has a curve $\mathcal{C}$ of A_{N-1} singularities, which corresponds to $SU(N)$ enhanced gauge symmetry. Close to the singularity there is a field theory description in terms of $\mathcal{N}=2$ $SU(N)$ gauge theory with g adjoint hypermultiplets, with the Lagrangian

$$
\begin{aligned}
&2\pi\mathcal{L} = \mathrm{Im}\left[\mathrm{Tr}\int d^4\theta\left(M_i^\dagger e^V M^i + \tilde{M}_i^\dagger e^V \tilde{M}^i\right) + \Phi^\dagger e^V \Phi + \frac{\tau}{2}\int d^2\theta \mathrm{Tr} W^2 + i\int d^2\theta \mathcal{W}\right] \\
&\mathcal{W} = \mathrm{Tr}\tilde{M}^i[\Phi, M_i]. \qquad (4.7.138)
\end{aligned}
$$

Here, in $(M^i, \tilde{M}^i)$ are g adjoint hypermultiplets, representing complex structure moduli, V is an $\mathcal{N}=1$ vector multiplet superfield with field strength W, Φ is an $\mathcal{N}=1$ adjoint chiral multiplet, representing Kähler moduli, and the scalar potential is given by

$$\mathcal{V} = \mathrm{Tr}\left[[m_i, m^{\dagger i}]^2 + [\tilde{m}_i, \tilde{m}^{\dagger i}]^2 + [\phi, \phi^\dagger]^2 + 2[m^{\dagger i}, \phi][\phi^\dagger, m_i] + 2[\tilde{m}^{\dagger i}, \phi][\phi^\dagger, \tilde{m}_i] + \right.$$
$$\left. + 2[\tilde{m}_j^\dagger, m^{\dagger j}][m_i, \tilde{m}^i]\right], \tag{4.7.139}$$

where m_i, $\tilde{m}_i$, and ϕ are the scalar components of the corresponding superfields. The moduli space of this theory can be parametrized by diagonal traceless matrices ϕ and $(m_i, \tilde{m}_i)$ and has the form $\mathbb{C}^{N-1} \times \mathbb{C}^{2g(N-1)}$, where the first factor comes from vector multiplet moduli, and the second - from hypermultiplets. The point of enhanced $SU(N)$ gauge symmetry occurs at codimension $N-1$ in vector moduli space and in codimension $2g(N-1)$ in hypermultiplet moduli space, which translates to codimension $N-1$ in Kähler and $2g(N-1)$ in complex structure moduli spaces in the full IIA string theory. As we are interested in singularities of codimension 1 in Kähler moduli space, we put $N = 2$.

The special locus $m_i = 0, \tilde{m}_i = 0$ is a complex plane, parametrized by a, $\phi = a\sigma_3$. The spectrum is that of a $U(1)$ $N = 2$ SYM with g hypermultiplets, that is enhanced to $SU(2)$ at the origin. The multiplet with charge 1 under this $U(1)$ that becomes massless corresponds to W^+ boson in field theory and to a state with charge γ in string theory. It has second helicity supertrace $2g-2$ and thus

$$\Omega(\gamma) = 2g - 2,$$

where $2g$ comes from g hypermultiplets and -2 comes from the vectormultiplet. The modulus a corresponds to the period of the charge γ in string theory. Denoting by a_D the period of the dual charge γ_D, $\langle \gamma, \gamma_D \rangle = -2$, [65] give the monodromy of these periods around the singularity in the a-plane to be

$$\begin{cases} a \to a \\ a_D \to a_D - 4(g-1)a, \end{cases} \tag{4.7.140}$$

which translates to the monodromy of the charge lattice as follows

$$\Gamma \to \Gamma - (2g-2)\langle \Gamma, \gamma \rangle \gamma = \Gamma - \Omega(\gamma)\langle \Gamma, \gamma \rangle \gamma, \tag{4.7.141}$$

for any charge Γ. As we mentioned above, going around the singularity the Hilbert spaces of halo states $\Gamma + m\gamma + n\gamma_D$ will change in a complicated way due to the presence of hybrid conjugation/recombination walls.

Now we change the complex structure away from the special point, for example take non-zero $m_1 \neq 0$. Careful examination of the scalar potential (4.7.139) shows that in this case the

point $a = 0$ does not have enhanced gauge symmetry, but there is a massive $N = 4$ vector multiplet[14] $(V^+, \Phi^+)$with charge $+1$ under the unbroken $U(1)$ as well as $(g-1)$ massless $N = 2$ hypermultiplets $(M_i^+, \tilde{M}_i^+)$, $i = 2, .., g$ of the same charge. This massless spectrum has the same BPS index but different spin character than the one at the special complex structure value. In particular the Hilbert space of γ became purely fermionic. From IIA string theory point of view, there are $2g-2$ spheres in the same homology class shrinking to zero ([65]) and the BPS index of massless state is $\Omega(\gamma) = 2g-2$. If we now go around the $a = 0$ singularity, the picture will be exactly the same as in Sections 4.3.4,4.3.5. In particular the monodromy of the charge lattice (4.7.141) is consistent with what we find in (4.3.50),(4.3.32). The index will be preserved across the conjugation wall, the Hilbert spaces of halo states will undergo the Fermi flip and the spin character will also be preserved.

4.7.3 Extremal Transitions

In this Section we consider an example that was discussed in a number of papers on geometric engineering and heterotic/type II dualities. It first appeared in the discussion of chains of heterotic/type II dual models in [66]. The spectrum at the singularity was analyzed from the type IIA side in [67].

We will be interested only in the last step of the chain of heterotic/II duals, connected by extremal transitions, as described in [67]. On the type II side there are two CY manifolds denoted by X_4 and X_3, and given, roughly, [15] by hypersurfaces in weighted projective spaces $WP(1,1,2,6,10)[20]^{4,190}$ and $WP(1,1,2,8,12)[24]^{3,243}$. Each of these models has a heterotic dual, given by certain $\mathbb{Z}_6$ orbifolds. The main hero is the manifold X_4 with four Kähler moduli t_i. It develops a singularity on the locus $t_4 = 0$ and transitions to the X_3 model.

The description of the singularity in the IIA language is the following: for $t_4 \neq 0$ X_4 contains a $\mathbb{P}^1$ of blown-up A_1 singularities with 28 double points, where the blown-up $\mathbb{P}^1$ splits into two. This family of $\mathbb{P}^1$'s fibered over the base $\mathbb{P}^1$ represents a divisor of X_4, which is nothing else than just a family of conics in $\mathbb{P}^2$ over $\mathbb{P}^1$ with 28 degenerate fibers. In the limit $t_4 \to 0$ the fiber $\mathbb{P}^1$ shrinks and this gives rise to massless particles. One gets an enhanced gauge symmetry at this locus and the massless spectrum consists of a massless $SU(2)$ vectormultiplet and 28 hypermultiplets, fundamental under the new $SU(2)$. This has an interpretation on the heterotic side, where the IIA modulus t_4 corresponds to a Wilson line, of a point of perturbative enhanced

[14] Here for instance $V^+ := V^1 + iV^2$.

[15] We say roughly because the polytope, used to define X_4 in the language of toric geometry, has one additional vertex and correspond to a different toric variety than just $WP(1,1,2,6,10)$.

gauge symmetry with hypermultiplets coming from the E_8 instanton degrees of freedom.

The transition to X_3 occurs at $t_4 = 0$ and on the IIA side consists of blowing-up the singularities and obtaining a new CY with $N_v = 3$ vector moduli and $N_h = 243$ hypermultiplet moduli. The transition has a nice interpretation in field theory, where one goes from the Coulomb to Higgs branch [70]. On the Higgs branch the gauge group is completely broken and one is left with $2 \times 28 - 3 = 53$ additional hypermultiplet moduli.

One way to verify the spectrum at the singularity, that does not involve the heterotic dual of this model, is to compute the periods of X_4 and find their monodromy around the singularity. In this example it is possible to do this explicitly by using a Mellin-Barnes representation of the periods and analytically continuing the periods of X_4 from the large volume point to the neighborhood of the singularity. The advantage of the method of analytic continuation is that it automatically gives an integral symplectic basis for the periods, since we start with such a basis from the large volume point. The details of the computation as well as some background material is given in Appendix G. Performing this computation one finds that there are two dual vanishing periods at the singularity, denoted t_4 and t_4^D, and given in terms of algebraic coordinates z_i on the complex structure moduli space of the mirror X_4, by

$$\begin{aligned} t_4 &= \sqrt{z_4}(1 + O(z_i)) \\ t_4^D &= -\frac{\sqrt{z_4}}{2\pi i}\left((24\log z_4 + 2\log z_2 + 4\log z_3 + 8\log z_1)(1 + O(z_i)) + O(z_i)\right) \end{aligned} \tag{4.7.142}$$

These periods correspond to a pair of charges γ, γ_D with $\langle \gamma, \gamma_D \rangle = 2$, respectively. From these periods we see that there is a monodromy around singularity in the z_4 plane of the form

$$\begin{aligned} t_4 &\to -t_4 \\ t_4^D &\to -t_4^D + 24 t_4, \end{aligned} \tag{4.7.143}$$

which is the monodromy, expected in the $SU(2)$ gauge theory with 28 fundamental flavors. Nevertheless, as we argued in Section 4.6.3, the spectrum will also contain massless monopoles, and the fact that the dual period t_4^D vanishes at the singularity confirms this fact. The physical argument of Section 4.6.3 implies that this charge is populated, but we can supply further evidence for the existence of a monopole (and indeed an infinite tower of dyons) becoming massless together with the W boson at the singularity. In IIA language the W boson is a D2 brane wrapping the generic fiber of the shrinking divisor. The monopole is a D4 brane wrapping the divisor itself (perhaps with some flux). The intersection product of this D2 and D4 is 2 as it should be. Classically, when the D2 volume vanishes at $t_4 = 0$, the D4 volume vanishes

also. On the other hand, the IR freeness of the theory implies that this fact is not spoiled by quantum corrections, as we have seen directly from the periods. So the W-boson and monopole become massless together. The quantum corrections do not spoil this relation, although from the periods we see there is some logarithmic running of the proportionality factor $\frac{1}{g^2}$, again as expected from field theory with $\beta = 48$ and

$$\frac{\mu}{v} = \frac{z_1^{-1/6} z_2^{-1/24} z_3^{-1/12}}{\sqrt{z_4}}.$$

In the mapping of IIA with heterotic variables one identifies $z_2 \sim e^{-2\pi S}$, where S is the heterotic dilaton $S = \frac{4\pi}{g_0^2} - i\frac{\theta}{2\pi}$. Looking at the periods (4.7.142) we see that in the limit of weak heterotic coupling $z_2 \to 0$ for fixed t_4 the dual period t_4^D becomes infinitely massive and disappears from the spectrum. This is as expected in the IR-free theory since the mass of the monopole is proportional to $\frac{1}{g^2}$. If we keep the coupling constant non-zero and take the limit $t_4 \to 0$ then we find that in fact both periods vanish at the singularity and the monopole becomes massless. Moreover, the monopole state cannot be seen in the perturbative spectrum in the IR limit, but it does become massless at the singularity. In this sense the perturbative heterotic string is *misleading* with regards to the massless spectrum. Of course there might be other dyonic massless states and the full massless spectrum depends on the UV completion of the field theory. To determine the full spectrum one has to do a detailed analyses of the singularity in the IIB picture and find all the special Lagrangian cycles, that shrink at the singularity. Regrettably, this computation appears to be out of reach at present. We want to stress that, as follows from the discussion in Section 4.3.4, the massless spectrum of the IR-free gauge theory with fundamental matter is *inconsistent* with the wall-crossing phenomenon. Indeed, the massless electric spectrum gives for the product P in (4.3.33)

$$P(q) = \frac{(1-q)^{28}}{(1-q^2)^4} \tag{4.7.144}$$

which is clearly not a polynomial.

If one goes through the extremal transition to the Higgs branch of the gauge theory, the monopoles get confined via the dual Meissner effect. Thus on that side of the extremal transition they will not be seen in the spectrum. If one wishes to go back and transition to the Coulomb branch the flux tubes confining the monopoles shrink and become tensionless at the transition point, so one again gains free massless monopoles. For some related discussion see [71].

To summarize, this model has a spectrum at the singularity, that does not satisfy the requirements of Section 4.3.1. We still expect that the BPS indices are preserved as one crosses BST walls. To verify this we need to know the full massless spectrum at the singularity. We do

not have this information, and even if we did, as discussed in Section 4.7.1, it is not clear how to sum all contributions to the given BPS state on both sides of the BST wall.

Similarly in the spirit of Section 4.3.4 and [38], we can form a partition function of the BPS indices of states $\Gamma + m\gamma + n\gamma_D$. Here γ is the charge of the hypermultiplet that becomes massless and γ_D is the charge of magnetic monopole. The partition function changes as we go around the singularity and the net change is just the monodromy of the local system of charges. As we discuss in chapter 5 and in [38] this gives a restriction on the spectrum at the singularity in the form of a generalized KS formula which relates the product of KS transformations around the singularity to the monodromy of the local system of charges. Unfortunately we cannot check this statement here since we do not know the full spectrum.

Chapter 5

Wall-crossing from supersymmetric galaxies

In this chapter we give an elementary physical derivation of the Kontsevich-Soibelman wall crossing formula, valid for any theory with a 4d $\mathcal{N} = 2$ supergravity description. The basic strategy we follow is similar to that of [15], which gave a proof of the (motivic) KS wall-crossing formula in the context of $\mathcal{N} = 2$ *field theory*. The essential physical idea used halo configurations of particles bound to line operators. Our analysis will generalize this idea to gravity, without introducing external objects such as line operators. The surrogate for the line operator will be an infinitely massive BPS black hole, to which the BPS objects of interest are bound. The physical cartoon to have in mind is that of a galaxy with a supermassive black hole at its center, where the BPS objects of interest are the solar systems orbiting around it. These galactic configurations exhibit jumping phenomena when dialing the moduli: when crossing certain walls, halos of objects of a particular charge can be pushed out to infinity or conversely come in from infinity. The generating function for the BPS indices of these galactic bound states transforms in a simple way when such a wall is crossed, by the action of a certain operator on the generating function, which follows directly from the simple halo wall crossing formula (a.k.a. the semiprimitive wall crossing formula) of [5]. Collections of walls intersect on real codimension two loci, together also with marginal stability walls for the individual solar systems. Circling around these intersection loci will produce a sequence of wall crossing operations on the generating function. For a contractible loop in moduli space, the product of these operators must be the identity. This turns out to be nothing but the KS formula. For a noncontractible loop in moduli space we find a generalization of the KS formula. This chapter is based on [38].

5.1 BPS galaxies and the halo wall crossing operator

In Section 4.3.2 we gave the main properties of halo BPS states and here we recall the necessary details. A halo is a BPS configuration consisting of an arbitrary number N of particles with electromagnetic charge proportional to a primitive charge γ surrounding a core of charge Γ. For

simplicity of exposition (only!) we will initially consider only halo particles of charge γ. The charges are valued in a symplectic lattice L. The equilibrium distance R between core and halo particles is given by [72]

$$R = \frac{\langle \gamma, \Gamma \rangle}{2\,\mathrm{Im}(e^{-i\alpha} Z_\gamma)}\,, \tag{5.1.1}$$

where $\langle \gamma, \Gamma \rangle$ is the electric-magnetic symplectic product of γ and Γ, Z_γ is the central charge of γ, measured at spatial infinity (where the vector multiplet moduli are set at $t = t_\infty$), and $\alpha = \arg Z_{\Gamma+N\gamma}$. A necessary condition for existence is $R > 0$. When the phases of the central charges of the core and halo line up, i.e. $\arg Z_\Gamma = \arg Z_\gamma = \alpha$, the radius diverges and the halo decays. Both core and halo particles can in turn be composites. The above formula for the equilibrium distance still holds as long as R is much larger than the size of these composites.

In the limit $R \to \infty$, the halo particles can be considered to be noninteracting electric point particles, confined to a sphere threaded by a uniform magnetic flux. The supersymmetric one particle ground states are given by the lowest Landau levels, and the N-particle halo states are constructed from those as an N particle Fock space $\mathcal{F}_\Gamma(N\gamma)$ [10, 5]. We denote the Witten index of these halo states by[1]

$$\Omega^{\mathrm{Fock}}_\Gamma(N\gamma; t_\infty) \equiv \mathrm{Tr}_{\mathcal{F}_\Gamma(N\gamma)}(-1)^F\,. \tag{5.1.2}$$

For $N = 1$, we have $\Omega^{\mathrm{Fock}}_\Gamma(\gamma) = |\langle \gamma, \Gamma \rangle| \Omega(\gamma)$. Here $\Omega(\gamma)$ is the usual $\mathcal{N} = 2$ BPS index, and $|\langle \gamma, \Gamma \rangle|$ is the lowest Landau level degeneracy factor. For general N it is convenient to define a generating function. Introduce formal variables X_i, $i = 1, \ldots, \mathrm{rank} L$, and write $X^\Delta := \prod_i X_i^{\Delta_i}$ for a charge Δ with components Δ_i with respect to some chosen basis for L. Then the generating function is

$$G^{\mathrm{Fock}}_\Gamma(X) := \sum_N \Omega^{\mathrm{Fock}}_\Gamma(N\gamma)\, X^{\Gamma+N\gamma} = \left(1 - (-1)^{\langle \gamma, \Gamma \rangle} X^\gamma\right)^{\Omega(\gamma)|\langle \gamma, \Gamma \rangle|}\, X^\Gamma \tag{5.1.3}$$

This follows from standard Fock space combinatorics [5].

In general $\Omega(\Gamma + N\gamma) \neq \Omega(\Gamma)\, \Omega^{\mathrm{Fock}}_\Gamma(N\gamma)$ in the full theory. The reason is that the true index $\Omega(\Gamma + N\gamma)$ in general gets contributions from many other configurations of charges summing up to the same total charge. For instance a core black hole of charge Γ with two halo particles of charge γ and a core black hole of charge $\Gamma + \gamma$ and one halo particle of charge γ will both contribute to $\Omega(\Gamma + 2\gamma)$. At finite R, the corresponding Fock spaces can be expected to get mixed due to quantum tunneling between these configurations. Only the sum over all possible configurations is guaranteed to give a well defined index. Phrased differently, whereas

[1] The indices depend on the background moduli t_∞. For notational compactness we will sometimes suppress this dependence.

the supersymmetric quantum mechanics of halo particles trapped in their potential minimum at finite R is a well-defined closed system in perturbation theory, nonperturbative tunneling between this minimum and the minimum corresponding to merging with the black hole core causes the wave function of the halo configuration to "leak out" and mix with configurations with different core black hole charges. It is no longer a well-defined closed system.

The leaking can be prevented, however, by taking the limit of infinite core black hole size, as black hole tunneling is generically exponentially suppressed in the size of the black hole. This is entirely an entropic effect. For example the amplitude for fragmentation of an extremal Reissner-Nordström black hole of charge $Q = Q_1 + Q_2$ into black holes of charge Q_1 and Q_2 — a process unobstructed by any potential barrier — is nevertheless suppressed as $e^{-\frac{1}{2}\Delta S}$ where $\Delta S = \pi Q^2 - \pi Q_1^2 - \pi Q_2^2 = 2\pi Q_1 Q_2$ [73]. Therefore in the $Q \to \infty$ limit, taking into account charge quantization, the extremal RN black hole becomes absolutely stable; there is no more mixing with fragmented configurations. Stability of large black holes is a universal phenomenon — even Schwarzschild black holes stop radiating and become stable in the infinite size limit.

Thus, we will consider configurations of BPS objects orbiting around a supermassive black hole core of charge Γ_c, where we eventually send $\Gamma_c \to \infty$ while keeping the total charge of the objects in the orbits finite. The objects themselves can be multicentered BPS bound states. We can loosely think of this system as a galaxy consisting of many solar systems orbiting around a supermassive black hole, and we therefore refer to these objects as "BPS galaxies". The simplest situation is when we have a single halo of particles of charge γ around the hole, but we also allow multiple halos, or more general, non-halo configurations involving interacting solar systems with mutually nonlocal charges. So the most general BPS galaxy will be a complex multi-particle bound state, with potentially strong position-constraining interactions between neighboring solar systems, and intricate exchanges of suns and planets between different solar systems possible when dialing the moduli.

To make this more precise, we have to specify more carefully how we take the limit $\Gamma_c \to \infty$. For our purpose of deriving the KS formula, it turns out to be convenient to single out a particular $U(1)$, give the core large electric and magnetic charges with respect to this $U(1)$, and keep the orbiting solar systems uncharged under this $U(1)$. More precisely, we choose a set of charges $C \equiv \{\Gamma_0, \Gamma_0', \gamma_c\}$ such that Γ_0 supports a single centered BPS black hole, $\langle \Gamma_0, \Gamma_0' \rangle \neq 0$, and $\langle \gamma_c, \Gamma_0 \rangle = 0 = \langle \gamma_c, \Gamma_0' \rangle$. We then set

$$\Gamma_c = \Lambda^2 \Gamma_0 + \Lambda \Gamma_0' + \gamma_c \tag{5.1.4}$$

and take $\Lambda \to \infty$. The anisotropic scaling is chosen for reasons that will become clear later

(see footnote 1). To avoid infinite lowest Landau level degeneracies, we restrict the charges γ of the solar systems orbiting around this core to be orthogonal to both Γ_0 and Γ_0', which means they are uncharged under the $U(1)$ associated to Γ_0 and Γ_0'. More formally, the sublattice of orbiting charges $L_{\rm orb}$ is thus

$$L_{\rm orb} := \{\gamma \in L \,|\, \langle \gamma, \Gamma_0 \rangle = 0 = \langle \gamma, \Gamma_0' \rangle\}. \tag{5.1.5}$$

With this definition, we also have $\gamma_c \in L_{\rm orb}$.

The Hilbert space of BPS galaxies with core charge Γ_c and total orbital charge $\Gamma_{\rm orb}$ has an overall factor corresponding to the internal states of the core black hole, which we can factor out to produce a factor space $\mathcal{H}_{\Gamma_c}(\Gamma_{\rm orb}; t_\infty)$, which can be thought of as the Hilbert space of the orbiting solar systems in a background sourced by the core black hole. We obtain a closed supersymmetric quantum system with this Hilbert space provided there is no mixing between galaxies of different core charges, nor mixing with galaxies which do contain charges in orbit which are *not* in the restricted lattice $L_{\rm orb}$. This turns out to be generically the case in the limit $\Lambda \to \infty$, essentially because such tunneling events are either infinitely entropically suppressed along the lines mentioned above, or infinitely suppressed because they require tunneling over infinite distances. We give detailed arguments for this in appendix H, and prove that there is just one exception, namely when it so happens that the attractor point of Γ_0 lies on a locus with massless particles with charge in $L_{\rm orb}$, in which case there may be mixing between galaxies with cores differing by the charges becoming massless. This situation is nongeneric, and we will assume this is not the case.

Thus, at fixed $\Gamma_{\rm orb}$, in the limit $\Lambda \to \infty$, we can define a proper Witten index for this supersymmetric closed system, which we call the "framed" BPS galaxy index, in analogy with the framed BPS indices of [15]:

$$\overline{\Omega}_C(\Gamma_{\rm orb}; t_\infty) := \lim_{\Lambda\to\infty} {\rm Tr}_{\mathcal{H}_{\Gamma_c}(\Gamma_{\rm orb}; t_\infty)} (-1)^F . \tag{5.1.6}$$

Here $C \equiv \{\Gamma_0, \Gamma_0', \gamma_c\}$ is the set of charges determining the one parameter family $\Gamma_c(\Lambda)$ of core charges as in (5.1.4). It will be useful to introduce the generating function of framed BPS indices:

$$G_C(X; t_\infty) := \sum_{\Gamma_{\rm orb} \in L_{\rm orb}} \overline{\Omega}_C(\Gamma_{\rm orb}; t_\infty)\, X^{\gamma_c + \Gamma_{\rm orb}}. \tag{5.1.7}$$

The presence of singularities and associated monodromies gives rise to some subtleties, which we discuss in section 5.3. For the time being we simply assume we stay in a sufficiently small open set of moduli space, away from singular loci, in which case we can ignore these subtleties altogether.

The key observation that makes this construction useful is that although the generic BPS galaxy has a very complicated structure, its wall crossing behavior when varying t_∞ is very simple. It is entirely governed by pure halo decays, since the galactic core black hole cannot decay and serves as a fixed, primitively charged center. Whenever the central charge $Z(\gamma)$ of some charge γ supporting BPS states lines up with the total central charge $Z = Z(\Gamma_c)+Z(\Gamma_{\rm orb})$ of the galaxy, a halo of objects with charge γ can be added or subtracted at spatial infinity. We again restrict to $\gamma \in L_{\rm orb}$. In the $\Lambda \to \infty$ limit the wall in moduli space where this happens is independent of the solar system charge, since in this limit $Z/Z(\Gamma_c) = 1$, so $\arg Z = \arg Z(\Gamma_c) = \arg Z(\Gamma_0)$ and we can set $\alpha = \alpha_0 := \arg Z(\Gamma_0; t_\infty)$ in (5.1.1). Hence the wall of marginal stability for the halo is [2]

$$W_\gamma = \{t_\infty | \arg[e^{-i\alpha_0} Z(\gamma, t_\infty)] = 0\}\,, \qquad \text{stable side:} \quad \langle \gamma, \gamma_c + \Gamma_{\rm orb}\rangle \, {\rm Im}[e^{-i\alpha_0} Z(\gamma, t_\infty)] > 0\,. \tag{5.1.8}$$

We will call these "BPS walls."

The part of the Hilbert space of all BPS galaxies with fixed core charge Γ_c that jumps across a BPS wall W_γ is given by the halo Fock space described earlier, with an effective core charge Γ, as seen by this halo, given by the *total* interior galactic charge $\Gamma = \Gamma_c + \Gamma_{\rm orb}$ enclosed by the halo. The corresponding transformation of the framed galactic indices can therefore be inferred from (5.1.3). Roughly speaking, the terms in the generating function G_C in (5.1.7) get multiplied by the factor appearing in (5.1.3). However, as we have just explained, the effective Γ appearing in (5.1.3) depends on $\Gamma_{\rm orb}$ and hence is different for the different terms in G_C, and so the multiplication factor will be different. This is easily formalized by introducing a linear operator D_γ acting on monomials X^δ by pulling down the symplectic product:

$$D_\gamma X^\delta := \langle \gamma, \delta \rangle X^\delta\,. \tag{5.1.9}$$

With this and an eye on (5.1.3), we define the following operator acting on polynomials in X: [3]

$$T_\gamma := \left(1 - (-1)^{D_\gamma} X^\gamma\right)^{D_\gamma}\,. \tag{5.1.10}$$

Notice that this operator effectively acts as a diffeomorphism on the coordinates X^i. The transformation of the generating function when crossing the wall W_γ in the direction of *increasing*

[2] These are analogs of the "BPS walls" of [15] with $e^{i\alpha_0}$ playing the role of ζ. However, an important difference is that now $e^{i\alpha_0}$ depends on t_∞ and is only an independent variable to the extent that Γ_0 is.

[3] We remark that the operators $\tau_\gamma := (-1)^{D_\gamma} X^\gamma$ satisfy $\tau_\gamma \tau_{\gamma'} = (-1)^{\langle \gamma, \gamma' \rangle} \tau_{\gamma+\gamma'}$, and hence the operators τ_γ provide a natural quadratic refinement of the mod-two intersection form, a point which aficionados of the KSWCF will surely appreciate. (A related point was made in equations (3.27)-(3.29) of [15].)

$\arg[Z_\gamma e^{-i\alpha_0}]$ is then

$$G_C(X) \to U_\gamma(t)\, G_C(X)\,, \qquad U_\gamma(t) := \prod_{k\in\mathbb{Z}^+} T_{k\gamma}^{\Omega(k\gamma;t)}\,, \tag{5.1.11}$$

where we made the dependence on the point t where the wall is crossed explicit. We take γ to be primitive. The product over k comes from the fact that the walls $W_{k\gamma}$ coincide. (Thus, we have now relaxed our initial assumption that only halo particles of primitive charge γ enter.) To check that this formula is correct when going in the direction of increasing $\arg[Z_\gamma e^{-i\alpha_0}]$, note that on the part of the generating function for which $D_\gamma > 0$, going in this direction means by (5.1.8) going from the unstable to the stable side, and vice versa for the $D_\gamma < 0$ part. Therefore, the wall crossing formula should multiply the $D_\gamma > 0$ terms by halo factors (5.1.3), and conversely remove such factors from the $D_\gamma < 0$ part (or alternatively add such factors when the inverse operation is performed, corresponding to decreasing $\arg[Z_\gamma e^{-i\alpha_0}]$). This is indeed implemented by the fact that we dropped in (5.1.11) the absolute value signs appearing in the exponent of (5.1.3).

Finally, we come to the central formula of this chapter. Consider a closed contractible loop $\mathcal{P}$ in moduli space (noncontractible loops will be discussed in section 5.3). Along this loop, the generating function G_C will undergo a sequence of wall crossing operations $U_{\gamma_i}(t_i)$. Since $\mathcal{P}$ is contractible, the composition of these operations must act trivially on G_C, for any choice of γ_c and starting point t:

$$\prod_i U_{\gamma_i}(t_i) \cdot G_C = G_C\,, \tag{5.1.12}$$

where the product is ordered according to the sequence of walls crossed: points crossed later in the path are placed to the left. At the core attractor point $t_*(\Gamma_c)$ there are no multicentered bound states involving Γ_c, and hence no BPS galaxies. So at this point we have simply

$$G_C(X)|_{t_\star(\Gamma_c)} = X^{\gamma_c}\,. \tag{5.1.13}$$

Starting from this expression, the wall crossing formula (5.1.11) uniquely determines all framed galactic indices given all $\Omega(k\gamma)$. This shows that G_C is well defined as a function to the extent that the wall crossing factors are. (It is conceivable that a dense set of BPS walls can lead to an ill-defined expression.) Furthermore by varying γ_c we can generate as many independent functions $G_C(X)$ as there are independent variables X_k associated to charges in $L_{\rm orb}$. [4] This in combination with the fact that the wall crossing operators U_γ act as diffeomorphisms implies

[4] This corresponds to the condition, discussed in [15], that there are "enough" line operators to deduce the KSWCF.

that the product of the sequence of halo wall crossing operators around a contractible loop must be the identity

$$\prod_i U_{\gamma_i}(t_i) = 1\,. \tag{5.1.14}$$

We will prove in detail in the next section that this is in essence equivalent to the KS wall crossing formula.

5.2 Derivation of the KS formula

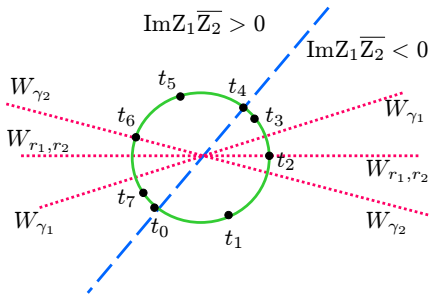

Figure 5.1: This shows the neighborhood $\mathcal{U}$ in the normal bundle to $W_{\gamma_1} \cap W_{\gamma_2}$. The wall of marginal stability is given by $\mathrm{Im}[Z(\gamma_1;t)\overline{Z(\gamma_2;t)}] = 0$ since $\mathrm{Re}[Z(\gamma_1;t)\overline{Z(\gamma_2;t)}]$ is nonzero throughout $\mathcal{U}$. We choose the ordering of γ_1, γ_2 so that W_{γ_1} is counterclockwise from W_{γ_2} with opening angle smaller than π. Then the BPS walls $W_{r_1\gamma_1+r_2\gamma_2}$ are ordered so that increasing r_1/r_2 gives walls in the counterclockwise direction. We consider a path $\mathcal{P}$ in $\mathcal{U}$ circling the origin in the counterclockwise direction. The central charges of vectors $r_1\gamma_1 + r_2\gamma_2$ with $r_1, r_2 \geq 0$ at representative points $t_0, \ldots, t_7$ along $\mathcal{P}$ are illustrated in the next figure.

We now demonstrate that when $\mathcal{P}$ is a small contractible loop intersecting a wall of marginal stability the Kontsevich-Soibelman wall crossing formula is a consequence of (5.1.14). Let us therefore consider two mutually nonlocal charges γ_1, γ_2 and a generic *non-singular* point $t_{ms} \in MS(\gamma_1, \gamma_2)$ where both central charges are nonzero and γ_1, γ_2 support BPS states. Using the attractor equation it is easy to show that we can always find a Γ_0 (and hence a phase α_0) so that Γ_0 supports single-centered black holes and t_{ms} lies on the intersection of BPS walls $W_{\gamma_1} \cap W_{\gamma_2}$. [5] This intersection is real codimension two in moduli space and we now consider a small neighborhood $\mathcal{U}$ of t_{ms} so that the only other BPS walls $W_{\gamma'}$ passing through t_{ms} arise from charges of the form $\gamma' = r_1\gamma_1 + r_2\gamma_2$ for rational r_1, r_2. We will denote charges of this

[5] We can take for example $\Gamma_0 \equiv -2\mathrm{Im}[\bar{X}\Omega^{(3,0)}]$, where $\Omega^{(3,0)}$ is the holomorphic 3-form evaluated at t_{ms} and X is an arbitrary complex constant with $\arg X \equiv \arg Z_1 = \arg Z_2$. This Γ_0 has a regular attractor point, namely t_{ms}, because the equation we used to define Γ_0 is nothing but the attractor point equation. Taking the symplectic product of this equation with γ_1, γ_2 shows that $\langle\gamma_1, \Gamma_0\rangle = 0 = \langle\gamma_2, \Gamma_0\rangle$. Taking the symplectic product with $\Omega^{(3,0)}$ shows that $X = Z(\Gamma_0 : t_{ms})$, so, as we wished, the central charges line up at t_{ms}. Although Γ_0 will in general not be quantized, this is acceptable since all we care about in the end is the limit $\Lambda \to \infty$.

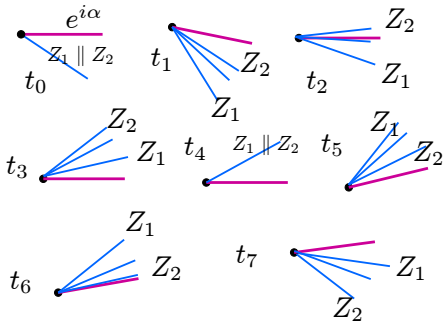

Figure 5.2: As t moves along the path $\mathcal{P}$ the central charges evolve as in this figure. Note that $\mathrm{Im}(Z_1\overline{Z_2}) > 0$ means that Z_1 is counterclockwise to Z_2 and rotated by a phase less than π. In that case the rays parallel to $r_1Z_2 + r_2Z_2$ for $r_1, r_2 \geq 0$ are contained in the cone bounded by $Z_1\mathbb{R}_+$ and $Z_2\mathbb{R}_+$, and ordered so that increasing r_1/r_2 corresponds to moving counterclockwise. When t crosses the marginal stability wall the cone collapses and the rays reverse order. As t moves in the region t_2 the quantity $\arg[Z_\gamma e^{-i\alpha_0}] > 0$ is increasing for all γ_{r_1,r_2} with $r_1, r_2 \geq 0$ while at the point t_6 the argument is decreasing.

form by γ_{r_1,r_2}. Since the point t_{ms} is non-singular a loop around it is contractible and (5.1.14) holds.

Below we will argue that, perhaps after choosing suitable linear combinations, we can assume that the only populated charges of type γ_{r_1,r_2} in $\mathcal{U}$ in fact have $(r_1, r_2) \in \mathbb{Z}^2$ with r_1, r_2 both ≥ 0 or both ≤ 0. We can order γ_1, γ_2 so that the configuration of BPS walls and the marginal stability wall are arranged as shown in Figure 5.1. Suppose we begin at the point t_1 and move along the path $\mathcal{P}$ in the counterclockwise direction. We first cross the BPS walls in the region $\mathrm{Im}Z_1\overline{Z_2} < 0$ in order of increasing r_1/r_2 and *increasing* $\arg[Z_{\gamma_{r_1,r_2}} e^{-i\alpha_0}]$. Then we cross in the region $\mathrm{Im}Z_1\overline{Z_2} > 0$ again with increasing r_1/r_2 but now this corresponds to *decreasing* values of $\arg[Z_{\gamma_{r_1,r_2}} e^{-i\alpha_0}]$. Thus we have

$$\prod_{\frac{r_1}{r_2}\nearrow}^{\leftarrow} T_{r_1,r_2}^{-\Omega^+_{r_1,r_2}} \prod_{\frac{r_1}{r_2}\nearrow}^{\leftarrow} T_{r_1,r_2}^{\Omega^-_{r_1,r_2}} = 1 \tag{5.2.15}$$

where the arrows on the product mean that increasing values of r_1/r_2 are written to the left, and $\Omega^\pm_{r_1,r_2}$ is the BPS index of $r_1\gamma_1 + r_2\gamma_2$ in the region $\mathcal{U}$ with $\mathrm{Im}Z_1\bar{Z}_2 > 0$ and < 0 respectively. Taking into account the relation between the ordering of r_1/r_2 and the ordering of the phases of the central charges illustrated in figures 5.1 and 5.2 we can also write this in the more traditional way:

$$\prod_{\arg Z_{r_1,r_2}\nearrow}^{\rightarrow} T_{r_1,r_2}^{\Omega^+_{r_1,r_2}} = \prod_{\arg Z_{r_1,r_2}\nearrow}^{\rightarrow} T_{r_1,r_2}^{\Omega^-_{r_1,r_2}}. \tag{5.2.16}$$

This is the KS wall crossing formula.

We still need to fill in a gap above and justify the important claim that we can choose

γ_1, γ_2 so that only r_1, r_2 both ≥ 0 or ≤ 0 are populated. This "root basis property" can be rigorously proven in certain field theory examples [50]. We offer an alternative justification here by requiring that the spectrum of BPS masses should not have an accumulation point at zero. (We are therefore using that the point t_{ms} is not at a singularity of moduli space since that assumption is violated, for example at a superconformal point.) Denoting the central charges of γ_1, γ_2 at t_{ms} by ρ_1, ρ_2 we therefore know that there is an $\epsilon > 0$ so that populated charges γ_{r_1,r_2} must have $|r_1\rho_1 + r_2\rho_2| > \epsilon$. In the (r_1, r_2)-plane this is a strip of width 2ϵ centered on the line with slope $-\rho_2/\rho_1$. (Since t_{ms} is on the marginal stability wall ρ_2/ρ_1 is real.) If our point t_{ms} is generic then there is in fact a neighborhood of t_{ms} in the marginal stability wall so that, moving along this wall the spectrum of BPS particles of charges of the form γ_{r_1,r_2} must remain constant. But the slope $-\rho_2/\rho_1$ will vary in this neighborhood. This means that there must be an unpopulated wedge (and its negative) in the (r_1, r_2)-plane. By choosing a suitable redefinition $\gamma_1 \to a\gamma_1 + b\gamma_2, \gamma_2 \to c\gamma_1 + d\gamma_2$ we can ensure that the populated states in the complementary wedges are of the form γ_{r_1,r_2} with r_1, r_2 both ≥ 0 or both ≤ 0.

We end with two remarks

1. The root basis property of BPS states is addressed in the mathematical framework of Kontsevich and Soibelman [7] in a slightly different way. A part of their "stability conditions," used a quadratic form on the lattice of charges $\mathcal{Q} : L \to \mathbb{R}$ and only the charges that satisfied $\mathcal{Q}(\gamma) \geq 0$ were considered. The quadratic form also has the property that $\mathcal{Q}|_{\mathrm{Ker}\, Z} < 0$, where Z is the central charge map $Z : L \to \mathbb{C}$. Thus, restricting the set of charges entering the WCF to $\mathcal{Q}(\gamma) \geq 0$ means that we have to discard certain wedges in the space of charges surrounding the directions with $Z(\gamma) = 0$.

2. Finally, we comment on the "motivic" or "refined" version of the wall-crossing formula [7] which takes into account spin degrees of freedom [74, 75]. The field theoretic derivation of the motivic KSWCF given in [15] can also be carried over directly in the present context: We now let X_γ be valued in the quantum torus. We replace G_C by the generating function of the spin characters, and across the walls W_γ we will find that G_C is conjugated by certain combinations of quantum dilogarithms. However, we stress that the justification for the derivation in [15] relied on the existence of "*protected spin characters*," which can only be defined if there is an $SU(2)_R$ symmetry in the supersymmetry algebra. In general this symmetry is not present in supergravity, and hence the validity of "motivic" generalization of the wall-crossing formula is a little mysterious. In fact, as is well-known, the spin character depends on hypermultiplet moduli as well as vectormultiplet moduli.

(For examples in the weakly coupled heterotic strings with type II duals see [69, 76].)

5.3 Generalization to noncontractible loops

In our derivation of the KS formula, we considered a contractible loop $\mathcal{P}$ in moduli space. Nothing prevents us from considering instead a non-contractible loop, in particular a loop circling around a point on the discriminant locus. Such a loop will be closed in moduli space but not in covering space, and the local system of charges undergoes nontrivial monodromy $M_{\mathcal{P}} : L \to L$ after going around it.[6] As a result the generating function will not be exactly preserved, and (5.1.12) must be modified.

As mentioned under (5.1.7), the proximity of singularities associated to nontrivial monodromies can lead to some subtleties in the definition of the framed BPS indices $\overline{\Omega}_C(\Gamma_{\rm orb}, t_\infty)$. Besides the usual jumps at marginal stability, there are two other kinds of formal index "jumps" (or rather relabelings) related to the presence of singularities and monodromies. The first occurs when t_∞ crosses a cut, where the choice of charge lattice basis jumps by convention. This is just a relabeling of indices, equating framed indices involving charges related by the corresponding basis transformation. If desired it can be eliminated by going to the moduli covering space. The second event occurs when t_∞ crosses a conjugation wall in the language of chapter 4, i.e. when the core attractor flow gets "pulled through" a singular locus in moduli space. In this case new particles (becoming massless at the singularity) appear in orbit while the apparent core charge as seen from infinity jumps, keeping the total charge (and index) unchanged. This is again some kind of relabeling of indices, equating framed indices involving shifted core and orbit charges, but this time the jump cannot be eliminated by going to the covering space.

More formally, when crossing a cut from t_∞ to t'_∞, charges $\Gamma|_{t'_\infty}$ and $M\cdot\Gamma|_{t_\infty}$ get identified. Thus the indices on the respective sides of the cut are related by

$$\overline{\Omega}_C(\Gamma_{\rm orb}; t'_\infty) = \overline{\Omega}_{M\cdot C}(M\cdot\Gamma_{\rm orb}; t_\infty)\,. \tag{5.3.17}$$

A short computation shows that the generating functions get accordingly identified as

$$G_C(X; t_\infty) = \hat{M}\cdot G_{M^{-1}C}(X, t'_\infty)\,, \tag{5.3.18}$$

where we defined for any automorphism M of the charge lattice a map on generating functions by

$$\hat{M}\cdot\sum_\Gamma a_\Gamma X^\Gamma := \sum_\Gamma a_\Gamma X^{M\cdot\Gamma}\,. \tag{5.3.19}$$

[6] To avoid cluttering the discussion, in the following we will not bother specifying at each step in which direction we orient loops, monodromies etc.

When crossing a conjugation wall from t_∞ to t'_∞, by definition, the core attractor flow gets pulled through the discriminant locus, so that if initially the core attractor flow did not cross the cut ending on the discriminant locus, it now does, or vice versa. By physical continuity, the core charge as seen by a local observer at the core must remain Γ_c. Hence, if the monodromy transformation associated to the cut is $\Gamma \to M \cdot \Gamma$, the apparent core charge as seen by an observer at spatial infinity jumps from Γ_c to $M \cdot \Gamma_c$. Since the total charge must remain the same, the charge in the galactic orbit must jump from $\Gamma_{\rm orb}$ to $\Gamma_{\rm orb} + (1 - M) \cdot \Gamma_c$ (see [34] for a detailed discussion of how this happens physically). Note that to remain in the picture in which the orbit charge remains finite when $\Lambda \to \infty$, we should therefore require

$$M \cdot \Gamma_0 = \Gamma_0 \,, \qquad M \cdot \Gamma'_0 = \Gamma'_0 \,. \tag{5.3.20}$$

The framed indices on the respective sides of the conjugation wall are then related by

$$\overline{\Omega}_C(\Gamma_{\rm orb}; t_\infty) = \overline{\Omega}_{M \cdot C}(\Gamma_{\rm orb} + (1 - M) \cdot \gamma_c; t'_\infty) \,. \tag{5.3.21}$$

The corresponding generating functions are related even more simply by

$$G_C(X, t_\infty) = G_{M \cdot C}(X, t'_\infty) \,. \tag{5.3.22}$$

We can now collect these results and state the generalization of (5.1.12) to the case of a noncontractible loop $\mathcal{P}$ around a point t_0 of the discriminant locus, with associated monodromy M. As before, we assume that no massless BPS particles exist at $t_*(\Gamma_0)$. Since in general there are massless BPS particles present at the discriminant locus, we assume in particular that we have chosen Γ_0 to be such that $t_0 \neq t_*(\Gamma_0)$. There are two cases to distinguish:

1. **Singularity without conjugation wall**: This is the case for singularities at infinite distance, such as the infinite volume limit of IIA on the quintic. We can assume there is a single cut ending on the singularity, across which the generating function transforms as in (5.3.18). Going infinitesimally across the cut in one direction or along the full loop $\mathcal{P}$ in the other direction (along which the generating function undergoes a series of wall crossing operations as before), should give the same result. Thus (5.1.12) generalizes to

$$\prod_i U_{\gamma_i}(t_i) \cdot G_C = \hat{M} \cdot G_{M^{-1} \cdot C} \,. \tag{5.3.23}$$

2. **Singularity with conjugation wall**: This is the case typically for singularities at finite distance, such as the conifold point of IIA on the quintic. Assuming (5.3.20) and taking without loss of generality the cut on top of the conjugation wall for convenience, the

transformation of the generating function when crossing the wall is given simply by $G_C \to G_{M\cdot C} \to \hat{M} \cdot G_C$, and the analog of (5.1.12) becomes

$$\prod_i U_{\gamma_i}(t_i) \cdot G_C = \hat{M} \cdot G_C \,. \tag{5.3.24}$$

By the same arguments as before, we can infer from this the operator equation

$$\prod_i U_{\gamma_i}(t_i) = \hat{M} \,, \tag{5.3.25}$$

which generalizes (5.1.14).

As an application of this formula, consider a singularity t_0 where a charge γ becomes massless, but no other linearly independent charges do. Because $Z(\gamma)$ acquires all phases around t_0, the loop $\mathcal{P}$ will necessarily cross both W_γ and $W_{-\gamma}$. If the loop is chosen such that these are the only walls that are crossed, equation (5.3.25) becomes

$$\begin{aligned} \hat{M} &= U_{-\gamma} \cdot U_\gamma \\ &= \prod_k \left(1 - (-1)^{-kD_\gamma} X^{-k\gamma}\right)^{-k\Omega(k\gamma)D_\gamma} \prod_k \left(1 - (-1)^{kD_\gamma} X^{k\gamma}\right)^{k\Omega(k\gamma)D_\gamma} \\ &= X^{\sum_k k^2 \Omega(k\gamma)\, \gamma D_\gamma} \,. \end{aligned} \tag{5.3.26}$$

Recalling (5.3.19), we see this is equivalent to

$$M \cdot \Gamma = \Gamma + \sum_k k^2 \Omega(k\gamma) \langle \gamma, \Gamma \rangle \, \gamma \,. \tag{5.3.27}$$

Thus this generalized KS formula relates monodromy to the the BPS spectrum. In the case of the simple conifold, $\Omega(k\gamma) = \delta_{k,0}$ and the above formula reduces to the well know Picard-Lefschetz monodromy formula $M \cdot \Gamma = \Gamma + \langle \gamma, \Gamma \rangle \, \gamma$. We discuss such relations in much more detail in chapter 4.

Appendix A

Attractor flow trees near the large volume point

In this appendix we summarize some facts about attractor flow trees. It was conjectured in [11, 27] that the existence of multicentered BPS solutions of supergravity can be analyzed in terms of the the existence of split attractor flow trees. Some attempts at making this conjecture more precise were made in [5, 9].

Split Attractor Flow Conjecture (SAFC):

a) The components of the moduli spaces (in $\vec{x}_i$) of the multicentered BPS solutions with constituent charges Γ_i and background t_∞, are in 1-1 correspondence with the attractor flow trees beginning at t_∞ and terminating on attractor points for Γ_i.

b) For a fixed t_∞ and total charge Γ there are only a finite number of attractor flow trees.

A practical recipe of identifying the intervals with the corresponding tree topologies is the following: tune the moduli at infinity such that they approach the first MS wall of a given attractor flow tree. Then, as we change the moduli across that MS wall, the corresponding component of moduli space of solutions to (2.7.58) ceases to exist.

We now give an explicit description of an attractor flow tree. First, we introduce some notation. For a general tree we will denote vertices of the tress by $\vec{\epsilon}$, which is a vector of $+$ and $-$ signs and the sequence of $+$ and $-$ corresponds to sequence of right and left turns that one needs to make when going from the origin of the tree to that vertex. Quantity X related to a particular vertex $\vec{\epsilon}$ will be denoted by $X^{(\vec{\epsilon})}$. The attractor equation for the edge starting at vertex (a), looks like:

$$2e^{-U} Im(e^{-i\alpha^{(a)}}\Omega(t)) = -H(s^{(a)}), \tag{1.0.1}$$

where $\Omega(t) = -\frac{1}{\sqrt{4/3J^3}} e^{B+iJ}$ (in IIA picture), e^U is the metric warp factor, $\alpha^{(a)}$ is the phase of central charge $Z(\Gamma^{(a)})$, $s^{(a)}$ is a parameter of the flow on this edge, and

$$H(s^{(a)}) = \Gamma^{(a)} s^{(a)} - \Delta H^{(a)}. \tag{1.0.2}$$

$\Delta H^{(a)}$ depends only on the moduli at infinity and is determined recursively by summing contributions from the origin of the tree up to vertex (a):

$$\begin{aligned}
&\Delta H = 2Im(e^{-i\alpha}\Omega)|_{t_\infty} \\
&\Delta H^{(+)} = \Delta H^{(-)} = \Delta H - \Gamma s_{ms} \\
&\Delta H^{(++)} = \Delta H^{(+-)} = \Delta H^{(+)} - \Gamma^{(+)} s^{(+)}_{ms} \\
&\Delta H^{(-+)} = \Delta H^{(--)} = \Delta H^{(-)} - \Gamma^{(-)} s^{(-)}_{ms}, \ ...
\end{aligned} \tag{1.0.3}$$

where $s^{(a)}_{ms}$ are values of parameters along the flow, for which surfaces of marginal stability are crossed:

$$\begin{aligned}
s_{ms} &= \frac{\langle \Gamma^{(+)} \Delta H \rangle}{\langle \Gamma^{(+)} \Gamma \rangle} \\
s^{(+)}_{ms} &= \frac{\langle \Gamma^{(++)} \Delta H^{(+)} \rangle}{\langle \Gamma^{(++)} \Gamma^{(+)} \rangle} \\
s^{(-)}_{ms} &= \frac{\langle \Gamma^{(-+)} \Delta H^{(-)} \rangle}{\langle \Gamma^{(-+)} \Gamma^{(-)} \rangle}, \ ...
\end{aligned} \tag{1.0.4}$$

The solution to the attractor equations (1.0.1), that is, the image of the flow in moduli space, can be written in closed form in terms of the entropy function $S(p,q)$ [28]:

$$t^A(s^{(a)}) = \left. \frac{\frac{\partial S}{\partial q_A} + \pi i p^A}{\frac{\partial S}{\partial q_0} - \pi i p^0} \right|_{(p,q)=H(s^{(a)})} . \tag{1.0.5}$$

Here, the parameter $s^{(a)}$ varies as: $s^{(a)} \in (0, \infty)$ for the terminal edge, and $s^{(a)} \in (0, s^{(a)}_{ms})$ for an internal edge.

For a given attractor tree to exist, all its edges have to exist. Terminal edges exist if the discriminants of terminal charges are positive, or if the terminal charge is pure electric or magnetic, which corresponds to the flow going to the boundary of moduli space. Inner edges exist if:

1. the flow reaches the MS wall at a positive flow parameter $s^{(a)}_{ms} > 0$
2. MS wall (not an anti-MS wall) is crossed, i.e. $\frac{Z(\Gamma^{(a+)})}{Z(\Gamma^{(a-)})}|_{s^{(a)}_{ms}} > 0$
3. MS wall is crossed before the flow hits a zero of the central charge (if present):

$$s^{(a)}_{ms} \leq s^{(a)}_0 \quad \text{or} \quad s^{(a)}_0 \leq 0.$$

where $s^{(a)}_0$ is the value where the flow crashes on a zero.

For a D4-D2-D0 charge we give explicit formulae for attractor flow in moduli space:

$$
\begin{aligned}
&t^a(s) = D(P(s))^{ab}Q_b(s) + iP^a(s)\sqrt{-6\hat{q}_0(s)/P^3(s)} \\
&\Gamma(s) = p^0(s) + P(s) + Q(s) + q_0(s)dV = s\Gamma - \Delta H \\
&\Delta H = \frac{2Im(\bar{Z}\Omega)}{|Z|}|_\infty = \\
&= \frac{2}{\sqrt{\frac{4}{3}J^3}}\left(2\frac{-Q\cdot J + P\cdot B\cdot J}{P\cdot J^2} - J + J^2\frac{-Q\cdot J + P\cdot B\cdot J}{P\cdot J^2} + \frac{J^3}{6}\right)|_\infty. \qquad (1.0.6)
\end{aligned}
$$

In the formula for ΔH we used the large J_∞ approximation and dropped relative corrections of order $O(J_\infty^{-2})$. The expression for $t^a(s)$ was found from (1.0.5) putting $p^0(s) = 0$. Strictly speaking, this is not true because already ΔH contains non-zero contribution to $p^0(s)$. To estimate the error that we make, take the expression for the moduli for a 1-parameter moduli space and expand it around $p^0(s) = 0$. The first correction looks like:

$$
\delta_1 t(s) = \left[\frac{2Q(s)^2 - 3P(s)q_0(s)}{P(s)^3} + i\frac{\sqrt{3}P(s)Q(s)(2Q(s)^2 - 3P(s)q_0(s))}{3P(s)^3\sqrt{P(s)^2(Q(s)^2 - 2P(s)q_0(s))}}\right]p^0(s). \qquad (1.0.7)
$$

Focusing on J_∞ dependence, $\Gamma(s)$ in (1.0.6) can be written as

$$
\Gamma(s) = \left(O(J_\infty^{-5/2}), sP + O(J_\infty^{-1/2}), sQ + O(J_\infty^{-1/2}), sq_0 + O(J_\infty^{3/2})\right). \qquad (1.0.8)
$$

This means that, for instance, for s of order $s \sim J_\infty^{-1/2+\epsilon}$ with $0 \leq \epsilon \leq 2$ (which covers all the cases of interest of chapter 2) the correction in (1.0.7) is of order

$$
\delta_1 t(s) \sim O(J_\infty^{-2\epsilon}) + iO(J_\infty^{-1-3/2\epsilon}). \qquad (1.0.9)
$$

and can be neglected in large J_∞ limit.

Appendix B

Lefschetz $SU(2)$ action on the Higgs branch ground states

In this Appendix we demonstrate that Lefschetz $SU(2)$ action on the cohomology of the Higgs branch moduli space coincides with spatial group of rotations. We give a brief derivation of the Hamiltonian of SSQM on it's Higgs branch, together with the rotation generators. Given the two we will conclude how rotations act on the eigenfunctions of the Hamiltonian.

We rewrite the Lagrangian of SSQM (3.1.1) after integrating out auxiliary fields and for simplicity the case of only "-" fields present:

$$L = \frac{\mu}{2}(\dot{x}^2 + 2i\bar{\lambda}\dot{\lambda}) + |\partial_\tau \phi^a|^2 + \frac{i}{2}\left(\bar{\psi}^a \partial_\tau \psi^a - \partial_\tau \bar{\psi}^a \psi^a\right) - r^2|\phi^a|^2 - \frac{1}{2\mu}(|\phi^a|^2 + \theta)^2 - \bar{\psi}^a \vec{x}\cdot\vec{\sigma}\psi^a - \\ -i\sqrt{2}\left(\bar{\phi}^a \lambda^\alpha \psi^a_\alpha + \phi^a \bar{\psi}^{a\,\alpha}\bar{\lambda}_\alpha\right) \tag{2.0.1}$$

In the regime (3.1.9) we will integrate out fields $\vec{x}, \lambda$ as well as "radial" components of ϕ, ψ, which become massive due to the potential $\frac{1}{2\mu}(|\phi^a|^2 + \theta)^2$. In order to decompose fields into "radial" and "angular" components we choose a patch in the field space where $\phi^1 \neq 0$. Introduce the following coordinates:

$$\phi = (\phi^1, ..., \phi^n) = \tilde{\phi}\frac{(1, z^1, ..., z^{n-1})}{\sqrt{1 + \sum |z^i|^2}} := \tilde{\phi}\vec{n}. \tag{2.0.2}$$

Here, z^i are coordinates on one patch of CP^{k-1}, $\tilde{\phi}$ is the "radial" field, whose modulus will become massive and $\|n\|^2 = (\vec{n}^\dagger, \vec{n}) = 1$. Fermions are decomposed according to the supersymmetry transformations:

$$\psi^a = \frac{\partial \phi^a}{\partial \tilde{\phi}}\xi_{\tilde{\phi}} + \frac{\partial \phi^a}{\partial z^i}\xi_i + \frac{\partial \phi^a}{\partial \bar{z}^i}\bar{\xi}_i = \vec{n}\xi_{\tilde{\phi}} + \tilde{\phi}\partial_i \vec{n}\xi_i - \frac{1}{2}A_{\bar{i}}\tilde{\phi}\partial_i \vec{n}\bar{\xi}_i. \tag{2.0.3}$$

Here, $A_{\bar{i}} = \frac{z^i}{(1+\sum |z^i|^2)}$ is the antiholomorphic part of the connection on the canonical bundle of

CP^{k-1}. Let's list a number of expressions for later use:

$$
\begin{aligned}
&(\vec{n}^\dagger, \partial_i \vec{n}) = \frac{1}{2} A_i = \frac{\bar{z}^i}{2(1+\sum |z^i|^2)} \\
&(\partial_{\bar{i}} \vec{n}^\dagger, \vec{n}) = \frac{1}{2} A_{\bar{i}} = \frac{z^i}{2(1+\sum |z^i|^2)} \\
&(\vec{n}^\dagger, \dot{\vec{n}}) = \frac{1}{2}(A_i \dot{z^i} - A_{\bar{i}} \dot{\bar{z}^j}) \\
&(\bar{\partial}_{\bar{j}} \vec{n}^\dagger, \partial_i \vec{n}) = \frac{\delta_{ij}}{(1+\sum |z^i|^2)} - \frac{3}{4} \frac{\bar{z}^i z^j}{(1+\sum |z^i|^2)^2} \\
&(\vec{n}^\dagger, \partial_{\bar{i}} \dot{\vec{n}}) = -\frac{\dot{\bar{z}^j}}{2(1+\sum |z^i|^2)} - \frac{\bar{z}^i}{4} \frac{\bar{z}^k \dot{z}^k - z^k \dot{\bar{z}}^k}{(1+\sum |z^i|^2)^2} \\
&(\bar{\partial}_{\bar{i}} \vec{n}^\dagger, \dot{\vec{n}}) = \frac{\dot{z^i}}{(1+\sum |z^i|^2)} - \frac{z^i}{4} \frac{3\bar{z}^k \dot{z}^k + z^k \dot{\bar{z}}^k}{(1+\sum |z^i|^2)^2} \\
&(\bar{\partial}_{\bar{i}} \vec{n}^\dagger, \partial_j \dot{\vec{n}}) = -\frac{\delta_{ij}(\bar{z}^k \dot{z}^k + z^k \dot{\bar{z}}^k)}{2(1+\sum |z^i|^2)^2} - \frac{2\bar{z}^j \dot{z}^i + z^i \dot{\bar{z}}^j}{4(1+\sum |z^i|^2)^2} - \frac{\bar{z}^j z^i (7\bar{z}^k \dot{z}^k + 5 z^k \dot{\bar{z}}^k)}{8(1+\sum |z^i|^2)^3}.
\end{aligned} \tag{2.0.4}
$$

Introducing the notation $\tilde{\phi} = \rho e^{i\alpha}$ the kinetic term for ϕ can be written as

$$
|\partial_\tau \phi^a|^2 = (\partial_\tau \rho)^2 + \rho^2 \left(\partial_\tau \alpha - i(\vec{n}^\dagger, \dot{\vec{n}}) \right)^2 + \rho^2 \omega^{FS}_{i\bar{j}} \partial_\tau z^i \partial_\tau \bar{z}^{\bar{j}}, \tag{2.0.5}
$$

where $\omega^{FS}_{i\bar{j}}$ is the Fubini-Studi metric:

$$
\omega^{FS}_{i\bar{j}} = \frac{\delta_{ij}}{(1+\sum |z^i|^2)} - \frac{\bar{z}^i z^j}{(1+\sum |z^i|^2)^2}. \tag{2.0.6}
$$

To write fermion kinetic term we introduce fermion field

$$
\chi = \xi_{\tilde{\phi}} - \frac{1}{2} \tilde{\phi} A_{\bar{j}} \bar{\xi}^j + \frac{1}{2} \tilde{\phi} A_i \xi^i, \tag{2.0.7}
$$

and direct calculation gives:

$$
\begin{aligned}
&\frac{i}{2} \left(\bar{\psi}^a \partial_\tau \psi^a - \partial_\tau \bar{\psi}^a \psi^a \right) = \frac{i}{2} \left(\bar{\chi} (\partial_\tau + (\vec{n}^\dagger, \dot{\vec{n}})) \chi - (\partial_\tau - (\vec{n}^\dagger, \dot{\vec{n}})) \bar{\chi} \chi \right) + \\
&+ \frac{i}{2} \omega^{FS}_{i\bar{j}} \left(\tilde{\phi}^\dagger \bar{\xi}^j (\partial_\tau + (\vec{n}^\dagger, \dot{\vec{n}}))(\tilde{\phi} \xi^i) + \rho^2 \Gamma^i_{km} \bar{\xi}^j \xi^k \dot{z}^m - (\partial_\tau - (\vec{n}^\dagger, \dot{\vec{n}}))(\tilde{\phi}^\dagger \bar{\xi}^j) \tilde{\phi} \xi^i - \rho^2 \Gamma^{\bar{j}}_{\bar{k}\bar{m}} \bar{\xi}^k \xi^i \dot{\bar{z}}^m \right) - \\
&- i \bar{\chi} \tilde{\phi} \xi^i \left((\dot{\vec{n}}, \partial_i \vec{n}) - (\vec{n}^\dagger, \partial_i \vec{n})(\dot{\vec{n}}, \vec{n}) \right) + i \tilde{\phi}^\dagger \bar{\xi}^i \chi \left((\bar{\partial}_{\bar{i}} \vec{n}^\dagger, \dot{\vec{n}}) - (\partial_{\bar{i}} \vec{n}^\dagger, \vec{n})(\vec{n}^\dagger, \dot{\vec{n}}) \right).
\end{aligned} \tag{2.0.8}
$$

Finally introducing $\chi' = e^{-i\alpha} \chi$, we can write the full Lagrangian as

$$L = \frac{\mu}{2}\dot{x}^2 + i\bar{\lambda}\dot{\lambda} + (\partial_\tau\rho)^2 + \rho^2\left(\partial_\tau\alpha - i(\vec{n}^\dagger, \dot{\vec{n}})\right)^2 + \rho^2\omega^{FS}_{i\bar{j}}\partial_\tau z^i\partial_\tau\bar{z}^{\bar{j}} +$$
$$+\frac{i}{2}\left(\bar{\chi}'D\chi' - \bar{D}\bar{\chi}'\chi'\right) + \frac{i}{2}\rho^2\omega^{FS}_{i\bar{j}}\left(\bar{\xi}^j D\xi^i + \Gamma^i_{km}\bar{\xi}^j\xi^k\dot{z}^m - \bar{D}\bar{\xi}^j\xi^i - \Gamma^{\bar{j}}_{\bar{k}\bar{m}}\bar{\xi}^k\xi^i\dot{\bar{z}}^m\right) -$$
$$-i\rho\bar{\chi}'\xi^i C^i + i\rho\bar{\xi}^i\chi'\bar{C}^i -$$
$$-r^2\rho^2 - \frac{1}{2\mu}(\rho^2+\theta)^2 - \bar{\chi}'\vec{x}\cdot\vec{\sigma}\chi' - \rho^2\omega^{FS}_{i\bar{j}}\bar{\xi}^j\vec{x}\cdot\vec{\sigma}\xi^i - i\sqrt{\frac{2}{\mu}}\rho\left(\lambda\chi' + \bar{\chi}'\bar{\lambda}\right), \qquad (2.0.9)$$

where $D = \partial_\tau + (\vec{n}^\dagger, \dot{\vec{n}}) + i\dot{\alpha}$, $\bar{D} = \partial_\tau - (\vec{n}^\dagger, \dot{\vec{n}}) - i\dot{\alpha}$, $C^i = (\dot{\vec{n}}^\dagger, \partial_i\vec{n}) - (\vec{n}^\dagger, \partial_i\vec{n})(\dot{\vec{n}}^\dagger, \vec{n})$ and $\Gamma^{\bar{j}}_{\bar{k}\bar{m}}$ are Christoffel symbols of the moduli space metric. Note that this Lagrangian, though first written for certain patch in field space, is valid everywhere in field space. Phase α is a gauge degree of freedom. In order to restrict to gauge invariant configuration we have to find the canonical momentum, corresponding to α and put it equal to zero. As α enters the Lagrangian quadratically this amounts to just integrating it out and gives:

$$L = \frac{\mu}{2}\dot{x}^2 + i\bar{\lambda}\dot{\lambda} + (\partial_\tau\rho)^2 + \rho^2\omega^{FS}_{i\bar{j}}\partial_\tau z^i\partial_\tau\bar{z}^{\bar{j}} +$$
$$+\frac{i}{2}\left(\bar{\chi}'\partial_\tau\chi' - \partial_\tau\bar{\chi}'\chi'\right) + \frac{i}{2}\rho^2\omega^{FS}_{i\bar{j}}\left(\bar{\xi}^j\partial_\tau\xi^i + \Gamma^i_{km}\bar{\xi}^j\xi^k\dot{z}^m - \partial_\tau\bar{\xi}^j\xi^i - \Gamma^{\bar{j}}_{\bar{k}\bar{m}}\bar{\xi}^k\xi^i\dot{\bar{z}}^m\right) -$$
$$-\frac{1}{4\rho^2}(\bar{\chi}\chi + \omega^{FS}_{i\bar{j}}\bar{\xi}^j\xi^i)^2 - i\rho\bar{\chi}'\xi^i C^i + i\rho\bar{\xi}^i\chi'\bar{C}^i -$$
$$-r^2\rho^2 - \frac{1}{2\mu}(\rho^2+\vartheta)^2 - \bar{\chi}'\vec{x}\cdot\vec{\sigma}\chi' - \rho^2\omega^{FS}_{i\bar{j}}\bar{\xi}^j\vec{x}\cdot\vec{\sigma}\xi^i - i\sqrt{\frac{2}{\mu}}\rho\left(\lambda\chi' + \bar{\chi}'\bar{\lambda}\right) \qquad (2.0.10)$$

Dropping prime in χ' for ease of notation we can write down the corresponding Hamiltonian

$$H = \frac{p_x^2}{2\mu} + \frac{p_\rho^2}{4} + \frac{1}{\rho^2}\omega^{l\bar{k}}_{FS}\left(p_{\bar{k}} + \frac{i}{2}\rho^2\Gamma_{m\bar{n}\bar{k}}\bar{\xi}^n\xi^m + \frac{i\rho\bar{\chi}\xi^k}{(1+\sum|z^i|^2)} + \frac{i\rho\bar{\xi}^m\chi z^m z^k}{(1+\sum|z^i|^2)^2}\right)\times$$
$$\times\left(p_l - \frac{i}{2}\rho^2\Gamma_{\bar{m}nl}\bar{\xi}^m\xi^l - \frac{i\rho\bar{\xi}^l\chi}{(1+\sum|z^i|^2)} - \frac{i\rho\bar{\chi}\xi^m\bar{z}^m\bar{z}^l}{(1+\sum|z^i|^2)^2}\right) + \frac{1}{4\rho^2}(\bar{\chi}\chi + \rho^2\omega^{FS}_{i\bar{j}}\bar{\xi}^j\xi^i)^2 +$$
$$+r^2\rho^2 + \frac{1}{2\mu}(\rho^2+\theta)^2 + \bar{\chi}\vec{x}\cdot\vec{\sigma}\chi + \rho^2\omega^{FS}_{i\bar{j}}\bar{\xi}^j\vec{x}\cdot\vec{\sigma}\xi^i + i\sqrt{\frac{2}{\mu}}\rho\left(\lambda\chi + \bar{\chi}\bar{\lambda}\right). \qquad (2.0.11)$$

In the limit we are considering, namely $\mu \ll 1$, $\alpha \gg 1$, $\mu\alpha^{3/2} \gg 1$, fields $\vec{x}, \lambda$ and ρ, ξ will become massive with a Hamiltonian

$$H = H^{(2)}_{x,\rho,\lambda,\chi} + V$$
$$H^{(2)}_{x,\rho,\lambda,\chi} = \frac{p_x^2}{2\mu} + \frac{p_\rho^2}{4} + r^2\rho^2 + \frac{1}{2\mu}(\rho^2+\vartheta)^2 + i\sqrt{\frac{2}{\mu}}\rho\left(\lambda\chi + \bar{\chi}\bar{\lambda}\right), \qquad (2.0.12)$$

where we separated the quadratic part from the interaction with other massless fields. We see that ρ gets an expectation value and becomes massive with large mass $m_\rho = \sqrt{\frac{2|\vartheta|}{\mu}}$ and we have

to put this field into it's oscillator ground state. Fermion fields λ, χ should be put into the state, annihilated by operator $\left(\lambda\chi + \bar{\chi}\bar{\lambda}\right)$. Expectation value of ρ gives mass to x field, $m_x = \sqrt{\frac{2|\vartheta|}{\mu}}$, but since the kinetic term for x contains $\frac{1}{\mu}$ we have to take into account exchanges of x, or in Hamiltonian language, take into account first excited states of x-oscillators. In all, the effective Hamiltonian for massless fields z^i and ξ^i will look like:

$$H^{eff}_{z^i,\xi^i} =< \Psi^0_{x,\rho,\lambda,\chi}|V|\Psi^0_{x,\rho,\lambda,\chi} > + \sum_n \frac{| < \Psi^n_{x,\rho,\lambda,\chi}|V|\Psi^n_{x,\rho,\lambda,\chi} > |^2}{E_0 - E_n} \tag{2.0.13}$$

where we need to account for excited states of x only. The result is as expected

$$H^{eff}_{z^i,\xi^i} = \frac{1}{|\theta|}\left(p_{\bar{k}} + \frac{i}{2}\rho^2\Gamma_{m\bar{n}\bar{k}}\bar{\xi}^n\xi^m\right)\omega^{l\bar{k}}_{FS}\left(p_l - \frac{i}{2}\rho^2\Gamma_{\bar{m}nl}\bar{\xi}^m\xi^l\right) +$$
$$+\frac{1}{4}\rho^2 R_{i\bar{k}l\bar{j}}(\bar{\xi}^i\bar{\xi}^k)(\xi^l\xi^j). \tag{2.0.14}$$

We choose fermionic ground state $|0\rangle$ to be

$$\xi^n_1|0\rangle = \bar{\xi}^2_{\bar{n}}|0\rangle = 0, \quad \forall\, n. \tag{2.0.15}$$

The order of spinors in the Hamiltonian itself should be normal order, as usual. Ground states of this Hamiltonian have a general form

$$\Phi_{n_1\ldots n_k\bar{m}_1\ldots\bar{m}_l}\xi^{n_1}_2\ldots\xi^{n_k}_2\bar{\xi}^{\bar{m}_1\,1}\ldots\bar{\xi}^{\bar{m}_l\,1}, \tag{2.0.16}$$

and correspond to elements of Dolbeault cohomology of the moduli space through identification

$$\begin{aligned} \bar{\xi}^{\bar{n}\,1} &\to d\bar{z}^{\bar{n}} \qquad & \xi^n_1 &\to \theta^{-1}w^{n\bar{m}}_{FS}\frac{\partial}{\partial d\bar{z}^{\bar{m}}} \\ \xi^n_2 &\to dz^n \qquad & \bar{\xi}^{\bar{n}\,2} &\to \theta^{-1}w^{\bar{n}m}_{FS}\frac{\partial}{\partial dz^m}. \end{aligned} \tag{2.0.17}$$

Forms $\Phi_{n_1\ldots n_k\bar{m}_1\ldots\bar{m}_l}dz^{n_1}\ldots dz^{n_k}d\bar{z}^{\bar{m}_1}\ldots d\bar{z}^{\bar{m}_l}$ are harmonic representatives of Dolbeault cohomology $\mathrm{H}^{k,l}(\mathcal{M})$ and Hamiltonian (2.0.14) acts as a Laplacian on them. Now we can write spatial rotation generators M_i,$i = 1, 2, 3$, following from the Lagrangian (2.0.10) as :

$$M^i = \mu\epsilon^{ijk}\dot{x}_j x_k - \bar{\lambda}\tau^i\lambda - \rho^2 w^{FS}_{l\bar{k}}\bar{\xi}^{\bar{k}}\tau^i\xi^l \tag{2.0.18}$$

Once we go to the Higgs branch we have to take expectation of these generators in the ground state of massive oscillators which gives

$$M^i = \theta w^{FS}_{l\bar{k}} \bar{\xi}^{\bar{k}} \tau^i \xi^l. \tag{2.0.19}$$

Using the identification (2.0.17) we get

$$\begin{aligned}
M^3 &= \theta w^{FS}_{l\bar{k}} \left(\bar{\xi}^{\bar{k}\,1} \xi^l_1 - \bar{\xi}^{\bar{k}\,2} \xi^l_2 \right) = \frac{1}{2} \left(d\bar{z}^{\bar{m}} \frac{\partial}{\partial d\bar{z}^{\bar{m}}} + dz^m \frac{\partial}{\partial dz^m} \right) - \frac{\dim_{\mathbb{C}}}{2} \\
M^+ &= \theta w^{FS}_{l\bar{k}} \bar{\xi}^{\bar{k}\,1} \xi^l_2 = -\theta w^{FS}_{l\bar{k}} dz^l \wedge d\bar{z}^{\bar{k}} \\
M^- &= \theta w^{FS}_{l\bar{k}} \bar{\xi}^{\bar{k}\,2} \xi^l_1 = \theta^{-1} w^{l\bar{k}}_{FS} \frac{\partial}{\partial dz^l} \wedge \frac{\partial}{\partial d\bar{z}^{\bar{k}}}
\end{aligned} \tag{2.0.20}$$

which is exactly (3.2.29) if we put $\theta = 1$.

Appendix C
Properties of Attractor Flow trees

In this appendix we review some properties of the attractor mechanism and attractor flow trees relevant to the discussion in chapter 4. The attractor flow equations for the Kähler moduli t^a for given charge Γ have the form [19, 20]:

$$\begin{aligned}\frac{d}{d\tau}t^a(\tau) &= -2e^U g^{a\bar{b}}\partial_{\bar{b}}|Z(\Gamma;t(\tau)| \\ \frac{d}{d\tau}e^{-U} &= |Z(\Gamma;t(\tau))|,\end{aligned} \tag{3.0.1}$$

where τ is the parameter along the flow, e^U is metric warp factor, $g_{a\bar{b}}$ is the metric on the moduli space. The attractor flow can be written in an integrated form, which is particularly useful for multicentered generalization [11]:

$$2e^{-U}\mathrm{Im}(e^{-i\alpha}\Omega(t)) = -\tau\Gamma + H_\infty(t_\infty), \tag{3.0.2}$$

where $\Omega(t)$ is the period vector, $\alpha = \arg Z(\Gamma;t)$, t_∞ is the starting point of the flow and

$$H_\infty = 2\mathrm{Im}\left[e^{-i\alpha_\infty}\Omega(t_\infty)\right]. \tag{3.0.3}$$

Now we list and prove a number of properties of attractor flows that are useful in the main text.

Property 1: *For any two charges Γ and γ the attractor flow for charge $\Gamma+\gamma$ crosses the (anti)marginal stability locus $\mathrm{Im}\left[\bar{Z}(\Gamma;t)Z(\gamma;t)\right]=0$ at most once.*

Proof: (3.0.2) determines the value of the flow parameter τ, for which the locus $\mathrm{Im}\left[\bar{Z}(\Gamma;t)Z(\gamma;t)\right] = 0$ is crossed to be

$$\tau_{ms}(t_\infty) = \frac{2\mathrm{Im}\left[Z(\Gamma;t_\infty)\overline{Z(\gamma;t_\infty)}\right]}{\langle\Gamma,\gamma\rangle|Z(\Gamma+\gamma;t_\infty)|} \tag{3.0.4}$$

As (3.0.2) is linear in τ, there is only one solution (3.0.4).■

Let's denote the point where the attractor flow of $\Gamma+\gamma$, starting at t, hits the locus $\mathrm{Im}\left[\bar{Z}(\Gamma;t)Z(\gamma;t)\right]=0$ by $B(t)$.

Property 2: *For any $t \notin AMS(\gamma,\Gamma)$, the distance in the moduli space from t to $B(t)$ along the flow of $\Gamma+\gamma$ is finite.*

Proof: Using (3.0.1) one can write an identity:

$$\int d\tau \left(\frac{dl}{d\tau}\right)^2 = \int d\tau \dot{t}^a g_{a\bar{b}} \bar{\dot{t}}^{\bar{b}} = \frac{1}{2}\int d\tau e^U \left(-2\dot{t}^a \partial_a |Z| - 2\bar{\dot{t}}^{\bar{b}} \partial_{\bar{b}} |Z|\right) = -\int e^U d|Z|, \quad (3.0.5)$$

where dl is a line element along the flow, parametrized by τ. Using the fact that $d|Z| < 0$ along the flow and $e^U \leq 1$, we get

$$\int_0^{\tau_{ms}(t)} d\tau \left(\frac{dl}{d\tau}\right)^2 \leq |Z(\Gamma+\gamma;t)|. \quad (3.0.6)$$

Th parameter τ_{ms} is finite, since the only place where it can go to infinity is on the locus $Z(\Gamma+\gamma;t)=0$, which belongs to $AMS(\gamma,\Gamma)$. Thus we can conclude that

$$\int_0^{\tau_{ms}} d\tau \left(\frac{dl}{d\tau}\right)^2 < \infty, \quad (3.0.7)$$

which means that the distance is indeed finite

$$\int_0^{\tau_{ms}} d\tau \frac{dl}{d\tau} < \infty. \quad (3.0.8)$$

■

Property 3: *The attractor flow of charge Γ in the neighborhood of $(A)MS(\gamma,\Gamma)$ always has the direction from stable to unstable side.*

Proof: Indeed, writing the attractor equation for charge Γ as in (3.0.1) and taking intersection product of it with γ we get:

$$2e^U \mathrm{Im}\left(\frac{\bar{Z}(\Gamma;t)}{|Z(\Gamma;t)|} Z(\gamma;t)\right) = -\tau\langle\gamma,\Gamma\rangle + 2\mathrm{Im}\left(\frac{\bar{Z}(\Gamma;t_\infty)}{|Z(\Gamma;t_\infty)|} Z(\gamma;t_\infty)\right). \quad (3.0.9)$$

Dividing both sides by $\langle\gamma,\Gamma\rangle$ we get

$$2\frac{e^U}{|Z(\Gamma;t)|}\frac{\mathrm{Im}\left(\bar{Z}(\Gamma;t)Z(\gamma;t)\right)}{\langle\gamma,\Gamma\rangle} = -(\tau-\tau_{ms}), \quad (3.0.10)$$

which proves the Property after taking into account the definition of stable/unstable side (4.2.4).

■

Appendix D

Arrangement of conjugation walls near $\mathcal{Z}(\gamma)$

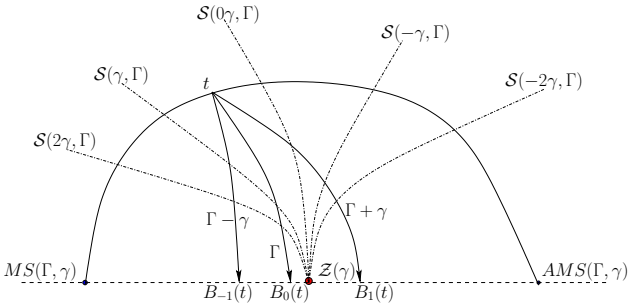

Figure D.1: Location of conjugation walls $\mathcal{S}(n\gamma,\Gamma)$ as a function of n. Two attractor flows for charges $\Gamma+\gamma$ and $\Gamma-\gamma$ are shown.

In figure D.1 we show the general arrangement of the walls $\mathcal{S}(p\gamma,\Gamma)$ walls for $p\in\mathbb{Z}$ in a sufficiently small neighborhood of $\mathcal{Z}(\Gamma)$. Let us give a schematic proof that this arrangement of walls is correct. To do this we find the gradient vectors, entering the attractor equations for charges $\Gamma+p\gamma$, at the locus $\mathcal{Z}(\gamma)$. For this purpose we can neglect all the moduli except the one parameterizing the plane in figure D.1 and can further choose it to be the period of γ, so that $Z_h(\gamma;z)=z$ in a small neighborhood of $\mathcal{Z}(\gamma)$.[1] In this effectively one complex dimensional case the attractor equation will look like:

$$\dot{z}=-2e^U g^{z\bar{z}}\partial_{\bar{z}}|Z(\Gamma+p\gamma;z)|, \tag{4.0.1}$$

This can be written out as

$$\dot{z}=-e^U g^{z\bar{z}}\partial_{\bar{z}}K|Z(\Gamma+p\gamma;z)|-e^U g^{z\bar{z}}e^{K/2}\sqrt{\frac{Z_h}{\bar{Z}_h}}\partial_{\bar{z}}\left(\bar{Z}_h(\Gamma;\bar{z})+p\bar{z}\right), \tag{4.0.2}$$

and we want to study this flow in the leading approximation near $z=0$ as a function of p.

Making a further choice of the phase of z we can assume without loss of generality that $\arg Z_h(\Gamma;z)|_{z=0}=\pi$, so that $AMS(\gamma,\Gamma)$ is the positive real axis and $MS(\gamma,\Gamma)$ is the negative real axis. In the neighborhood of $z=0$ the metric will in general be singular. For example the

[1] A more complete calculation would involve writing the general attractor equation for the moduli y^a, assuming that close to the zero of γ's central charge we can write $Z_h(\gamma;z)\simeq\alpha_a y^a:=z$ and then projecting the attractor flow $\dot{y}^a$ on to the direction $\dot{z}=\alpha_a\dot{y}^a$. It gives the same result as we get below.

metric will typically behave like $g^{z\bar{z}} \sim -\frac{R}{\log|z|^2}$. Nevertheless, we can choose a gauge so that $\partial_{\bar{z}} K$ is continuous and then we can write the leading approximation to the flow equation for $\Gamma + pz$ near $z = 0$ in the form

$$\frac{dz}{d\tau} = -Kg^{z\bar{z}}(\Delta - p) \tag{4.0.3}$$

where $K > 0$ is constant and Δ is a complex constant. The stable side is determined by the sign of $\langle \Gamma, \gamma \rangle$ and taking $\langle \Gamma, \gamma \rangle > 0$ the stable side will be on top of figure D.1. According to Property 3 from Appendix C the attractor flow will cross $(A)MS(\gamma, \Gamma)$ from stable to unstable side which corresponds to $\mathrm{Im}\Delta > 0$. Then even if $g^{z\bar{z}}$ is singular, we know that it is positive, and hence the tangent vectors to the flow have $\frac{dy}{d\tau} < 0$ while $\frac{dx}{d\tau}$ is *positive* for $p > \mathrm{Re}\Delta$ and *negative* for $p < \mathrm{Re}\Delta$. Thus, in a suffciently small neighborhood of $z = 0$ the flows will look as shown in Figure D.1.

Appendix E

The BST walls on the conifold

In this section we determine the positions of $\mathcal{S}(\gamma_{m,n}, \Gamma_{m',n'})$ walls in the conifold example of Section 4.4. As discussed on Section 4.4, we are going to use large volume approximation[1] to solve (4.4.68) and find the branching point of the flow $\Gamma_{\tilde{m},\tilde{n}} := \Gamma_{m',n'} + \gamma_{m,n}$ from (4.4.69). The starting point of the flow is $t_\infty = zP + L\tilde{P}e^{i\phi}$ and the large volume approximation of the holomorphic central charges are given by

$$\begin{aligned} Z^h(\Gamma_{m',n'}; t_\infty) &= \frac{t_\infty^3}{6} - m'z - n' \\ Z^h(\gamma_{m,n}; t_\infty) &= -mz - n \\ Z^h(\Gamma_{\tilde{m},\tilde{n}}; t_\infty) &= \frac{t_\infty^3}{6} - \tilde{m}z - \tilde{n}. \end{aligned} \tag{5.0.1}$$

In terms of the harmonic functions $H = -\tau\Gamma + H_\infty$, entering (4.4.68), the moduli on the first branch of the attractor tree are given by [77, 28].

$$\begin{aligned} t^A &= \frac{H^A - \frac{M}{Q^{3/2}} y^A}{H^0} + i\frac{\Sigma}{Q^{3/2}} y^A \\ D_{ABC} y^B y^C &= -2H^0 H_A + D_{ABC} H^B H^C \\ Q^{3/2} &= 1/3 D_{ABC} y^A y^B y^C \\ M &= H_0 (H^0)^2 + 1/3 D_{ABC} H^A H^B H^C - H^A H_A H^0 \end{aligned} \tag{5.0.2}$$

The branching point corresponds to $\tau_{ms} = \langle \gamma_{m,n}, H_\infty \rangle = \sqrt{\frac{3}{J_\infty^3}} \frac{\mathrm{Im}\left[\frac{\bar{Z}^h(\Gamma_{\tilde{m},\tilde{n}}; t_\infty)}{|Z^h(\Gamma_{\tilde{m},\tilde{n}}; t_\infty)|} Z^h(\gamma_{m,n}; t_\infty)\right]}{\langle \gamma_{m,n}, \Gamma_{\tilde{m},\tilde{n}} \rangle}$, and the only problem in finding the moduli at the brancing point is solving the equation $D_{ABC} y^B y^C = -2H^0 H_A + D_{ABC} H^B H^C$ from (5.0.2). In the present case this reduces to

$$\begin{aligned} D_{222} y^2 y^2 + 2D_{122} y^1 y^2 + D_{112} y^1 y^1 &= -2H^0 H_2 + D_{222} H^2 H^2 + 2D_{122} H^1 H^2 + D_{112} H^1 H^1 \\ D_{122} y^2 y^2 + 2D_{112} y^1 y^2 + D_{111} y^1 y^1 &= -2H^0 H_1 + D_{122} H^2 H^2 + 2D_{112} H^1 H^2 + D_{111} H^1 H^1 \end{aligned} \tag{5.0.3}$$

[1] We use the large volume periods in what follows. Close to the discriminant locus, the periods get finite quantum corrections, but one can check that the effect of these corrections is subleading in $1/\Lambda$.

It is easy to see that $H^1 \sim O(L^0)$ and $H^2 \sim O(L^1)$ and we will look for the solution of (5.0.3) of the form

$$\begin{aligned} y^1 &= y^1_{(1)} + \frac{1}{L} y^1_{(2)} + \dots \\ y^2 &= L y^2_{(1)} + y^2_{(2)} + \dots \end{aligned} \tag{5.0.4}$$

This allows to solve (5.0.3) as an expansion in $\frac{1}{L}$ and gives

$$\begin{aligned} y^2_{(1)} &= L\sqrt{\frac{3}{J^3_\infty}}\sqrt{\sin^2 2\phi - \frac{m}{n}\sin\phi\,\mathrm{Im}\left[ze^{-3i\phi}\right]} \\ y^1_{(1)} &= \frac{\sqrt{\frac{3}{J^3_\infty}}\left(-2\mathrm{Im}\left[e^{-2i\phi}(-\frac{m}{n}z-1)\right]\mathrm{Im}\left[ze^{-3i\phi}\right]\right)}{2\sqrt{\sin^2 2\phi - \frac{m}{n}\sin\phi\,\mathrm{Im}\left[ze^{-3i\phi}\right]}}. \end{aligned} \tag{5.0.5}$$

Note that triple-intersection numbers completely disappeared from the answer! Now we can write our final expression for the moduli at the branching point :

$$\begin{aligned} z_{br} &= -\frac{n}{m} + \frac{\mathrm{Im}\left[e^{-2i\phi}(-\frac{m}{n}z-1)\right]}{\left(\sin^2 2\phi - \frac{m}{n}\sin\phi\,\mathrm{Im}\left[ze^{-3i\phi}\right]\right)^2}\left(\frac{n}{m}\sin 2\phi\left(\sin^2 2\phi - \frac{3}{2}\frac{m}{n}\sin\phi\,\mathrm{Im}\left[ze^{-3i\phi}\right]\right) - \right. \\ &\left. -i\sin\phi\mathrm{Im}\left[ze^{-3i\phi}\right]\sqrt{\frac{3}{4}\sin^2 2\phi - \frac{m}{n}\sin\phi\,\mathrm{Im}\left[ze^{-3i\phi}\right]}\right) \\ L_{br} &= L\frac{\sin\phi}{\sqrt{\sin^2 2\phi - \frac{m}{n}\sin\phi\,\mathrm{Im}\left[ze^{-3i\phi}\right]}} \\ \tan\phi_{br} &= \sqrt{\tan^2\phi + \frac{\mathrm{Im}[e^{-3i\phi}(-\frac{m}{n}z-1)]}{\sin\phi\cos^2\phi}} \end{aligned} \tag{5.0.6}$$

The BST wall is determined by the fact that the branching point is on the locus $Z^h(\gamma_{m,n}; t_{br}) = -mz_{br} - n = 0$. Using (5.0.6) we find that this happens when

$$\begin{cases} \mathrm{Im}\left[e^{-2i\phi}(-\frac{m}{n}z-1)\right] = 0 \\ \frac{3}{4}\sin^2 2\phi - \frac{m}{n}\sin\phi\,\mathrm{Im}\left[ze^{-3i\phi}\right] > 0. \end{cases} \tag{5.0.7}$$

which leads to the final answer (4.4.70).

Appendix F

Enumerating Flow Trees in the FHSV Example

Let us consider attractor flow trees of the form (4.7.116)

$$\Gamma_{m,n} \to (\gamma_{m_1,n_1} + (\gamma_{m_2,n_2} + ...(\gamma_{m_{L-1},n_{L-1}} + (\Gamma + \gamma_{m_L,n_L}))...)), \tag{6.0.1}$$

where $\sum m_i = m$ and $\sum n_i = n$. We make the simplifying assumptions described in Section 4.7.1. In particular $\tau = i$ and z is arbitrarily small. We can assume without loss of generality that $n > 0$.

If the terminal point is in the lower half-plane (for z) then each successive split drives the flow further into the lower half-plane. On the other hand $\sum n_i = n$ must be positive, so some of the n_i must be positive, but all the walls MS_{m_i,n_i} with n_i positive are in the upper half-plane. Therefore, the initial point must be in the upper half-plane.

Now consider a single split $\Gamma_{m,n} \to \Gamma + \gamma_{m,n}$. The marginal stability wall $MS_{m,n}$ is always to the right of the BST wall $\mathcal{S}(\gamma_{m,n}, \Gamma)$. If the initial point is to the right of the BST wall we can construct the tree, otherwise, there is no intersection with the marginal stability wall.

In general, we cannot construct any flow tree with initial point to the left of the BST wall $\mathcal{S}(\gamma_{m,n}, \Gamma)$ because the initial branching (which must take place in the lower half-plane) must necessarily proceed from unstable to stable region, which is forbidden.

Now, consider a point infinitesimally to the right of the BST wall. When enumerating trees further to the right we find a subset of these flows. We first claim that all the n_i are positive. One can check that if n_i becomes negative, then the conservation of charge and the stable-to-unstable rule forces the next n_{i+1} to be negative and so on so that the n-value of the core flow grows without bound. Since we explicitly want the terminal core flow to be Γ this cannot happen. Thus, the n_i are all positive and form a partition of n, in particular, there are finitely many choices for the n_i.

Next, the flow tree will intersect a series of marginal stability walls for

$$\gamma_{m_1,n_1}, \gamma_{m_2,n_2}, \ldots, \gamma_{m_L,n_L},$$

in that order. Since the flow proceeds to the right (stable to unstable) the walls must be

ordered so that successive walls are in the clockwise direction. It is easy to check that the wall $MS_{m_{i+1},n_{i+1}}$ is on the clockwise side of MS_{m_i,n_i} iff

$$m_i n_{i+1} - n_i m_{i+1} > 0 \tag{6.0.2}$$

One way to see this is to require the slope $-n_i/m_i$ to be decreasing. Another way is to require $\mathrm{Im}(m_j - in_j)\overline{(m_{j+1} - in_{j+1})} > 0$. Since m_i can be positive, zero, or negative, but n_i must be positive it is more convenient to write:

$$\frac{m_1}{n_1} > \frac{m_2}{n_2} > \cdots > \frac{m_L}{n_L}. \tag{6.0.3}$$

Now, if $m - a \leq 0$ then all the successive walls have $m_i < 0$. It follows that $-m_i$ forms a partition of $-m$ and hence there are finitely many choices for the m_i. In that case, the trees are labeled by two partitions of $-m$ and n, respectively, subject to (6.0.3).

If $m-a > 0$ the situation is a little more complicated. The walls of marginal stability divide up into the first set with $m_i \geq 0$, which are met first in moving downstream the flow tree and the second set with $m_i < 0$. For the first set there will be inequalities bounding the allowed values of m_i. Then the second set must form a partition to saturate total charge conjugation. For example, if the first branching happens at MS_{m_1,n_1} with $m_1 > 0$ then requiring that the subsequent flow with tangent vector $-a + m - m_1 - i(n - n_1)$ proceed into the unstable region forces

$$\mathrm{Im}(-a + m - m_1 - i(n - n_1))\overline{(m_1 - in_1)} > 0 \quad \Rightarrow \quad \frac{m-a}{n} > \frac{m_1}{n_1} \tag{6.0.4}$$

There are therefore finitely many possible values for m_1. If the next branching is at MS_{m_2,n_2} with $m_2 > 0$ then we similarly get

$$\frac{-a + m - m_1}{n - n_1} > \frac{m_2}{n_2} \tag{6.0.5}$$

giving finitely many values of m_2, and so on.

Of course, the walls are only relevant for wall-crossing provided the Hilbert spaces of halo particles are nonvanishing. Thus $gcd(m_i, n_i)$ must be 1 or 2.

Appendix G
Computation of the periods

In this Appendix we give some details of the computation of periods near the singularity for the X_4 CY manifold of [67]. We start with a review of mirror symmetry and construction of mirror manifold pairs via toric geometry, after that we go over the techniques used to compute the periods using Picard-Fuchs equations. Finally we use these methods to compute the periods near the singularity with massless vector multiplets by explicitly solving Picard-Fuchs equations and using the method of analytic continuation of the periods from the large volume point. We find consistence between the two methods and confirm the existence of two vanishing periods at the singularity.

Construction of mirror manifolds

First we briefly review the construction of the X_4 manifold with it's mirror $\tilde{X}_4$ as a hypersurface in a 4-dimensional toric variety, given in [67]. As pioneered in the works of Batyrev [78] mirror pair of CY manifolds $(\mathcal{M}, \tilde{\mathcal{M}})$ can be described as hyper surfaces in a pair of toric varieties $(\mathbb{P}_\Delta, \mathbb{P}_{\Delta^*})$. Here Δ and Δ^* are a pair of reflexive polyhedra, describing the varieties in the language of toric geometry. The dual polyhedra belong to the two dual rank 4 lattices $(\mathbb{N}, \mathbb{M})$ and are defined by the set of their vertices $\{v^i\}$ and $\{v^*_j\}$. We also denote by $\Sigma^{(k)}_i$ the set of k-dimensional cones who's edges are formed by rays going from the origin to each vertex of the polytope. To a given polytope Δ^* one can associate a number of toric fans: take the set of one dimensional cones $\Sigma^{(1)}(\Delta^*)$ and then choose a set T of 4-dimensional cones $\Sigma^{(4)}_i(\Delta^*)$ such that

$$\begin{aligned} &\Sigma^{(4)}_i \cap \Sigma^{(4)}_j \in \Sigma^{(k)},\ k < 4 \\ &\cup_{i\in T}\, \Sigma^{(4)}_i = R^4. \end{aligned} \tag{7.0.1}$$

This set gives a triangulation of the polytope Δ^* and is called a fan. Each fan T corresponds to certain phase of the toric variety $\mathbb{P}_\Delta$. To construct it explicitly as a holomorphic quotient we associate a coordinate y_i to each one-dimensional cone $\Sigma^{(1)}_i(\Delta^*)$ so that $y_i \in C^n$, $n =$

$\dim\Sigma^{(1)}(\Delta^*)$ and write

$$\mathbb{P}_\Delta(T) = \frac{C^n - Z(\Delta;T)}{G_\Delta}. \tag{7.0.2}$$

Here $Z(\Delta;T)$ is the subset of C^n where the action of toric group G_Δ becomes singular. For each subset of vertices $S \subset \Sigma^{(1)}(\Delta^*)$, that do not form a cone of the fan T but such that each subset of S does form a cone, take the locus $y_i = 0, i \in S$. $Z(\Delta)$ is given by the union of all these loci. Finally the group G_Δ is defined as

$$\begin{aligned} &G_\Delta := Ker[Hom(\Sigma^{(1)}(\Delta^*), C^*) \to Hom(\mathbb{N}, C^*)], \text{ where} \\ &Hom(\Sigma^{(1)}(\Delta^*), C^*) \to Hom(\mathbb{N}, C^*) : \ (\lambda_1, ...\lambda_n) \to (\prod_{i=1}^{n} \lambda_i^{v^*_{(i)\,1}}, ..., \prod_{i=1}^{n} \lambda_i^{v^*_{(i)\,4}}). \end{aligned} \tag{7.0.3}$$

Here $v^*_{i\,a}$, $a = 1..4$ are the coordinates of vertices in lattice $\mathbb{M}$ and the action of group G_Δ on C^n is

$$g_\lambda \in G_\Delta : (y_1, ..., y_n) \to (\lambda_1 y_1, ..., \lambda_n y_n). \tag{7.0.4}$$

The variety (7.0.2) might still be singular. In order to resolve the singularities we have to add integral points of $\mathbb{M}$ inside 1- and 2-dimensional faces of Δ^* and construct refined triangulations. These triangulations will give smooth toric varieties, connected to each other through a sequence of flops.

CY manifold X_4 is a hyper surface in the above toric variety $\mathbb{P}_\Delta$ defined by a polynomial:

$$P(b, y) := \sum_{i \in \Sigma^{(1)}(\Delta)} b_i \prod_{j=1}^{n} y_j^{\langle v^i, v_j^* \rangle + 1}, \tag{7.0.5}$$

where b_i are coefficients, parameterizing complex structure deformations of X_4. In practice, in each C^4 patch of the toric variety (7.0.2) we can choose 4 complex coordinates $y_{j_1}, ...y_{j_4}$ and (7.0.5) will give 3-dimensional surface in this patch.

The whole story repeats itself in describing the mirror CY $\tilde{X}_4$ as a hypersurface in $\mathbb{P}_{\Delta^*}$ given by a polynomial:

$$\tilde{P}(a, x) := \sum_{j \in \Sigma^{(1)}(\Delta^*)} a_j \prod_{i=1}^{\dim\Sigma^{(1)}(\Delta)} x_i^{\langle v^i, v_j^* \rangle + 1}. \tag{7.0.6}$$

The parameters a_j now parametrize complex structure moduli space of the mirror and by mirror symmetry this is isomorphic to the Kähler moduli space of X_4.

To be more specific we proceed to writing down the details of two manifolds X_4 and $\tilde{X}_4$ from [67]. The polytopes are given by their vertices as

$$\Delta:\ v^{(1)}=(0,0,1,-1)\quad v^{(2)}=(0,0,-2,1)\quad v^{(3)}=(6,-6,1,1)\quad v^{(4)}=(6,4,1,1)$$
$$v^{(5)}=(-14,4,1,1)\quad v^{(6)}=(2,2,-1,1)\quad v^{(7)}=(-6,2,-1,1). \tag{7.0.7}$$

$$\Delta^*:\ v^{*(1)}=(-1,0,2,3)\quad v^{*(2)}=(0,0,-1,0)\quad v^{*(3)}=(0,0,0,-1)\quad v^{*(4)}=(0,\ 0,2,3)$$
$$v^{*(5)}=(0,1,2,3)\quad v^{*(6)}=(1,2,2,3)\quad v^{*(7)}=(0,-1,2,3)\quad v^{*(8)}=(0,-1,1,2). \tag{7.0.8}$$

In principle, polytope Δ contains 194 integral points, including all internal points inside 1-, 2- and 3-dimensional faces and the corresponing polynomial, defining X_4 will contain 194 monomials. However, following [67] we can restrict ourselves to a subspace of the full complex structure moduli space, given only by the vertices of Δ. X_4 will be given by a hypersurface

$$P(b,y)=b_0y_1...y_8+b_1y_3^2+b_2y_2^3y_8+b_3y_4^6y_7^{12}y_8^{10}+b_4y_4^6y_5^{10}y_6^{20}y_7^2+b_5y_1^{20}y_4^6y_5^{10}y_7^2+$$
$$+b_6y_2^2y_4^2y_5^4y_6^8+b_7y_1^8y_2^2y_4^2y_5^4 \tag{7.0.9}$$

inside the toric variety $\mathbb{P}_\Delta$. [67] analyzed in detail the rational curves inside X_4. Of particular interest is the family of conics fibered over $\mathbb{P}^1$, which shrinks when one dials certain Kähler parameter of X_4. This family can be seen if we put $y_8=0$ and $y_4=y_5=1$ in the above equation:

$$b_1y_3^2+f_{20}(y_1,y_6)y_7^2+f_8(y_1,y_6)y_2^2=0, \tag{7.0.10}$$

where f_i are homogeneous polynomials of given degree. It is easy to see that (y_1,y_6) parametrize $\mathbb{P}^1$ and for each point on this $\mathbb{P}^1$ we have a plain conic. The discriminant of the above equation has degree 28, which means that there 28 points on the $\mathbb{P}^1$ where the conic degenerates into a pair of $\mathbb{P}^1$'s, intersecting over a point. Note that this is different from the claim made in [67] that the discriminant has degree 24.

We can give the corresponding formulas for the mirror manifold $\tilde{X}_4$. As mentioned above, for a given polytope one can construct a number of fans, corresponding to toric varieties, related to each other by flop transitions. For $\tilde{X}_4$ with vertices (7.0.7) the 3-dimensional faces are

$$((1,2,3,4,6),(1,2,3,5,7),(1,2,6,7),(1,3,4,5),(1,4,5,6,7),(2,3,4,5,6,7)), \tag{7.0.11}$$

where the numbers label vertices (7.0.7). We can associate a fan to this polytope by triangulating the above 3-faces and then making each tetrahedron into a cone with vertex at the point (0,0,0,0). One possible triangulation is:

$$T := ((1,2,3,6),(1,3,4,6),(1,2,3,5),(1,2,5,7),(1,2,6,7),(1,3,4,5),(1,4,5,6),(1,5,6,7),$$
$$(2,3,4,5),(2,4,5,6),(2,5,6,7)). \tag{7.0.12}$$

For T we can find $Z(\Delta^*;T)$ to be

$$Z(\Delta) = \{x_3 = x_7 = 0\} \cup \{x_4 = x_7 = 0\} \cup \{x_1 = x_2 = x_4 = 0\} \cup \{x_3 = x_5 = x_6 = 0\} \cup$$
$$\cup \{x_1 = x_2 = x_5 = x_6 = 0\} \cup \{x_2 = x_3 = x_4 = x_6 = 0\}. \tag{7.0.13}$$

The gauge group G_{Δ^*} will have a $(C^*)^3$ subgroup, generated by the elements:

$$n^{(1)} = (20,10,3,2,0,0,5)$$
$$n^{(2)} = (0,-10,1,-6,0,15,0)$$
$$n^{(3)} = (30,20,4,3,3,0,0), \tag{7.0.14}$$

with $g^{\lambda}_{n^{(i)}} : x_j \to e^{i\lambda n^{(i)}_j} x_j$. In addition there will be a discrete subgroup that will produce quotient singularities. CY $\tilde{X}_4$ is a hypersurface in $\mathbb{P}_{\Delta^*}$ given by a polynomial equation:

$$P_4(a,x) = a_0 x_1 ... x_7 + a_1 x_5^{20} x_7^8 + a_2 x_2^3 x_6^2 x_7^2 + a_3 x_1^2 + a_4 x_3^6 x_4^6 x_5^6 x_6^2 x_7^2 + a_5 x_4^{10} x_5^{10} x_6^4 x_7^4 + a_6 x_4^{20} x_6^8 +$$
$$+ a_7 x_3^{12} x_4^2 x_5^2 + a_8 x_2 x_3^{10}. \tag{7.0.15}$$

a_j parametrize complex structure moduli space of $\tilde{X}_4$ which is isomorphic to the Kähler moduli space of X_4. Our main goal here is to study the singularities of $\mathcal{M}_{Kahler}$ and identify the massless BPS spectrum at those singularities. To achieve this in the next Section we will study the complex structure moduli space of $\tilde{X}_4$. We will find the periods of the holomorphic 3-form around the point $a_8 = 0$, which as explained in [67] corresponds to shrinking the $\mathbb{P}^1$ family of conics (7.0.10). On the other hand, in order to find the spectrum we need to identify special Lagrangian cycles of (7.0.15), that vanish as we dial $a_8 \to 0$. This is not possible to do in the current setting since the toric variety $\mathbb{P}_{\Delta^*}$ has quotient singularities and in order to resolve them we need to add all 194 points of Δ and consider a holomorphic quotient of a subvariety of C^{194}. This calculation seems to be out of reach. Nevertheless, computing the periods only will already give us some evidence about the spectrum.

Periods near the large volume point

In this section we compute the periods of the holomorphic 3-form of the mirror $\tilde{X}_4$, using the techniques described in ([79], [80], [81], [82]). It turns out that one needs only the polytope data in order to do that and in particular the phase of toric variety, in which $\tilde{X}_4$ is embedded, is irrelevant.

First let's introduce the notion of the Mori cone of a toric variety $\mathbb{P}_\Delta$ in a given phase determined by a triangulation T of Δ^*. It is convenient to enlarge the lattice $\mathbb{M}$ and consider a polytope in this enlagred lattice with vertices $\bar{v}_i^* := (1, v_i^*)$. There is a linear space given by $L := \{l \in R^{\mathrm{dim}\Sigma^{(1)}(\Delta^*)+1} : l_i \bar{v}_i^* = 0\}$. Dimension of this space is $\mathrm{dim}L = \mathrm{dim}\Sigma^{(1)}(\Delta^*) - 4$. For triangulation T take the set of 4-dimensional cones, comprising T. For each cone $\Sigma_a^{(4)}(T)$ denote the set of it's 1-dimensional generators by S_a. Then to each $\Sigma_a^{(4)}(T)$ we can associate a cone in L space given by

$$\mathcal{C}_T^a = \{l \in L : \, l_i \geq 0 \ \forall i, \, l_i = 0 \ \ i \in S_a\}. \tag{7.0.16}$$

Intersection of all such cones is called the Mori cone for given triangulation:

$$\mathcal{C}_T = \cap_a \mathcal{C}_T^a. \tag{7.0.17}$$

The Kähler cone of $\mathbb{P}_\Delta$ for this triangulation T is dual to $\mathcal{C}_T$. As discussed in detail in [31], a family of CY manifolds can have many phases, connected with each other through flops or more general transitions. In what follows we will be interested in finding the periods of X_4 in the large volume phase and also near the singularity given $a_8 = 0$. The Mori cone generators for the large vomue phase are given in [67]:

$$\begin{aligned} l^1 &= (-2, 0, 0, 1, 1, 0, 0, -2, 2) \\ l^2 &= (0, 1, 0, 0, 0, -2, 1, 0, 0) \\ l^3 &= (0, 0, 0, 0, -2, 1, 0, 1, 0) \\ l^4 &= (-2, 0, 1, 1, 0, 0, 0, 1, -1). \end{aligned} \tag{7.0.18}$$

The period vector $\Pi(a)$ is a function of a_i from (7.0.15), parametrizing the complex structure moduli space of $\tilde{X}_4$ and satisfies the Picard-Fuchs equations:

$$\left[\prod_{i: l_i^m > 0} a_i^{l_i^m} \left(\frac{\partial}{\partial_{a_i}} \right)^{l_i^m} - z_l \prod_{i: l_i^m < 0} a_i^{-l_i^m} \left(\frac{\partial}{\partial_{a_i}} \right)^{-l_i^m} \right] \Pi(a) = 0, \ m = 1..4. \tag{7.0.19}$$

It is very convenient to introduce $z_m = \prod_i a_i^{l_i^m}$, $m = 1..4$ as complex coordinates on the CS moduli space of $\tilde{X}_4$. These coordinates are called algebraic and have direct relation to the Kähler moduli of X_4. In particular, near the large volume point, which is given in these coordinates by $z_m = 0$ the mirror map between moduli space of $\tilde{X}_4$ and Kähler moduli space of X_4 is given by

$$z_m \sim e^{i2\pi t_m}. \tag{7.0.20}$$

A crucial property of the large volume point is the presence of a unique period $\Pi_0(a)$, called fundamental period, which is analytic around this point and non-vanishing at this point. It is convenient to choose a "gauge" such that

$$\Pi(a) = \frac{1}{a_0}\tilde{\Pi}(a). \tag{7.0.21}$$

In this gauge the fundamental period is a regular power series in a_j around the large volume point given by $z_i = 0$. Using the identities

$$a^n \left(\frac{\partial}{\partial_a}\right)^n = (a\partial_a)(a\partial_a - 1)(a\partial_a - 2)...(a\partial_a - n + 1), \quad a_i\partial_{a_i} = \sum_k l_k^i z_k \partial_{z_k}, \tag{7.0.22}$$

and denoting $\theta_k := z_k\partial_{z_k}$ we can rewrite the Picard-Fuchs operators (7.0.19) as:

$$\begin{aligned}
&D_1 = (\theta_1 + \theta_4)(\theta_1 - 2\theta_3)(2\theta_1 - \theta_4)(2\theta_1 - \theta_4 - 1) - \\
&-z_1(-2\theta_1 - 2\theta_4 - 1)(-2\theta_1 - 2\theta_4 - 2)(-2\theta_1 + \theta_4 + \theta_3)(-2\theta_1 + \theta_4 + \theta_3 - 1) \\
&D_2 = \theta_2^2 - z_2(-2\theta_2 + \theta_3)(-2\theta_2 + \theta_3 - 1) \\
&D_3 = (-2\theta_1 + \theta_4 + \theta_3)(\theta_3 - 2\theta_2) - z_3(\theta_1 - 2\theta_3)(\theta_1 - 2\theta_3 - 1) \\
&D_4 = \theta_4(\theta_1 + \theta_4)(-2\theta_1 + \theta_4 + \theta_3) - \\
&-z_4(-2\theta_1 - 2\theta_4 - 1)(-2\theta_1 - 2\theta_4 - 2)(2\theta_1 - \theta_4).
\end{aligned} \tag{7.0.23}$$

Such generalized hypergeometric systems were studied first by Gelfand, Kapranov and Zelevinski(GKZ) in [83]. Without going into too much details, the above system is incomplete, which means that the space of solution to this system is much larger than the number of periods. In order to compete it we first write it with all z's being on the right of θ's and possible factorizing

the operators D_i by polynomials of θ_j from the left:

$$
\begin{aligned}
&D_1 = (\theta_1 - 2\theta_3)(2\theta_1 - \theta_4)(2\theta_1 - \theta_4 - 1) - \\
&-2(2\theta_1 + 2\theta_4 - 1)(-2\theta_1 + \theta_4 + \theta_3 + 2)(-2\theta_1 + \theta_4 + \theta_3 + 1)z_1 \\
&D_2 = \theta_2^2 - (-2\theta_2 + \theta_3 + 2)(-2\theta_2 + \theta_3 + 1)z_2 \\
&D_3 = (-2\theta_1 + \theta_4 + \theta_3)(\theta_3 - 2\theta_2) - (\theta_1 - 2\theta_3 + 2)(\theta_1 - 2\theta_3 + 1)z_3 \\
&D_4 = \theta_4(-2\theta_1 + \theta_4 + \theta_3) - 2(2\theta_1 + 2\theta_4 - 1)(2\theta_1 - \theta_4 + 1)z_4. \qquad (7.0.24)
\end{aligned}
$$

Now we consider all possible integral vectors insides the Mori cone, write the corresponding operators D_l as above, and then look for linear combinations of them with polynomial in θ_k coefficients such that the resulting operators can be factorized from the left by some polynomial in θ_k, reducing the order of operators. This procedure must give us in this case 6 2nd order operators, and this turns out to be a complete GKZ system:

$$
\begin{aligned}
&\mathcal{D}_1 = \theta_2^2 - (-2\theta_2 + \theta_3 + 2)(-2\theta_2 + \theta_3 + 1)z_2 \\
&\mathcal{D}_2 = (-2\theta_1 + \theta_4 + \theta_3)(\theta_3 - 2\theta_2) - (\theta_1 - 2\theta_3 + 2)(\theta_1 - 2\theta_3 + 1)z_3 \\
&\mathcal{D}_3 = \theta_4(-2\theta_1 + \theta_4 + \theta_3) - 2(2\theta_1 + 2\theta_4 - 1)(2\theta_1 - \theta_4 + 1)z_4 \\
&\mathcal{D}_4 = \theta_4(\theta_1 - 2\theta_3) - 24(2\theta_1 + 2\theta_4 - 1)(2\theta_1 + 2\theta_4 - 5)z_1 z_4^2 - \\
&-4(2\theta_1 + 2\theta_4 - 1)(-2\theta_1 + \theta_4 + \theta_3 + 1)z_1 z_4 \\
&\mathcal{D}_5 = (\theta_1 - 2\theta_3)(2\theta_1 - \theta_4) - 2(-2\theta_1 + \theta_4 + \theta_3 + 1)(-2\theta_1 + \theta_4 + \theta_3 + 2)z_1 - \\
&-4(2\theta_1 + 2\theta_4 - 3)(-2\theta_1 + \theta_4 + \theta_3 + 1)z_1 z_4 \\
&\mathcal{D}_6 = (\theta_3 - 2\theta_2)(2\theta_1 - \theta_4) - 2(-2\theta_1 + \theta_4 + \theta_3 + 1)(\theta_1 - 2\theta_3 + 1)z_1 z_3 - \\
&-12(2\theta_1 + 2\theta_4 - 3)(\theta_1 - 2\theta_3 + 1)z_1 z_3 z_4. \qquad (7.0.25)
\end{aligned}
$$

Before proceeding further we briefly discuss the general approach to solving such systems. We will apply this approach in the next section in order to find the periods around the point inside the moduli space, namely the point with massless vector multiplets. Near the large volume point $z = 0$ we can look for the solution of (7.0.25) in the form of a general power series in z:

$$
w(z, \rho) = \sum_{n \geq 0} c(n; \rho) z^{n+\rho}, \qquad (7.0.26)
$$

where $n = (n_1, ...n_4)$ is a multi-index and $\rho = (\rho_1, ...\rho_4) \in C^4$. Plugging this in (7.0.25) allows us to determine the coefficients $c(n; \rho)$ for all n and in addition to get an algebraic equation on ρ, called indicial equation. This equation can be obtained by taking the principal parts of Picard-Fuchs operators by putting $z = 0$ in them and replacing $\theta_i \to \rho_i$:

$$\rho_2^2=0 \quad (-2\rho_1+\rho_4+\rho_3)(\rho_3-2\rho_2)=0 \quad \rho_4(-2\rho_1+\rho_4+\rho_3)=0$$
$$\rho_4(\rho_1-2\rho_3)=0 \quad (\rho_1-2\rho_3)(2\rho_1-\rho_4)=0 \quad (\rho_3-2\rho_2)(2\rho_1-\rho_4)=0. \quad (7.0.27)$$

This system has only one solution $\rho=0$, which is 10-fold degenerate. The 10 solutions of (7.0.25) corresponding to 10 periods of X_4 are given by

$$w(z,\rho)|_{\rho=0},\ \partial_i w(z,\rho)|_{\rho=0},\ C^{jk}\partial_j\partial_k w(z,\rho)|_{\rho=0},\ C^{ijk}\partial_i\partial_j\partial_k w(z,\rho)|_{\rho=0}, \quad i,j,k=1..4, \quad (7.0.28)$$

where all the derivatives are taken w.r.t ρ. There are much more than 10 independent functions here, however, the coefficients C^{jk} and C^{ijk} are not arbitrary but satisfy the following conditions:

$$C^{jk}\partial_j\partial_k\ pp_a(\rho)|_{\rho=0}=0 \quad C^{ijk}\partial_i\partial_j\partial_k\ pp_a(\rho)|_{\rho=0}=0, \quad (7.0.29)$$

where $pp_a(\rho)$ are the principal parts given in (7.0.27). Of course any combination of these solutions is also a solution. Recall now that the period vector in the IIB picture (corresponding to the mirror CY manifold $\tilde{X}_4$) can be defined in any integral symplectic basis $(\alpha_0,\alpha_a,\beta^a,\beta^0)$ of $\mathrm{H}^3(X;Z)$. The basis is called symplectic if

$$(\alpha_0,\beta^0)=1 \quad (\alpha_a,\beta^b)=\delta_a^b, \quad (7.0.30)$$

and the rest of intersection numbers are zero. There is a particular basis which is most useful in applications of mirror symmetry, namely the basis in which the period vector, given by

$$\Pi(z):=\left(\int_{\alpha_0}\Omega(z),\int_{\alpha_a}\Omega(z),\int_{\beta^a}\Omega(z),\int_{\beta^0}\Omega(z)\right) \quad (7.0.31)$$

can be written in terms of the Kähler moduli t^a of X_4 as

$$\Pi(z)=\left(1,t^a,\frac{1}{2}D_{abc}t^bt^c,\frac{1}{6}D_{abc}t^at^bt^c\right)+O(e^{2\pi it}), \quad (7.0.32)$$

where D_{abc} are the triple intersection numbers of X_4 manifold. In the IIA description, given by X_4, the components of the period have interpretation of holomorphic central charges of BPS states, formed by wrapping (D0,D2,D4,D6)-branes on a symplectic basis of $\mathrm{H}_{2*}(X_4,Z)$. In other words, the above basis is particularly useful since it has a direct geometrical interpretation on the IIA side. In this basis the period vector, being a solution to the Picard-Fuch system (7.0.25) is given by

$$\Pi_0(z) = w(z,\rho)|_{\rho=0}$$
$$\Pi_i(z) = \frac{1}{(2\pi i)}\partial_i w(z,\rho)|_{\rho=0}, \quad i = 1..4$$
$$\Pi^i(z) = \frac{1}{2(2\pi i)^2} D^{ijk}\partial_j\partial_k w(z,\rho)|_{\rho=0},$$
$$\Pi^0(z) = -\frac{1}{6(2\pi i)^3} D^{ijk}\partial_i\partial_j\partial_k w(z,\rho)|_{\rho=0}, \quad i,j,k = 1..4. \tag{7.0.33}$$

This defines the period vector in an integral symplectic basis (unique up to monodromy) around the large volume point. The general form of function (7.0.26) for Mori vectors $l^{(k)}$ is:

$$w(z,\rho) = G(\rho) z^\rho \sum_{n\geq 0} \frac{\Gamma(1-\sum_k l_0^{(k)}(n_k+\rho_k))}{\prod_{i>0}\Gamma(\sum_k l_i^{(k)}(n_k+\rho_k)+1)} z^n, \text{ where}$$
$$G(\rho) = \frac{\prod_{i>0}\Gamma(\sum_k l_i^{(k)}\rho_k + 1)}{\Gamma(1-\sum_k l_0^{(k)}\rho_k)}. \tag{7.0.34}$$

Plugging in the Mori cone vectors (7.0.18) we get:

$$w(z,\rho) = G(\rho) z^\rho \sum_{n_1,n_2,n_3,n_4\geq 0} \frac{\Gamma(1+2(n_1+\rho_1)+2(n_4+\rho_4))z^n}{\Gamma(n_2+\rho_2+1)^2\Gamma(n_4+\rho_4+1)\Gamma(n_1+\rho_1+n_4+\rho_4+1)} \times$$
$$\times \frac{1}{\Gamma(n_1+\rho_1-2(n_3+\rho_3)+1)\Gamma(n_3+\rho_3-2(n_2+\rho_2)+1)} \times$$
$$\times \frac{1}{\Gamma(n_3+\rho_3+n_4+\rho_4-2(n_1+\rho_1)+1)\Gamma(2(n_1+\rho_1)-(n_4+\rho_4)+1)},$$
$$G(\rho) = \frac{\Gamma(\rho_2+1)^2\Gamma(\rho_4+1)\Gamma(\rho_1+\rho_4+1)\Gamma(\rho_1-2\rho_3+1)\Gamma(\rho_3-2\rho_2+1)}{\Gamma(1+2\rho_1+2\rho_4)} \times$$
$$\times\Gamma(\rho_3+\rho_4-2\rho_1+1)\Gamma(2\rho_1-\rho_4+1). \tag{7.0.35}$$

Periods around the singularity with massless vector multiplets

In this section we finally find the periods around the singularity with massless vector multiplets. As mentioned above it is given by the complex codimension one locus $a_8 = 0$. In terms of algebraic coordinates, introduced under (7.0.19)

$$
\begin{aligned}
z_1 &= \frac{a_3 a_4 a_8^2}{a_0^2 a_7^2} \\
z_2 &= \frac{a_1 a_6}{a_5^2} \\
z_3 &= \frac{a_5 a_7}{a_4^2} \\
z_4 &= \frac{a_2 a_3 a_7}{a_0^2 a_8},
\end{aligned} \tag{7.0.36}
$$

the locus looks like

$$
z_1 \to 0 \quad z_4 \to \infty \quad z_1 z_4^2 = const. \tag{7.0.37}
$$

There are two ways to get the periods around this locus: we can either write the GKZ system (7.0.25) around this locus and solve it or we can take the periods (7.0.33) and analytically continue them to this locus. We will use both ways and find a consistent answer. To write (7.0.25) near the $a_8 = 0$ locus we pass to new coordinates

$$
\begin{aligned}
z_1' &= z_1 z_4^2 \\
z_{2,3}' &= z_{2,3} \\
z_4' &= 1/z_4,
\end{aligned} \tag{7.0.38}
$$

in which the system becomes:

$$
\begin{aligned}
&\mathcal{D}_1 = \theta_2'^2 - (-2\theta_2' + \theta_3' + 2)(-2\theta_2' + \theta_3' + 1) z_2' \\
&\mathcal{D}_2 = (-\theta_4' + \theta_3')(\theta_3' - 2\theta_2') - (\theta_1' - 2\theta_3' + 2)(\theta_1' - 2\theta_3' + 1) z_3' \\
&\mathcal{D}_3 = (6\theta_1' - 2\theta_4' + 1)\theta_4' - \frac{1}{2}(2\theta_1' - \theta_4' + 1)(-\theta_4' + \theta_3' + 1) z_4' \\
&\mathcal{D}_4 = (2\theta_1' - \theta_4')(\theta_1' - 2\theta_3') - 24(6\theta_1' - 2\theta_4' - 1)(6\theta_1' - 2\theta_4' - 5) z_1' - \\
&-4(6\theta_1' - 2\theta_4' - 1)(-\theta_4' + \theta_3' + 1) z_1' z_4' \\
&\mathcal{D}_5 = (\theta_1' - 2\theta_3')\theta_4' - 2(-\theta_4' + \theta_3' + 1)(-\theta_4' + \theta_3' + 2) z_1' z_4'^2 - \\
&-4(6\theta_1' - 2\theta_4' - 3)(-\theta_4' + \theta_3' + 1) z_1' z_4' \\
&\mathcal{D}_6 = (\theta_3' - 2\theta_2')\theta_4' - 2(-\theta_4' + \theta_3' + 1)(\theta_1' - 2\theta_3' + 1) z_1' z_4'^2 z_3' - \\
&-12(6\theta_1' - 2\theta_4' - 3)(\theta_1' - 2\theta_3' + 1) z_1' z_3' z_4'.
\end{aligned} \tag{7.0.39}
$$

Notice that the principal parts of Picard-Fuchs operators are not homogeneous in this new

coordinates. This is expected since such homogeneity is really the unique property of the large volume point. The indicial equations will now have two degenerate solutions:

$$\begin{aligned} &S_1 : \rho_i = 0 \ \ \forall i, \ 8 \text{ times degenerate} \\ &S_2 : \rho_i = 0 \ \ i \neq 4, \quad \rho_4 = \frac{1}{2}, \ 2 \text{ times degenerate.} \end{aligned} \tag{7.0.40}$$

To construct the solutions we need to obtain a function $w(z', \rho)$, analogous to (7.0.34), but constructed using the new Mori cone vectors:

$$\begin{aligned} l'^{(1)} &= l^{(1)} + 2l^{(4)} \\ l'^{(2,3)} &= l^{(2,3)} \\ l'^{(4)} &= -l^{(4)}. \end{aligned} \tag{7.0.41}$$

To prove this recall that the Mori cone is dual to the Kahler cone. Kähler cones, corresponding to different patches of the moduli space form "secondary fan", which describes compactification of the moduli space and the coordinate transformation between the two chambers is given by linear relations between Mori cones, corresponding to these two chambers. Provided that the algebraic coordinates in the chamber, containing the divisor $a_8 = 0$, are related to the large volume coordinates as in (7.0.38), the transformation of Mori cone generators must be given by (7.0.41). Using these vectors we can write the function $w'(z', \rho)$:

$$\begin{aligned} w'(z, \rho) = G'(\rho) z'^{\rho} \sum_{n_1, n_2, n_3, n_4 \geq 0} & \frac{\Gamma(1 + 6(n_1 + \rho_1) - 2(n_4 + \rho_4)) z'^{n}}{\Gamma(n_2 + \rho_2 + 1)^2 \Gamma(n_4 + \rho_4 + 1) \Gamma(3n_1 + 3\rho_1 - n_4 - \rho_4 + 1)} \times \\ \times & \frac{1}{\Gamma(n_1 + \rho_1 - 2(n_3 + \rho_3) + 1) \Gamma(n_3 + \rho_3 - 2(n_2 + \rho_2) + 1) \Gamma(n_3 + \rho_3 - n_4 - \rho_4 + 1)} \times \\ \times & \frac{1}{\Gamma(2(n_1 + \rho_1) - (n_4 + \rho_4) + 1)}. \end{aligned} \tag{7.0.42}$$

In terms of this function the periods corresponding to S_2 from (7.0.40) are given by

$$\begin{aligned} \tilde{w}_0(z') &= w'(z', \rho)|_{S_2} \\ \tilde{w}_1(z') &= \tfrac{1}{(2\pi i)} (4\partial_{\rho_1} + \partial_{\rho_2} + 2\partial_{\rho_3} + 12\partial_{\rho_4}) w'(z', \rho)|_{S_2}, \end{aligned} \tag{7.0.43}$$

where to get the second solution, we take a general linear combination of first derivatives ∂_{ρ_i}, act on the principal parts of the Picard-Fuchs operators (7.0.39) and find combinations that

annihilate those principal parts at S_2. Around the point $z_i' = 0$ these two periods will look like

$$\tilde{w}_0(z') \approx \sqrt{z_4'}\,(1 + O(z'))$$
$$\tilde{w}_1(z') \approx \tfrac{1}{(2\pi i)}\sqrt{z_4'}(4\log z_1' + \log z_2' + 2\log z_3' + 12\log z_4')\,(1 + O(z'))\,. \qquad (7.0.44)$$

It is clear that the two periods will both vanish at the singular locus, given in the new coordinates by $z_4' = 0$. What is not clear is how these two periods are related to the integral sympectic basis (7.0.33). We will find the precise relation in the next Section. Now let's proceed to the solution S_1. The fundamental solution here is just $w_0 := w'(z', \rho)_{\rho=0}$. To get first order in logs solution we again find linear combinations of the first ρ derivatives, that annihilate the principal parts of Picard-Fuchs operators:

$$w_1(z') = \frac{1}{(2\pi i)}\partial_{\rho_1} w'(z', \rho)|_{\rho=0} \quad w_2(z') = \frac{1}{(2\pi i)}\partial_{\rho_2} w'(z', \rho)|_{\rho=0} \quad w_3(z') = \frac{1}{(2\pi i)}\partial_{\rho_3} w'(z', \rho)|_{\rho=0}. \qquad (7.0.45)$$

Using second order derivatives gives 4 linear combinations:

$$\begin{aligned}
w_4(z') &= \frac{1}{(2\pi i)^2}(\partial_{\rho_1}^2 + \partial_{\rho_1}\partial_{\rho_3}) w'(z', \rho)|_{\rho=0} \\
w_5(z') &= \frac{1}{(2\pi i)^2}\partial_{\rho_1}\partial_{\rho_2} w'(z', \rho)|_{\rho=0} \\
w_6(z') &= \frac{1}{(2\pi i)^2}(\partial_{\rho_3}^2 + \partial_{\rho_2}\partial_{\rho_3}) w'(z', \rho)|_{\rho=0} \\
w_7(z') &= \frac{1}{(2\pi i)^2}(4\partial_{\rho_1}\partial_{\rho_4} - \partial_{\rho_2}\partial_{\rho_3} + \partial_{\rho_2}\partial_{\rho_4} + 2\partial_{\rho_3}\partial_{\rho_4} + 6\partial_{\rho_4}^2) w'(z', \rho)|_{\rho=0}. \qquad (7.0.46)
\end{aligned}$$

but the last one is not independent but is related to $\tilde{w}_1$ found above through $\theta_4 w_7 = \frac{1}{(\pi i 2)\sqrt{z_4'}}\tilde{w}_1$. Finally the third order ρ derivatives give:

$$w_8(z') = \frac{1}{(2\pi i)^3}\left(8\partial_1^3 + 6\partial_1^2\partial_2 + 12\partial_1^2\partial_3 + 6\partial_1\partial_2\partial_3 + 6\partial_1\partial_3^2\right) w'(z', \rho)|_{\rho=0}. \qquad (7.0.47)$$

The periods $w_1, ..., w_8$ can be written in a much more suggestive way. Recall that according to [67] at the locus $a_8 = 0$ of X_4 it is possible to go through an extremal transition to another CY manifold with 3 Kähler moduli, denoted by X_3. Geometrically on the IIA side we freeze the Kähler modulus $z_4' = 0$ and resolve the singularities by deforming the complex structure moduli to get to X_3 manifold with Hodge numbers $\dim \mathrm{H}^{1,1}(X_3) = 3$, $\dim \mathrm{H}^3(X_3) = 243$. It is easy to

see that we can write siutable linear combinations of $w_1, ..., w_8$ in the form:

$$
\begin{aligned}
w_0^{X_3}(z') &= w'(z', \rho)|_{\rho=0} \\
w_i^{X_3}(z') &= \frac{1}{(2\pi i)} \partial_i w(z', \rho)|_{\rho=0}, \\
w_{i+3}^{X_3}(z') &= \frac{1}{2(2\pi i)^2} D_{X_3}^{ijk} \partial_j \partial_k w'(z', \rho)|_{\rho=0}, \\
w_7^{X_3}(z') &= -\frac{1}{6(2\pi i)^3} D_{X_3}^{ijk} \partial_i \partial_j \partial_k w'(z', \rho)|_{\rho=0}, \quad i, j, k = 1..3,
\end{aligned} \tag{7.0.48}
$$

where $D_{X_3}^{ijk}$ are the intersection numbers of X_3. After putting $z_4' = 0$ these 8 periods become exactly the periods of X_3 around it's large volume point. This is a manifestation of the extremal transition on the level of periods. It is instructive to find the map between the found periods and the periods of the heterotic description of the same extremal transition. Now let's discuss the meaning of the above periods, and in particular, compare our results with the heterotic string. The details of the heterotic description of this extremal transition as well as the IIA/heterotic map in the weak coupling limit can be found in [84]. The Kähler moduli in the heterotic description comprise of the dilaton field S, the toroidal moduli T, U and Wilson lines of the gauge fields on the torus. Using the IIA/Het map, given in Eq.(65) of [84], we can identify

$$
\begin{aligned}
V = t_4 &= \tilde{w}_0 = \sqrt{z_4'}(1 + O(z')) \\
U = t_1 &= \frac{w_1}{w_0} = \frac{1}{(2\pi i)} \log z_1' + O(z') \\
S - T = t_2 &= \frac{w_2}{w_0} = \frac{1}{(2\pi i)} \log z_2' + O(z') \\
T - U = t_3 &= \frac{w_3}{w_0} = \frac{1}{(2\pi i)} \log z_3' + O(z') \\
V_D = const\, \tilde{w}_1 &= const \sqrt{z_4'}(4 \log z_1' + \log z_2' + 2 \log z_3' + 12 \log z_4' + O(z')).
\end{aligned} \tag{7.0.49}
$$

The last equality holds because the periods $(\tilde{w}_0, \tilde{w}_1)$ have the correct monodromy transformation around the singularity $z_4' = 0$. To give even more convincing argument we use (4.9), (5.14), (5.15) from [84] to write the period, dual to the Wilson line near $V = 0$ as:

$$
V_D \approx -\frac{24}{i\pi} V \left(\log V + \frac{T + U}{12} \right). \tag{7.0.50}
$$

Using the mirror map (7.0.49) above this takes the form

$$
V_D \approx -\frac{2}{i2\pi} \sqrt{z_4} \left(12 \log z_4 + 4 \log z_1 + 2 \log z_2 \right), \tag{7.0.51}
$$

which is exactly our $\tilde{w}_1$ (in the weak-coupling limit) and the correct normalization is

$$V_D = -2\tilde{w}_1. \tag{7.0.52}$$

The main result of this relation between IIB and heterotic string periods is that $(\tilde{w}_0, -2\tilde{w}_1, w_0, ..., w_7)$ form an integral symplectic basis of periods. In the next section we confirm this using Mellin-Barnes method of analytic continuation of the periods from the large volume point to the neighborhood of $z' = 0$ point.

Analytic continuation of the periods

The "period generating function" (7.0.34) can be rewritten in the new coordinates (7.0.38) as

$$\begin{aligned}
&w(z',\rho) = G(\rho) z_1'^{\rho_1} z_2'^{\rho_2} z_3'^{\rho_3} z_4'^{2\rho_1-\rho_4} \times \\
&\times \sum_{n_1,n_2,n_3\geq 0} \frac{z_1'^{n_1} z_2'^{n_2} z_3'^{n_3} F(z_4',\rho;n_1,n_2,n_3)}{\Gamma(n_2+\rho_2+1)^2\Gamma(n_1+\rho_1-2(n_3+\rho_3)+1)\Gamma(n_3+\rho_3-2(n_2+\rho_2)+1)} \\
&F(z_4',\rho;n_1,n_2,n_3) = \sum_{m\leq 2n_1} \frac{\Gamma(1+6n_1-2m+2\rho_1+2\rho_4) z_4'^m}{\Gamma(2n_1-m+\rho_4+1)\Gamma(3n_1-m+\rho_1+\rho_4+1)} \times \\
&\times \frac{1}{\Gamma(n_3-m+\rho_3+\rho_4-2\rho_1+1)\Gamma(m+2\rho_1-\rho_4+1)},
\end{aligned} \tag{7.0.53}$$

where $m = 2n_1 - n_4$. Doing the Mellin-Barnes trick to analytically continue $F(z_4', \rho; n_1, n_2, n_3)$ to the neighborhood of $z_4' = 0$ we get:

$$\begin{aligned}
&z_4'^{2\rho_1-\rho_4} F(z_4',\rho;n_1,n_2,n_3) = -\sum_{m>2n_1} \frac{\Gamma(1+6n_1-2m+2\rho_1+2\rho_4)}{\Gamma(2n_1-m+\rho_4+1)\Gamma(3n_1-m+\rho_1+\rho_4+1)} \times \\
&\times \frac{1}{\Gamma(n_3-m+\rho_3+\rho_4-2\rho_1+1)\Gamma(m+2\rho_1-\rho_4+1)}\, z_4'^{m+2\rho_1-\rho_4} + \\
&+ \sum_{m\geq 0} \frac{\Gamma(1+6n_1-2m+6\rho_1)}{\Gamma(m+1)\Gamma(2n_1-m+2\rho_1+1)\Gamma(3n_1-m+3\rho_1+1)\Gamma(n_3-m+\rho_3+1)} z_4'^m + \\
&+ (-1)^{3n_1} \frac{\sqrt{z_4'}\sin\pi(\rho_4-2\rho_1)}{2\sqrt{\pi}\cos\pi(\rho_4+\rho_1)} \times \\
&\times \sum_{m\geq 0} \frac{\Gamma(-3n_1-m-3\rho_1-\frac{1}{2})\, z_4'^{3n_1+m+3\rho_1}}{2^{2m}\Gamma(m+1)\Gamma(-n_1-m-\rho_1+\frac{1}{2})\Gamma(n_3-3n_1-m-3\rho_1+\rho_3+\frac{1}{2})}.
\end{aligned} \tag{7.0.54}$$

An interesting technical point is that the the first sum would not give any contribution to the periods.[1] Using this function we can find all the periods, using (7.0.33), which in the case of X_4 transforms into

[1] As $m > 2n_1$ the first Γ-function downstairs would give ρ_4 and it's higher powers in the numerator.For $n_3 \leq n_1/2$ we get powers of $(\rho_3+\rho_4-2\rho_1)$ from $\Gamma(n_3-m+\rho_3+\rho_4-2\rho_1+1)$, and for $n_3 > n_1/2$ $\Gamma(n_1+\rho_1-2(n_3+\rho_3)+1)$ will give $\rho_1 - 2\rho_3$. In all this first term will be proportional to either $\rho_4(\rho_3+\rho_4-2\rho_1)$ or $\rho_4(\rho_1-2\rho_3)$, but these both are principal parts of GKZ system, and as such will be annihilated by all ρ-derivatives.

$$\Pi_5(z') = \frac{1}{2(2\pi i)^2}(8\partial_1^2 + 4\partial_1\partial_2 + 8\partial_1\partial_3 + 2\partial_2\partial_3 + 2\partial_3^2 + 32\partial_1\partial_4 + 8\partial_2\partial_4 +$$
$$+16\partial_3\partial_4 + 24\partial_4^2)w(z',\rho)|_{\rho=0}$$
$$\Pi_6(z') = \frac{1}{2(2\pi i)^2}(2\partial_1^2 + 2\partial_1\partial_3 + 8\partial_1\partial_4 + 4\partial_3\partial_4 + 6\partial_4^2)w(z',\rho)|_{\rho=0}$$
$$\Pi_7(z') = \frac{1}{2(2\pi i)^2}(4\partial_1^2 + 2\partial_1\partial_2 + 4\partial_1\partial_3 + 16\partial_1\partial_4 + 4\partial_2\partial_4 + 8\partial_3\partial_4 + 12\partial_4^2)w(z',\rho)|_{\rho=0}$$
$$\Pi_8(z') = \frac{1}{2(2\pi i)^2}(16\partial_1^2 + 8\partial_1\partial_2 + 16\partial_1\partial_3 + 4\partial_2\partial_3 + 4\partial_3^2 + 48\partial_1\partial_4 + 12\partial_2\partial_4 +$$
$$+24\partial_3\partial_4 + 36\partial_4^2)w(z',\rho)|_{\rho=0}$$
$$\Pi_9(z') = -\frac{1}{6(2\pi i)^3}\left(8\partial_1^3 + 6\partial_1^2\partial_2 + 12\partial_1^2\partial_3 + 6\partial_1\partial_2\partial_3 + 6\partial_1\partial_3^2 + 48\partial_1^2\partial_4 + 24\partial_1\partial_2\partial_4 +\right.$$
$$\left.+48\partial_1\partial_3\partial_4 + 12\partial_2\partial_3\partial_4 + 12\partial_3^2\partial_4 + 72\partial_1\partial_4^2 + 18\partial_2\partial_4^2 + 36\partial_3\partial_4^2 + 36\partial_4^3\right) w(z',\rho)|_{\rho=0} \quad (7.0.55)$$

Some algebra finally gives the periods of X_4 near the $z_4' = 0$ locus:

$$\Pi_0 = w'(z',\rho)_{S_1} \sim 1 + O(z')$$
$$\Pi_1 = w_1^{X3} - 2\Pi_4 \sim \frac{1}{(2\pi i)}\log z_1' + 2\sqrt{z_4'}(1 + O(z'))$$
$$\Pi_2 = w_2^{X3} \sim \frac{1}{(2\pi i)}\log z_2' + O(z')$$
$$\Pi_3 = w_3^{X3} \sim \frac{1}{(2\pi i)}\log z_3' + O(z')$$
$$\Pi_4 = -\frac{1}{(2\pi i)}w'(z',\rho)_{S_2} \sim -\frac{1}{(2\pi i)}\sqrt{z_4'}(1 + O(z'))$$
$$\Pi_5 = w_4^{X3}$$
$$\Pi_6 = w_5^{X3}$$
$$\Pi_7 = w_6^{X3}$$
$$\Pi_8 = 2w_4^{X3} + 2\frac{1}{(2\pi i)^2}(4\partial_1 + \partial_2 + 2\partial_3 + 12\partial_4)w'(z',\rho)_{S_2} - 8(\log 4 + 6)\Pi_4$$
$$\Pi_9 = w_7^{X3} - \frac{56}{3}\Pi_4. \quad (7.0.56)$$

Due to the fact that these periods are obtained from the large volume ones through analytic continuation, we automatically get an integral symplectic basis of periods. Performing a symplectic

transformaion we can bring these periods to the form:

$$\begin{aligned}
\Pi_0 &= w_0^{X3}(z'),\\
\Pi_1 &= w_1^{X3}\\
\Pi_2 &= w_2^{X3}\\
\Pi_3 &= w_3^{X3}\\
\Pi_4 &= -\frac{1}{(2\pi i)}\tilde{w}_0(z')\\
\Pi_5 &= w_4^{X3}\\
\Pi_6 &= w_5^{X3}\\
\Pi_7 &= w_6^{X3}\\
\Pi_8 &= 2\frac{1}{(2\pi i)^2}\tilde{w}_1(z')\\
\Pi_9 &= w_7^{X3}.
\end{aligned} \tag{7.0.57}$$

Thus we confirmed the relation between the two dual vanishing periods, following from (7.0.52). The monodromy around the singularity $z_4 \to e^{2\pi i} z_4$ in this basis will look like:

$$\begin{aligned}
\Pi_4 &\to -\Pi_4\\
\Pi_8 &\to -\Pi_8 + 24\,\Pi_4,
\end{aligned} \tag{7.0.58}$$

Finally, we can give the physical interpretation of the vanishing periods. Near the large volume point the periods (Π_4, Π_8) correspond to central charges of D2 and D4 branes, wrapping the corresponding cycles in X_4. After analytic continuation and the change of basis, that brought us to (7.0.57), the periods (Π_4, Π_8) are interpreted as central charges of a D2 brane and a D4 brane with some flux. We see that both BPS states become massless at the singularity. This supports the statements, made in 4.7.3, that we have two mutually non-local BPS states, becoming massless at the singularity.

Appendix H

No-mixing conditions in supersymmetric galaxies

A crucial element in our derivation of the KS wall crossing formula and its generalization in chapter 5 was the argument for the absence of quantum mixing between galaxies with different core charges, and between galaxies with orbit charges $\gamma \in L_{\rm orb}$ and galaxies with some orbit charges $\gamma \notin L_{\rm orb}$. As promised we will now examine this argument in more detail, and show that mixing is absent in the $\Lambda \to \infty$ limit except if there exist massless charged particles at the attractor point of Γ_0, with charge in $L_{\rm orb}$.

We first investigate nonperturbative quantum mixing between the perturbative semiclassical states corresponding to a galaxy with all orbiting charges $\gamma \in L_{\rm orb}$, i.e. $\langle \gamma, \Gamma_0 \rangle = 0 = \langle \gamma, \Gamma_0' \rangle$, and those corresponding to a galaxy with some orbiting charges $\gamma \notin L_{\rm orb}$. The core charge is $\Gamma_c = \Lambda^2 \Gamma_0 + \Lambda \Gamma_0' + \gamma_c$ for both galaxies. This kind of mixing could in principle be mediated by a tunneling process in which a charge γ in orbit splits into a charge $\gamma_1 + \delta$ and a charge $\gamma_2 - \delta$, with $\gamma_1, \gamma_2 \in L_{\rm orb}$, $\gamma_1 + \gamma_2 = \gamma$, and $\delta \notin L_{\rm orb}$, followed by tunneling of the two charges to their respective BPS equilibrium positions. If the charges are held fixed in the $\Lambda \to \infty$ limit, then since $\delta \notin L_{\rm orb}$ the symplectic product $\langle \delta, \Gamma_c \rangle$ is at least of order Λ and therefore by (4.1.1) the distance to which the charges would have to tunnel diverges when $\Lambda \to \infty$. Since tunneling over infinite distances is infinitely suppressed, the amplitude for such a process vanishes in the limit. If on the other hand we allow δ to grow with Λ, then in particular for $\delta \equiv \Lambda \Gamma_0 + \Gamma_0'$, it is no longer true that $\langle \delta, \Gamma_c \rangle$ diverges. So for such δ the tunneling trajectory does not have to be infinitely long. However, such diverging charges carry diverging entropy, and hence, by the arguments we will give below, we get infinite entropic tunneling suppression of the splitting event. An even stronger argument is that BPS configurations containing such charge pairs $(\gamma_1 + \delta, \gamma_2 - \delta)$ actually cannot exist, since in the limit $\Lambda \to \infty$, these two charges are essentially opposite (as they diverge but sum up to a finite fixed charge γ), so they are essentially each others antiparticles, and it is not possible to have particles and anti-particles at the same time in orbit and still be BPS (since particle annihilation would clearly be energetically favorable). Thus, either way, mixing with galaxies with orbiting charges not in $L_{\rm orb}$ does not occur in the

limit $\Lambda \to \infty$.[1]

Now we investigate mixing between different cores. Consider a BPS galaxy with core charge $\Gamma_c = \Lambda^2\Gamma_0 + \Lambda\Gamma_0' + \gamma_c$ and total orbiting charge $\Gamma_{\rm orb}$, and a galaxy with core charge $\Gamma_c' = \Gamma_c - \delta$ and orbiting charge $\Gamma_{\rm orb}' = \Gamma_{\rm orb} + \delta$. The perturbative semiclassical states corresponding to these classical configurations can mix nonperturbatively through tunneling of a BPS particle of charge δ between the core black hole and a solar system orbiting the galaxy. We will now argue that such tunneling is infinitely suppressed in the limit $\Lambda \to \infty$, except if δ lies in $L_{\rm orb}$ and becomes massless at the attractor point $t_*(\Gamma_0)$ of Γ_0.

The infinite suppression when $\delta \notin L_{\rm orb}$ in the limit $\Lambda \to \infty$ follows by essentially the same arguments as we used above to show the absence of mixing between galaxies with all orbiting charges in $L_{\rm orb}$ and galaxies with some orbiting charges not in $L_{\rm orb}$: charges $\delta \notin L_{\rm orb}$ would either have to tunnel infinitely far (when they are kept finite), or (when $\delta \propto \Lambda\Gamma_0 + \Gamma_0'$) have infinite entropy themselves and give rise to an infinite change in entropy of the core. Either way, tunneling is infinitely suppressed.

When $\delta \in L_{\rm orb}$, the particle can tunnel to finite distance, but tunneling will be infinitely suppressed in the limit due to the fact that the change in entropy of the core is infinite, *except* when the mass $m_\delta = |Z_\delta|$ of δ vanishes at $t_*(\Gamma_0)$. We first show the steps in the proof of this claim and then explain them. The entropy difference is

$$\begin{aligned}
\Delta S &= S_{\rm BH}(\Lambda^2\Gamma_0 + \Lambda\Gamma_0' + \gamma_c) - S_{\rm BH}(\Lambda^2\Gamma_0 + \Lambda\Gamma_0' + \gamma_c - \delta) && (8.0.1)\\
&= \Lambda^4\left[\frac{\delta^I}{\Lambda^2}\frac{d}{d\Gamma^I}S(\Gamma)|_{\Gamma=\Gamma_0} + \mathcal{O}(\frac{1}{\Lambda^4})\right] && (8.0.2)\\
&= \pi\Lambda^2\delta^I\frac{d}{d\Gamma^I}|Z(\Gamma, t_*(\Gamma))|^2|_{\Gamma=\Gamma_0} + \mathcal{O}(1) && (8.0.3)\\
&= 2\pi\Lambda^2\,{\rm Re}(\overline{Z}_{\Gamma_0}Z_\delta)|_{t_*(\Gamma_0)} + \mathcal{O}(1) && (8.0.4)\\
&= \pm 2\pi\Lambda^2|Z_{\Gamma_0}|\,m_\delta\,|_{t_*(\Gamma_0)} + \mathcal{O}(1)\,, && (8.0.5)
\end{aligned}$$

which indeed diverges when $\Lambda \to \infty$ except if $m_\delta|_{t_*(\Gamma_0)} = 0$. In going from the first to the second line we used the fact that the Bekenstein-Hawking entropy of a BPS black hole scales quadratically with the charges, and we expanded around $\Lambda = \infty$. In the third line we used the expression of the entropy in terms of the central charge. In going to the next to last line we were allowed to ignore the dependence on Γ through $t_*(\Gamma)$ because $|Z(\Gamma, t)|$ has a critical point at $t = t_*(\Gamma)$, i.e. $\partial_t|Z(\Gamma,t)||_{t_*(\Gamma)} = 0$. In the final step we used the attractor point equation

[1] The preceding reasoning makes clear why we added the somewhat peculiar term $\Lambda\Gamma_0'$ in (5.1.4): without it there would be unsuppressed tunneling processes for $\delta \propto \Gamma_0$, and with a term $\Lambda^2\Gamma_0'$ instead, the there would be unsuppressed tunneling for $\delta \propto \Gamma_0 + \Gamma_0'$. Dropping the $\Lambda\Gamma_0'$ term while adding Γ_0 to $L_{\rm orb}$ would be an alternative, but then the awkward situation arises that all walls $W_{k\gamma+m\Gamma_0}$ coincide, spoiling the derivation of the KS formula.

$2\,\mathrm{Im}(\overline{Z}_{\Gamma_0} Z_\delta)|_{t_*(\Gamma_0)} = \langle \Gamma_0, \delta \rangle = 0$. Thus, in the absence of massless BPS particles at $t_*(\Gamma_0)$ with charge in $L_{\rm orb}$, there can be no mixing between galaxies with different core charges.

In conclusion, if no massless charged particles exist at $t_*(\Gamma_0)$, our BPS galaxies are closed quantum systems in the limit $\Lambda \to \infty$, and the framed index is well defined. Massless charged particles only appear at loci of complex codimension 1. Thus, for a generic Γ_0, there will be no massless charged particles at $t_*(\Gamma_0)$, and there will be no mixing.

There might however be special circumstances in which we are interested precisely in the situation where $L_{\rm orb}$ contains charges becoming massless at $t_*(\Gamma_0)$. In this case, mixing may occur, so to be guaranteed a well-defined index we should sum over values of the core charge differing by multiples of the charges becoming massless. It is indeed natural to consider such nongeneric situations in compactifications with codimension 1 loci of enhanced gauge symmetry, as we now explain. Near such loci, there are light vector bosons, say of charge γ, and typically also light monopoles of charge γ_D. Their central charges are related by $Z_{\gamma_D} \sim \tau Z_\gamma$, where τ is the (moduli-dependent) complexified coupling, and $Z_\gamma \to 0$ at the enhanced symmetry locus. When we want to allow both the vector boson and the monopole in a galactic orbit, i.e. $\gamma, \gamma_D \in L_{\rm orb}$, the attractor equations for Γ_0 imply $\mathrm{Im}(Z_\gamma \overline{Z}_{\Gamma_0}) = 0 = \mathrm{Im}(Z_{\gamma_D} \overline{Z}_{\Gamma_0})$ at $t_*(\Gamma_0)$. Given the relation $Z_{\gamma_D} \sim \tau Z_\gamma$ and $\mathrm{Im}\,\tau \neq 0$, this implies $Z_\gamma|_{t_*(\Gamma_0)} = 0$ — that is, we necessarily have massless particles at the attractor point. In Section 4.7.1 we discuss an example of this sort, and show explicitly that it is indeed necessary to sum over core charges to get a well-defined index.

To make this more precise, we could try to define a generalized framed index by summing over the entire lattice V_0 of multiples of charges in $L_{\rm orb}$ becoming massless at $t_*(\Gamma_0)$:

$$\underline{\overline{\Omega}}_C(\Gamma_{\rm orb}; t_\infty) := \sum_{\nu \in V_0} \lim_{\Lambda \to \infty} \mathrm{Tr}_{\mathcal{H}_{\Gamma_c+\nu}(\Gamma_{\rm orb}-\nu; t_\infty)} (-1)^F \,. \tag{8.0.6}$$

There is some redundancy among these objects, as $\underline{\overline{\Omega}}_{\{\Gamma_0, \Gamma_0', \gamma_c\}}(\Gamma_{\rm orb}) = \underline{\overline{\Omega}}_{\{\Gamma_0, \Gamma_0', \gamma_c+\nu\}}(\Gamma_{\rm orb} - \nu)$ for any $\nu \in V_0$. Consequently, the associated generating function

$$G_{[C]}(X; t_\infty) := \sum_{\Gamma_{\rm orb} \in L_{\rm orb}} \underline{\overline{\Omega}}_C(\Gamma_{\rm orb}; t_\infty)\, X^{\gamma_c + \Gamma_{\rm orb}} \,, \tag{8.0.7}$$

depends only on the equivalence class $[C] := \{\Gamma_0, \Gamma_0', \gamma_c \bmod V_0\}$. We could now try to repeat the analysis of the previous sections using these generalized definitions. It is however not immediately obvious that the objects we have defined here are finite or computable in practice, and indeed it is only in special cases possible to restrict the sum over cores to a finite subset.

References

[1] N. Seiberg and E. Witten, "Monopole Condensation, And Confinement In N=2 Supersymmetric Yang-Mills Theory," *Nuclear Physics B*, vol. 426, p. 19, 1994, hep-th/9407087v1.

[2] J. M. Maldacena, "The large N limit of superconformal field theories and supergravity," *Adv. Theor. Math. Phys.*, vol. 2, pp. 231–252, 1998, hep-th/9711200.

[3] A. Strominger and C. Vafa, "Microscopic Origin of the Bekenstein-Hawking Entropy," *Physics Letters B*, vol. 379, p. 99, 1996, hep-th/9601029.

[4] H. Ooguri, A. Strominger, and C. Vafa, "Black Hole Attractors and the Topological String," *Physical Review D*, vol. 70, p. 106007, 2004, hep-th/0405146.

[5] F. Denef and G. W. Moore, "Split States, Entropy Enigmas, Holes and Halos," 2007, hep-th/0702146v1.

[6] F. Denef, B. Greene, and M. Raugas, "Split attractor flows and the spectrum of BPS D-branes on the Quintic," 2001, hep-th/0101135v2.

[7] M. Kontsevich and Y. Soibelman, "Stability structures, motivic Donaldson-Thomas invariants and cluster transformations," 2008, 0811.2435v1.

[8] E. Diaconescu and G. W. Moore, "Crossing the Wall: Branes vs. Bundles," 2007, 0706.3193v1.

[9] J. d. Boer, F. Denef, S. El-Showk, I. Messamah, and D. V. d. Bleeken, "Black hole bound states in $AdS_3 \times S^2$," *JHEP0811*, vol. 050, 2008, 0802.2257v1.

[10] F. Denef, "Quantum Quivers and Hall/Hole Halos," *JHEP*, vol. 0210, p. 023, 2002, hep-th/0206072.

[11] F. Denef, "Supergravity flows and D-brane stability," *JHEP0008*, vol. 050, 2000, hep-th/0005049.

[12] D. L. Jafferis and G. W. Moore, "Wall crossing in local Calabi Yau manifolds," 2008, 0810.4909v1.

[13] A. Strominger, "Massless Black Holes and Conifolds in String Theory," *Nuclear Physics B*, vol. 451, p. 96, 1995, hep-th/9504090v1.

[14] D. Gaiotto, G. W. Moore, and A. Neitzke, "Four-dimensional wall-crossing via three-dimensional field theory," 2008, 0807.4723v1.

[15] D. Gaiotto, G. W. Moore, and A. Neitzke, "Framed BPS States," 2010, 1006.0146.

[16] E. Andriyash and G. W. Moore, "Ample D4-D2-D0 Decay," 2008, 0806.4960.

[17] J. Maldacena, A. Strominger, and E. Witten, "Black Hole Entropy in M-Theory," *JHEP*, vol. 9712, p. 002, 1997, hep-th/9711053.

[18] M. Bershadsky, S. Cecotti, H. Ooguri, and C. Vafa, "Kodaira-Spencer Theory of Gravity and Exact Results for Quantum String Amplitudes," *Communications in Mathematical Physics*, vol. 165, p. 311, 1994, hep-th/9309140.

[19] S. Ferrara, R. Kallosh, and A. Strominger, "N=2 Extremal Black Holes," *Physical Review D*, vol. 52, p. 5412, 1995, hep-th/9508072.

[20] A. Strominger, "Macroscopic Entropy of $N = 2$ Extremal Black Holes," *Physics Letters B*, vol. 383, p. 39, 1996, hep-th/9602111.

[21] F. Denef and G. W. Moore, "How many black holes fit on the head of a pin?," *Gen. Rel. Grav.*, vol. 39, pp. 1539–1544, 2007, 0705.2564.

[22] D. Gaiotto, A. Strominger, and X. Yin, "From AdS3/CFT2 to Black Holes/Topological Strings," *JHEP*, vol. 0709, p. 050, 2007, hep-th/0602046v1.

[23] J. d. Boer, M. C. N. Cheng, R. Dijkgraaf, J. Manschot, and E. Verlinde, "A Farey Tail for Attractor Black Holes," *JHEP0611*, vol. 024, 2006, hep-th/0608059.

[24] J. Manschot and G. W. Moore, "A Modern Fareytail," *Commun. Num. Theor. Phys.*, vol. 4, pp. 103–159, 2010, 0712.0573.

[25] P. Candelas, X. d. l. Ossa, A. Font, S. Katz, and D. R. Morrison, "Mirror Symmetry for Two Parameter Models I," *Nuclear Physics B*, vol. 416, p. 481, 1994, hep-th/9308083v2.

[26] G. Moore, "Arithmetic and Attractors," 1998, hep-th/9807087v3.

[27] F. Denef, "On the correspondence between D-branes and stationary supergravity solutions of type II Calabi-Yau compactifications," 2000, hep-th/0010222.

[28] B. Bates and F. Denef, "Exact solutions for supersymmetric stationary black hole composites," 2003, hep-th/0304094.

[29] C. V. Johnson, "D-Brane Primer," 2000, hep-th/0007170.

[30] G. Moore, "Unpublished notes.," 2007.

[31] P. S. Aspinwall, B. R. Greene, and D. R. Morrison, "Calabi-Yau Moduli Space, Mirror Manifolds and Spacetime Topology Change in String Theory," *Nuclear Physics B*, vol. 416, p. 414, 1994, hep-th/9309097v3.

[32] E. Witten, "Topological Sigma Models," *Commun. Math. Phys.*, vol. 118, p. 411, 1988.

[33] E. Witten, "Topological Quantum Field Theory," *Commun. Math. Phys.*, vol. 117, p. 353, 1988.

[34] E. Andriyash, F. Denef, D. L. Jafferis, and G. W. Moore, "Bound state transformation walls," 2010, 1008.3555.

[35] G. Lopes Cardoso, B. de Wit, J. Kappeli, and T. Mohaupt, "Stationary BPS solutions in N = 2 supergravity with R**2 interactions," *JHEP*, vol. 12, p. 019, 2000, hep-th/0009234.

[36] T. Dimofte, "Refined BPS Invariants, Chern-Simons Theory,and the Quantum Dilogarithm," *PhD thesis*.

[37] G. W. Moore, "PiTP Lectures on Wall Crossing,"

[38] E. Andriyash, F. Denef, D. L. Jafferis, and G. W. Moore, "Wall-crossing from supersymmetric galaxies," 2010, 1008.0030.

[39] F. Denef, "(Dis)assembling special Lagrangians," 2001, hep-th/0107152.

[40] G. Chalmers, M. Rocek, and R. von Unge, "Monopoles in quantum corrected N = 2 super Yang-Mills theory," 1996, hep-th/9612195.

[41] J. Manschot, "Wall-crossing of D4-branes using flow trees," 2010, 1003.1570.

[42] S. Cecotti, P. Fendley, K. A. Intriligator, and C. Vafa, "A New supersymmetric index," *Nucl. Phys.*, vol. B386, pp. 405–452, 1992, hep-th/9204102.

[43] S. Cecotti and C. Vafa, "On classification of N=2 supersymmetric theories," *Commun. Math. Phys.*, vol. 158, pp. 569–644, 1993, hep-th/9211097.

[44] D. Berenstein and M. R. Douglas, "Seiberg duality for quiver gauge theories," 2002, hep-th/0207027.

[45] M. Aganagic and K. Schaeffer, "Wall Crossing, Quivers and Crystals," 2010, 1006.2113.

[46] M. R. Gaberdiel, T. Hauer, and B. Zwiebach, "Open string-string junction transitions," *Nucl. Phys.*, vol. B525, pp. 117–145, 1998, hep-th/9801205.

[47] O. Bergman and A. Fayyazuddin, "String junctions and BPS states in Seiberg-Witten theory," *Nucl. Phys.*, vol. B531, pp. 108–124, 1998, hep-th/9802033.

[48] A. Mikhailov, N. Nekrasov, and S. Sethi, "Geometric realizations of BPS states in N = 2 theories," *Nucl. Phys.*, vol. B531, pp. 345–362, 1998, hep-th/9803142.

[49] K. Behrndt, D. Lust, and W. A. Sabra, "Stationary solutions of N = 2 supergravity," *Nucl. Phys.*, vol. B510, pp. 264–288, 1998, hep-th/9705169.

[50] D. Gaiotto, G. W. Moore, and A. Neitzke, "Wall-crossing, Hitchin Systems, and the WKB Approximation," 2009, 0907.3987v1.

[51] J. A. Harvey and G. W. Moore, "On the algebras of BPS states," *Commun. Math. Phys.*, vol. 197, pp. 489–519, 1998, hep-th/9609017.

[52] G. W. Moore, "String duality, automorphic forms, and generalized Kac- Moody algebras," *Nucl. Phys. Proc. Suppl.*, vol. 67, pp. 56–67, 1998, hep-th/9710198.

[53] M. Kontsevich and Y. Soibelman, "Cohomological Hall algebra, exponential Hodge structures and motivic Donaldson-Thomas invariants," 2010, 1006.2706.

[54] G. Moore, "Attractors and Arithmetic," 1998, hep-th/9807056.

[55] P. S. Aspinwall, R. P. Horja, and R. L. Karp, "Massless D-Branes on Calabi-Yau Threefolds and Monodromy," *Communications in Mathematical Physics*, vol. 259, p. 45, 2005, hep-th/0209161v2.

[56] K. Nagao and H. Nakajima, "Counting invariant of perverse coherent sheaves and its wall-crossing," 2008, 0809.2992v4.

[57] K. Nagao, "Derived categories of small toric Calabi-Yau 3-folds and counting invariants," *ArXiv e-prints*, sep 2008, 0809.2994.

[58] A. Iqbal, N. Nekrasov, A. Okounkov, and C. Vafa, "Quantum Foam and Topological Strings," *JHEP*, vol. 0804, p. 011, 2008, hep-th/0312022.

[59] B. Szendroi, "Non-commutative Donaldson-Thomas theory and the conifold," 2007, 0705.3419v3.

[60] J. d. Boer, S. El-Showk, I. Messamah, and D. V. d. Bleeken, "Quantizing N=2 Multicenter Solutions," 2008, 0807.4556v1.

[61] P. S. Aspinwall, "An N=2 Dual Pair and a Phase Transition," *Nuclear Physics B*, vol. 460, p. 57, 1996, hep-th/9510142v2.

[62] S. Kachru and C. Vafa, "Exact Results for N=2 Compactifications of Heterotic Strings," *Nuclear Physics B*, vol. 450, p. 69, 1995, hep-th/9505105v3.

[63] S. Kachru, A. Klemm, W. Lerche, P. Mayr, and C. Vafa, "Nonperturbative Results on the Point Particle Limit of N=2 Heterotic String Compactifications," *Nuclear Physics B*, vol. 459, p. 537, 1996, hep-th/9508155v1.

[64] S. Katz, A. Klemm, and C. Vafa, "Geometric Engineering of Quantum Field Theories," *Nuclear Physics B*, vol. 497, p. 173, 1997, hep-th/9609239v2.

[65] S. Katz, D. R. Morrison, and M. R. Plesser, "Enhanced Gauge Symmetry in Type II String Theory," *Nuclear Physics B*, vol. 477, p. 105, 1996, hep-th/9601108v2.

[66] G. Aldazabal, L. E. Ibanez, A. Font, and F. Quevedo, "Chains of N=2, D=4 heterotic/type II duals," *Nuclear Physics B*, vol. 461, p. 85, 1996, hep-th/9510093v1.

[67] P. Berglund, S. Katz, A. Klemm, and P. Mayr, "New Higgs Transitions between Dual N=2 String Models," *Nuclear Physics B*, vol. 483, p. 209, 1997, hep-th/9605154v3.

[68] S. Ferrara, J. A. Harvey, A. Strominger, and C. Vafa, "Second-Quantized Mirror Symmetry," *Physics Letters B*, vol. 361, p. 59, 1995, hep-th/9505162v2.

[69] J. A. Harvey and G. Moore, "Algebras, BPS States, and Strings," *Nuclear Physics B*, vol. 463, p. 315, 1996, hep-th/9510182v2.

[70] B. R. Greene, D. R. Morrison, and A. Strominger, "Black Hole Condensation and the Unification of String Vacua," *Nuclear Physics B*, vol. 451, p. 109, 1995, hep-th/9504145v2.

[71] B. R. Greene, D. R. Morrison, and C. Vafa, "A Geometric Realization of Confinement," *Nuclear Physics B*, vol. 481, p. 513, 1996, hep-th/9608039v2.

[72] F. Denef, "Supergravity flows and D-brane stability," *JHEP0008*, vol. 050, 2000, hep-th/0005049v2.

[73] J. M. Maldacena, J. Michelson, and A. Strominger, "Anti-de Sitter fragmentation," *JHEP*, vol. 02, p. 011, 1999, hep-th/9812073.

[74] T. Dimofte and S. Gukov, "Refined, Motivic, and Quantum," 2009, 0904.1420v1.

[75] T. Dimofte, S. Gukov, and Y. Soibelman, "Quantum Wall Crossing in N=2 Gauge Theories," 2009, 0912.1346v1.

[76] A. Dabholkar, F. Denef, G. W. Moore, and B. Pioline, "Exact and Asymptotic Degeneracies of Small Black Holes," *JHEP0508*, vol. 021, 2005, hep-th/0502157.

[77] M. Shmakova, "Calabi-Yau Black Holes," *Physical Review D*, vol. 56, p. 540, 1997, hep-th/9612076.

[78] V. Batyrev, "Dual Polyhedra and Mirror Symmetry for Calabi-Yau Hypersurfaces in Toric Varieties," *arXiv.org/abs/alg-geom/9310003v1.*

[79] P. Berglund, S. Katz, and A. Klemm, "Mirror Symmetry and the Moduli Space for Generic Hypersurfaces in Toric Varieties," *Nuclear Physics B*, vol. 456, p. 153, 1995, hep-th/9506091v1.

[80] S. Hosono, A. Klemm, S. Theisen, and S. T. Yau, "Mirror Symmetry, Mirror Map and Applications to Calabi-Yau Hypersurfaces," *Communications in Mathematical Physics*, vol. 167, p. 301, 1995, hep-th/9308122v2.

[81] S. Hosono, A. Klemm, S. Theisen, and S.-T. Yau, "Mirror Symmetry, Mirror Map and Applications to Complete Intersection Calabi-Yau Spaces," *Nuclear Physics B*, vol. 433, p. 501, 1995, hep-th/9406055v2.

[82] S. Hosono, B. H. Lian, and S. T. Yau, "GKZ-Generalized Hypergeometric Systems in Mirror Symmetry of Calabi-Yau Hypersurfaces," *Communications in Mathematical Physics*, vol. 182, p. 535, 1996, alg-geom/9511001v1.

[83] A. I.M.Gelfand and M.M.Kapranov *Funct. Anal. Appl. 23, 2.*

[84] D. Lust, "String Vacua with N=2 Supersymmetry in Four Dimensions," 1998, hep-th/9803072v2.

Vita

Evgeny Andriyash

1997-2003	Master degree in physics, Department of Physics, Moscow State University, Moscow, Russia
2003-2005	Research Assistant, Institute for Theoretical and Experimental Physics, Moscow, Russia
2005-2010	Doctor of Philosophy, Department of Physics and Astronomy, Rutgers University, USA
2003-2004	Stipend for Young Scientists, Institute for Theoretical and Experimental Physics, Moscow
2005-2007	Graduate Fellowship, Rutgers University
2008-2009	Graduate Assistantship, Rutgers University
2009-2010	Research Assistantship, NHETC, Rutgers University

List of Publications

2002	E. Andriyash and K. Stepanyantz, "One loop renormalization of the Yang-Mills theory with BRST invariant mass term," Moscow Univ.Phys.Bull.58:28-32 (2003) [arXiv:hep-th/0204211]
2003	E. Andriyash, G. Ovanesyan, M. Vysotsky, "Difference of tilde epsilon and epsilon in fitting the parameters of CKM matrix," Phys.Lett.B599:253-259 (2004) [arXiv:hep-th/0310314]
2005	E. Andriyash, G. Ovanesyan, M. Vysotsky, "The Value of B(K) from the experimental data on CP-violation in K-mesons and up-to-date values of CKM matrix parameters," Phys.Atom.Nucl.69:286-292 (2006) [arXiv:hep-th/0502111]
2008	E. Andriyash and G. Moore, "Ample D4-D2-D0 Decay," [arXiv:0806.4960]
2010	E. Andriyash, F. Denef, D. Jafferis, G. Moore, "Wall-crossing from supersymmetric galaxies," [arXiv:1008.0030]
2010	E. Andriyash, F. Denef, D. Jafferis, G. Moore, "Bound state transformation walls," [arXiv:1008.3555]